Department of
Mechanical and Manufacturing Engineering
Trinity College Dublin

Human Thermoregulatory Response to Infrared Radiant Heating

Michelle Tannam

DECLARATION

I, Michelle Tannam, declare that this thesis has not been submitted as an exercise for a degree at another university and that this thesis is entirely my own work.

_____

Michelle Tannam

March 2012

ACKNOWLEDGEMENTS

I would like to express my sincerest gratitude to the following people whose support has made this project possible;

- My supervisor Dr. Tony Robinson, for his much appreciated guidance throughout the year.
- Gerry Byrne, and all of the thermodynamics postgraduate students for their continuous assistance and advice.
- Paul Normoyle, for taking the time to share his expertise in programming and circuitry.
- Frank Wilson and John Morehead for their interest and much appreciated feedback.
- My test subjects Christine, Tara, Mick, Dave, Martyn, Ciara, Aaron, Daire, David, Taro and Ciara for their time and patience.
- My family for their endless support and encouragement.
- And finally Judith Lee, Mick Reilly and everyone in the workshop for all of their help.

ABSTRACT

This report discusses the workings of infrared radiant heating and investigates its applicability for indoor comfort applications. The fundamental concepts of radiant heat transfer, the human thermoregulatory system, and human thermal comfort are introduced. The current applications of electric infrared radiant heating are discussed, and it is compared with conventional convective heating methods. Experiments are conducted to obtain temperature and heat flux distribution characteristics for two ceramic element heaters. It is found that for both heaters the temperature and heat flux distributions are symmetric about symmetric sections of heater shape and vary most significantly within 0.5m of the heat source, after which distributions become more uniform. The trends between temperature and heat flux distribution are found to be similar for each heater, and the most appropriate placement of each heater for comfort applications is discussed. Further experiments investigate the human thermoregulatory response to infrared heating. A series of tests are carried out on a group off four subjects involving the application of infrared heat to the face or hand area whilst core temperature, skin temperature, and heat flux measurements are recorded. Similar testing is carried out using convective heating, and the two heating types are compared. Differences in trend between infrared and convective heating are identified, and it is also found that human thermoregulatory response differs between individuals tested. It is shown that the thermoregulatory system has the ability to effectively redistribute heat from an area directly heated by an IR source to other areas of the body so that heat may be lost from the surface of the skin and core temperature maintained at an appropriate level. In most cases the hand is seen to be the primary area to which heat is transferred for dissipation to the surroundings.

CONTENTS

LIST OF FIGURES

LIST OF TABLES

ACRONYMS

ASHRAE	American Society of Heating, Refrigerating and Air Conditioning Engineers
DR	Draft Rating
IR	Infrared
Ni	National Instruments
PC	Personal Computer
PMV	Predicted Mean Vote
PPD	Percentage People Dissatisfied
USB	Universal Serial Bus
UV	Ultraviolet
WR	Warm Room

NOMENCLATURE

Unless stated otherwise, the nomenclature is defined as follows;

Symbol	Definition	Units
A	Area	$[m^2]$
A_r	Effective radiation area of the body	$[m^2]$
A_D	DuBois surface area	$[m^2]$
$\propto$	Absorptivity	[%]
C	Convective heat transfer	$[W]$
c	Speed of light in the medium	$[m/s]$
E	Evaporative heat transfer	$[W]$
ε	Emissivity	$[-]$
f_{cl}	Clothing surface area factor	$[-]$
h_c	Convective heat transfer coefficient	$[W/(m^2 \cdot K)]$
h_r	Radiant heat transfer coefficient	$[W/m^2 \cdot K]$
I_{cl}	Clothing insulation	$[m^2K/W]$
K	Conductive heat transfer	$[W]$
k	Thermal conductivity	$[W/m \cdot K]$
l	Body height	$[m]$
λ	Wavelength	$[\mu m]$
M	Metabolic energy production	$[Met]$
m	Body mass	$[kg]$
P_a	Partial vapour pressure of water	$[°C]$
q	Heat transfer rate	$[W]$
q"	Heat flux	$[W/m^2]$
R	Radiant heat transfer	$[W]$
ρ	Reflectivity	[%]
S	Heat storage	$[W]$
σ	Stefan-Boltzmann constant = 5.67 x 10^{-8}	$[W/m^2 \cdot K^4]$
T	Temperature	$[K]$
t_a	Local air temperature	[°C]
$\overline{t_{cl}}$	Average temperature of clothing surface	$[°C]$

$\overline{t_r}$	Mean radiant temperature	$[°C]$
T_s	Surface temperature	$[K]$
$\overline{t_{sk}}$	Average skin surface temperature	$[°C]$
T_{sur}	Temperature of surroundings	$[K]$
Tu	Local turbulence intensity	$[\%]$
T_∞	Flow temperature	$[K]$
τ	Transmissivity	$[\%]$
u	Local mean air velocity	$[m/s]$
v	Frequency	$[s^{-1}]$
v_{ar}	Relative air velocity	$[m/s]$
W	Mechanical work	$[W]$

1 Introduction

Infrared (IR) radiant heating has been found to be very appropriate for thermal comfort applications due to its ability to quickly and efficiently heat objects in the directional path of its rays. It is currently used extensively in incubation, saunas, and outdoor heating, and the characteristics of IR heating suggest that it could also be used successfully for indoor heating in conjunction with conventional convective systems, particularly for intermittently used areas.

This report concerns the response of the human thermoregulatory system to IR heating. The thermoregulatory system is designed to maintain the core body temperature at around 37°C. When heat is applied to the body and its temperature begins to rise the thermoregulatory system undertakes action to correct the body temperature. This is the basis of human thermal comfort. Thermal comfort models have been developed which enable some general ideas to be formed about what is required for satisfactory thermal comfort. Some of these models recognise that it is not only the physical and physiological conditions which pertain to a state of thermal satisfaction; however these are the only truly measurable conditions.

This report provides information on the basics of radiation heat transfer and on the workings and characteristics of IR heating as compared to conventional convective heating. The methods employed by the thermoregulatory system to regulate core temperature are also discussed along with the basics of human thermal comfort theory, thus giving a solid basis for understanding of the objectives to follow

1.1 Objectives

The overall objective of this project is to investigate the suitability of IR heating for use in human thermal comfort applications by obtaining qualitative information about the response of the human thermoregulatory system to IR heating.

This first stage of the project will be concerned with the quantitative analysis of the output of IR heaters, which will be characterised in two ways;

- The temperature distribution of the heaters will be documented by a thermal imaging camera over a 2D area at incremental distances from the heat source.
- The heat flux distribution of the heaters will be documented using a radiant heat flux sensor moved over a 2D plane. Again the results will be documented at incremental distances from the heat source.

The second stage of the project will be concerned with the qualitative analysis of the response of the human thermoregulatory system to both conventional convective and localised IR heating conditions. This will involve using skin temperature, core temperature and heat flux information in conjunction with knowledge of the workings of the thermoregulatory system to gain an understanding of the response of the body to different heating conditions. The thermoregulatory response of multiple test subjects will be analysed for the following heating conditions;

- Warm room (baseline test).
- Cold room with IR heat applied to the face area.
- Cold room with IR heat applied to the hand area.

2 Background Theory

2.1 Radiant Heat Transfer

2.1.1 Principal Modes of Heat Transfer

Heat transfer is defined as energy in transit due to a temperature difference. It can be quantified by rate equations which allow calculation of the heat flux; defined as the rate of heat transfer per unit area. The heat transfer rate can thus be found by multiplying the heat flux by the relevant area [1];

$$q = q'' \cdot A$$

There are three principle modes of heat transfer;

- Conduction is the transmission of heat through a substance without perceptible motion of the substance [2], i.e.: through a stationary solid or fluid medium. The conductive heat flux in the x direction is given by [1];

$$q''_x = -k\frac{dT}{dx}$$

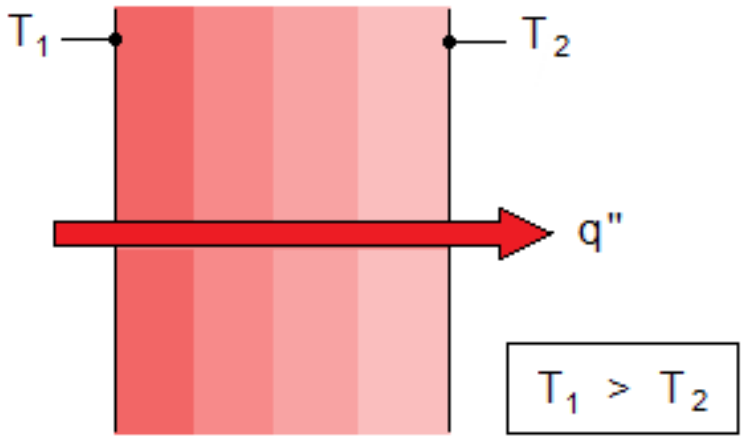

Figure 1 - Conduction through a solid or a stationary fluid [1]

- Convection is the transmission of heat due to the bulk movement of a fluid [2]. This usually occurs between a solid and a fluid. The convective heat flux is given by [1];

$$q" = h_c(T_s - T_\infty)$$

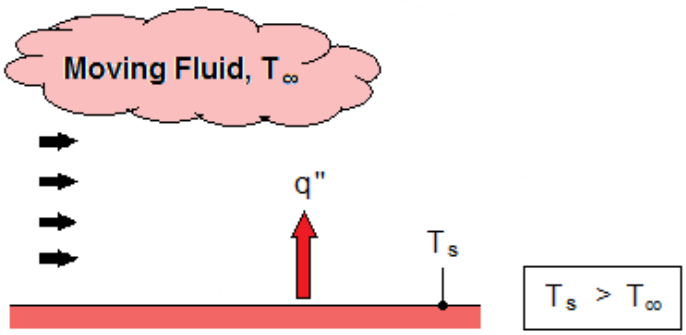

Figure 2 - Convection from a surface to a moving fluid [1]

- Radiation is the transmission of heat in the form of electromagnetic waves that occurs between surfaces in the absence of an intervening medium. All surfaces of a finite temperature emit radiant heat [1]. For the simple case of radiation between a small surface and a large enclosure, the radiant heat flux is given by;

$$q"_{rad} = \varepsilon\sigma(T_s^4 - T_{sur}^4)$$

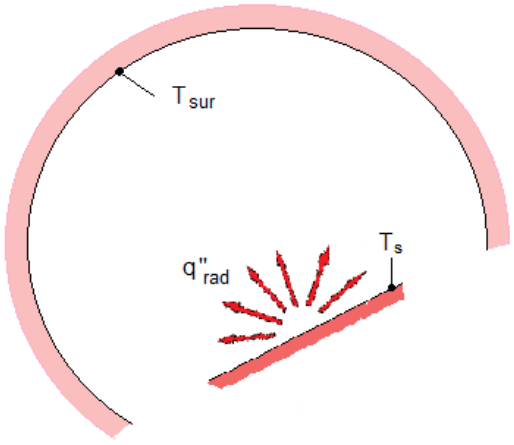

Figure 3 - Net radiation heat exchange between two surfaces [1]

Unlike conduction and convection, radiation does not require the presence of an intervening medium (and actually occurs most efficiently in a vacuum). Emission can be attributed to changes in the electron configurations of the constituent atoms or molecules, and can occur from liquids and gases as well as from solids [1], though here the focus will be on radiation from solid surfaces.

From comparison of the equations for each of the modes of heat transfer it can be seen that radiation heat exchange is the most affected by changes in temperature (being raised to the fourth power). This study is concentrated on the transfer of heat through radiation, and hence this will be the focus of discussion.

2.1.2 Fundamental Concepts of Radiation

Energy Propagation

Thermal radiation is energy emitted by matter which is at a finite temperature. The energy is propagated by electromagnetic waves, and so the standard wave properties of frequency and wavelength can be applied to radiation [1];

$$\lambda = \frac{c}{v}$$

The electromagnetic spectrum, in which the types of radiation are characterised by wavelength, is shown in Figure 4. Thermal radiation is the section of the spectrum ranging from approximately 0.1 to 100 microns [1]. It includes some of the UV range, the entire visible range, and much of the infrared range. This is the portion of the spectrum which is relevant to heat transfer. It can be seen that the infrared region ranges from approximately 0.7 to 1000 microns, and is split into near, medium and far infrared within that range [3].

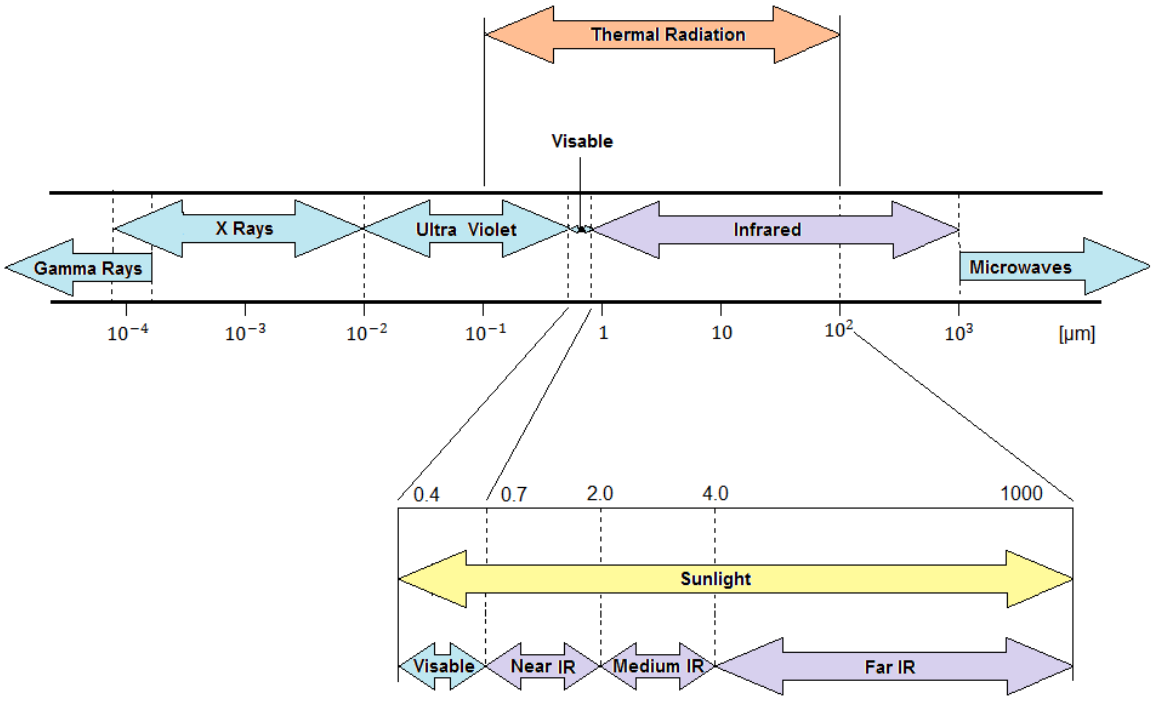

Figure 4 - The electromagnetic spectrum [3]

Blackbody

A blackbody is an ideal radiator [1];

- No surface can emit a greater amount of energy (for a set temperature and wavelength) than a blackbody.
- A blackbody absorbs all incident radiation regardless of wavelength or direction.
- A blackbody is a diffuse emitter, and hence is independent of direction.
- These properties allow the blackbody to be used as a standard against which the properties of real surfaces can be compared.

Emissivity

Emissivity is a measure of how efficiently a surface emits energy relative to a blackbody. For a real surface, the heat flux emitted is less than half that of a blackbody at the same temperature, and the emissivity value ranges between $\varepsilon = 0$ for a perfect reflector and $\varepsilon = 1$ for a blackbody. The property is strongly dependent on the surface material and finish [1].

The emissive power is the rate at which energy of wavelength λ is released from a surface per unit area, given by the Stefan-Boltzmann law;

$$E_\lambda = \varepsilon \sigma T_s^4$$

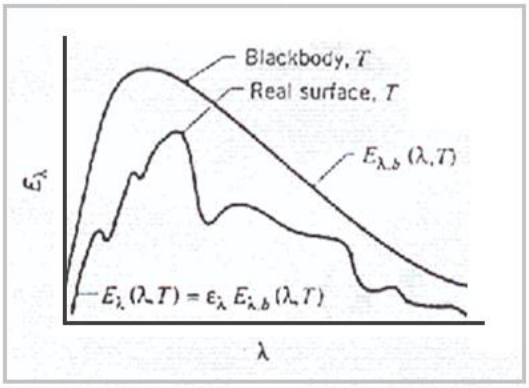

Figure 5 - Comparison of blackbody and real surface spectral distribution [1]

The Planck Distribution shown in Figure 6 displays the spectral distribution of blackbody emission. Observation of the Planck distribution shows that emitted radiation varies continuously with wavelength, and that wavelength is a function of temperature [1]. From Figure 6 it can be seen that higher temperatures produce shorter wavelengths, whilst lower temperatures produce longer wavelengths.

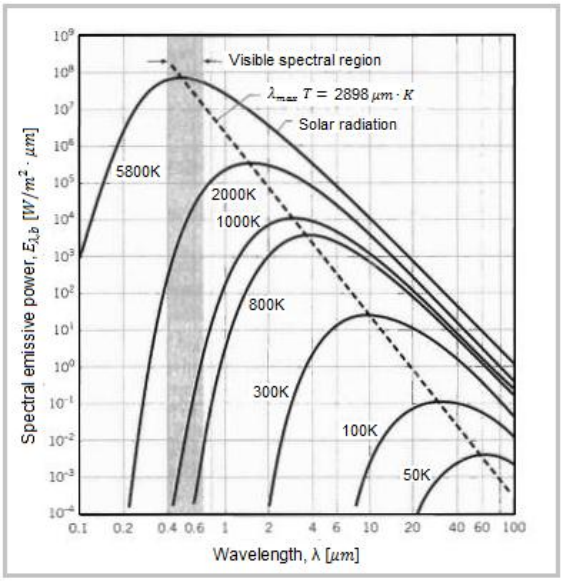

Figure 6 - Planck's spectral distribution of blackbody emission [1]

From the dotted line in Figure 6 it can be seen that the blackbody spectral distribution has a maximum for each temperature, along with a corresponding wavelength. These points are found using Wien's Displacement Law, given by [1];

$$\lambda_{max}\, T = 2897.8\, \mu m \cdot K$$

Intensity

The spectral intensity, $I_{\lambda\, e}$, is the rate at which radiant energy is emitted at wavelength λ in the (θ,ϕ) direction, per unit area of the emitting surface normal to this direction, per unit solid angle about this direction, per unit wavelength interval dλ about λ. Figure 7 shows (a) Emission of radiation from a differential area dA_1 into a solid angle $d\omega$ subtended by normal dA_n at a point on dA_1 and (b) the definition of a solid angle.

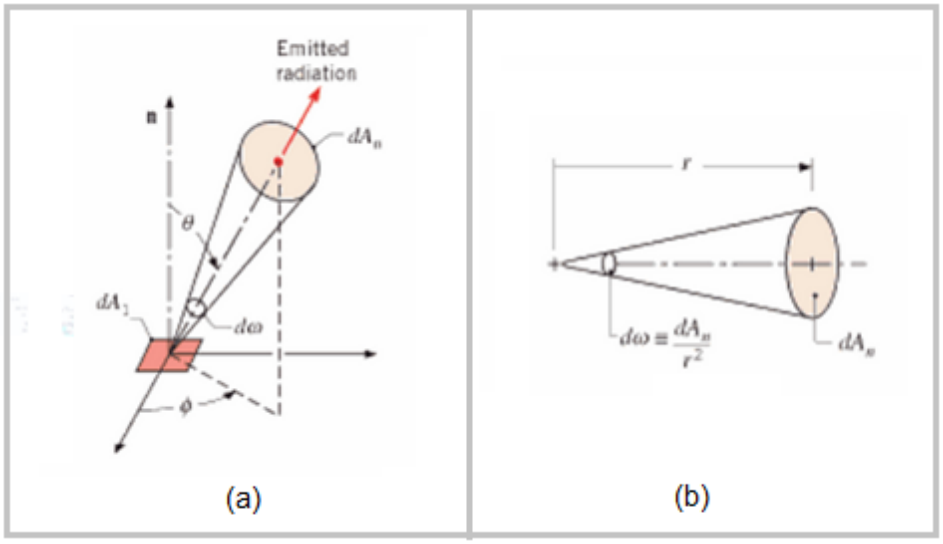

Figure 7 - Spectral intensity [1]

A blackbody is a diffuse emitter; it emits radiation independent of direction. However, a real surface may emit preferentially in certain directions. This is shown in Figure 8.

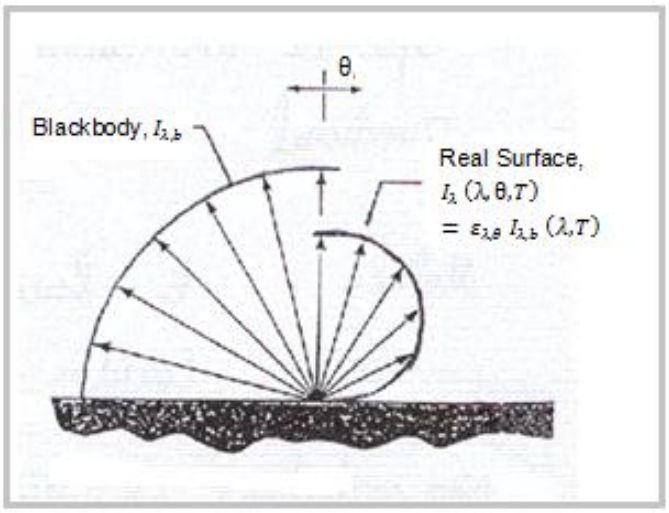

Figure 8 - Comparison of blackbody and real surface directional distribution [1]

Irradiation

The spectral irradiation, G_λ, is the rate at which radiation of wavelength λ is incident on a surface from all directions per unit surface area [4]. An irradiated surface will absorb, reflect or transmit radiation, depending on the surface. In the case of a semi-transparent medium, e.g.: glass, all three processes can occur.

The absorptivity is the fraction of radiant energy that is absorbed by the surface, the reflectivity is the fraction of the radiant energy reflected by the surface [1], and the transmissivity is the fraction of radiant energy transmitted by the surface [4]. Hence from a radiation balance, the total radiation of wavelength λ incident on a surface is given by [1];

$$G_\lambda = G_{\lambda\, absorbed} + G_{\lambda\, reflected} + G_{\lambda\, transmitted}$$

And therefore the sum of the fractions associated with absorption, reflection and transmission is equal to the total amount of energy;

$$\alpha + \rho + \tau = 1$$

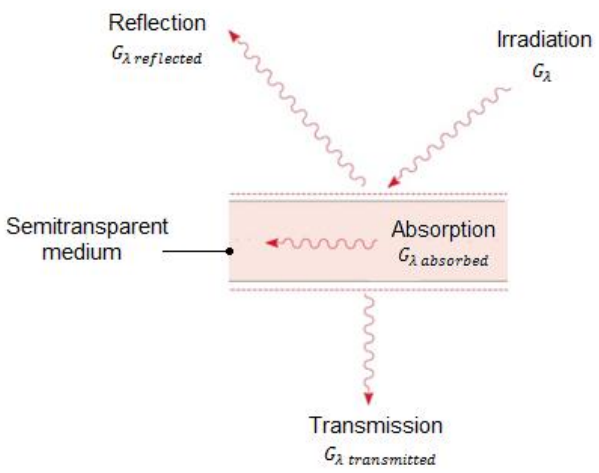

Figure 9 - Irradiation, absorption, reflection and transmission [1]

View Factor

As suggested by its directional nature, radiation is highly dependent on surface geometries and orientation. When calculating the radiation exchange between two surfaces, the amount of radiation leaving one surface that is actually intercepted by another surface must be calculated. The view factor defines the fraction of the radiation leaving surface i that is intercepted by a surface j. Figure 10 shows the elements of the view factor equation, given by [1];

$$F_{ij} = \frac{1}{A_i} \int_{A_i} \int_{A_j} \frac{\cos\theta_i \, \cos\theta_j}{\pi R^2} \, dA_i \, dA_j$$

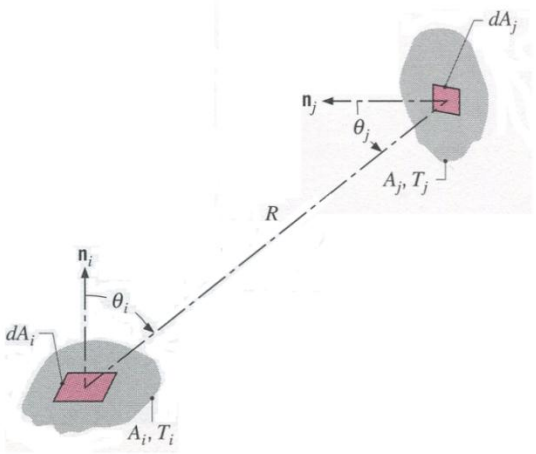

Figure 10 - Elements of the view factor equation [1]

2.2 Human Thermoregulation

2.2.1 Human Body Temperature Norms

The core body temperature should be maintained around 37°C, the normal range being between 36.2°C and 37.7°C [5]. If body temperature moves out of this range serious health issues can arise. The human thermoregulatory system must therefore be very effective in creating heat balance within wide limits of environmental variables. Figure 11 shows the health issues which would be expected over the course of extreme body temperature variations. It clearly shows the importance of effective body temperature regulation. The onset temperatures for the body's temperature regulation responses are also shown, and these will be discussed in section 2.2.2.

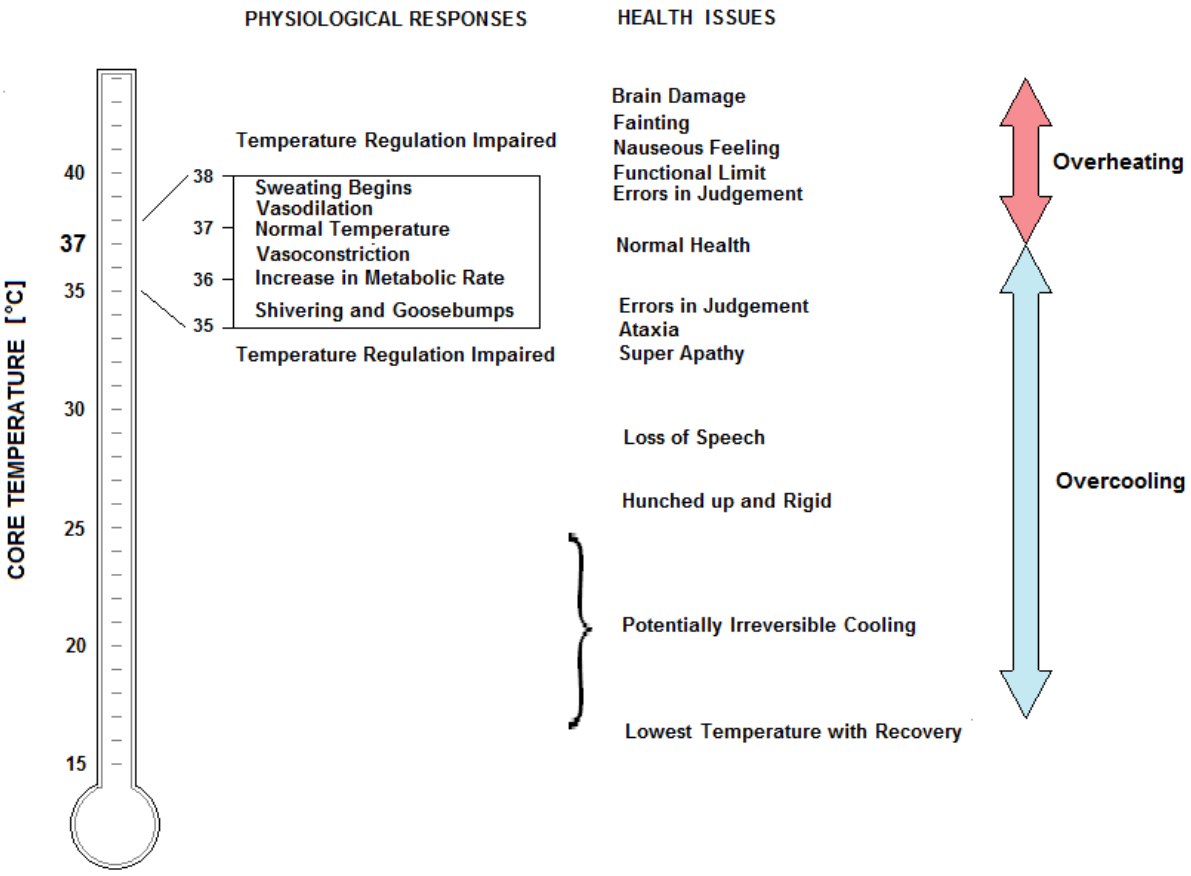

Figure 11 - Physiological reactions to body temperature [6]

Human skin is close to being a perfect blackbody, with an emissivity value of approximately 0.98 [7]. It acts as a heat sink when the body is hot, and an insulator when the body is cold. Local skin temperature generally ranges from 17- 40°C, with an average temperature of 33.2°C ± 1°C [8]. In a warm environment skin temperature tends to be more uniform, whilst in a cold environment it tends to be non-uniform, with the head and torso being warmer than the arms and legs [8]. Typical skin temperature variation for an adult human is shown in Figure 13.

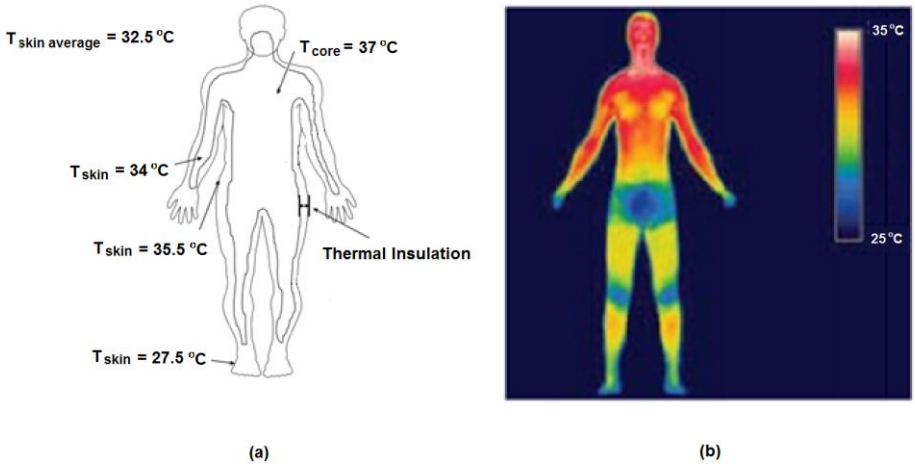

Figure 12 - Skin temperature distribution in the human body [9] [10]

2.2.2 Human Thermoregulatory System

Thermoregulation is the maintenance of a reasonably steady core body temperature under a variety of external conditions. The human thermoregulatory system conventionally comprises of three components or processes; afferent sensing, central control, and efferent response.

Afferent sensing is a process in which thermoreceptors send signals carrying body temperature information to the central control centre. Thermoreceptors are found throughout most of the body, not only on the skin surface but also within the body, in areas including the hypothalamus (central thermoregulatory control centre), deep core tissues and spinal cord [11]. Thermoreceptors within the body core are very sensitive to changes as small as 0.01°C and are critically important. For example, in the case of massive sweat evaporation skin thermoreceptors will respond to by incorrectly sending 'cold' signals to

the central control, even though the body is severely overheated [12]. However, thermoreceptors on the skin are highly useful in most circumstances as they allow individuals to consciously perceive temperature so that they might take appropriate action to warm or cool themselves, thus reducing the need for efferent response. Thermoreceptors for 'hot' and 'cold' are both anatomically and physiologically different. Hot thermoreceptors are excited by temperatures above a set threshold and generate signals that travel along unmyelinated C fibres, whilst cold thermoreceptors are excited by temperatures below a set threshold and generate signals that travel primarily along Aδ nerve fibres. Information is then integrated at several levels within the spinal cord and brain before arriving at the central control centre [13].

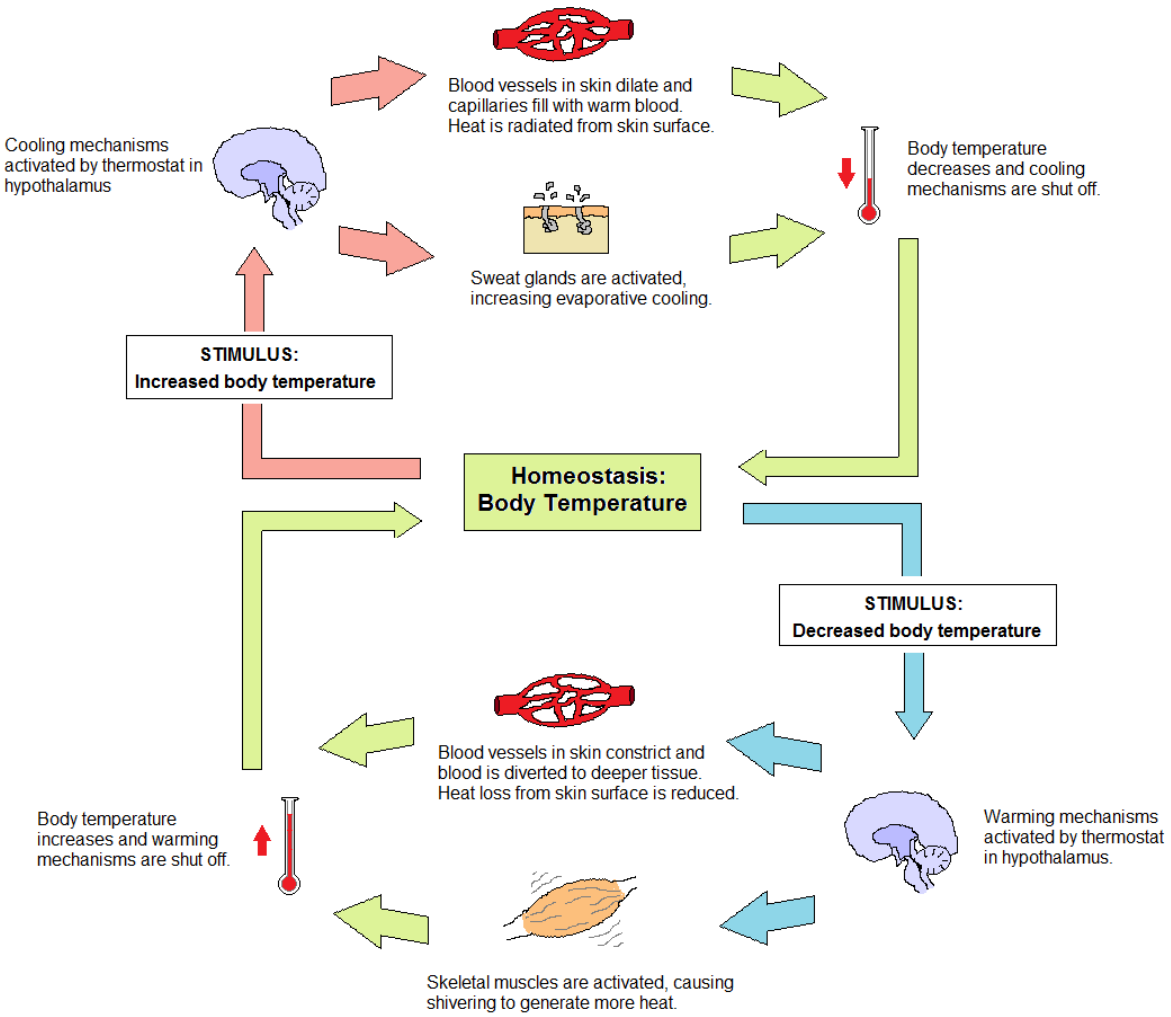

Figure 13 - Human thermoregulatory system [14]

The central control process is where the majority of efferent input is integrated and the various efferent outputs required to maintain an adequate temperature are coordinated [13]. The hypothalamus is the primary centre for thermoregulatory control. It regulates temperature by comparing the integrated thermal inputs with set 'hot' and 'cold' threshold temperatures. When these thresholds are exceeded the hypothalamus responds by initiating appropriate efferent responses that will return the body to the correct temperature [11]. The exact manner in which temperature thresholds are established is uncertain, but they are thought to depend on the interactions of several neurotransmitters, including dopamine, norepinephrine, serotonin and acetylcholine amongst others [13]. Factors which alter threshold temperatures include the circadian rhythm (daily variation of 1°C), exercise, food intake, menstrual cycle, infection and drugs such as anaesthetic, sedatives and alcohol [11] [13]. The interthreshold range encompasses the temperature range over which no thermoregulatory responses are required, generally only a few tenths of a degree Celsius, and so even a very small deviation from the ideal core temperature will cause initiation of some form of efferent response [11] [12].

The efferent response component of thermoregulatory system relates to the response mechanisms available to warm or cool the body. Each efferent response has its own threshold and gain (slope of response intensity to core temperature regression), and so responses occur in a systematic progression with intensities proportional to the heating or cooling requirement [11]. The different response mechanisms are briefly outlined as follows;

Behavioural Regulation is the most effective thermoregulatory response [11]. This can be considered as both a heating and cooling mechanism, and involves an individual taking conscious action to warm or cool themselves. Actions can include adding or removing clothing, modifying the surrounding temperature, increasing or decreasing voluntary movement, and assuming bodily positions that enhance or diminish heat loss [13].

❖ Heating Responses

The *endocrine system* is made up of glands that produce and secrete hormones which help to regulate the body's metabolism, thus affecting heat production in the body [15]. These include thyroxine from the thyroid gland, and catecholamines from the adrenal glands, which can both affect the metabolic rate throughout the body [12]. These hormones play a

greater role during cold stress when they increase the metabolic rate to increase heat production [16].

Vasoconstriction ensures that the core of the body is kept sufficiently warm (at the expense of the extremities). It operates by decreasing blood flow to the skin, thus increasing the effective insulation provided by the body shell [16]. Arteriovenous shunts are the thermoregulatory components of total digital skin blood flow (functionally distinct from the nutritional capillary component) and are atomically limited to the extremities such as the fingers, toes and nose [11]. If core temperature falls these shunts can be closed to constrict blood vessels; thus moving warm blood deeper within the body to prevent heat loss [15].

Involuntary thermogenesis (or shivering) is a heat generating mechanism of the skeletal muscle. In a cold environment, the brain centres controlling muscle tone stimulate small rapid neuromuscular reactions [12]. Since this muscle activity does not produce work it will generate heat, but will also increase blood flow to peripheral tissues which will lessen the net heating effect. Hence the activation threshold for shivering is a full degree Celsius below that for vasoconstriction, making it a last defence mechanism against hypothermia [11]. Many individual factors contribute to the onset of shivering, one of which is body fatness. A man with very little subcutaneous fat (say 2-3mm thickness) will begin to shiver after 40mins at 15°C and after 20mins at 10°C, whilst a man with more insulating fat (say 11mm) may not shiver at all at15°C and after 60mins at 10°C [16].

❖ Cooling responses

Vasodilation is a cooling mechanism which smooth's the muscle tissue of the blood vessels in the skin causing the blood vessels to vasodilate (increase in diameter). This causes increased blood flow from the body core to the skin [12]. The blood carries heat from the core, moving it to the skin where excess heat can be released to the environment [15]. The amount of heat carried from the core to the skin is a function of skin blood flow (SkBF), the temperature gradient between the core and the skin, and the specific heat of blood. SkBF at rest in a thermoneutral environment would be approximately 0.2-0.5l/min (5-10% of cardiac output). Under high heat stress however the temperature gradient between the core and skin will be lower meaning that a higher SkBF of up to 7-8l/min (~33% of cardiac output) will be required to achieve the necessary heat transfer.

Perspiration is a cooling mechanism which initiates impulses to the sweat glands causing them to secrete sweat so that the surface of the skin is moistened. This moisture then evaporates from the skin, thus cooling it [12] [13]. In humans, sweat is secreted from apocrine sweat glands (clustered glands which secrete sweat into hair follicles) and eccrine sweat glands (which are scattered non-uniformly over the surface of the body and secrete sweat directly onto the skin surface). This is a very effective cooling mechanism (for example, an individual producing a net metabolic heat of 640W would have an increase in body temperature of 1°C every 6-7mins without sweating, but with a reasonable sweat rate of 16g sweat per minute the rate of heat loss will match the rate of heat production) [16]. Perspiration is also the only mechanism by which an individual can release heat to an environment that is hotter than their core body temperature [11].

2.2.3 Conceptual heat balance equation

The conceptual heat balance equation describing the thermal exchange between the human body and the environment is shown below [17];

$$M - W = E + R + C + K + S$$

The metabolic rate of the body produces energy to enable the body to do mechanical work, releasing the remaining energy as heat. This remaining energy is the net metabolic rate, shown on the left hand side of the heat balance equation, the value of which is always positive. The right hand side of the equation shows the four heat loss mechanisms ($E, R, C\ and\ K$) along with the heat storage rate S. The heat loss mechanisms are shown here to be positive values in the conceptual heat balance equation, indicating heat loss; however heat can also be gained from the environment in which case these components would have negative values. When combined, the heat production rates and heat loss rates give the heat storage rate, which is zero for a body in heat balance [17].

Metabolic heat production is the rate of energy produced by the body. The basal metabolism is the minimum amount of energy the body uses to maintain vital processes; however there are many factors which effect metabolic rate, increasing it and thus increasing heat production within the body [15]. These include exercise (which raises the metabolic rate as much as 15 times above the resting level), hormones, body temperature (each 1°C increase further increases biochemical reactions by 10%), food ingestion (10-

20% increase depending on the food type). Other influencing factors are age (metabolic rate of a child is twice that of an elderly person with respect to size), gender (females generally have a lower metabolic rate than men), and other elements such as tropical climate, sleep and malnutrition, which can all lower metabolic rate [15].

The unit of metabolic heat production is the 'Met'. The metabolic rate for a standing person is $1.2\ Met$, or $70\ W/m^2$ [18], which assuming a DuBois surface area of $1.8m^2$ gives an energy production of $126\ W$. Even at mild to moderate work intensity, body core temperature would rise approximately one degree centigrade every 15 min were it not for an efficient means of heat dissipation [16]. The four aforementioned basic heat loss mechanisms employed by the human body are outlined below along with their proportional contribution to overall body heat loss at rest conditions and 21°C [15];

- Radiation heat loss through the emission of infrared rays (~60%)
- Evaporation heat loss through water removed from the surface of the skin (~22%)
- Convection heat loss to the surrounding medium (~15% through convection and conduction to the air)
- Conduction heat loss through physical contact (~3%)

This report is concerned with the radiant heat transfer between the human body and its surroundings. This part of the heat balance equation is given by [8];

$$R = h_r(\overline{t_{sk}} - \overline{t_r})$$

where $$h_r = 4\varepsilon\sigma\left(\frac{A_r}{A_D}\right)\left[273.2 + \frac{(\overline{t_{cl}} + \overline{t_r})}{2}\right]^3$$

$$A_D = 0.202\ m^{0.425}\ l^{0.725}$$

and where ε is the average emissivity of the clothing or body surface.

This equation shows that radiant heat transfer between the human body and its surroundings is given by the product of the radiation heat transfer coefficient and the difference between the average skin temperature and mean radiant temperatures. Further, the radiant heat transfer coefficient can be seen to be directly proportional to the effective radiation area of the body, the average emissivity of the clothing or body surface, and the

cubed average of the mean clothing and mean radiant temperatures. It can also be seen to be inversely proportional to the DuBois surface area (dependant on an individual's mass and height).

The ratio A_r/A_D is typically 0.70 for a sitting body, or 0.73 for a standing body, and for typical indoor temperatures and emissivity close to unity, the radiation heat transfer coefficient can be taken as $h_r = 4.7\ W/m^2 \cdot K$ [8].

2.3 Human Thermal Comfort Theory

From a physical point of view, thermal comfort relates to the body's balance between heat generated by the metabolism and heat dissipated from the body to the environment [19]. The definition of human thermal comfort is defined by ASHRAE [20] as:

> *'that condition of mind which expresses satisfaction with the thermal environment'*

This definition describes thermal comfort not as a state condition, but as a state of mind which can be influenced by many factors. It highlights the fact that an individual's judgement of comfort is a cognitive process involving multiple inputs which are influenced by physical, physiological and psychological factors amongst others [21]. In general, thermal comfort will occur when body temperatures are held within very narrow ranges, skin moisture is low, and the physiological effort required for regulation is minimal, i.e. if the heat generated by the metabolism is in balance with the heat dissipated to the surrounding environment [22].

Thermal comfort research falls into two categories; the rational heat balance approach and the adaptive approach. The heat balance approach is the conventional approach developed by Fanger [21] which emphasises the environmental conditions, whilst the more recent adaptive approach also takes into consideration the ability of people to adapt and change their environments to make themselves comfortable [19].

It must be noted that it is not considered possible to thermally satisfy an entire group of people at the same time, as individuals will respond differently to the same thermal state. The idea therefore is to attempt to create the thermal comfort situation in which the highest possible percentage of the group will feel comfortable [23]. In this report, a 90% thermal satisfaction rate will be considered sufficient, based on the Category B level of acceptability outlined in ISO 7730 [24].

2.3.1 The Heat Balance Approach to Thermal Comfort

Fanger's heat balance approach treats people as passive recipients to thermal stimuli, taking into account six factors which affect thermal sensation. The first four of these are physical environmental parameters and the final two are personal variables [23];

- Air temperature
- Mean radiant temperature
- Relative air velocity
- Vapour pressure in ambient air
- Activity level (metabolic rate)
- Thermal resistance of clothing

The method uses the Predicted Mean Vote (PMV) and Predicted Percentage of Dissatisfied (PPD) indices to predict information about the thermal comfort of a group under set conditions. The PMV index predicts the mean response to thermal comfort of a large group of people according to the ASHRAE thermal sensation scale [21]. The scale ranges from cold (-3) to hot (+3) with neutral (0) as shown in Figure 14. Experiments performed in climate chambers asked test subjects to rate their level of comfort according to this scale. The method allows a prediction to be made on what comfort vote would arise from a large group of individuals in a given set of environmental conditions for a given clothing insulation and metabolic rate [25]. A group would be considered sufficiently comfortable when the PMV lies within the range of $-0.5 < \text{PMV} < +0.5$ [20]. The PMV equation is given by [24];

$$PMV = [0.303\, exp(-0.036M) + 0.028]L$$

where L is the thermal load on the body, defined by the following equation;

$$\begin{aligned} L = {} & (M - W) - 3.05 \times 10^{-3} [5.733 - 6.99(M - W) - P_a] \\ & -0.42[(M - W) - 58.15] - 1.7 \times 10^{-5} M\,(5867 - P_a) - 0.0014\, M(34 - t_a) \\ & -3.96 \times 10^{-8}\, f_{cl}\, [(t_{cl} + 273)^4 - (\overline{t_r} + 273)^4] - f_{cl}\, h_c\, (t_{cl} - t_a) \end{aligned}$$

In which

$$\begin{aligned} t_{cl} = {} & 35..7 - 0.028\,(M - W) \\ & -I_{cl}\,\{3.96 \times 10^{-8}\, f_{cl}\, [(t_{cl} + 273)^4 - (\overline{t_r} + 273)^4] + f_{cl}\, h_c\, (t_{cl} - t_a)\} \end{aligned}$$

$$h_c = \begin{cases} 2.38\,|t_{cl} - t_a|^{0.25} & for \quad 2.38\,|t_{cl} - t_a|^{0.25} > 12.1\sqrt{v_{ar}} \\ 12.1\sqrt{v_{ar}} & for \quad 2.38\,|t_{cl} - t_a|^{0.25} < 12.1\sqrt{v_{ar}} \end{cases}$$

$$f_{cl} = \begin{cases} 1.00 + 1.290\,l_{cl} & for \quad l_{cl} \leq 0.078\,m^2 \cdot K/W \\ 1.05 + 0.645\,l_{cl} & for \quad l_{cl} > 0.078\,m^2 \cdot K/W \end{cases}$$

M Metabolic rate $[W/m^2]$

W Mechanical power $[W/m^2]$

These equations require several input values, such as metabolic rate and clothing insulation, which can be found in tables such as those provided in the appendices of the ISO 7730 [24]. As can be seen, this is quite a complicated equation and would be best solved by a computer program. It can also be used in a more simple way, in equations to find thermally neutral conditions, by setting $PMV = 0$ [24].

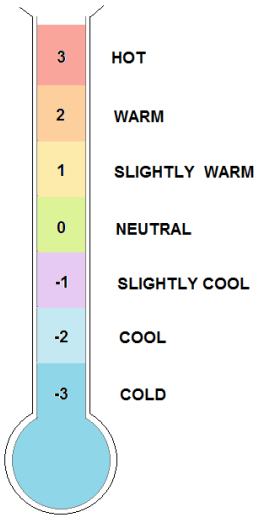

Figure 14 - ASHRAE thermal sensation scale [20]

The PPD index is used in conjunction with the PMV index to predict the percentage of people who would be dissatisfied with the thermal state i.e.: those who respond outside the range of ±1 [21]. It is related to the PMV by the following equation [24];

$$PPD = 100 - 95exp(0.03353\,PMV^4 + 0.2179\,PMV^2)$$

The relationship between PMV and PPD is shown in Figure 15. From this relationship it can be seen that even when the PMV index is zero there will still be some cases of dissatisfaction. This is due to the many cognitive processes involved in judgement of comfort. The PPD should be <10% for a group of people to be considered sufficiently comfortable [20].

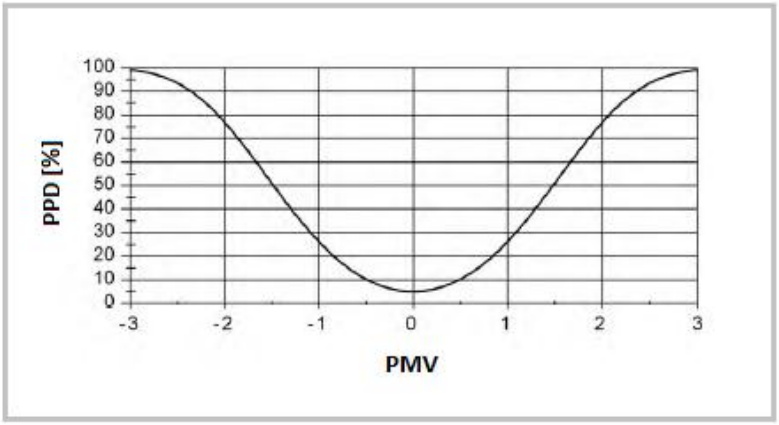

Figure 15 - Relationship between PMV and PPD [21]

Local Thermal Discomfort

Local thermal discomfort methods can be used in conjunction with the heat balance approach in order to get a more accurate assessment of thermal comfort. This section specifies the requirements for group thermal satisfaction of 90% in relation to the local thermal discomfort factors of draft, vertical air temperature difference, asymmetric thermal radiation and warm or cool floors.

❖ Draft

Draft is the undesired local cooling of the body caused by air movement, and is dependent on air speed, air temperature, turbulence intensity, airflow direction, frequency of velocity fluctuation, activity level and clothing [20], [26]. Sensitivity to draft is greatest on unclothed areas of the body, particularly the head, neck and shoulder region, but also on the leg region [20]. The predicted percentage of people dissatisfied with comfort due to the presence of a draft is given by the draft model [27];

$$DR = [(34 - t_a) \times (u - 0.05)^{0.62}] \times (0.37 \times v \times Tu + 3.14)$$

The maximum allowable air speed for a draft can be found either from the draft model or from the graphical method shown in Figure 16 where it is displayed as a function of air temperature and turbulence intensity. The percentage of people dissatisfied due to draft should be <20% [20].

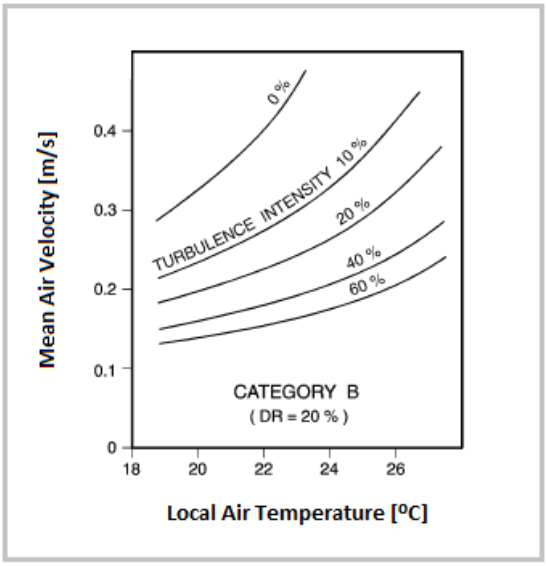

Figure 16 - Maximum allowable airspeed [27]

❖ Vertical Air Temperature Difference

A high vertical air temperature difference between head level and ankle level may cause thermal discomfort [27]. Thermal stratification generally occurs from heat rising in a room so as to cause warm discomfort at head level and cold discomfort at ankle level. Thermal stratification in the other direction rarely occurs, and if it does it is not usually perceived as a cause of discomfort [20].

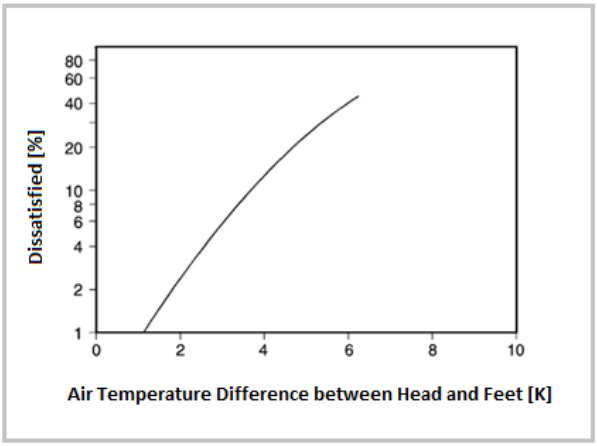

Figure 17 - Local discomfort caused by vertical air temperature difference [27]

The percentage of people dissatisfied due to vertical air temperature difference between head and feet should be <5% [20]. It can be seen from Figure 17 that the allowable vertical air temperature difference must therefore be <3°C.

❖ Asymmetric Thermal Radiation

Asymmetric thermal radiation involves a non-uniform radiation field around the body which can cause discomfort [20]. Its main causes are direct solar radiation through windows, hot roofs and overhead radiant heaters [27]. People tend to be the most sensitive to warm ceilings, but discomfort can also be caused by cool walls, cool ceilings and warm walls, as shown in Figure 18.

The percentage of people dissatisfied due to asymmetric thermal radiation should be < 5% [20]. The allowable radiant temperature asymmetry should therefore be < 5°C for a warm ceiling, < 10°C for a cool wall, < 14°C for a cool ceiling and <23°C for a warm wall, as shown in Figure 18.

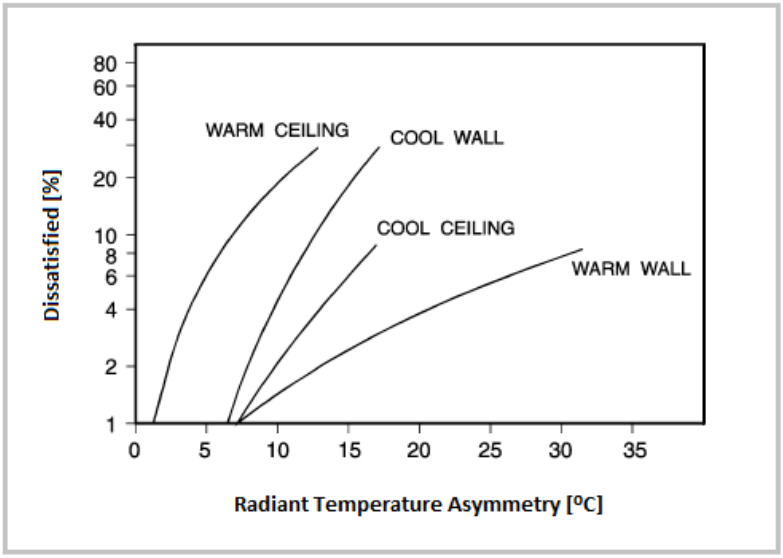

Figure 18 - Local discomfort caused by asymmetric thermal radiation [27]

Previous studies have investigated the acceptable asymmetric thermal radiation caused by overhead infrared heaters. It has been shown that the distance between ceiling level and head level has a significant impact on the acceptable level of asymmetry in these cases [27], [28].

❖ Warm or Cool Floors

Discomfort can be caused by floor temperatures that are either too warm or too cool. For people wearing shoes, it is the temperature of the floor rather than the material of the floor covering which is important for comfort [20].

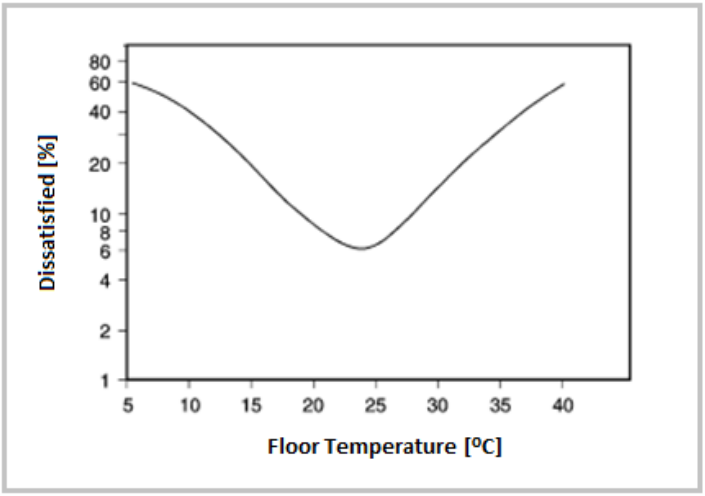

Figure 19 - Local discomfort caused by warm and cool floors [27]

The percentage of people dissatisfied due to warm or cool floors should be < 10%. It can be seen from Figure 19 that the allowable floor temperature range lies between 19°C and 29°C [20]. People with bare feet or people who may sit or lie on the floor will of course have different, and likely more specific, preferences for floor temperature e.g.: in Japan [27].

2.3.2 The Adaptive Approach to Thermal Comfort

The adaptive approach to thermal comfort is derived from field studies, which concentrate on gathering data about thermal environments and the responses of subjects in real life situations [29]. It recognises that people do not react passively to environmental conditions but will take action to make themselves comfortable by such actions as changing clothes, opening a window, changing position or drinking a hot/cold drink, amongst many others [21], [19]. It also recognises that in a real life situation activity levels and environmental conditions can vary within small timescales [25], and that expectations (e.g.: summer, winter) can also play a significant role in the perception of comfort [21].

The real life approach certainly provides more accurate results for a given situation. Subjects provide responses without the restrictions imposed by Fanger's model, in their normal environments and clothes and at a normal activity level. However, problems with this approach include the difficulty in accurately measuring the environmental conditions (which will vary with time) and the difficulty in applying the results from one survey to another [29]. In this respect, Fanger's approach could be considered to be a more useful model, as it deals with a steady state environment and set conditions. It would appear that the successful prediction of thermal comfort would use a combination of both models, as each have their own benefits and drawbacks.

2.4 Electric Infrared Radiant Heating

2.4.1 Convective Heating -v- Radiant Heating

Conventional space heating systems work by heating the air in a space by convection, which in turn warms our bodies. This process can take quite a long time, and systems can take up to an hour to reach 100% output. Heated air rises, thus creating vertical air temperature difference and wasting energy in heating the ceiling where there are no bodies to warm. Heating the air also means that heat escapes wherever air escapes causing further energy loss [30].

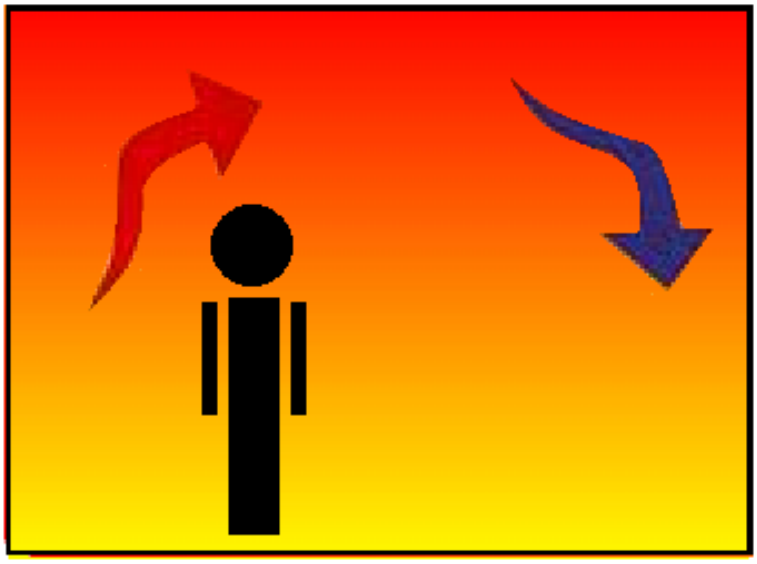

Figure 20 - Conventional convective heating [31]

Electric infrared radiant heating has many benefits over conventional systems. Infrared rays penetrate and warm the body directly, meaning energy is not wasted in heating the air. It works in the same manner as when you step out of the shade on a sunny day and are instantly warmed by the sun's rays [32]. It is an effective spot heating technique as the directional output of radiant heat allows for the heating of a small area within a space without the need to heat all of the air within the space. Electric energy is converted rapidly into infrared heat allowing radiant heaters to reach 100% output in a matter of minutes [30]. Spaces that are used only intermittently can therefore be heated very quickly when required, eliminating the need for preheating [33].

The most appropriate use of radiant heating for indoor comfort applications would likely see it used in conjunction with conventional heating systems. This would mean that the benefits of efficient directional heating could be used in intermittently required areas, for example in bathrooms, with conventional methods heating more frequently used areas. It should be noted that the placement of radiant heaters within a space is very important for comfort applications; heaters mounted on walls and ceilings must be positioned at an appropriate height and angle to radiate heat as uniformly as possible within the space to be heated and to avoid the object of the heating from becoming too warm.

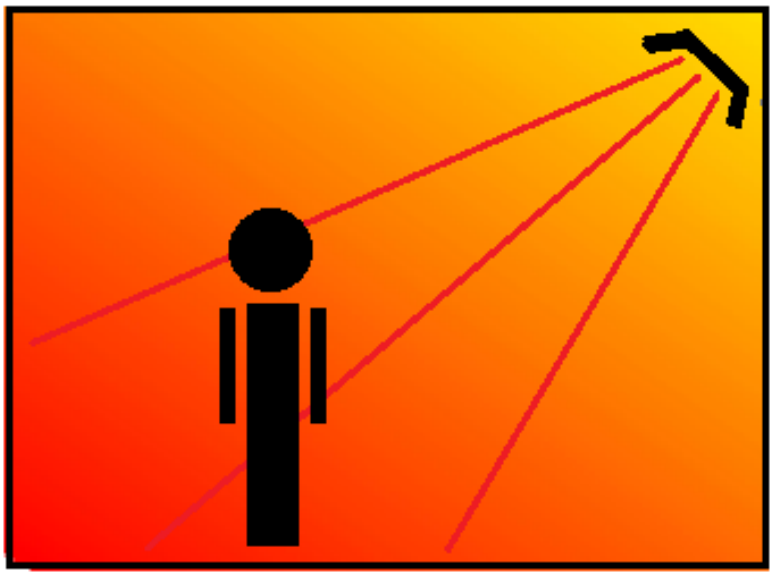

Figure 21 - Radiant heating system [31]

Aside from the basic working principals, it is also often easier and quicker to install electric heating than conventional systems as it requires connection to the electric circuitry

rather than extensive pipe work. This means fewer restrictions and more flexibility to a buildings layout and design [33]. The incorporation of radiant heaters into heating systems is also worth consideration when choosing heating technology for sustainable housing as it allows the use of electricity to supply power to the electric parts of heating systems rather than the entire system using combustible fuels or solar power.

2.4.2 Applications

Electric infrared radiant heating is currently used in a variety of industrial process and comfort heating applications amongst others. Table 1 shows some of the characteristics of four of the most popular types of radiant heaters. The near, medium and far parts of the infrared spectrum can all be used by choosing the appropriate type of heater, the appropriate waveband being chosen based on the given application.

Heater Type	Radiant Efficiency [%]	Physical strength	Response	Temperature [°C]
Metal sheath	56	High	Slow	760
Ceramic	96	Medium	Slow	871
Quartz tube	61	Low	Fast	2204
Quartz lamp	86	Very Low	Very Fast	704

Table 1 - Comparison of different infrared heaters [34]

Industrial processes will use near, medium and far infrared. Some heat processing applications will work within all of these ranges, whilst for others it is important to choose the correct waveband [35]. In the health sector the use of far infrared heating is growing and it is currently used in applications such as pain treatment, saunas and infant incubation [3], [36]. The most commonly used part of the infrared spectrum for such applications is the far region, generally in the 7 to 14 micron range [3]. Comfort applications use ceramic heaters to obtain high efficient gentle heating at relatively low source temperatures. The heaters used in this project were supplied by Ceramicx Ireland, whose ceramic elements operate within a temperature range of 300-700°C, producing wavelengths in the range of 2-10 microns [37].

Table 2 shows examples of temperatures associated with parts of the near, medium and far infrared regions, calculated using Wien's Displacement law (Section 2.1.2). These results confirm that the part of the infrared spectrum most suited to human comfort heating would be the medium range and the early part of the far range.

Infrared Region	Wavelength $[\mu m]$	Temperature $[K]$	Temperature $[°C]$
Near	1	2897.8	2624.7
Medium	3	965.9	692.8
Far	7	414.0	140.82

Table 2 - Relationship between wavelength and temperature within the infrared region

Infrared heating in Irelands outdoor comfort sector has become very popular in recent years, particularly in bars and hotels since the introduction of the smoking ban. Companies such as Glen Dimplex [38] and SSTS Infrared Ireland [39] offer a range of radiant heaters for this application. Attention is now being paid to similar solutions for indoor heating, with ceramic heaters such as the CXD from Glen Dimplex being suggested for use in garages, sunrooms and workshops as well as patios and balconies [40]. This trend suggests the move toward the use of electric infrared radiant heating in the domestic setting.

Figure 22 - (a) Pubsun 3 by SSTS IR Ireland [39] &(b) CXD by Glen Dimplex [38]

3 Experimental Apparatus

3.1 Temperature Distribution Testing

This test is carried out to analyse the three dimensional temperature distributions of two radiant infrared heaters supplied by Ceramicx Ireland. The heating elements tested are as follows;

- Ceramic 250W Edison Screw Bulb (ESER)
- 2 x horizontally aligned Ceramic 300W Full Trough Element (Double FTE)

The full technical details, schematics, and heat-up/cool-down curves can be found in Appendix A. The elements are mounted in reflectors similar to those shown in Figure 24. The heaters are mounted on a stand which can be moved over five axes. This allows the heater to be positioned exactly as required, but also means that the placement of the heater is subject to human error as it is positioned at various distances from the screen.

Figure 23 - Ceramic Heating elements (a) FTE & (b) ESER [37]

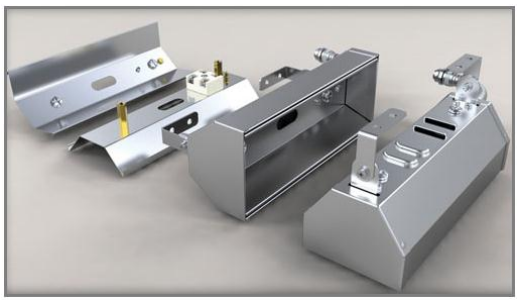

Figure 24 - Ceramic heater reflector mounts [37]

3.1.1 Test Rig

The experiment is set up as shown in Figure 25. An aluminium sheet with dimensions $2000 \times 1000 \times 2mm$ is used as a screen to capture the temperature distributions of the heaters in a 2D plane. The sheet is spray painted black to afford it a high and known emissivity (0.95 for matt black aluminium [41]). It is attached to wooden supports to prevent creasing of the sheet and to enable it to be freestanding within a space.

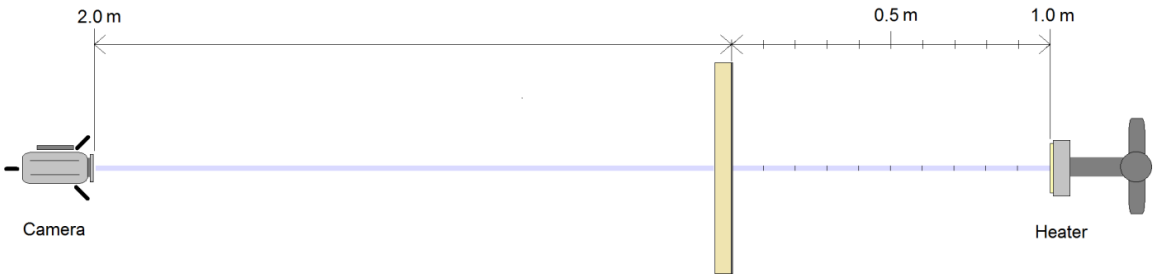

Figure 25 - Set up for temperature distribution testing

The heater is placed on one side of the screen. A thermal imaging camera is placed on the other side of the screen and used to capture the images of the temperature distribution that are displayed on the screen. The camera is a FLIR systems ThermaCAM P25, and is mounted on a fixed stand which is aligned with the heater and placed at a distance of $2m$ from the opposite side screen. This gives it a view area of just over $600 \times 800mm$.

3.1.2 Procedure

The procedure for the temperature distribution testing of both of the heaters is outlined as follows;

1) The heater left to heat up for 15 minutes away from the testing area. This allows it to reach full output as shown in the heating up curves included in Appendix A.
2) The heater is focused on the screen at an initial distance of $1m$ (early testing found that at distances greater than this the output for the tested heaters is negligible).
3) After 20 minutes a thermal image is captured. This timescale allows the screen to adjust to its new temperature.
4) The heater is moved closer to the screen by $0.1m$.
5) Steps 2 and 3 are repeated up to a final distance of $0.1m$ from the screen.

3.1.3 Data Reduction

The thermal images are processed in ThermaCAM Researcher Pro, MATLAB and Microsoft Excel. The basic MATLAB function 'contourf' is used to create filled contour plots of the temperature distribution over the entire test area (at each heater distance from the screen and for each heater) directly using the thermal images. This code is included in Appendix B.

ThermaCAM Researcher Pro allows the thermal images to be viewed and manipulated. Maximum and minimum temperature points and strings of single column data (taken horizontally across the point of the highest temperature in the distribution) are exported from ThermaCAM Researcher Pro to Microsoft Excel and plotted to show further information relating to temperature distribution across the centre of the heaters and also maximum and minimum temperature distribution across each image.

3.2 Heat Flux Distribution Testing

This test was carried out to analyse the three dimensional heat flux distributions of the same Ceramicx heaters described in Section 3.1.

3.2.1 Test Rig

Overview

The test rig is set up as shown in Figure 26 and Figure 27. It consists of two Rexroth linear ball screw drive units which are assembled to allow movement over a 2D plane; the horizontal (X-axis) is attached to the frame, and the vertical (Y-axis) axis is attached to the horizontal axis. These units are individually connected to a PC via a RS485 USB connector thus allowing their movements to be individually controlled by AcIA Easy software. A radiant heat flux sensor (details to follow) is fitted into an aluminium plate and mounted on the vertical unit, thus allowing it to move to any X-Y position over an area of approximately $1m^2$. Measurements from the heat flux sensor are amplified and sent to LabVIEW software on the PC via a Ni 6008 data acquisition device, where they can then be monitored.

A control box was designed to house the circuitry of the rig. Details of the design and the bill of materials for its manufacture are included in Appendix C. This addition to the rig allowed for the circuitry to be better organised and therefore more easily understood.

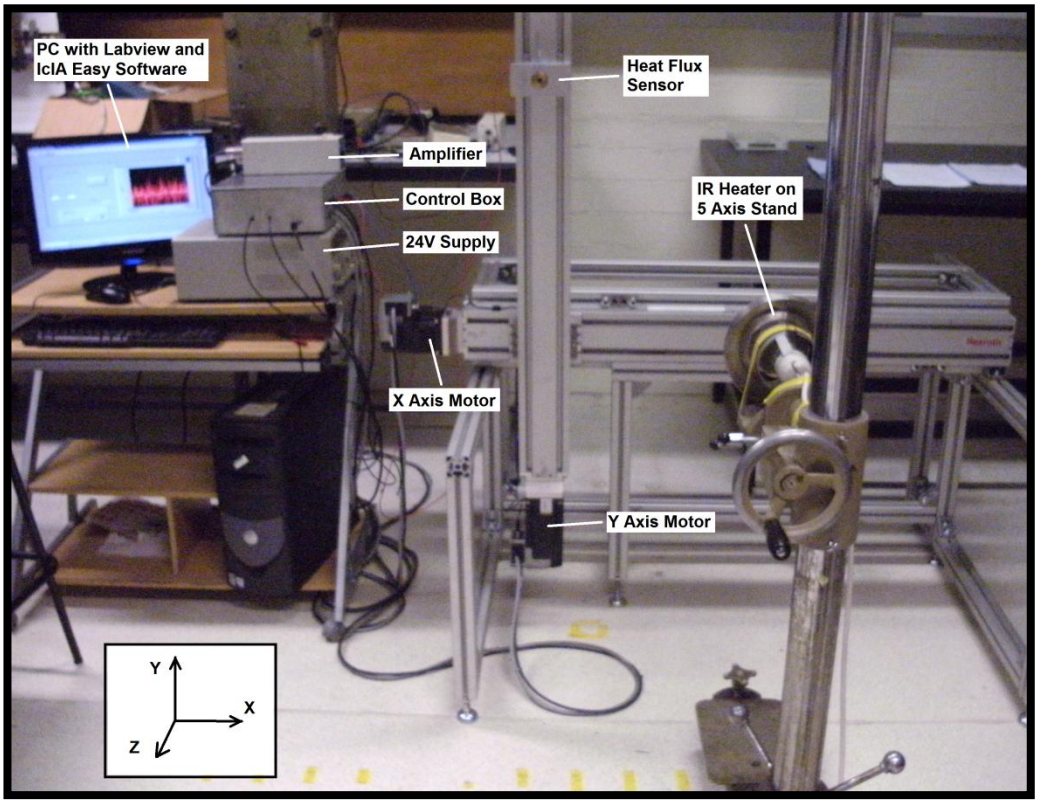

Figure 26 - Experimental set up for heat flux distribution testing

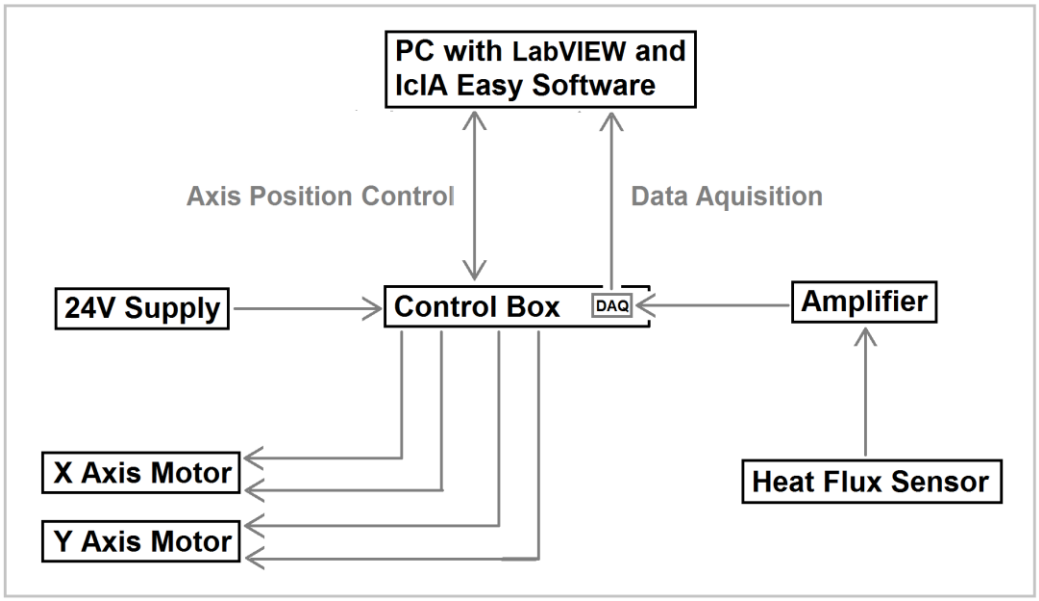

Figure 27 - Block Diagram of experimental rig set up for heat flux distribution testing

Radiant Heat Flux Sensing

A Series 9000 Thermogage (TG9000) by Vatell Corporation is used to measure incident heat flux. This circular foil heat flux gage measures only radiation heat transfer (although high convective heat transfers may skew measurements).

Figure 28 - TG9000 Radiant Heat Flux Sensor [42]

It uses a differential thermocouple as a transducer to measure the temperature difference between the centre and the circumference of a thin circular foil disc, which is bonded to a circular opening in a cylindrical heat sink. The constantan foil and copper heat sink produce a voltage output which is directly proportional to the heat flux [43]. The voltage output can then be converted to a heat flux measurement using the calibration sheet provided with the unit, which is shown in Appendix D. The transducer is designed for a maximum output of 10mV [43]. Although it is possible to water cool the unit, this is only required for temperatures exceeding 200°C which are not reached within the scope of this test.

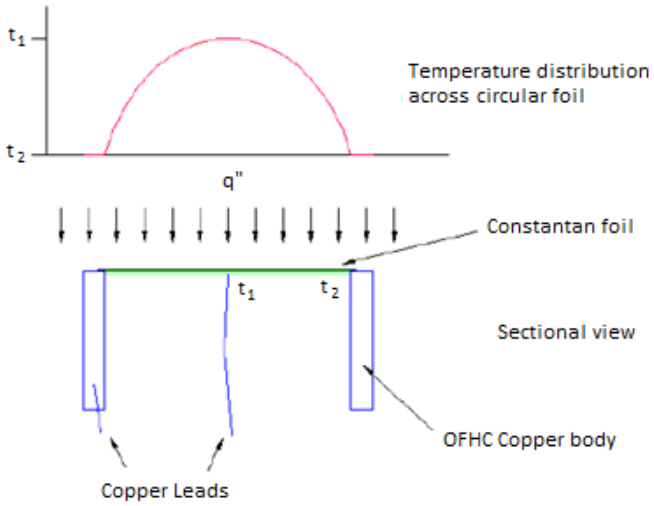

Figure 29 - Operating Principals of the TG9000 [44]

3.2.2 Procedure

The procedure for the heat flux distribution testing comprised of two main parts; drive unit positioning and the recording of heat flux data. As mentioned previously the drive unit positioning is controlled using AcIA Easy program and the heat flux data is recorded using a LabVIEW program. The procedures for the use of these programs are outlined further in Appendix E. Heat flux information is recorded over a test area of $0.8 \times 0.8m$ with $100mm$ increments between data set positions (giving a total of eighty-one data sets), with a data set numbering system as shown in Figure 30.

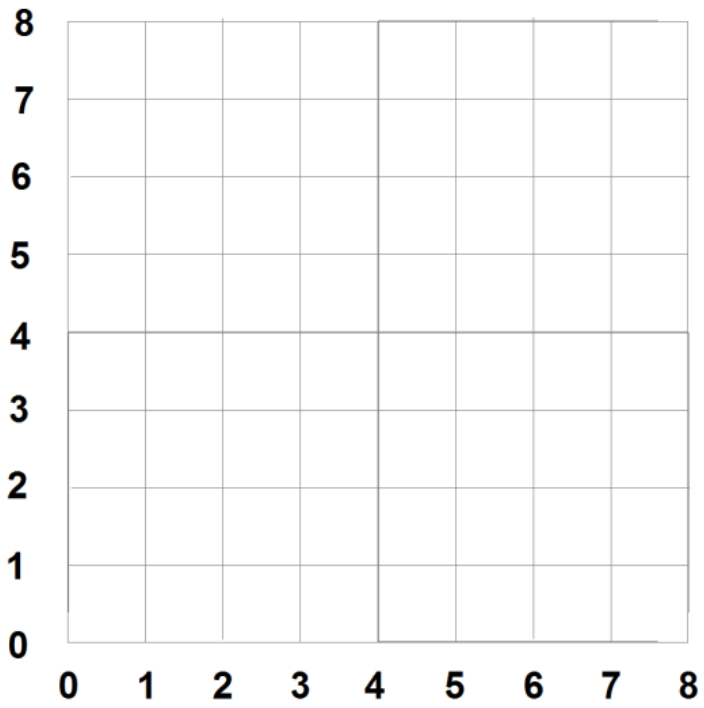

Figure 30 - Data set numbering system for heat flux distribution testing

The control flow diagram shown in Figure 31 outlines the procedure required to attain heat flux data for a heater at a single Z position from the sensor (i.e. the procedure is followed four times at different Z distances for each heater, with the sensor at positions 0.2m, 0.4m, 0.6m, and 0.8m from the heater). Together these tests give an idea of the three dimensional heat flux distribution for each heater.

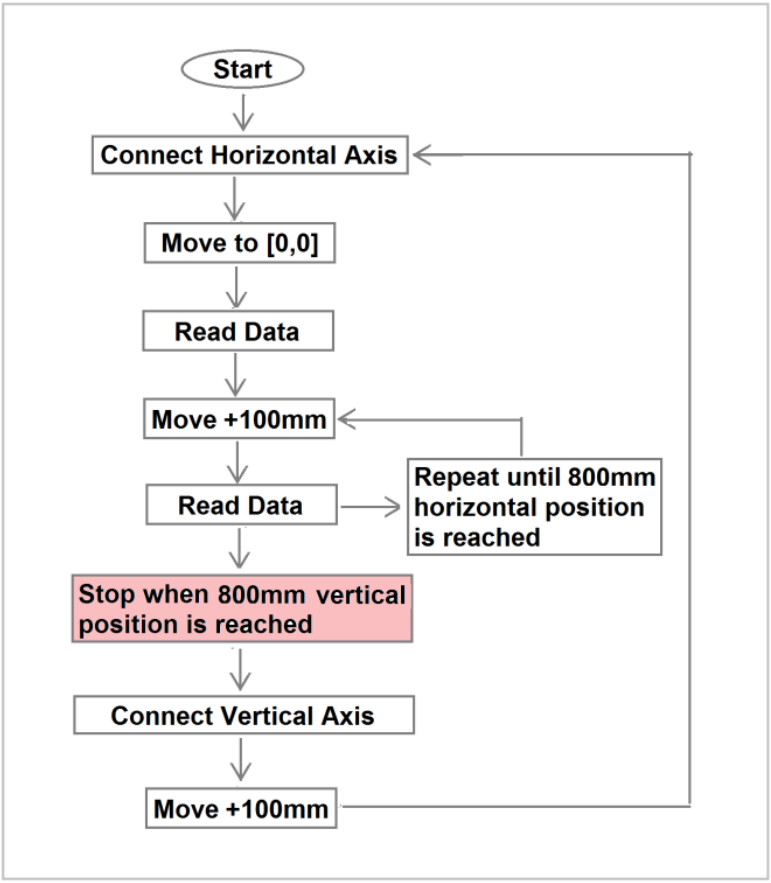

Figure 31 - Control Flow Diagram for heat flux distribution procedure

3.2.3 Data Reduction

The heat flux data in each .lvm file consists of five seconds of raw data for each data set position. There are eighty one data sets recorded in each file (along with a 'zero' data set) and there are four of these files for each heater, each containing the information over an area a set Z distance from the heater.

Each data set is averaged in Microsoft Office Excel, and Excel files are compiled containing the averaged heat flux data for each data set position during each test. The averaged data for each test area is then plotted in MATLAB using the basic 'contourf' function, the code for which is included in Appendix B.

Maximum and minimum temperature points and strings of single column data (taken horizontally across the point of the highest temperature in the distribution) are also plotted in Excel to show further information relating to heat flux distribution across the centre of the heaters and also maximum and minimum temperature distribution across each test area.

3.3 Human Thermoregulatory System Testing

3.3.1 Test Rig

The data acquisition apparatus is set up as shown in Figure 32 for both warm room (WR) and IR testing. This test is concerned with the distribution of heat within the body, and so there are three key factors to be monitored during this experiment; skin temperature, core temperature and heat flux, and the methods used to measure each of these will be discussed in more detail to follow.

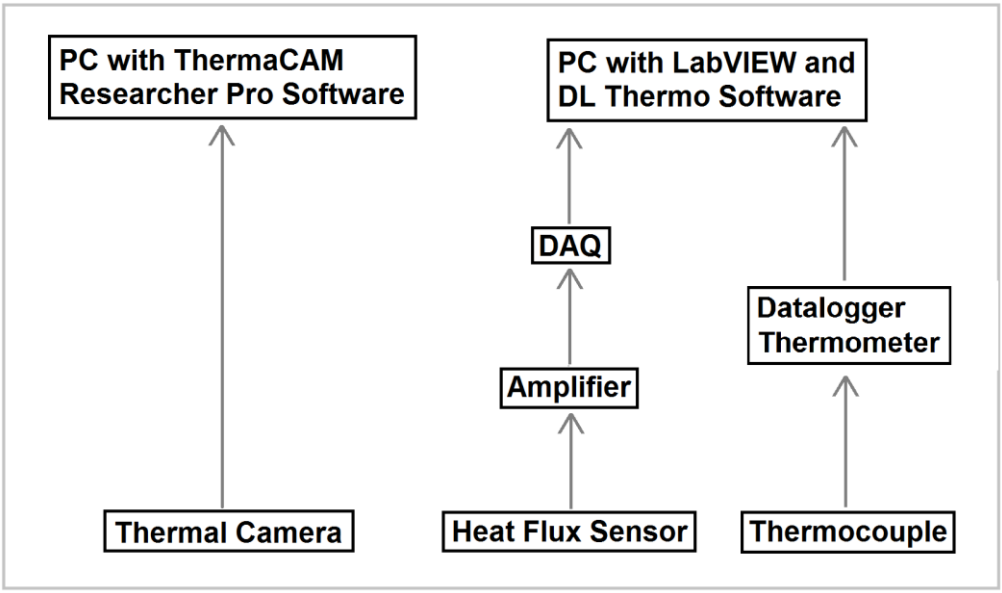

Figure 32 - Data acquisition set up for human thermoregulatory system testing

Skin Temperature Measurement

The FLIR systems ThermaCAM P25 is used to record images of the temperature distribution over the skin of the test subject. It is connected to a PC with ThermaCAM Researcher Pro software which allows video footage to be recorded and stored.

Core Temperature Measurement

A simple thermocouple is used to estimate core temperature. A sublingual (under the tongue) temperature measurement is taken that will underestimate the actual core temperature (36.2 -37.7°C) by approximately 0.3-0.8°C, making it a useful measurement

in approximating core temperature. The thermocouple is connected to a datalogger thermometer and hence to a PC where information is recorded and stored using DL Thermo Software.

Radiant Heat Flux Sensing

A thin foil radiant heat flux sensor is used to record the heat flux being transferred between the test subject and the surroundings. The calibration sheet for this sensor is included in Appendix D. It measures $25 \times 25mm$ and is attached using double sided tape to the flattest area on the back of the test subject's hand in the position shown in Figure 33. The effect of the tape on the heat transfer rate is assumed to be minimal and is ignored, but to ensure consistency the same type of tape is used for each test.

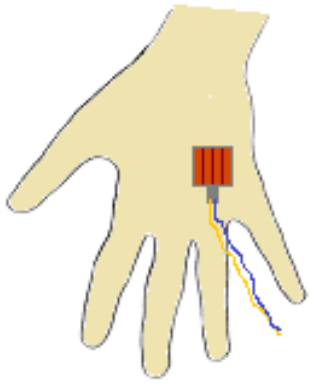

Figure 33 - Position of heat flux sensor on test subject's hand [45]

The IR testing is completed in a cold room using the ESER heater mentioned previously, and the test setup is shown in Figure 34. The ESER heater is placed at a distance of $0.4m$ from the area upon which heat is to be applied for each IR test. At this distance, the temperature and heat flux distributions of the ESER heater are as shown in Figure 53. This heater at a distance of $0.4m$ was chosen as being suitable for localised heating of areas of the body such as the face or hand for the following reasons;

- This heater is symmetrical and so the distributions across the centre of the heater are very similar in all directions.

- This selection gives a maximum temperature at the centre position of 26.5°C and maximum heat flux at the centre position of $30.8 \times 10^3 W/cm^2$ which is found from test subject feedback during early testing to be a comfortable amount of heat to apply.
- The distribution in temperature at this distance is fairly uniform at close to the maximum centre position temperature over a radius from the heater centre of 150mm, and the heat flux distribution over this same radius is at all points at least 65% of the maximum heat flux value. Outside of this radius both the temperature and heat flux magnitudes drop in value.

The set up for the WR testing is the same except for the heat source; these tests are completed in a preheated room which the subject enters at the beginning of the test having previously spent 10mins in the cold room. The warm room is heated by a basic electric convective space heater prior to testing.

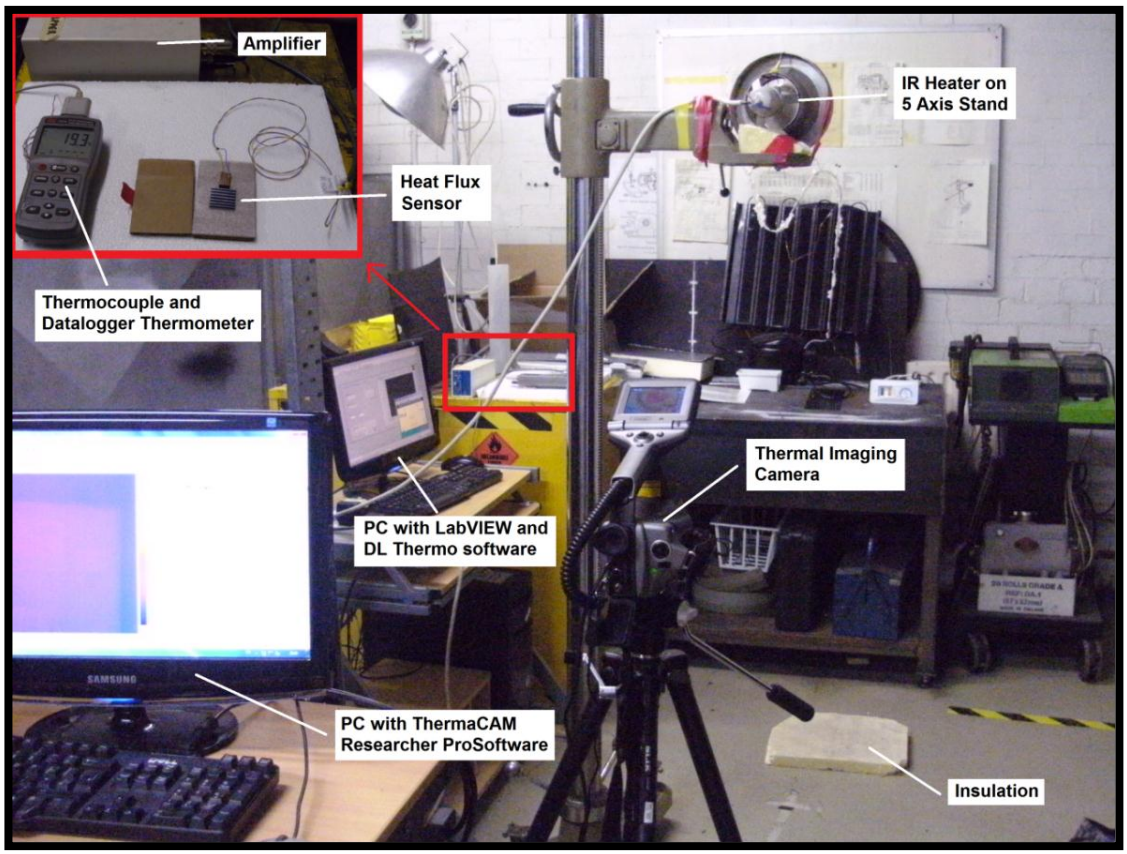

Figure 34 - Experimental set up for human thermoregulatory system testing

3.3.2 Procedure

This experiment consists of a set of seven tests which are outlined in Figure 35. Tests 1, 2 and 3 are baseline tests which show the heating behaviour of the body when in contact with warm air i.e. convective heating. This gives a baseline behaviour to which IR heating behaviour of tests 4, 5, 6 and 7 can be compared. There test group consists of four subjects and the thermoregulatory behaviour of each is assessed for each of tests 1 to 7.

Tests 1 and 4 record temperature distribution throughout the full body under WR and IR on Face conditions. Tests 2 and 5, and tests 3 and 6 repeat this experiment but focus on skin temperature distribution only in the face and hand areas respectively, thus allowing more accurate assessment of these areas. Test 7 focuses the IR heat on the subject's hand, and the opposite hand is monitored. All tests involve skin temperature and core temperature measurements, and tests 3 and 6 also include heat flux measurements for the monitored hand.

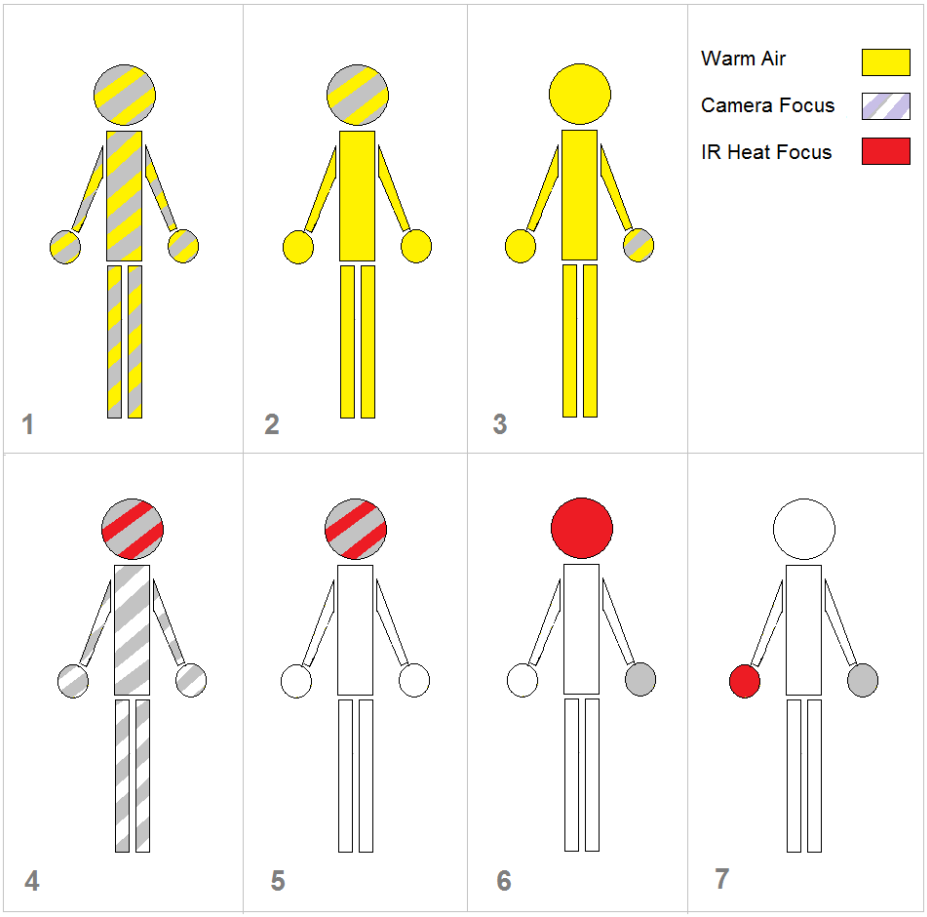

Figure 35 - Human thermoregulatory tests to be performed

The procedure for each of tests 1 to 7 is as follows;

1) The air temperature in the cold room (and warm room when applicable) is recorded.
2) The test subject is positioned standing on insulation to avoid heat loss by conduction to the cold floor.
3) The thermocouple is placed under the subjects tongue and the heat flux sensor (tests 3 and 6 only) is attached to the subject's hand.
4) The DL thermo and LabVIEW programs are run, and the camera is connected to the ThermaCAM Researcher Pro software and set to record images at 10second intervals. The LabVIEW program used here is the same as that used for the heat flux distribution testing, but with the elapsed time control for the data saving operation removed so that data is continuously acquired when the program is run. The ThermaCAM Researcher Pro and DL Thermo software both allow simple data recording operations to be performed and require no programming.
5) Data is acquired showing the initial thermal state of the subject. For the WR tests this corresponds to the time within 20seconds of the subject's entry into the warm room, and for the IR tests this corresponds to the time before the IR heat is applied to the body.
6) For the IR tests the heat is applied to the body at this time.
7) Data is recorded for 10mins while the subject is asked to remain in a still, standing position.

3.3.3 Data Reduction

The core temperature data is recorded to a text file, and the heat flux data to a .lvm file, each of which contains initial data and 10mins of test data. The core temperature data is ready for use in raw form, and the heat flux data is averaged in Microsoft Office Excel. The thermal images are processed using ThermaCAM Researcher Pro where temperature data at 30second intervals is selected from various body areas, as shown in Figure 36, and exported to Excel. Numerous combinations of data are then plotted in Excel to show temperature change and actual temperature data over the course of the tests.

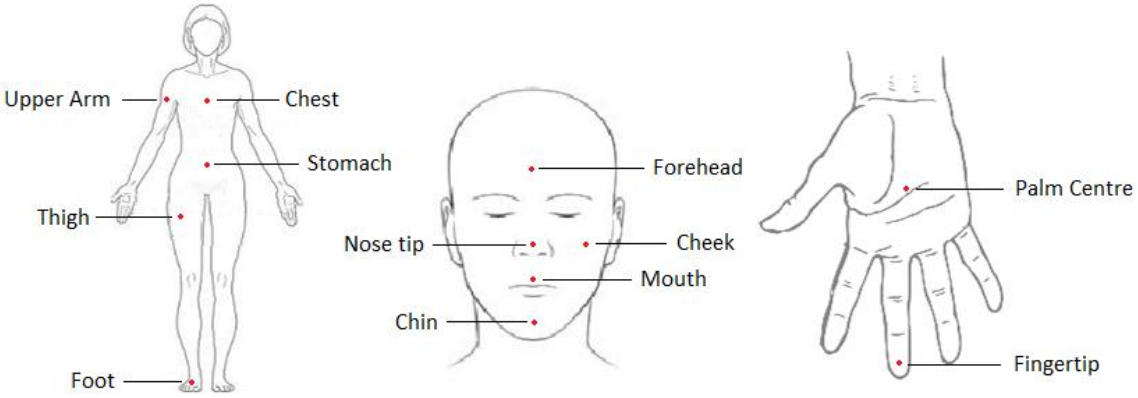

Figure 36 - Temperature measurement points [46] [47] [48]

4 Result and Discussion

4.1 Temperature Distribution Results

The following sections investigate the temperature distributions recorded in Section 3.1.

4.1.1 Overall Temperature Distribution

The following images show the variation in temperature across the 2D plane displayed on a screen as a heat source is placed at varying distances from it. The temperature legend is varied with each image to allow for the widely varying max-min temperature range which will be discussed in Section 4.1.2.

ESER

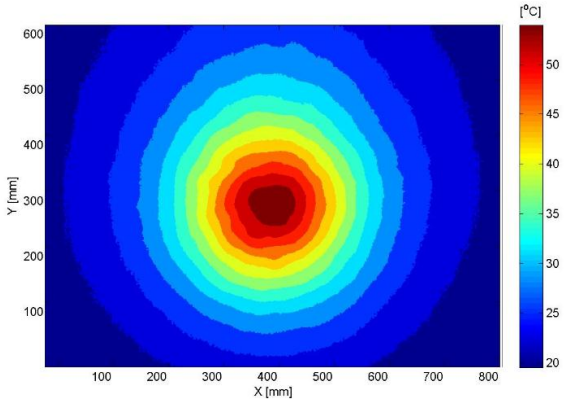

(a) 0.1m from source

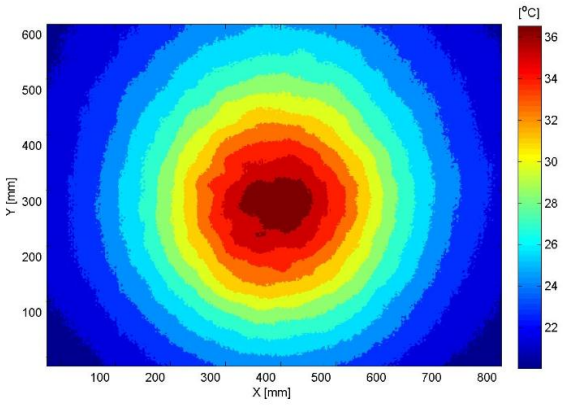

(b) 0.2m from source

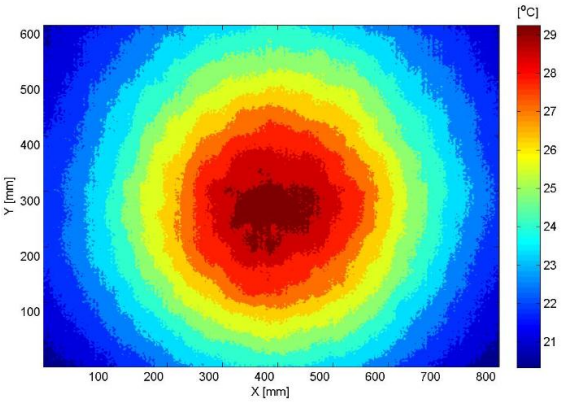

(c) 0.3m from source

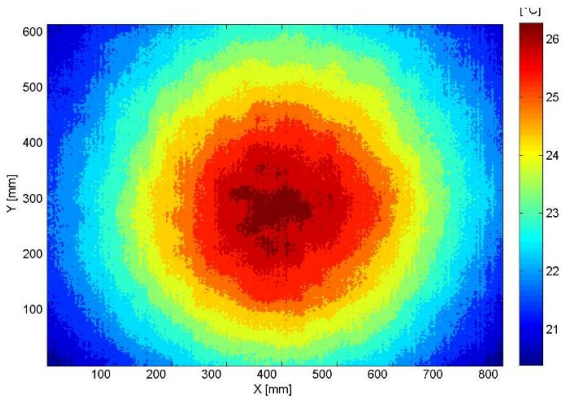

(d) 0.4m from source

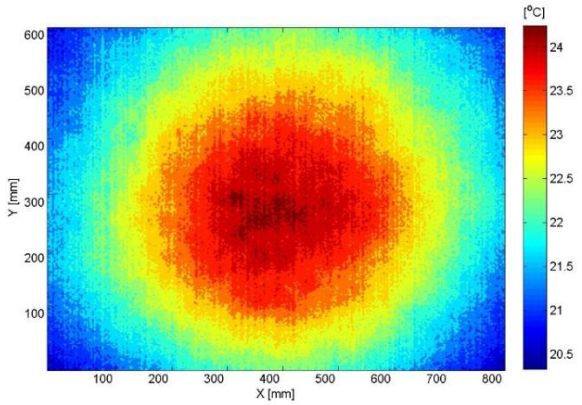

(e) 0.5m from source

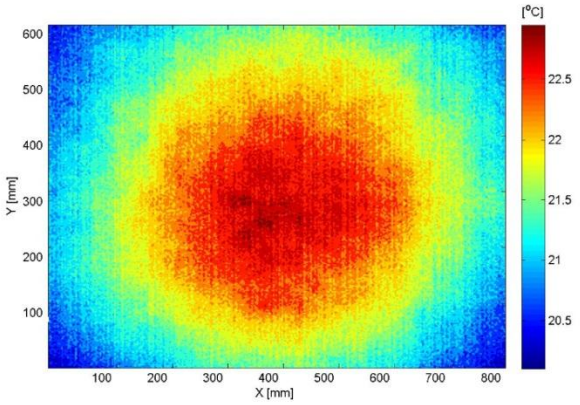

(f) 0.6m from source

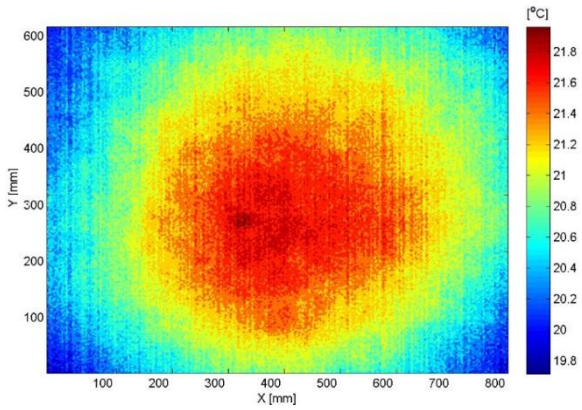

(g) 0.7m from source

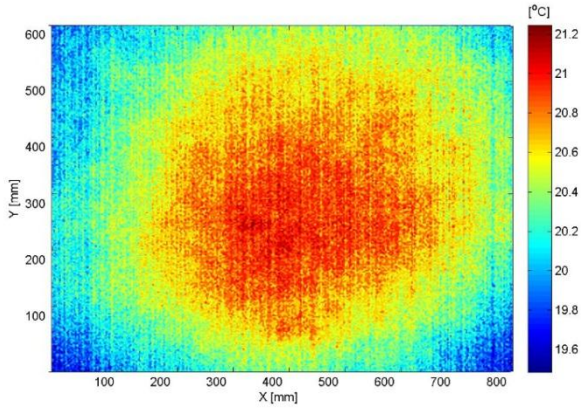

(h) 0.8m from source

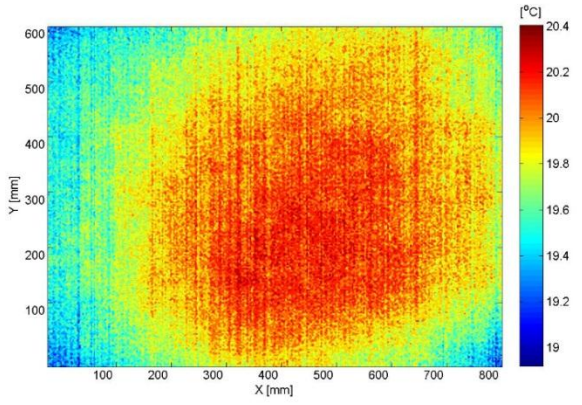

(i) 0.9m from source

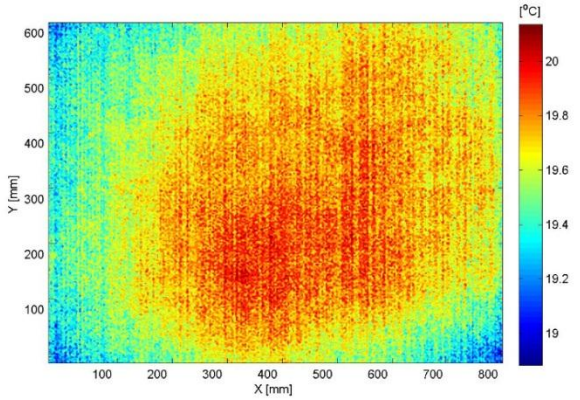

(j) 1.0m from source

Figure 37 - ESER temperature distribution

Figure 38 shows a section view of the temperature distribution, taken horizontally across the point of the highest temperature in the distribution i.e. the centre position. It can be seen from Figure 38 and from the preceding images that the temperature distribution is very symmetrical across all axes through the centre position and varies most dramatically at the closest point to the heat source, and this variation lessens as we move away from the source. The changes are most noticeable within the 0.5m closest to the source, whilst after that point the temperature variation settles down to within 2 - 3°C.

A human will feel warm in the 30°C rays of the sun [49], and so these results would suggest the placement of the ESER for comfort applications should be at least 0.3m away from the subject to be heated, where the maximum temperature is just under 30°C. This should avoid excessive heating, and at this point the temperature distribution is more uniform than at points closer to the source.

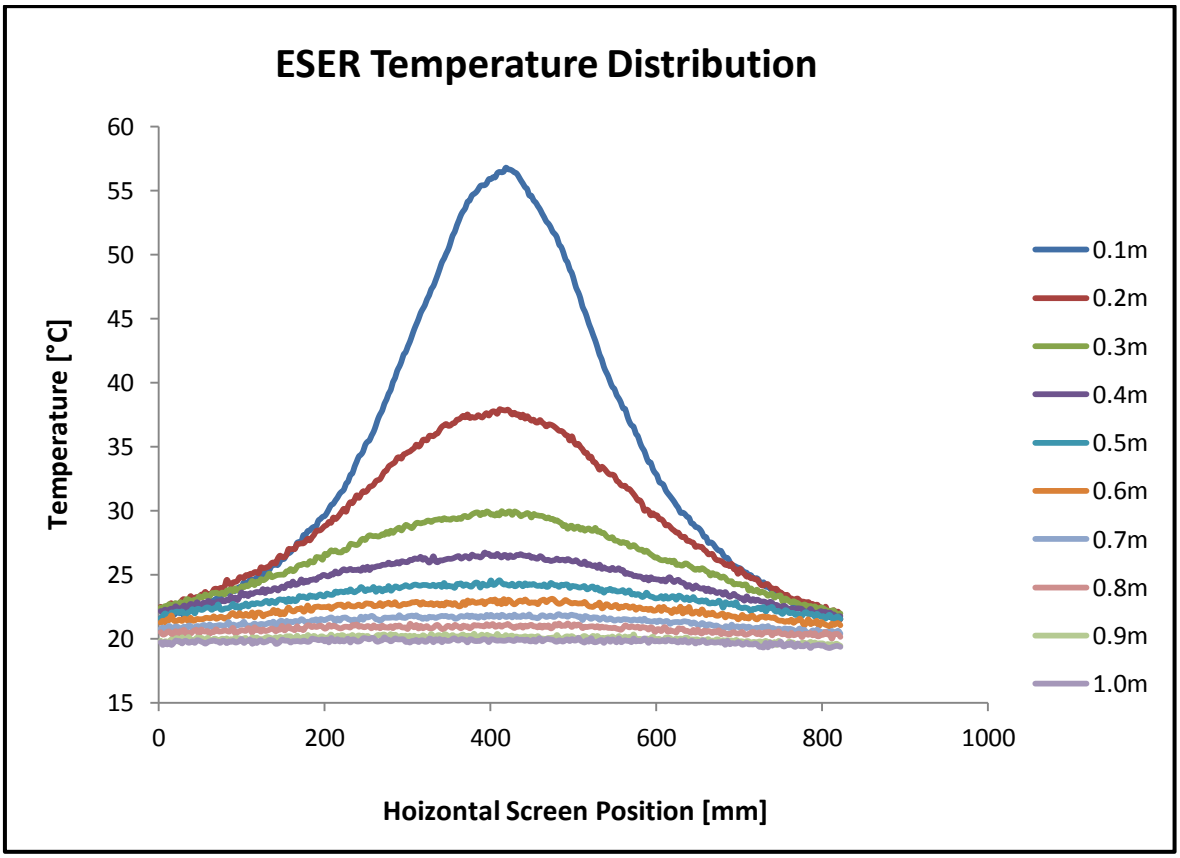

Figure 38 - Temperature Distribution for ESER

Double FTE

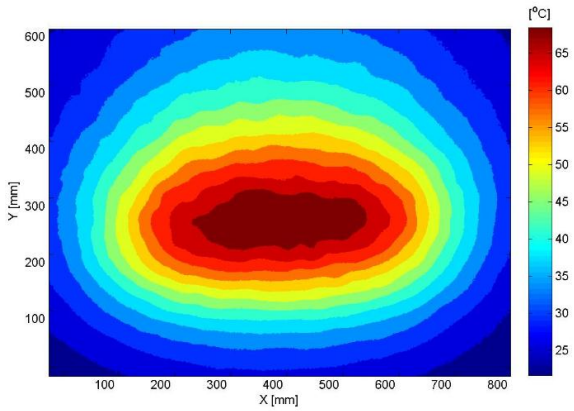

(a) 0.1m from source

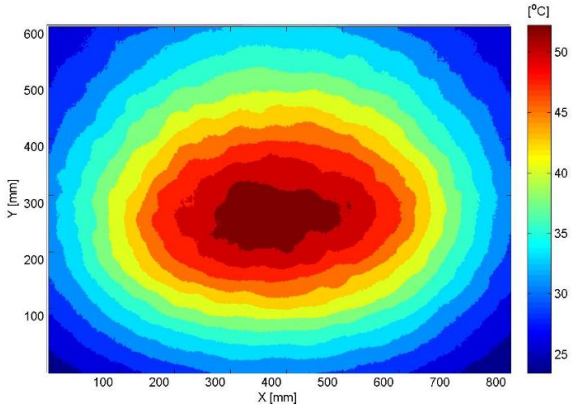

(b) 0.2m from source

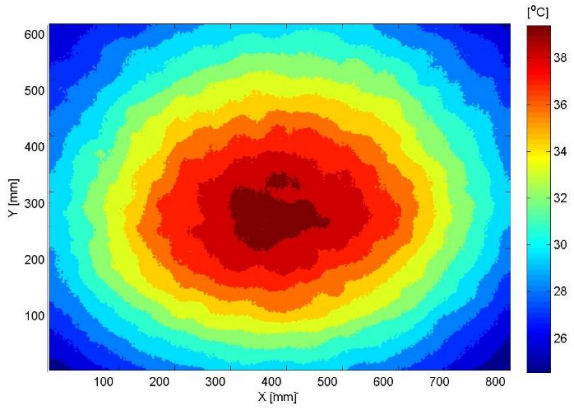

(c) 0.3m from source

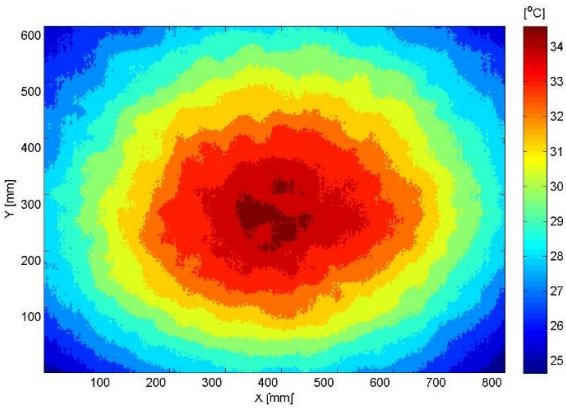

(d) 0.4m from source

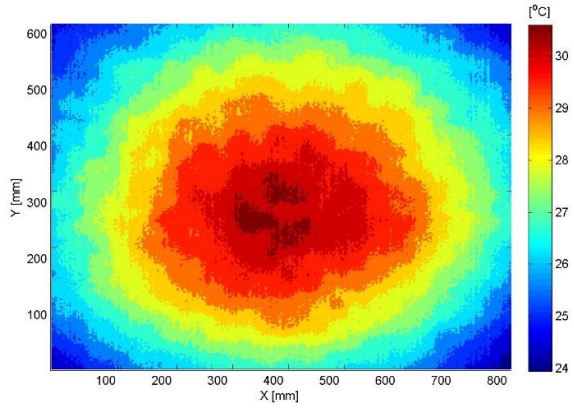

(e) 0.5m from source

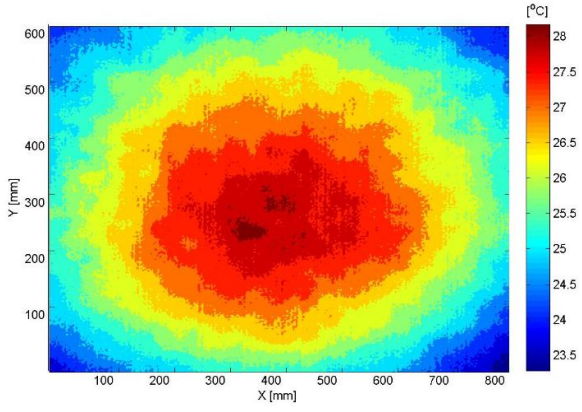

(f) 0.6m from source

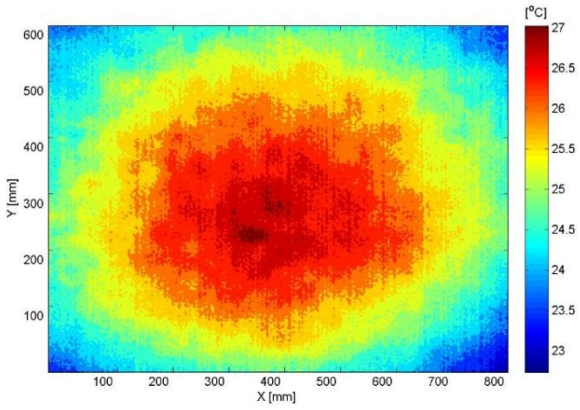

(g) 0.7m from source

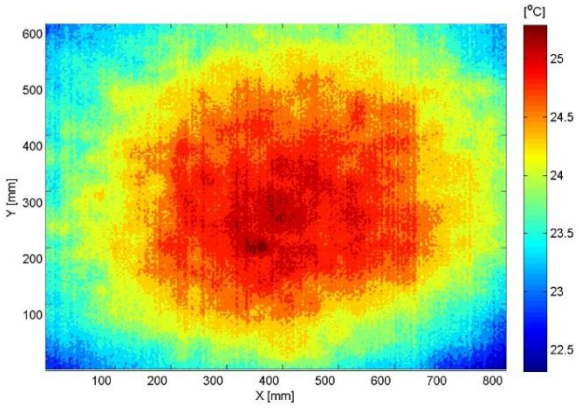

(h) 0.8m from source

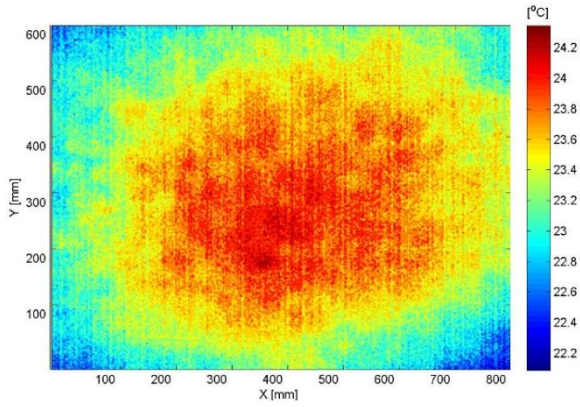

(a) 0.9m from source

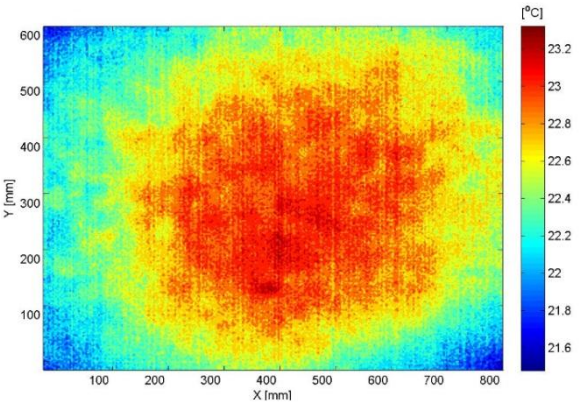

(b) 1.0m from source

Figure 39 - Double FTE distribution

As before, Figure 40 shows a section view of the temperature distribution taken horizontally across the point of the highest temperature in the distribution, i.e. the centre position. It can be seen from Figure 40 and from the preceding images that the temperature distribution for the Double FTE is symmetrical through the X and Y axes and varies most dramatically at the closest point to the heat source, and that this variation lessens with increased distance from the source. The changes are most noticeable within the 0.5m closest to the source, whilst after that point the temperature variation settles down to within 2 - 3°C.

The temperatures shown here would suggest that the placement of the ESER for comfort applications should be at least 0.5m away from the subject to be heated. At this distance

the maximum temperature is just over 30°C and the temperature distribution is more uniform than at points closer to the source.

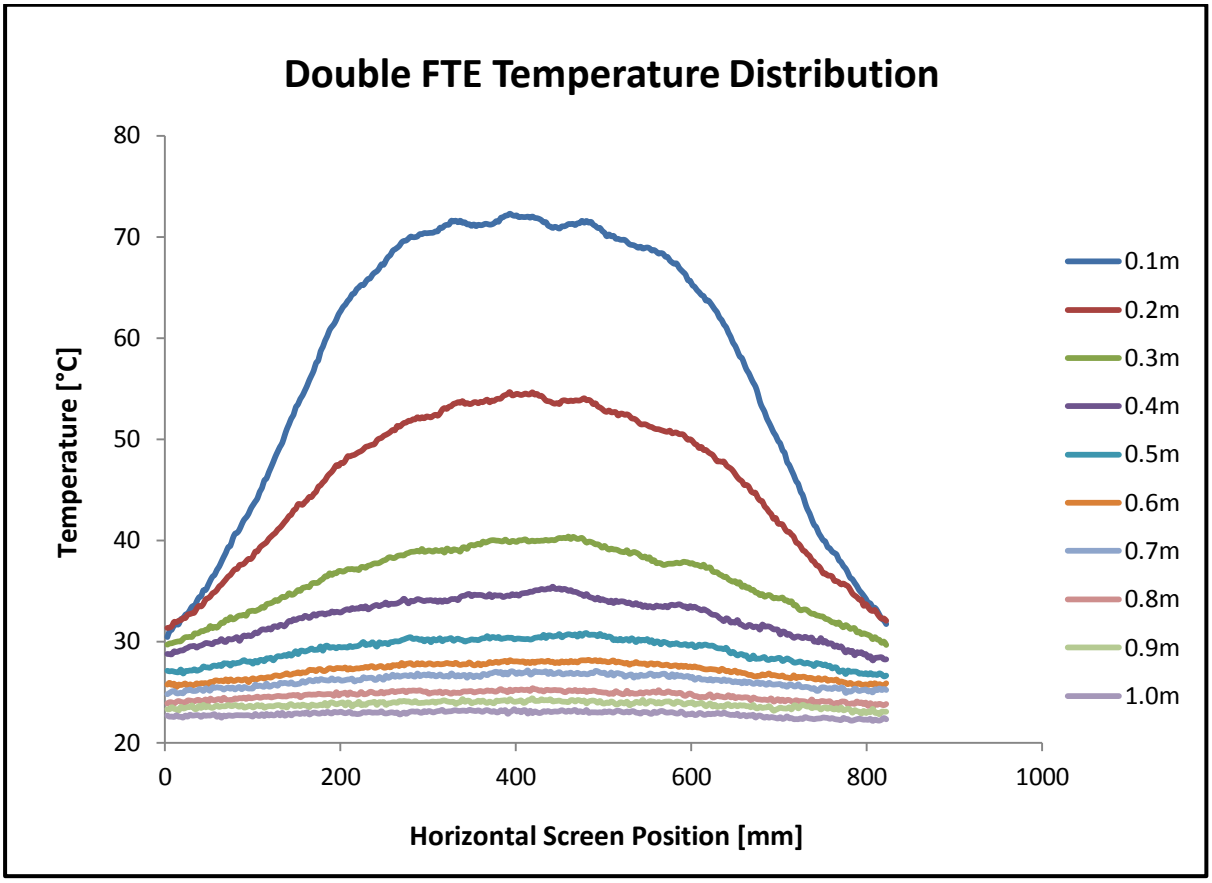

Figure 40 - Temperature Distribution for Double FTE

Figure 41 compares the temperature distributions for the ESER and Double FTE. It can be seen that the Double FTE gives a fairly even temperature distribution of approximately 70°C across a distance of 250mm at 0.1m from the source, whilst the ESER shows a sharp temperature peak of 55°C at 0.1m from the source. This result suggests that for more high temperature requirements the Double FTE would be more suited to heating a space than the ESER, which would be more suited to spot heating.

For comfort applications however, the suggested distances of 0.3m from the source for the ESER and 05m from the source for the Double FTE give much lower and more uniform temperature distributions across the horizontal section for both heaters. At these distances it can still be recognised that the Double FTE gives a more uniform distribution across a horizontal section than the ESER for which temperatures drop to a greater extent away from the centre of the heater.

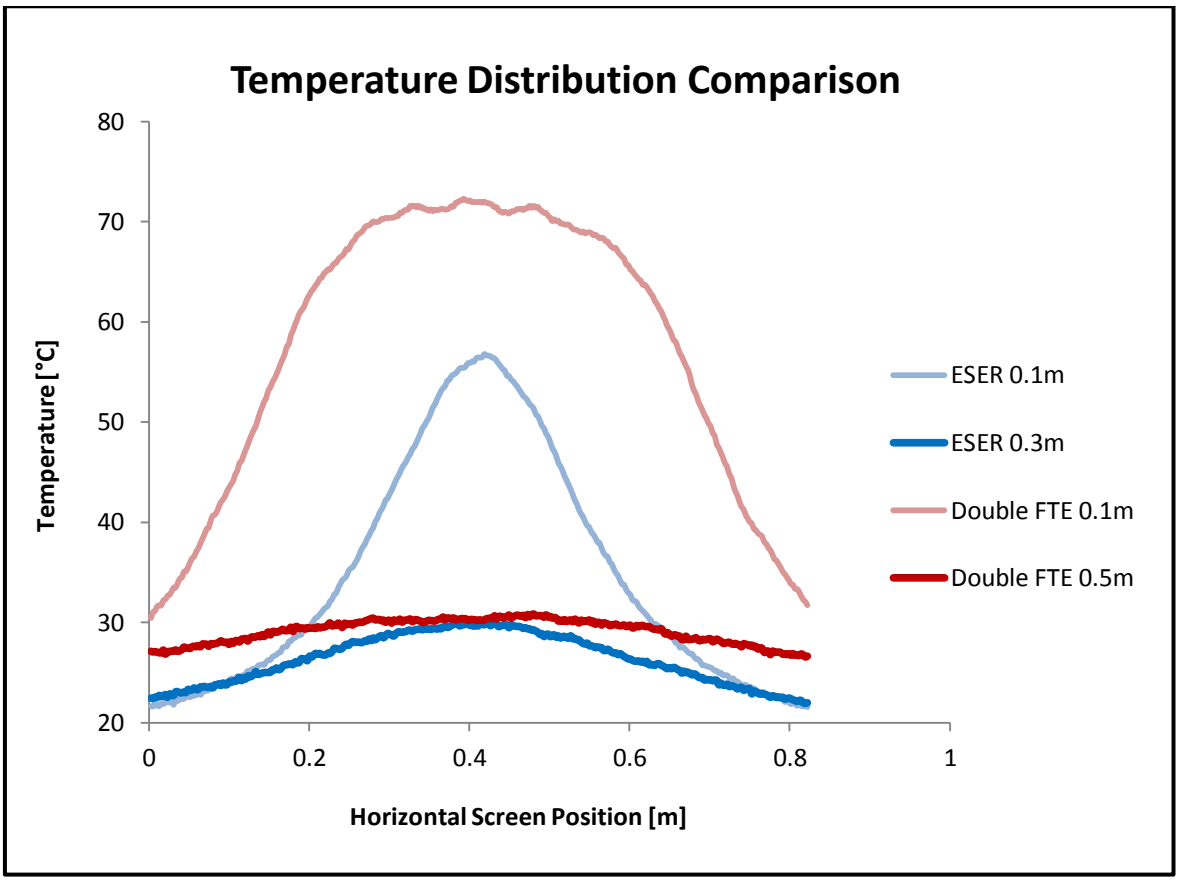

Figure 41 - Temperature Distribution Comparison for ESER and Double FTE

Figure 42 shows contour plots of the ESER and Double FTE at a distance of 0.1m from the source. The contour plots shown here suggest a non-uniform temperature distribution about symmetric parts of the heaters, which may have been noted upon observation of Figures 37a and 39a. It has been found from other testing however that this is not the case; the temperature distribution is in fact uniform across symmetric heater sections, as shown in the lower half of the contour plots. A possible cause of this is the use of an aluminium screen to capture the temperature distribution. As the screen is continually heated up close for prolonged periods of time, the heat may begin to rise up the screen.

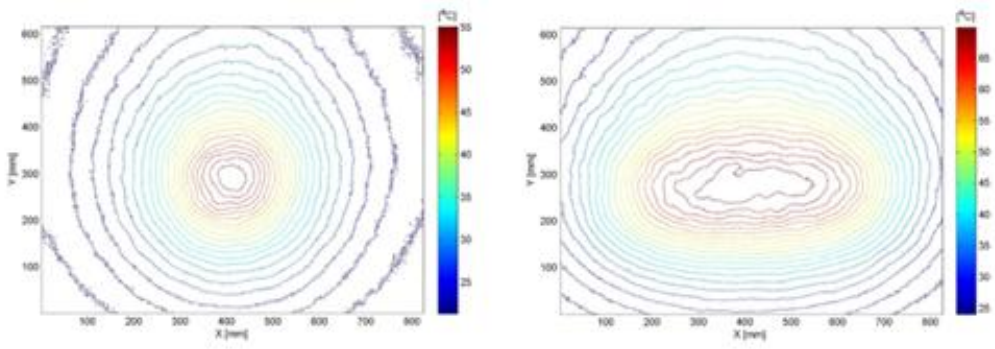

Figure 42 - Contour plots of ESER and Double FTE at 0.1m

4.1.2 Maximum and Minimum Temperature Distribution

Figure 43 shows the maximum temperature reading obtained at each distance from each of the heaters. These points correspond to the maxima shown in Figures 37 and 39. The same trend can be observed for both of the heaters in this case, consisting of an initially steep drop in maximum temperature which levels out towards a distance of $1m$ from the heat source. The Double FTE displays the higher maximum temperature at each distance from the source. As mentioned previously it can be seen that for both heaters most of the variation in maximum temperature occurs within the first $0.5m$ from the source.

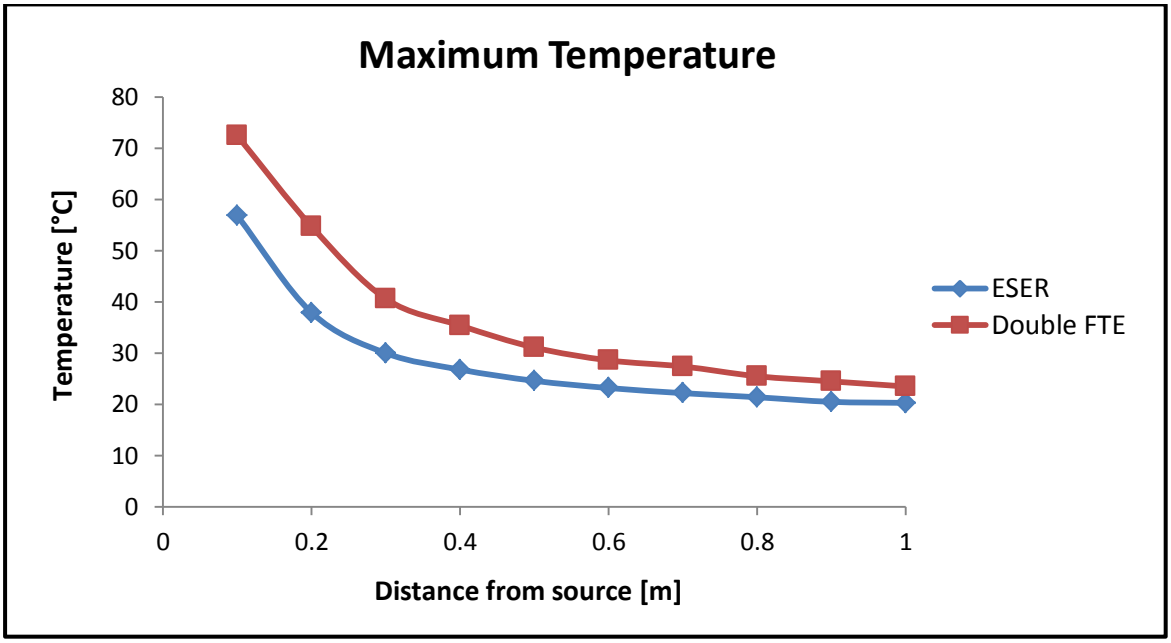

Figure 43 - Maximum Temperature for ESER and Double FTE

Figure 44 shows the minimum temperature reading obtained at each distance from each of the heaters. These points correspond to the corners of the view area where the least heat output is focused. Again, the same trend can be seen for both of the heaters, this time consisting of a gentle rise up to a maximum which occurs around $0.4m$ from the screen, followed by a gentle fall. The lowest minimum temperatures are therefore recorded up close to the heat source (where the directional nature of the IR waves means that their main heat is not reaching the edges of the view area) and far away from the heat source (where the overall temperatures are lowest). It can also be observed that the ESER hater has the more constant minimum temperature of the two.

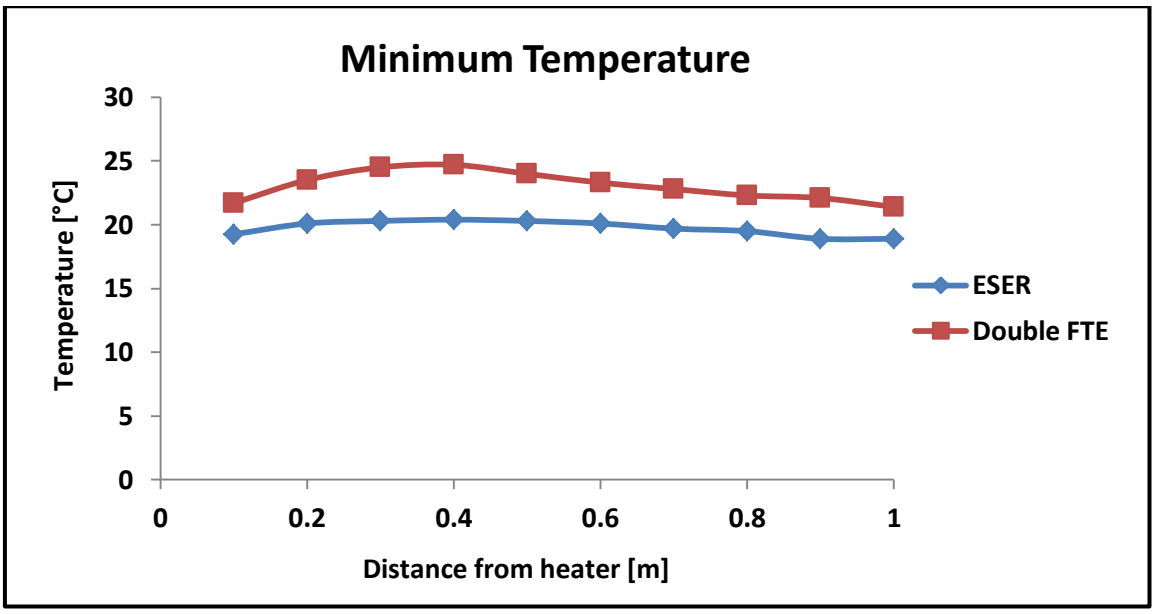

Figure 44 - Minimum Temperature for ESER and Double FTE

Figure 45 shows the difference between the maximum and minimum temperature readings obtained at each distance from the heaters. The trends are again similar for the two heaters; an initial steep decline up to a point around $0.3m$ from the screen, from which point the slope gradually becomes more gentle. It could be suggested here that the combination of maximum heat output and uniform temperature distribution occurs at a distance of around $0.3m$ from the heat source as at this point the maximum temperature and the temperature difference across the test area are within a middle range.

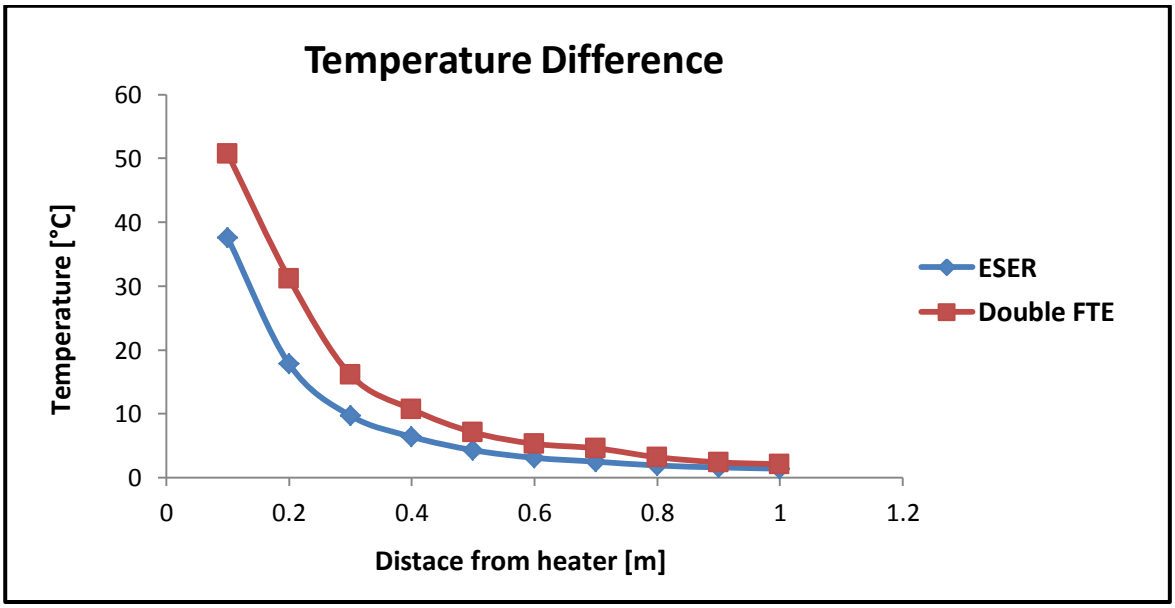

Figure 45 - Temperature Difference for ESER and Double FTE

4.2 Heat Flux Distribution Results

The following sections investigate the heat flux distributions recorded in Section 3.2.

4.2.1 Overall Heat Flux Distribution

The following images show the variation in heat flux across the 2D plane traversed by the radiant heat flux sensor as a heat source is placed at varying distances from it. The heat flux legend is varied with each image to allow for the widely varying max-min heat flux range which will be discussed in Section 4.2.2.

ESER

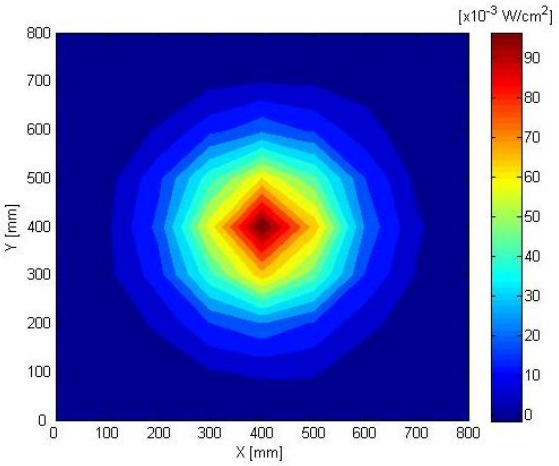

(a) 0.2m from source

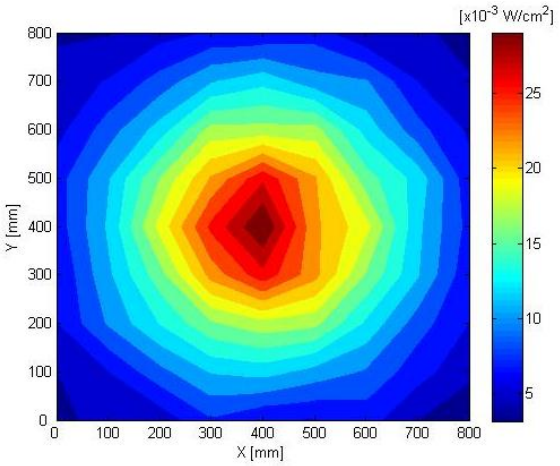

(b) 0.4m from source

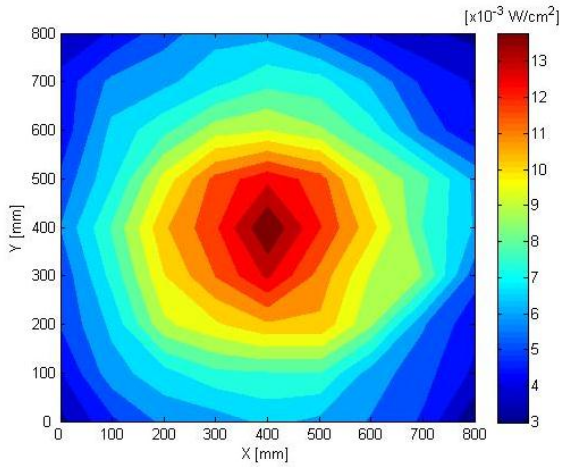

(a) 0.6m from source

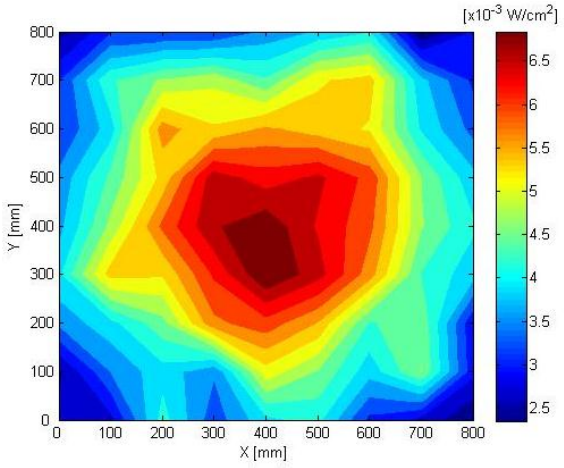

(b) 0.8m from source

Figure 46 - ESER Heat Flux Distribution Images

Figure 47 shows a section view of the heat flux distribution, taken horizontally across the point of the highest heat flux value in the distribution. It can be seen from Figure 47 and from the preceding images that the heat flux distribution is very symmetrical across all axes through the centre position, varies most dramatically at the closest point to the heat source, and that this variation lessens with increased distance from the source. The changes are most noticeable within the $0.4m$ closest to the source, whilst after that point the heat flux variation settles down to within $8.6 \times 10^{-3}\ W/cm^2$.

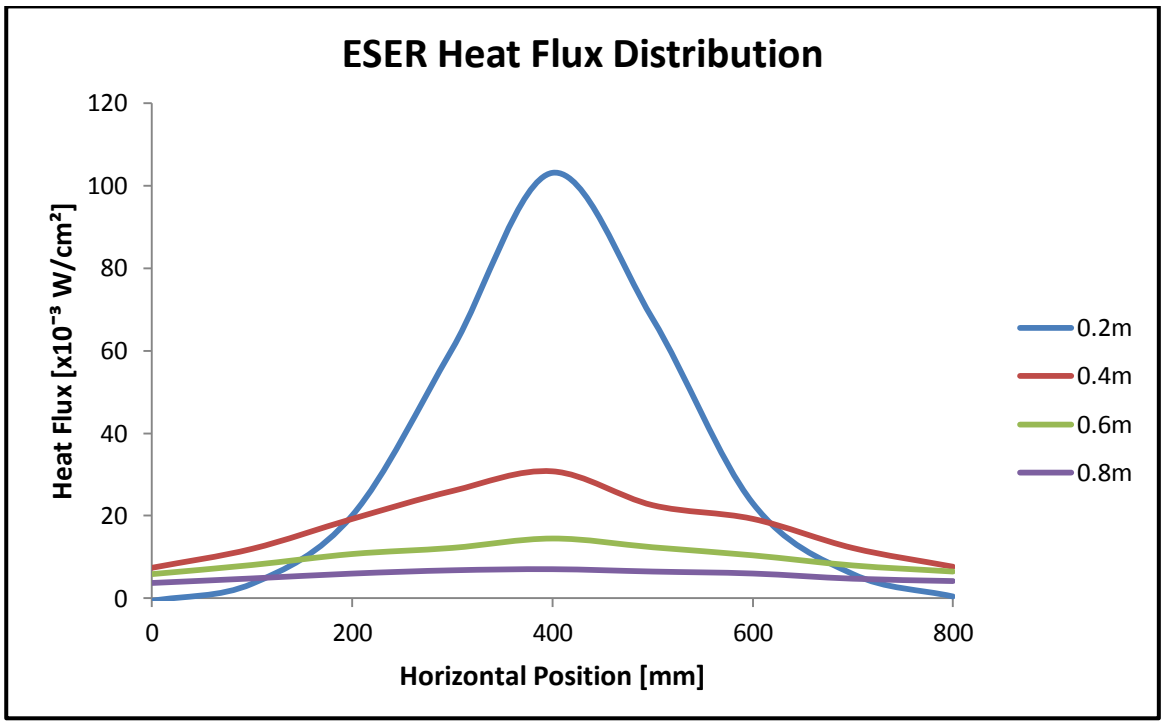

Figure 47 - ESER Heat Flux Distribution

Double FTE

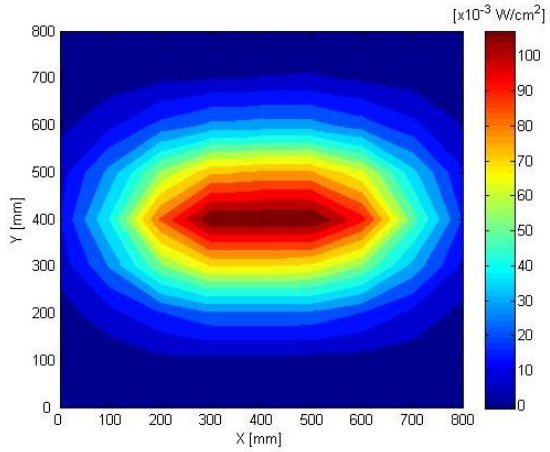

(a) 0.2m from source

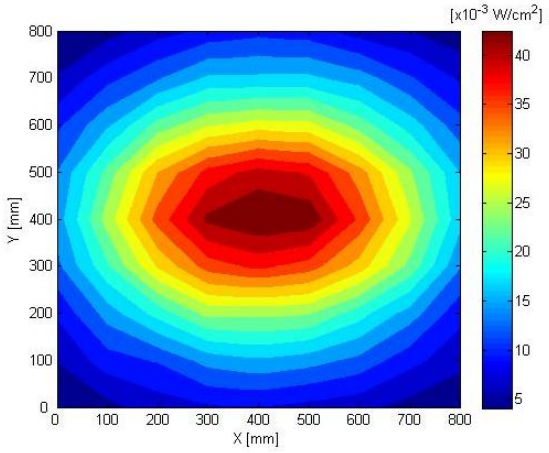

(b) 0.4m from source

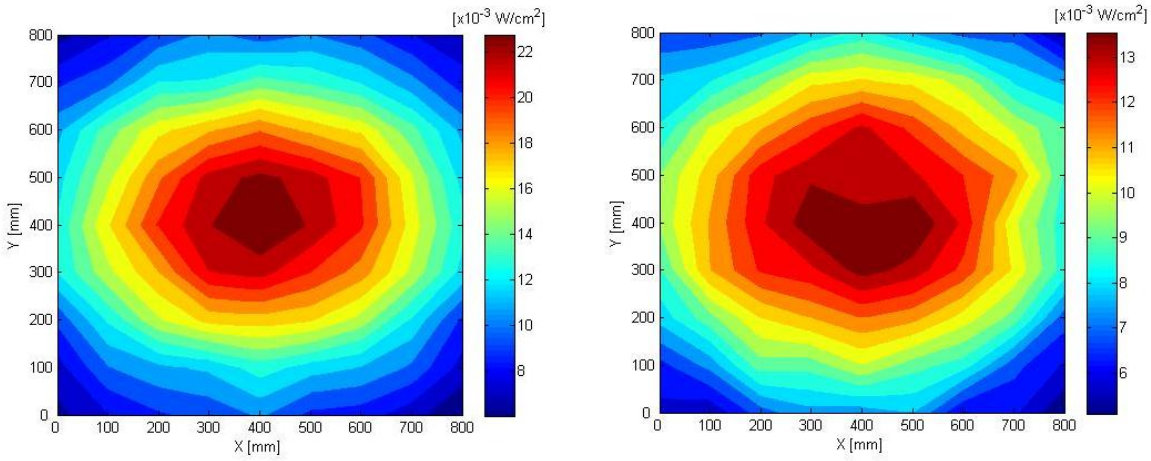

(a) 0.6m from source (b) 0.8m from source

Figure 48 - Double FTE Heat Flux Distribution Images

As for the ESER heater, Figure 49 shows a section view of the heat flux distribution taken horizontally across the point of the highest heat flux value in the distribution. It can be seen from Figure 49 and from the preceding images that, the temperature distribution is quite symmetrical about the X and Y axes and varies most dramatically at the closest point to the heat source, and that this variation lessens with distance from the source. Again, the changes are most noticeable within the $0.4m$ closest to the source, after which the temperature variation settles down to within $11 \times 10^{-3}\ W/cm^2$.

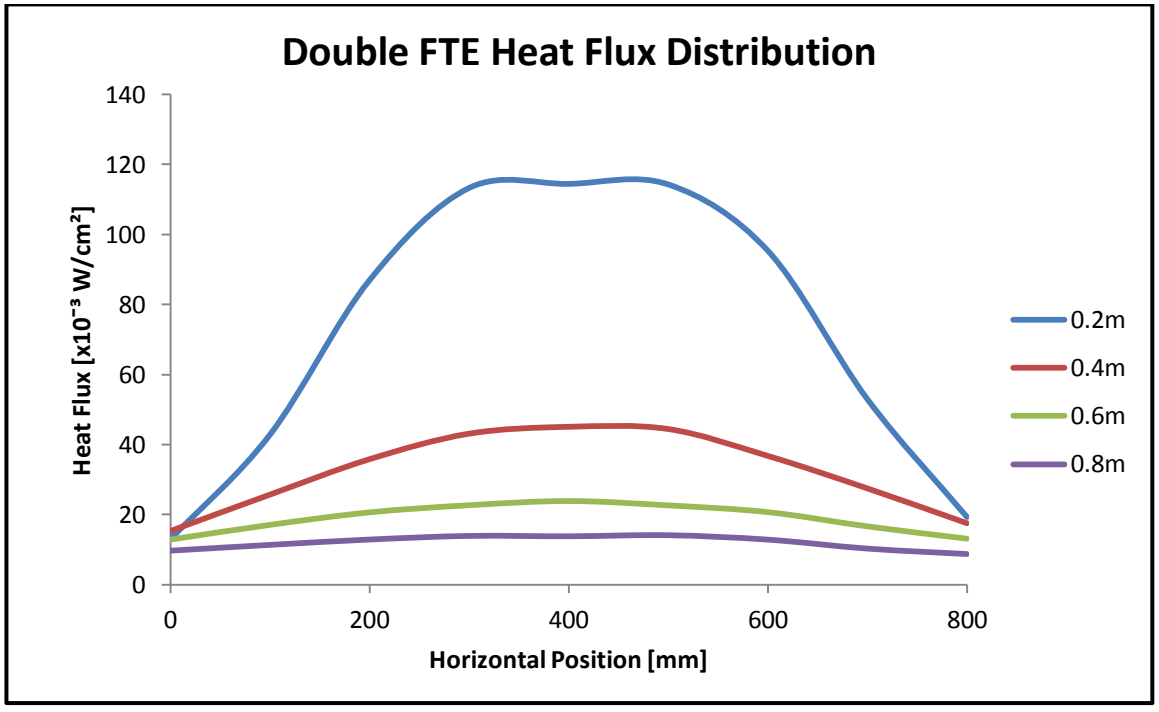

Figure 49 - Double FTE Heat Flux Distribution

Figure 50 compares the heat flux distributions for the ESER and Double FTE. It can be seen that the Double FTE gives a fairly even heat flux distribution of approximately $114 \times 10^{-3}\ W/cm^2$ across a distance of around 250mm at 0.2m from the source, whilst the ESER shows a sharp peak of $103 \times 10^{-3}\ W/cm^2$ at 0.2m from the source.

The suggested distances from the source for comfort applications has been suggested by the temperature distribution results to be 0.3m for the ESER and 0.5m for the Double FTE. The heat flux values across the horizontal section at a distance of 0.4m from the source are therefore also shown in Figure 50 (no data exists for 0.3m and 0.5m). At this distance the heat flux from the ESER and Double FTE is $30.8 \times 10^{-3}\ W/cm^2$ and $45 \times 10^{-3}\ W/cm^2$ respectively at the centre of the heated area. It can be seen that the heat flux distributions are more uniform at this point than at closer distances to the heater, both showing similar ranges of between 20-30 $\times\ 10^{-3} W/cm^2$ over the horizontal test position range.

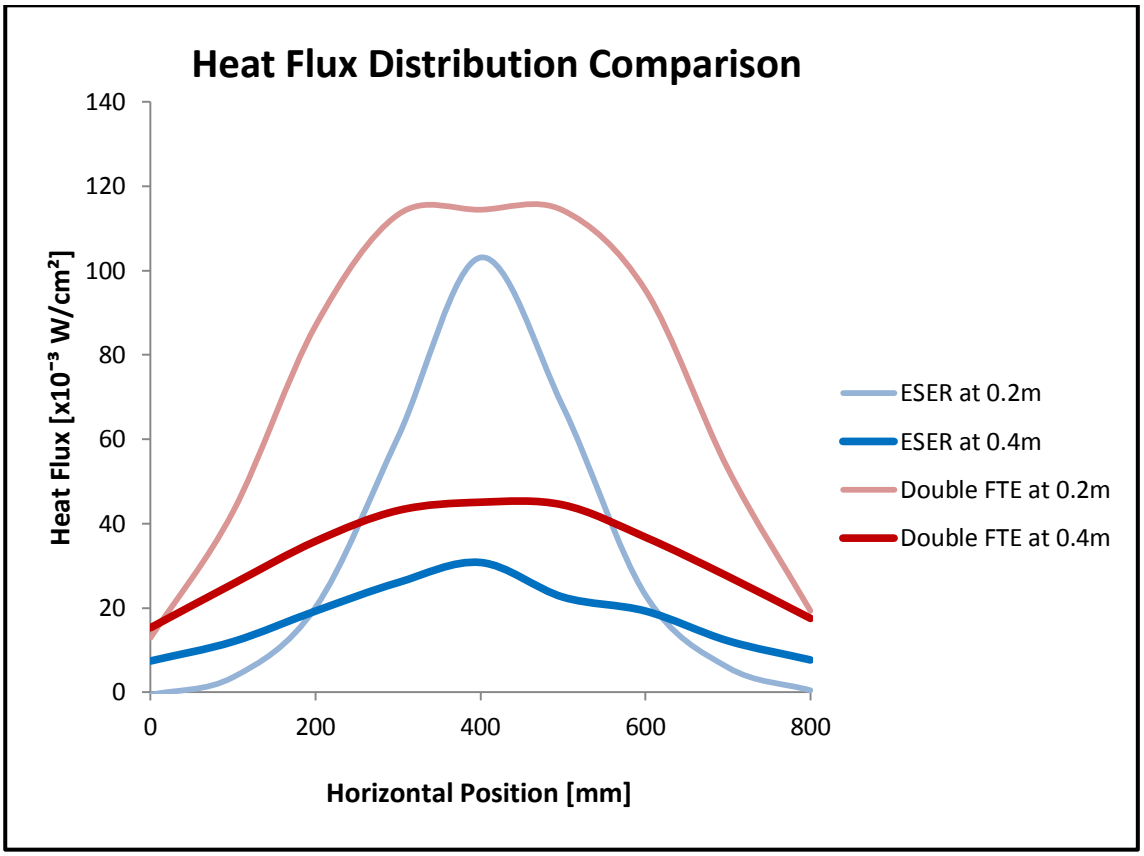

Figure 50 - Heat Flux Distribution Comparison for ESER and Double FTE

4.2.2 Maximum and Minimum Heat Flux Distribution

Figure 51 shows the maximum heat flux value obtained at each distance from each of the heaters. These points correspond to the maxima shown in Figures 46 and 48. The same trend can be observed for both heaters in this case, consisting of an initially steep drop in heat flux which levels out towards a distance of $0.8m$ from the heat source. It can be seen that for both heaters most of the variation occurs within the first 0.4m from the source.

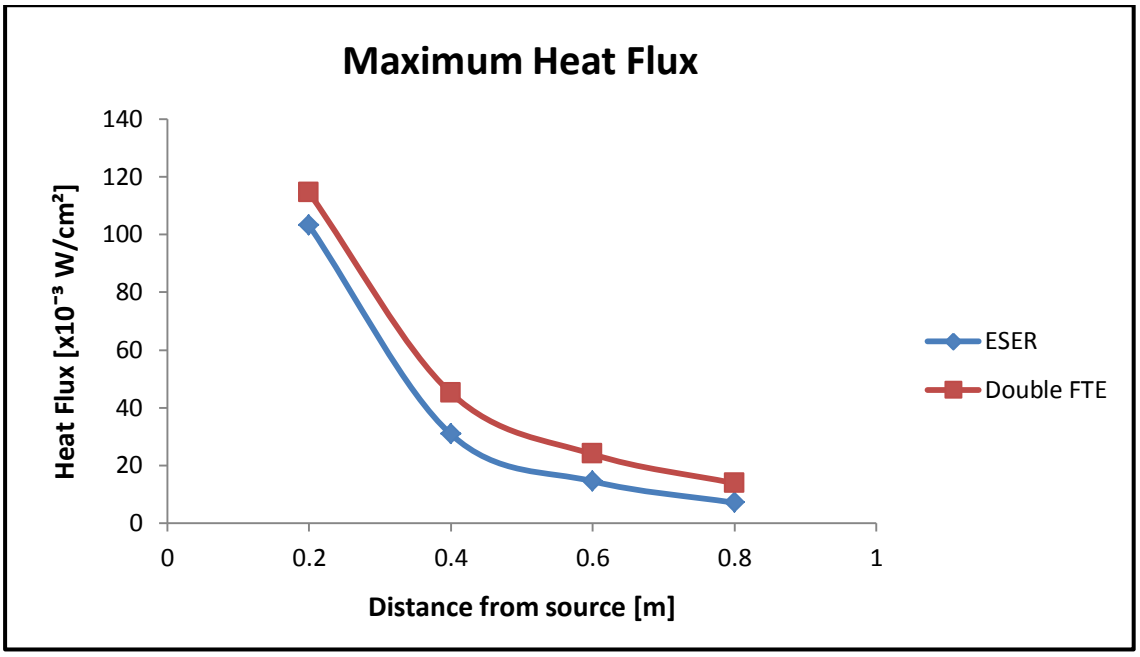

Figure 51 - Maximum Heat Flux for ESER and Double FTE

Figure 52 shows the minimum heat flux reading obtained at each distance from each of the heaters. These points correspond to the corners of the view area where the least heat output is focused. Again, the same trend can be seen for both of the heaters, consisting of a steep rise up to a maximum followed by a gentle fall. These maxima occur at 0.4m from the ESER source and at 0.6m from the Double FTE source. The lowest minimum heat flux values are therefore found up close to the heat source (where the directional nature of the IR waves means that their main heat is not reaching the edges of the view area) and to a lesser extent far away from the heat source (where the overall output is lowest).

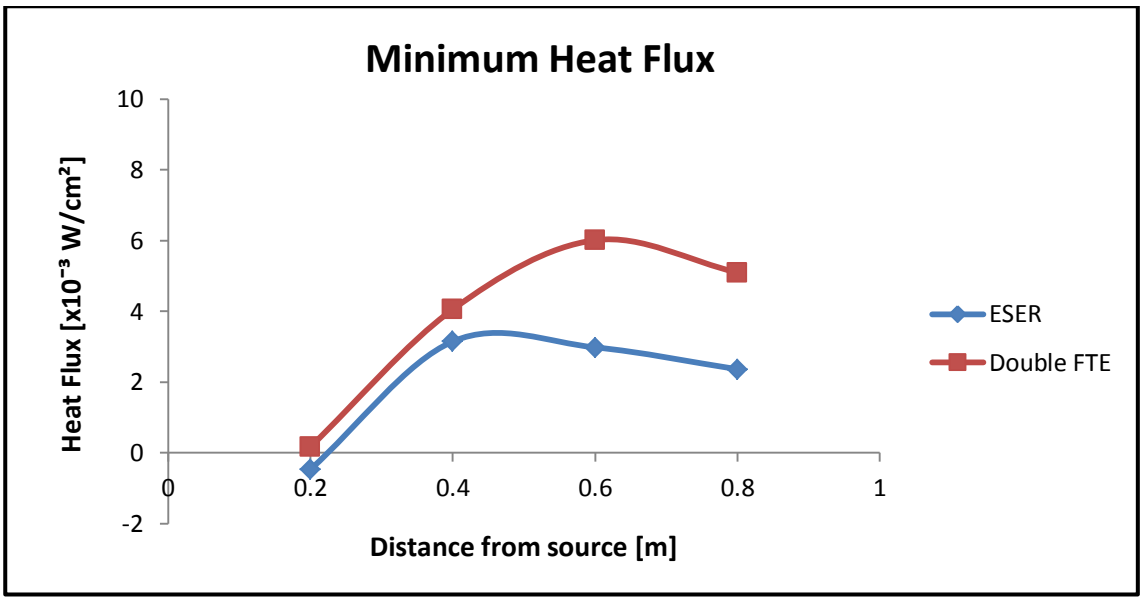

Figure 52 - Minimum Heat Flux for ESER and Double FTE

Figure 53 shows the difference between the maximum and minimum heat flux values obtained at each distance from each of the heaters. The trends are again similar for the two heaters; an initial steep decline up to a point around $0.3m$ from the screen, from which point the slope becomes more gentle. It could be suggested here that the combination of maximum heat flux output and uniform heat flux distribution occurs at a distance of around $0.4m$ from the heat source as at this point the maximum heat flux value and the difference between maximum and minimum heat flux values are within a middle range.

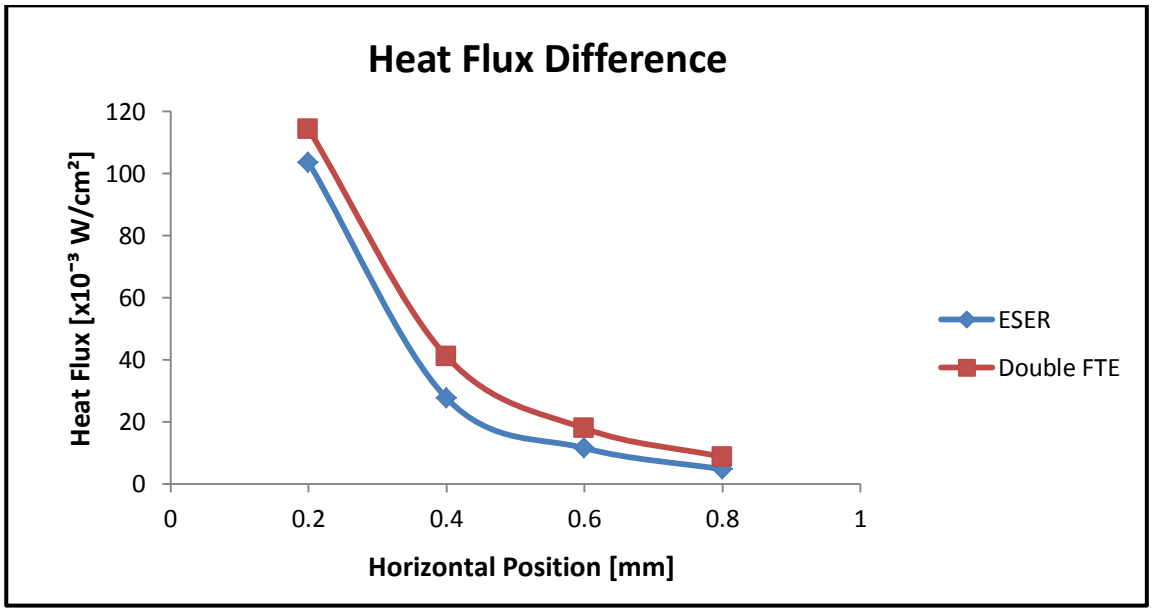

Figure 53 - Heat Flux Difference for ESER and Double FTE

4.2.3 Relationship between Heat Flux and Temperature

A comparative plot between the heat flux distribution and temperature distribution results at a distance of $0.4m$ from the source is shown in Figure 54. This highlights the relationship between heat flux and temperature and shows that their trends are closely linked.

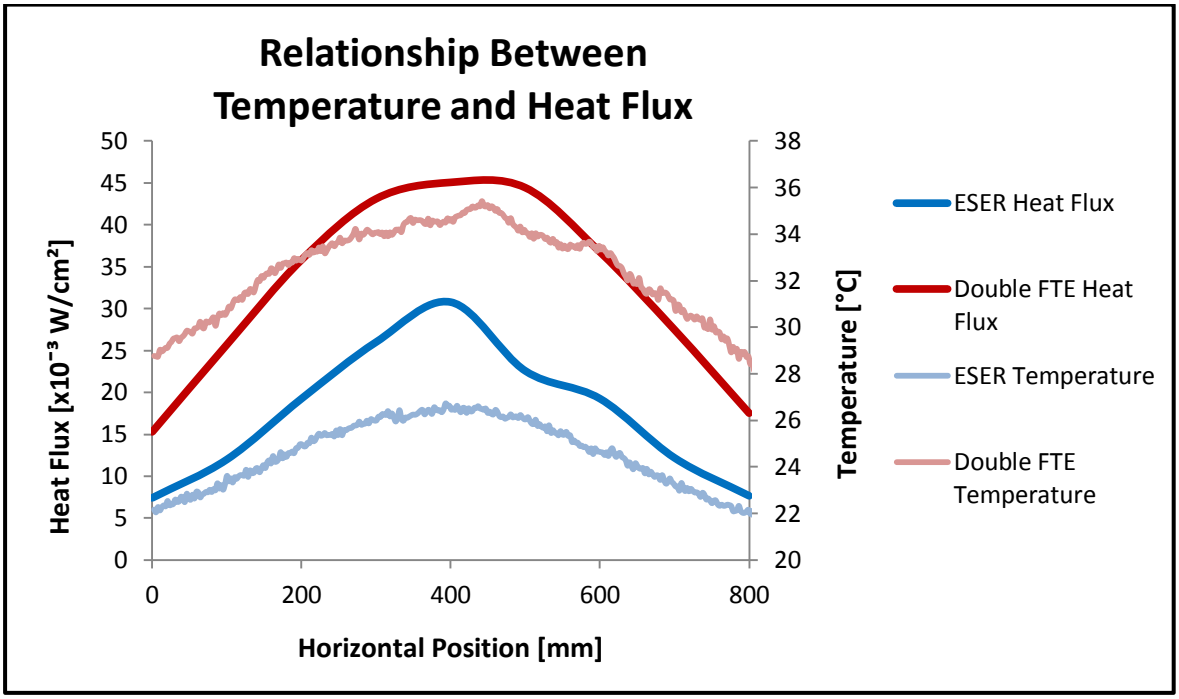

Figure 54 - Relationship between heat flux and temperature

4.3 Response of the Human Thermoregulatory System to IR Heating

The response of the thermoregulatory system was found to differ with each individual tested. This would be expected as thermoregulatory system behaviour is based on numerous individual factors. Therefore, in this section the results for each test subject will be discussed individually, and following this the overall findings will be discussed.

4.3.1 Individual Behaviour

4.3.1.1 Subject 1

Full Body Test - Warm Room

The subject is brought from a cold room (~20°C) into a warm room (~26°C). The resulting thermal images of skin temperature distribution about the body over the course of the test are shown in Figure 55.

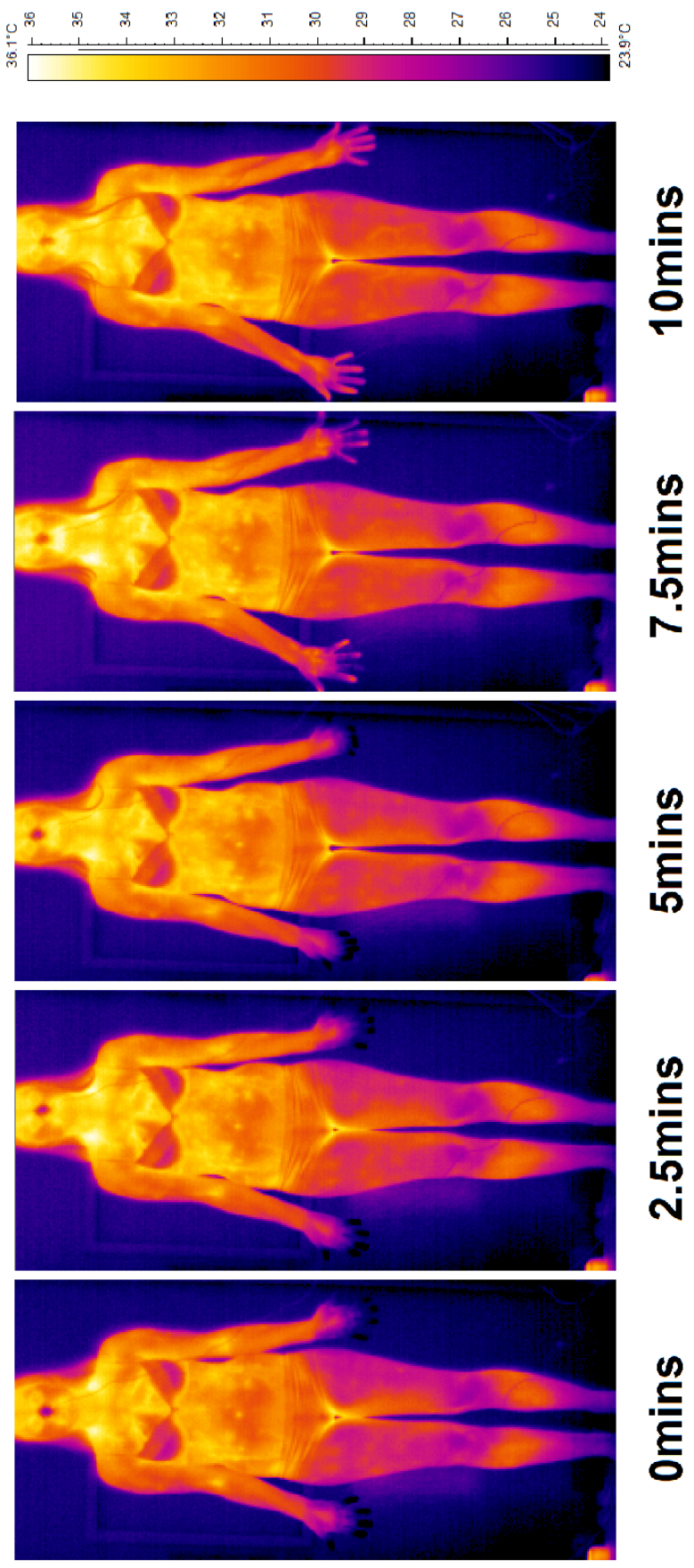

Figure 55 - Subject 1 Full Body Test: Thermal images of WR test

From observation of Figure 55 it can be seen that the most noticeable change in temperature over the course of the test occurs in the hands, in particular in the fingertip areas between the 5min and 7.5min images. Another visible change occurs in the nose area, which appears to gradually increase in temperature over the course of the test. Other areas of the body cannot be seen to noticeably change from inspection of this figure, but analysis of numerical data will allow more subtle changes to be observed.

Figure 56 shows the change in skin temperature experienced by different areas of the body regardless of initial temperature. *[Note: the numerical temperatures taken from the thermal images in this section follow the standard selection process set out in Figure 36].* The first observation to be made from Figure 56 is that there is at least a small increase in temperature for every area of the body over the course of the test. This would be expected as the whole of the body is in contact with the warm air in the room. A second point to note is that the areas which show the greatest increase in temperature over the course of the test are the fingertip (8°C), the nose (4.5°C), and the palm (3°C) areas, as observed from inspection of Figure 55. The remaining areas of the body show an increase of less than 1.3°C over the course of the test.

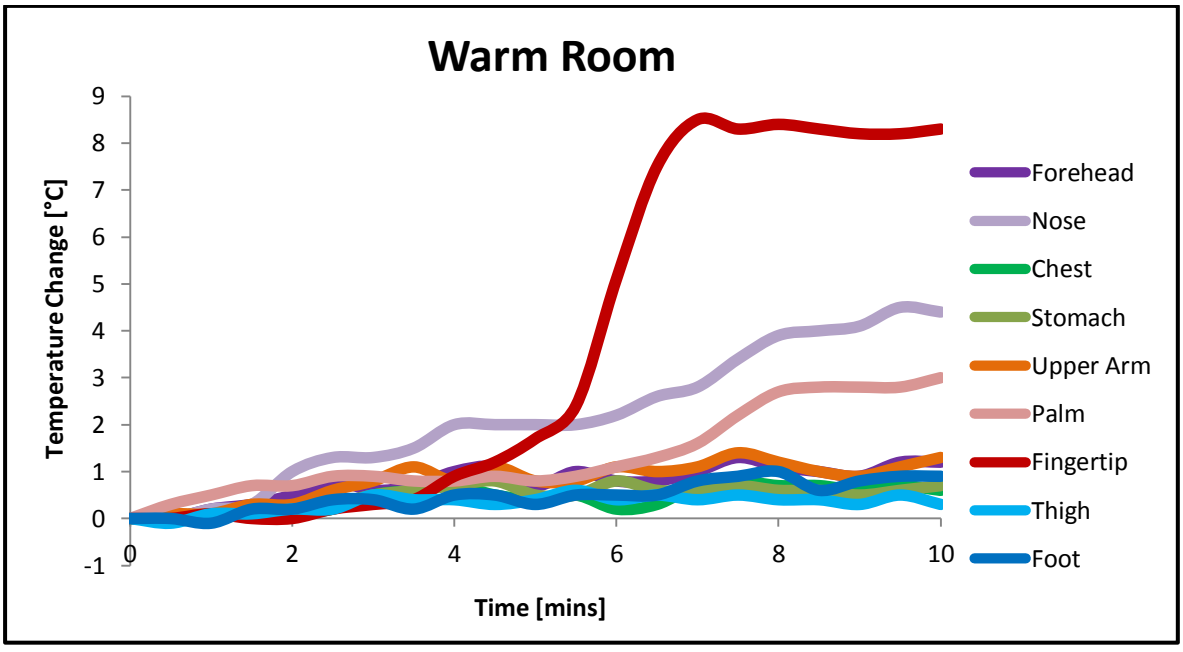

Figure 56 - Subject 1 Full Body Test: Temperature change data for WR test

The plot also reinforces the observation that the majority of the change in the fingertip area occurs within a small timescale; the temperature jumps by 6.5°C to its maximum value

between the times of 5.5mins and 7mins (accounting almost 80% of the overall fingertip temperature change of 8.3°C).

Figure 57 shows the actual temperatures of several areas of the body throughout the test. An observation that can be made at this point relates to apparent 'grouping' of the areas of the body according to temperature.

The areas of the body that hold the highest temperatures are considered the primary group, and these include areas of skin which lie over the core head and upper torso areas in the body i.e. the forehead and chest. These are shown to be the closest to the estimated core temperature, lying approximately 2°C below it throughout the test. The stomach, upper arm, thigh, and palm areas can be considered as a secondary group. These areas maintain a temperature 4.5-7°C below the estimated core temperature throughout the test. The nose temperature (9°C below the estimated core temperature) begins somewhat below the general temperature of this secondary group, but has joined it by the end of the test. The fingertip area has the lowest initial temperature at 14°C below the estimated core temperature, but has also joined the secondary group by the end of the test.

The result of this change is a more uniform temperature distribution across the body. The foot area does not fall into either of these groupings at any stage and is seen to be approximately 10°C lower in temperature than the estimated core throughout the test.

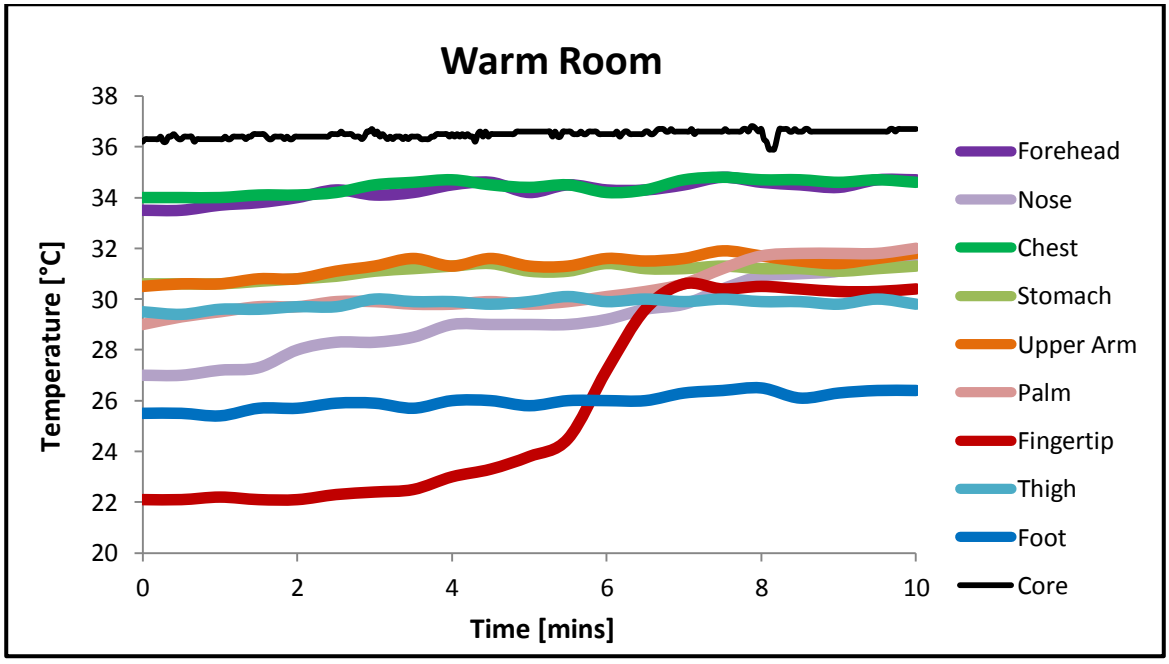

Figure 57 - Subject 1 Full Body Test: Actual temperature data for WR test

An interesting point to note here is that although the hand, foot and nose areas are all extremities of the body starting out at low temperatures, the hand (particularly in the fingertips) and nose areas have a much better heating capability once exposed to the warm air. The temperature of the fingertips is approximately 14°C below the estimated core temperature at the beginning of the test, but by the end of the test this difference has dropped to less than 7°C. Similarly, the nose temperature is approximately 9°C below the estimated core temperature at the beginning but only 4.5°C below at the end. The foot temperature however increases in temperature by less than 1°C over the course of the test.

Full Body Test - IR on Face in Cold Room

The subject is positioned in a cold room (~19.9°C) and IR heat (26.5°C at the centre position) is applied to the face area. Figure 58 shows the resulting changes in temperature distribution around the body. The most noticeable change in temperature which can be observed from this figure occurs in the face and upper torso areas. These areas appear to increase in temperature for the duration of the test as heat is applied. Another change which is just about perceivable occurs in the hands. A small heat spot in centre of the palm at the beginning of the test can be seen to spread further across the hand at 7.5mins. There is no visually obvious change in the fingertip temperature. *However, it should be noted that the fingertip area is difficult to discern from the thermal images due to lack of focus and so the accuracy of the observations and measurements in the case of this area may be impaired.* Other areas of the body appear unchanged throughout the test from inspection of this figure, and again a numerical analysis will be performed in order to obtain further information.

Figure 59 shows the change in skin temperature experienced by different areas of the body regardless of initial temperature. From this figure it can be seen that the areas with the largest temperature increase over the course of the test are indeed the areas that lie within the head and upper torso regions; the forehead (~4.8°C), the nose (~3.8°C), the chest and also the upper arm (both ~2.5°C). This would be expected as the main IR heat is focused on the face, with the peripheral emanating heat flux having a lesser heating effect on the upper torso and upper arm. It can also be observed that several areas of the body (foot, thigh, and stomach areas) show no temperature gain over the course of the test, with temperature change values fluctuating around the zero mark.

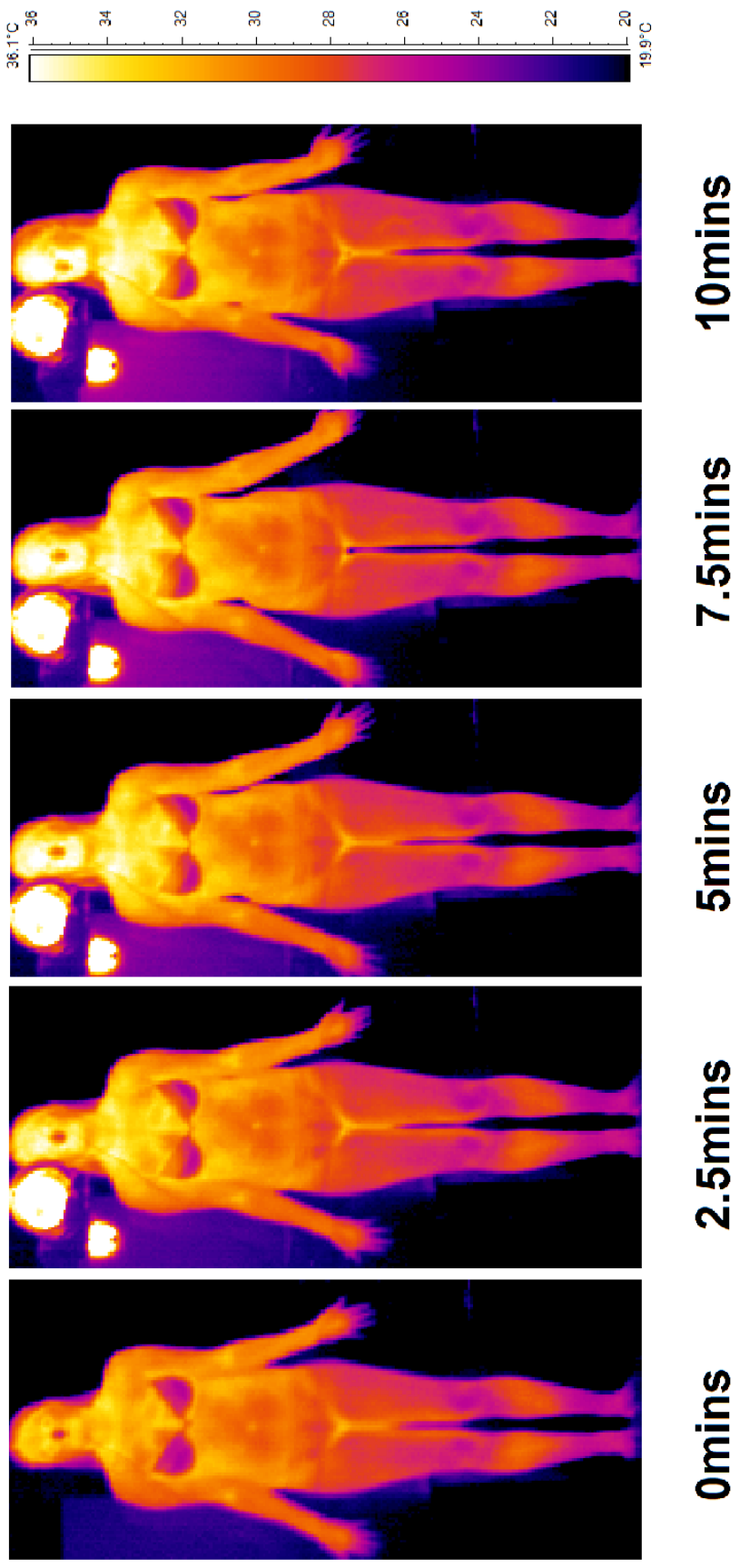

Figure 58 - Subject 1 Full Body Test: Thermal images of IR on Face test

Interestingly, the palm and fingertip areas do show some small increase in temperature (rising approximately 0.5-1.5°C over the test duration) thus suggesting that some amount of heat is being transferred to these areas by thermoregulation within the body, given that they are far outside the direct range of the IR heat.

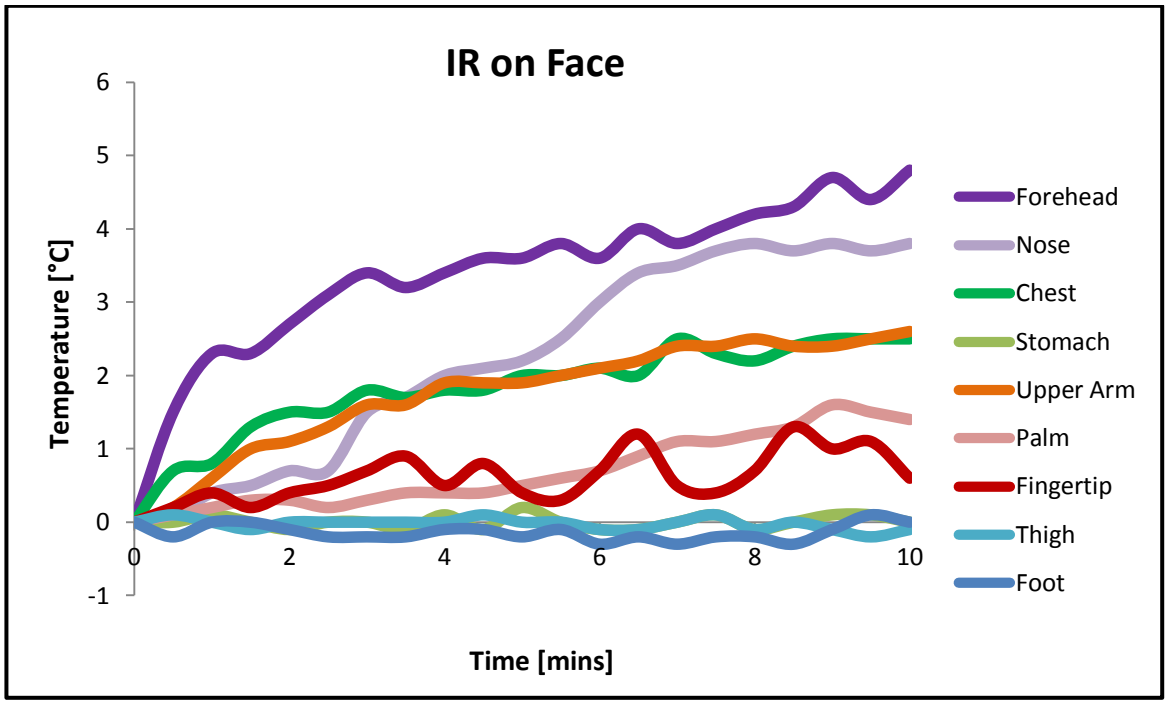

Figure 59 - Subject 1 Full Body Test: Temperature change data for IR on Face test

Figure 60 shows the actual temperatures of several areas of the body throughout the test. Though less distinct, the groupings of the core and secondary areas still generally hold. High forehead and chest temperatures are seen, both with initial temperatures 3.8°C below the estimated core temperature. These two areas diverge in temperature towards the end of the test, with a chest temperature 1.6°C below and a forehead temperature 0.6°C above the estimated core temperature. There is also a secondary grouping of lower stomach, upper arm, palm, and thigh temperatures ranging 5-9°C below the estimated core temperature throughout the test. The nose temperature varies over the range of the secondary group, gradually moving from its lower to upper temperatures. The foot temperature lies approximately 10°C below the estimated core temperature throughout, and the fingertip temperature lies even further from the core temperature, approximately 13°C below it for the duration of the test. In this case the temperature distribution across all areas of the body becomes less uniform over the test due to the localised heating of the primary areas to high temperatures.

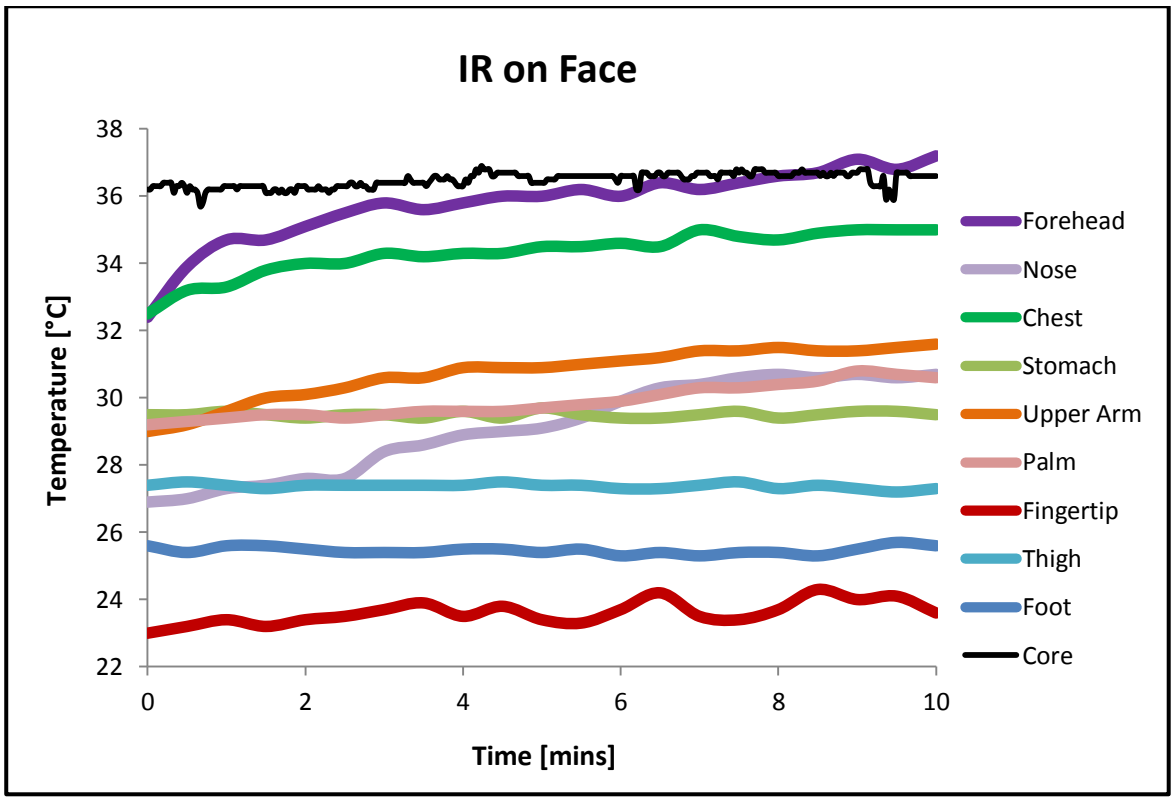

Figure 60 - Subject 1 Full Body Test: Actual temperature data for IR on Face test

Comparison of Full Body Heating under different conditions

In comparing the IR on Face test with the WR test, the most noticeable differences relate to the forehead area of the face and fingertip area of the hand, which are shown for comparison in Figure 61. The palm and nose temperatures differ less noticeably between the tests; they each have similar trends between tests and show only a slightly higher temperature increase during the WR test. This is somewhat unexpected of the nose area, as other areas of the body subject to direct IR heat (forehead, chest and upper arm) all heated to a greater extent during the IR on Face test. The forehead temperature is the best example of the difference in behaviour apparent in the forehead, chest and upper arm areas between the tests. It rises only 1.2°C during the WR test, but over the course of IR on Face test it rises by a total of 4.8°C, even reaching above the estimated core temperature. The fingertip shows the greatest difference in behaviour out of all areas examined. It has the lowest recorded temperature throughout the IR on Face test, with none of the rapid heating behaviour exhibited during the WR test. However, as previously stated the results for this area of the body may be inaccurate due to lack of camera focus on this area during the IR on Face test.

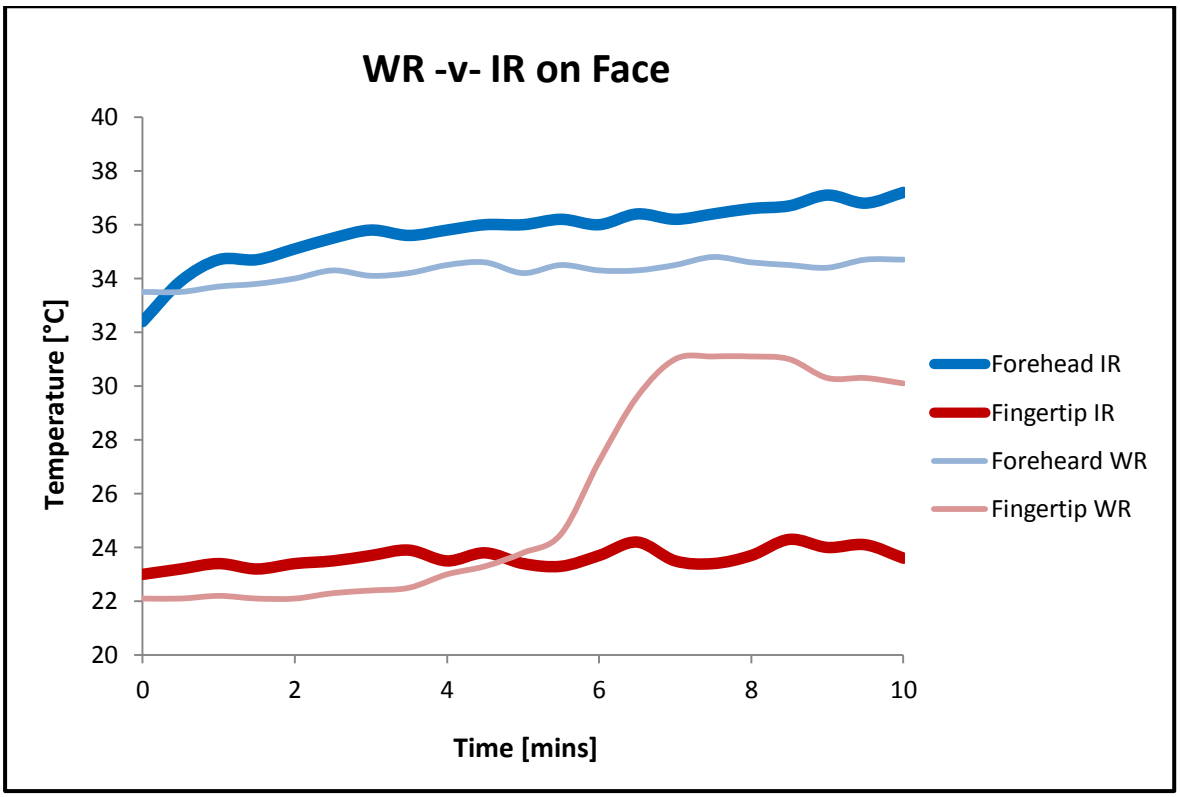

Figure 61 - Subject 1 Full Body Test: WR -v- IR on Face

From analysis of these two Full Body tests the areas of the body identified as being the most interesting from the point of view of their heating capabilities would be the hand and the face. Due to the limiting resolution of the thermal imaging camera at far distances from the test subject, both of these areas are difficult to accurately monitor when looking at the body as a whole. It is expected that there will be further and more interesting variations in these areas upon closer inspection with an improved image resolution. Therefore in order to gain a more accurate picture of the temperature distributions in these areas further tests are carried out focusing individually on these areas.

Face Test - Warm Room

The subject is brought from a cold room (~19.8°C) into a warm room (~25.6°C) and the temperatures in the face of the subject are monitored. The resulting changes in temperature distribution in the face are shown in Figure 62, and temperature change measurements are taken directly from these images.

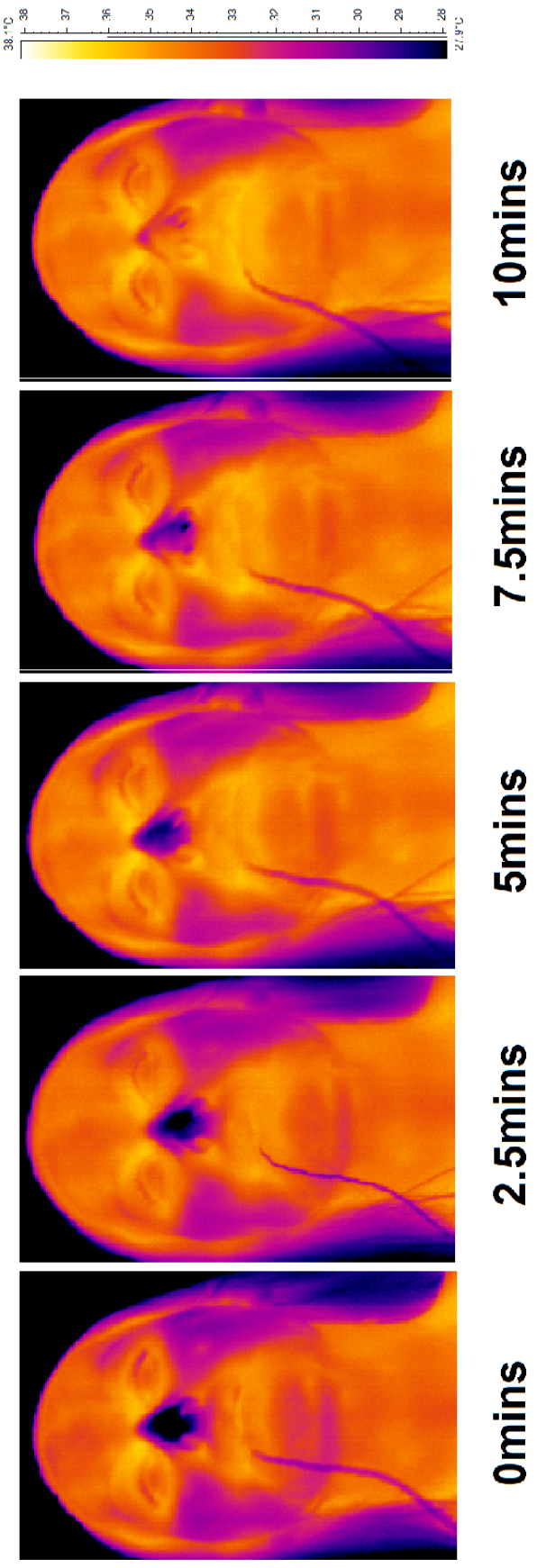

Figure 62 - Subject 1 Face Test: Thermal images of WR test

At the beginning of the test the warmest area of the face is the mouth at 34°C, followed by the forehead and chin areas at around 32.7°C. The cheeks are somewhat cooler, and the nose tip is the coldest area of the face at 26.5°C. Observation of the thermal images shows that the greatest temperature changes occur in the nose tip area, which very gradually rises in temperature to finish the test near to the forehead and chin temperatures. The cheeks can be seen to warm slightly but by the end of the test they are the coolest areas of the face.

Figure 63 allows for further inspection of the numerical results derived from the thermal images. It can be seen that the forehead and chin temperatures are very similar throughout the test, with the mouth and cheek temperatures remaining respectively 1.5°C above and 2°C below these areas throughout. Each of these three areas shows an increase between 1-2°C over the course of the test. The numerical results agree with the visual inspection in that the nose temperature begins far below the temperatures of the other areas of the face, but by the end of the test approaches the forehead and chin temperatures giving an overall nose temperature rise of 6.7°C. Hence the final temperature range within the face has dropped to 3.5°C from an initial range of 7.5°C resulting in a much more uniform temperature distribution.

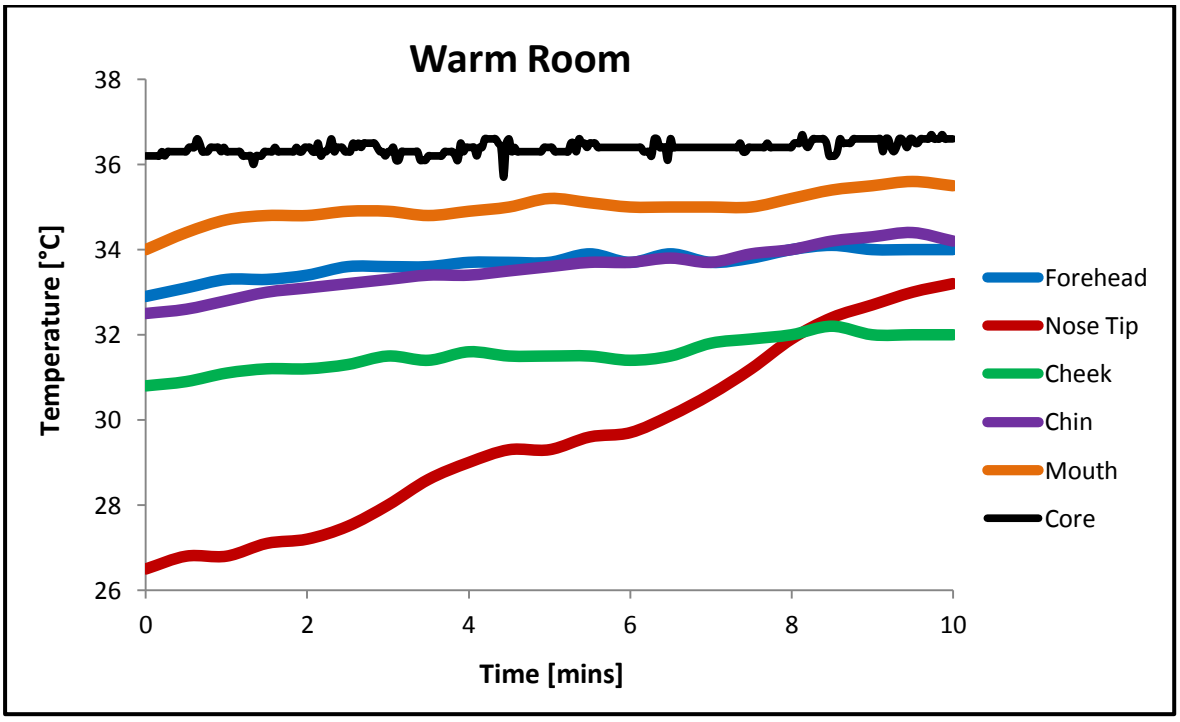

Figure 63 - Subject 1 Face Test: Actual temperature data for WR test

Face Test - IR on Face in Cold Room

The subject is positioned in a cold room (~20.8°C) and IR heat (26.5°C at the centre position) is applied to the face area. Monitoring of the temperatures in the face areas of the subject resulted in the changes in temperature distribution shown in Figure 64. At the start of the test the warmest area of the face is the mouth area at 34.1°C. The rest of the face is cooler, the nose tip being the coldest area at 28.7°C. At 2.5mins the temperatures in the face can be seen to have risen substantially throughout, most noticeably in the nose area. The highest temperatures at this point can be seen to be hot spots on the forehead, nose tip, cheek, chin, and around the mouth area, and the overall temperature of the face is fairly uniform if the sides of the face are ignored. From 2.5mins onwards the temperatures increase more gradually, appearing to maintain a fairly steady state from 5mins. The temperatures of the face areas appear even more uniform at this time.

The numerical results for this test are shown in Figure 65. The forehead, cheek and chin temperatures are similar throughout the test and give a good representation of the temperature of most of the centre of the face, disregarding the hot spot areas and sides of the face. These areas begin the test at temperatures of approximately 33°C, rise gradually until reaching a steady state at approximately 7mins, and finish at temperatures of around 36.5°C.

The overall temperature range across the face can be seen to have decreased dramatically by the end of the test, from an initial range of 5.1°C to only 1.1°C, giving an end result of quite an even temperature distribution.in the face area. The nose tip temperature at the beginning of the test is quite low at 28.5°C, but rises very rapidly upon the application of IR heat, reaching a temperature of around 36°C within 30seconds. The mouth area has the highest initial temperature, but converges with the nose temperature at this time. From this point on the nose tip and around the mouth are considered hot spot areas, rising above the estimated core temperature to 37.5°C. This temperature can be taken as an approximate value for all of the hot spot areas.

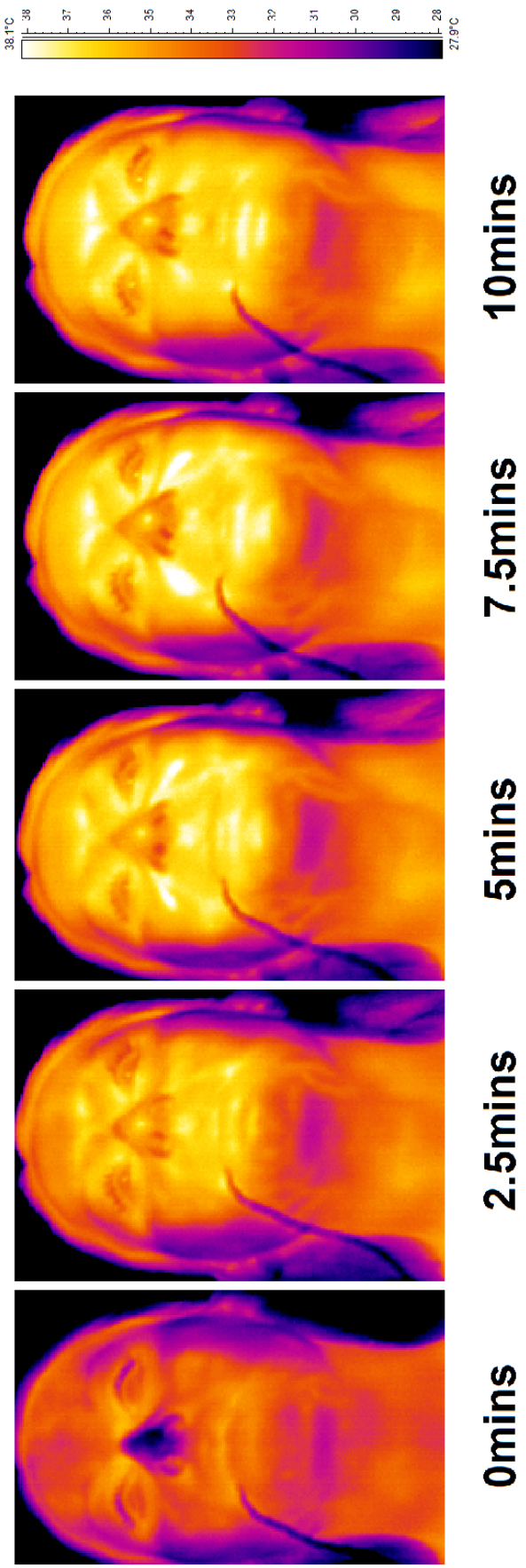

Figure 64 - Subject 1 Face Test: Thermal images of IR on Face test

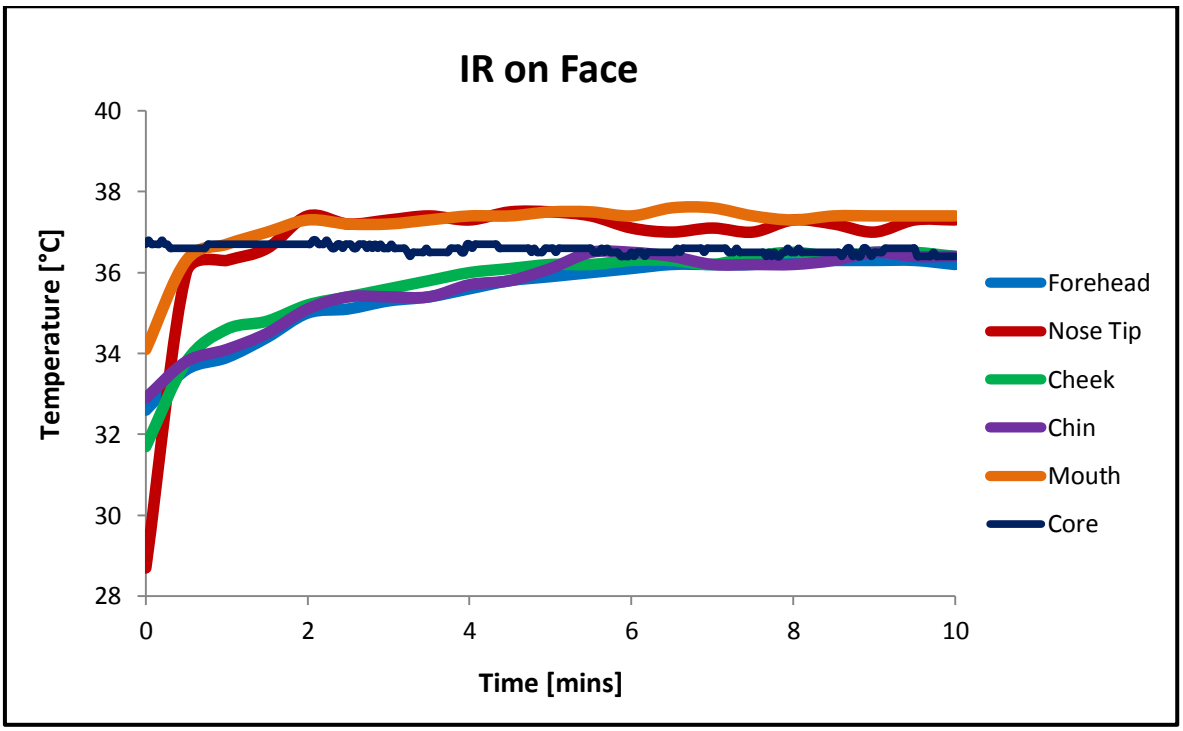

Figure 65 - Subject 1 Face Test: Actual temperature data for IR on Face test

Comparison of Face Heating under different conditions

Comparing the WR and IR on Face tests for the face it should be noted that the starting temperatures of the cheek and nose tip areas are somewhat dissimilar for the two tests, but are considered significantly close for qualitative comparisons to be made. The most obvious difference is that the temperature increases and overall temperatures for the IR on Face test are significantly higher for all face areas. This shows that the application of IR heat to the face at a maximum central temperature of 25.6°C heats the face more effectively than the air in a warm room maintained at a similar temperature. The common trend for the WR test can be seen to be an even gradual slope. The common trend for the IR on Face test differs most clearly from that of the WR test by being split into two stages; over first 30seconds showing a larger initial slope, and followed after by a more gentle slope and finally a relatively steady state. The area with the greatest difference with respect to trend is the nose tip temperature. The gradual temperature increase of the WR test is in clear contrast with the rapid initial increase during the IR on Face test. The WR test slowly heats the area over the entire 10mins of the test as the body remains in contact with the warm air, but the IR heat immediately affects the area directly in its path causing dramatic skin temperature increase to a steady state level within 2mins.

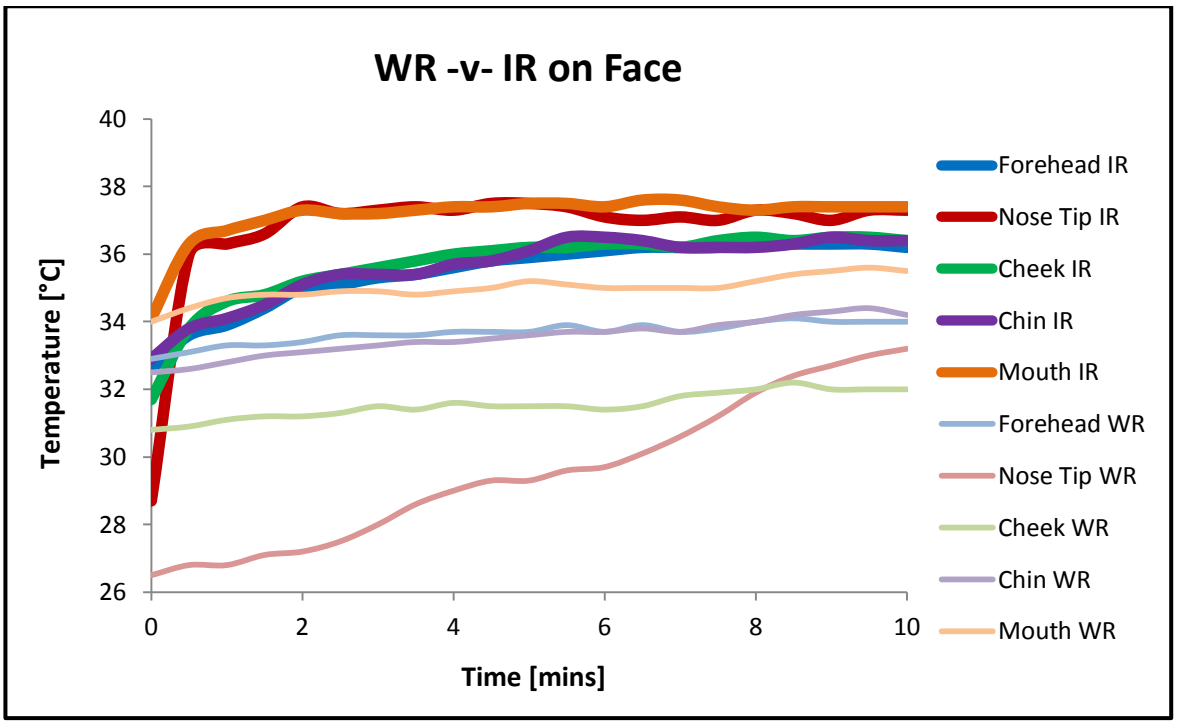

Figure 66 - Subject 1 Face Test: WR -v- IR on Face

Hand Test – Warm Room

The subject is brought from a cold room (~20°C) into a warm room (~25.8°C) and the hand temperatures of the subject are monitored. The resulting changes in temperature distribution about the hand are shown in Figure 67. It can be seen from the figure that the temperature of the whole hand increases dramatically over the course of the test. At the beginning, the warmest part of the hand is the centre of the palm (29.6°C), with temperatures falling towards the edges of the palm and beginning of the fingers. The coldest part of the hand is the fingertip areas, which have temperatures ranging from 21.3-23.3°C depending on the finger. The hand can be seen to heat very quickly, and at 2.5mins into the test change is already visible. At this point the centre palm temperature has risen to 32.3°C and most of the fingertips have reached temperatures of around 31.5°C. The fingertips are the first part of the hand to approach the centre palm temperature, and are at a higher temperature than the middle sections of the fingers and edges of the palm at the 2.5min point. At 5mins into the test the entire hand has been heated almost to its final temperature, and in the remainder of the test the temperatures level off and become stable at approximately 34°C for both the palm centre and the fingertips, with the edges of the palm at a slightly lower temperature.

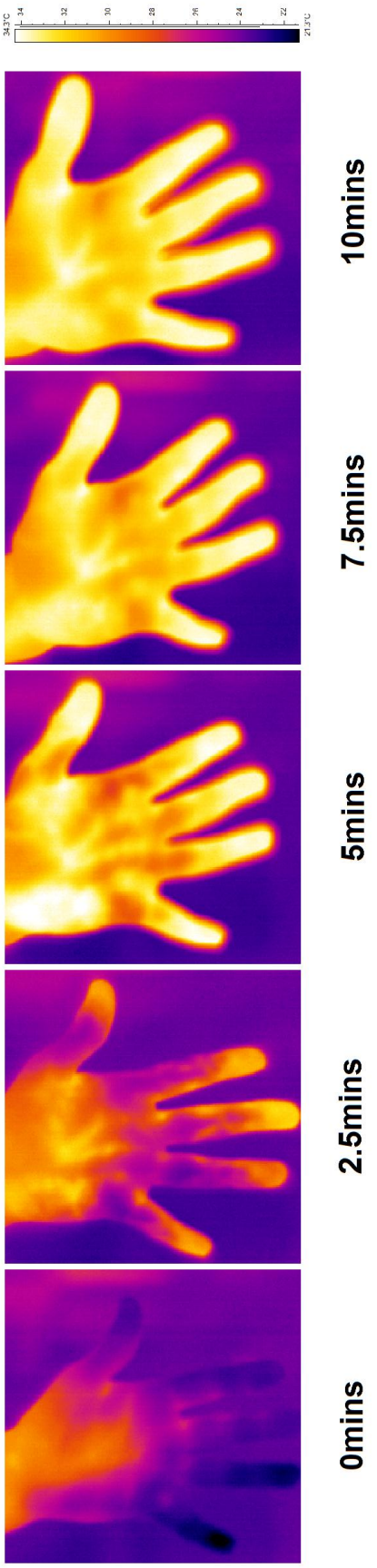

Figure 67 - Subject 1 Hand Test: Thermal images of WR test

Figure 68 presents the numerical data for the test. The interesting point to note here is that from a difference between palm and fingertip temperatures of 6.3°C at the beginning of the test, the values for the two areas converge after approximately 3-4mins and from that point onwards remain steady in temperature until the end of the test. The rapid rise in fingertip temperature can be seen clearly here, and it is shown to complete its entire rise in temperature between the times of 1min to 3.5mins. The palm temperature rise is more gradual and takes around 4mins to reach a steady state.

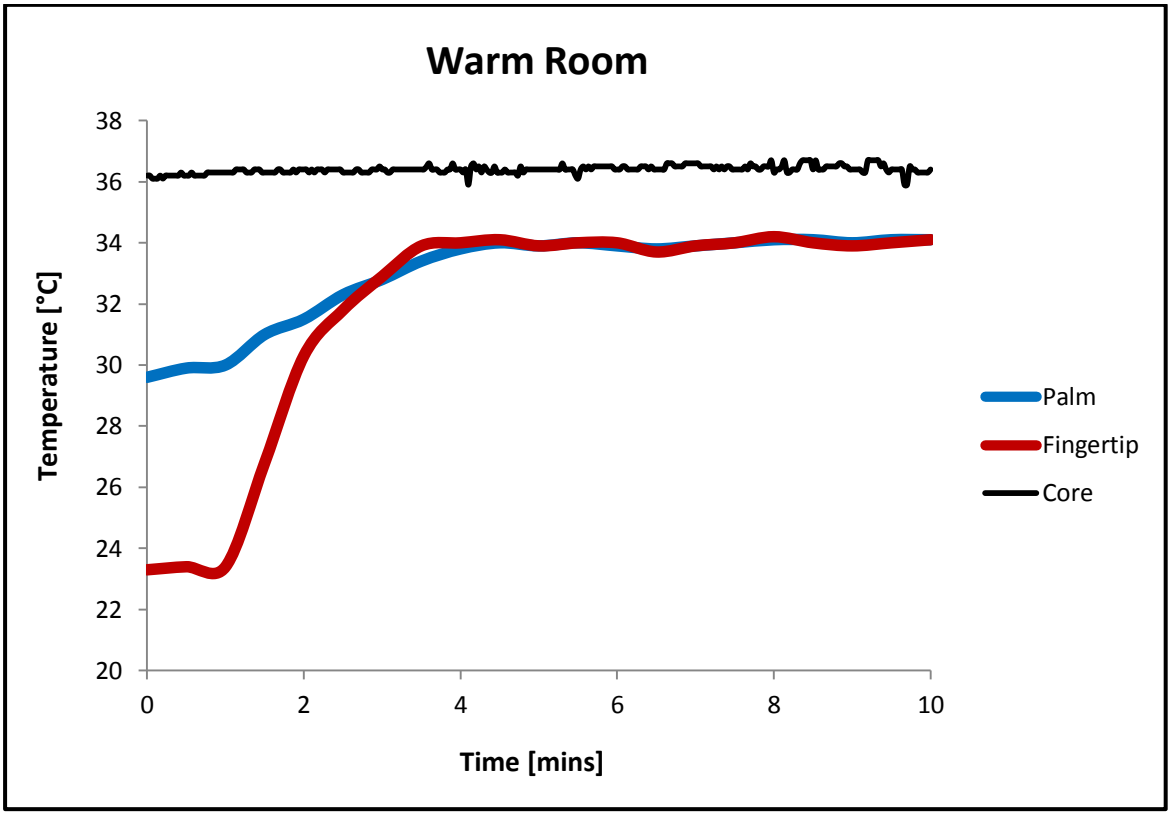

Figure 68 - Subject 1 Hand Test: Actual temperature data for WR test

Heat flux measurements recorded during this test are shown in Figure 69. *[Note: The primary axis shows the heat flux data, whilst the secondary axis shows the aforementioned palm and fingertip temperature variation data].* It can be seen from the figure that the heat flux value is negative for the first 2mins of the test, which shows that the hand is receiving energy from the surrounding warm air. The slope of the heat flux is also negative for the first 1min of the test, showing that the hand is further increasing its heat intake from the warm air at this time. The minimum heat flux value over the course of the test is $-1.26 \times 10^{-3}\, W/cm^2$ and after this point the slope of the heat flux becomes positive. This change in slope corresponds directly to the point where the hand temperatures begin to most rapidly increase (at 1min) and at this time heat intake begins to

be reduced. The heat flux value can be seen to change from a negative to positive value at the point where the palm temperature and fingertip temperatures are approximately 6.1°C and 5.2°C above the room temperature respectively. This change in value shows that the hand is now radiating heat to the surroundings. The heat flux increases with rising hand temperature and can be seen to level off just after the hand temperature reaches a steady state. However, a second rise in heat flux value is unaccompanied by a temperature rise in the palm and fingertip areas. The heat flux value is positive for the remainder of the test, reaching a maximum value of $4.05 \times 10^{-3} W/cm^2$ at 9.5mins.

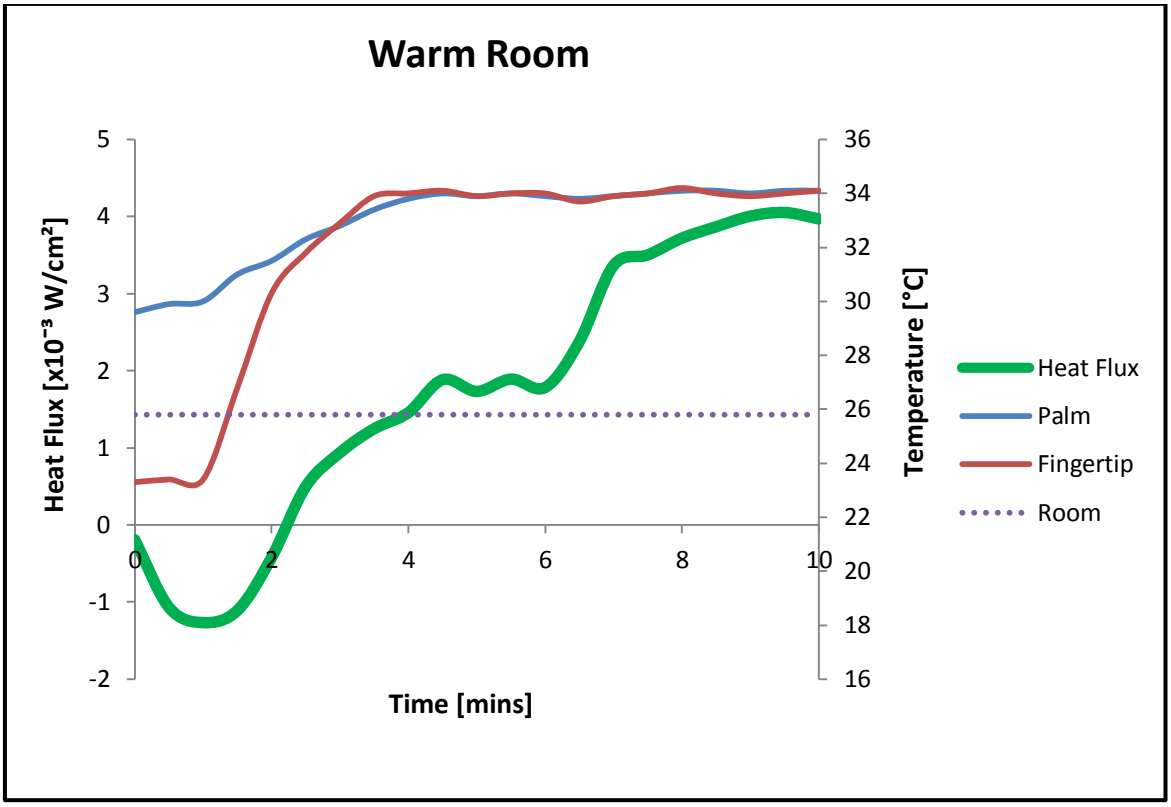

Figure 69 - Subject 1 Hand Test: Heat flux data for WR test

Hand Test –IR on Face in Cold Room

The subject is positioned in a cold room (~20.8°C) and IR heat (26.5°C at the centre position) is applied to the face area. The hand temperatures of the subject are again monitored. Figure 70 shows the resulting changes in temperature distribution about the hand. There is a dramatic increase in the temperature of the hand over the course of the test, particularly in the fingers. At the start of the test the entire palm (31.9°C) is noticeably warmer than the fingers (fingertips all of similar temperature at around 23.1°C).

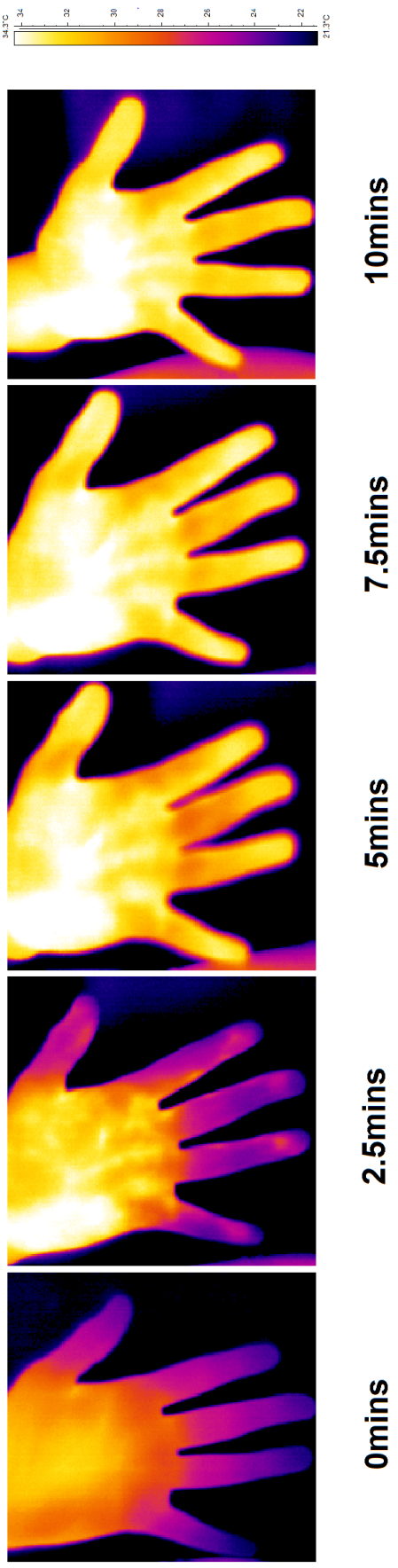

Figure 70 - Subject 1 Hand Test: Thermal images of IR on Face test

At 2.5mins the palm temperature has increased to over 34°C in parts and the first signs of warmer areas in the fingertips are visible. At 5mins the entire hand has been heated to almost its final temperature. All of the fingers have heated throughout over the course of the previous 2.5mins. After this point the temperatures in the hand remain relatively stable for the remainder of the test at 35°C for the palm and a cooler 32.2°C for the finger areas.

Figure 71 shows the numerical results of this test. The palm temperature shows a gentle positive slope up until a time of 6mins when it reaches a steady state of around 35°C having increased by a total of 3.2°C. The fingertip temperature remains constant for the first 2.5mins, and then rises very rapidly from this point up until 4mins into the test. A total fingertip temperature increase of 8.2°C occurs in this time. The overall effect is a more uniform hand temperature, which is now within a range of 2.9°C from an initial range of 8.8°C.

This increase in the hand area temperature is interesting as there is no heat being directly applied to this area. This suggests that a thermoregulatory response is responsible for the heating behaviour shown here.

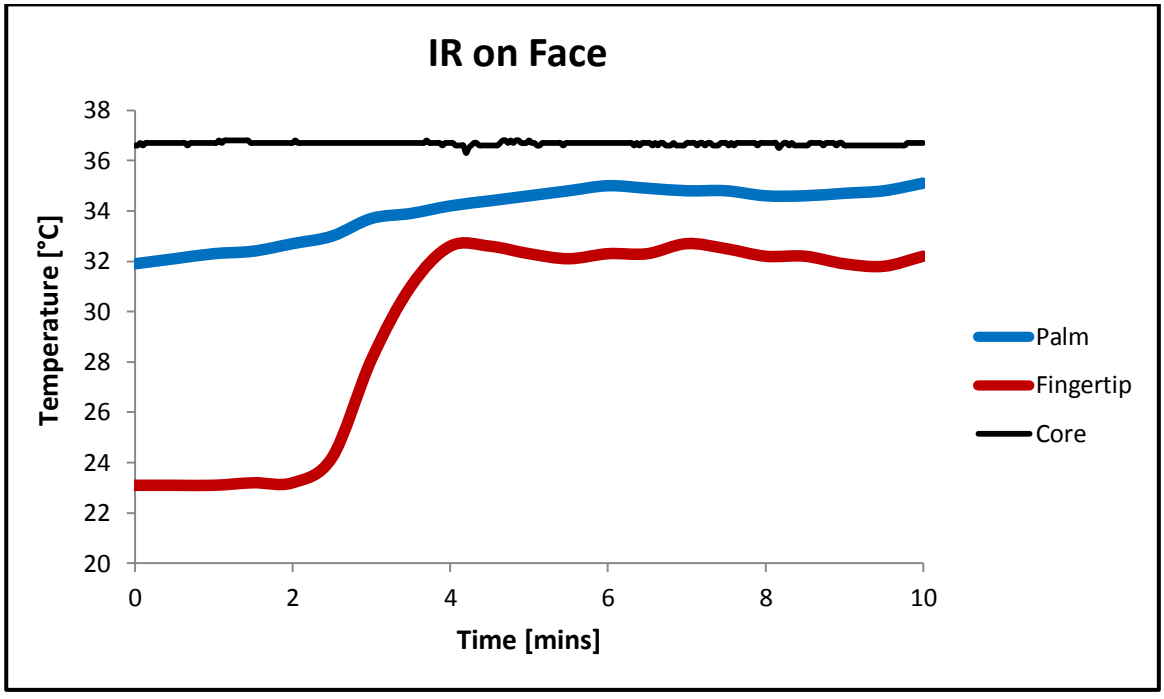

Figure 71 - Subject 1 Hand Test: Actual temperature data for IR on Face test

The heat flux data recorded for this test is displayed in Figure 72. The temperatures in the hand are higher than the room temperature throughout this test. The value for heat flux is

positive throughout which shows that the hand is radiating energy its cooler surroundings all through the test. Initially the slope of the heat flux is negative. The body may be cold at this time and making effort to reduce heat loss though the hands. The minimum heat flux value over the course of the test is $3.54 \times 10^{-3}\ W/cm^2$ and after this point the slope of the heat flux becomes positive. This change in slope corresponds directly to the point where the fingertip temperature begins to rapidly increase (at 2.5min) and at this time heat output begins to increase. The heat flux can be seen to increase with rising fingertip temperature, then to drop off slightly as the fingertip temperature stabilises at 4mins. The palm temperature however continues to rise up until 6mins and so too does the heat flux, after which time it fluctuates around a value of approximately $5.7 \times 10^{-3}\ W/cm^2$. Hence the heat flux is again seen to change with respect to varying temperature in the hand.

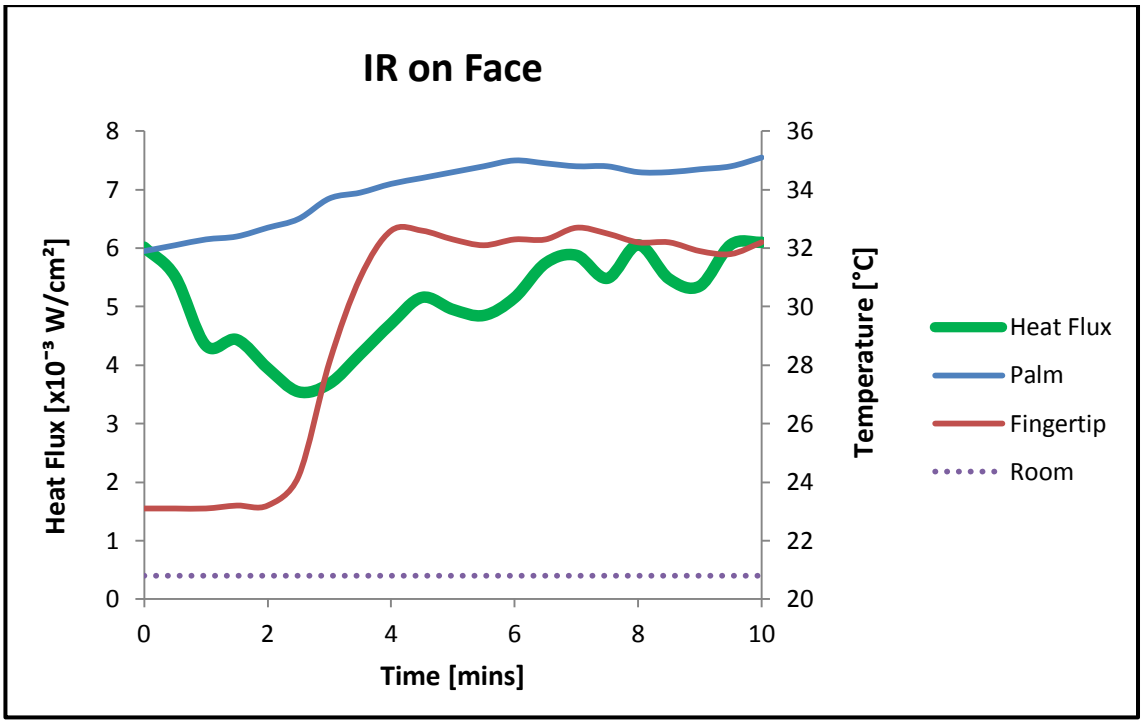

Figure 72 - Subject 1 Hand Test: heat flux data for IR on Face test

Hand Test –IR on Hand in Cold Room

The subject is positioned in a cold room (~20.4°C) and IR heat (26.5°C at the centre position) is applied to the hand area. Figure 73 shows the resulting changes in temperature distribution about the unheated hand. It can be seen here that the temperature distribution behaviour is similar to that of the hand under the application of IR heat to the face area.

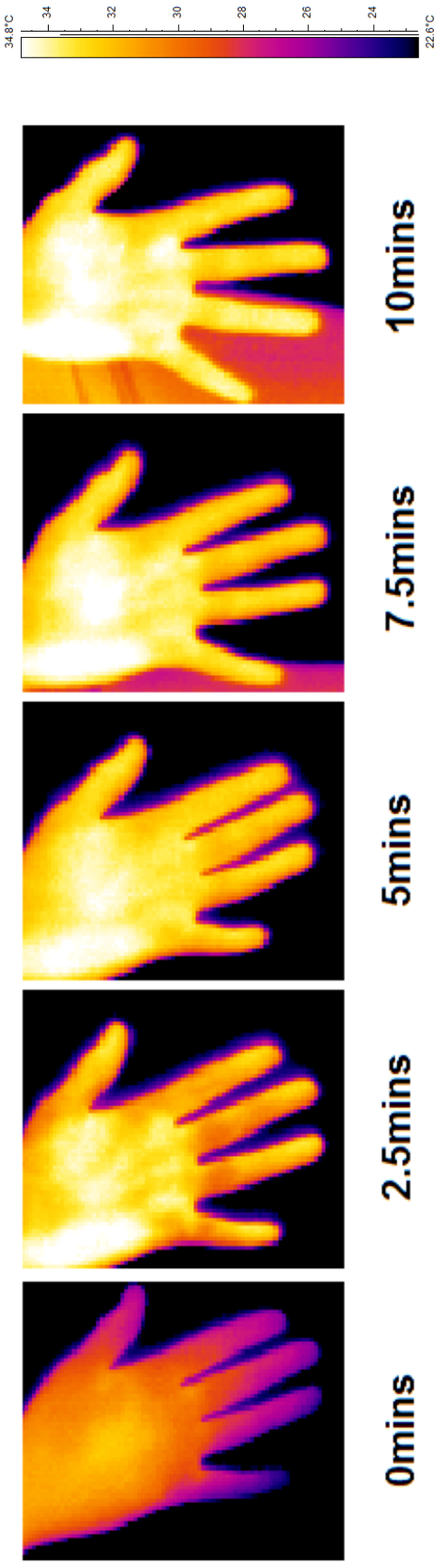

Figure 73 - Subject 1 Hand Test: Thermal images of IR on Hand test

At the beginning of the test the palm centre is noticeably the warmest area at 32.2°C and the fingertips are the coolest areas at 27.2°C, with temperatures in the fingers lying between. The greatest change in temperatures that can be observed from these thermal images occurs over the first 2.5mins, when the temperature across the whole hand rises; the palm centre to 33.4°C and the fingertips to 31.5°C. By 5mins the temperatures in the hand appear quite uniform, with the exception of the palm centre, and temperatures increase by only small amounts for the remainder of the test.

The numerical results from this test are plotted in Figure 74. Both the palm and fingertip areas can be seen here to undergo almost all of their temperature increase within the first 4mins. Overall the palm displays the more gentle rise in temperature, and its temperature increases by a total of 3.7°C over the course of the test. The fingertip temperature increases by 6°C over the course of the test, with over half of this increase occurring between the times of 0.5mins and 1.5mins. The hand is much more uniform at the end of the test with the temperature range across the hand at less than half that at the beginning of the test

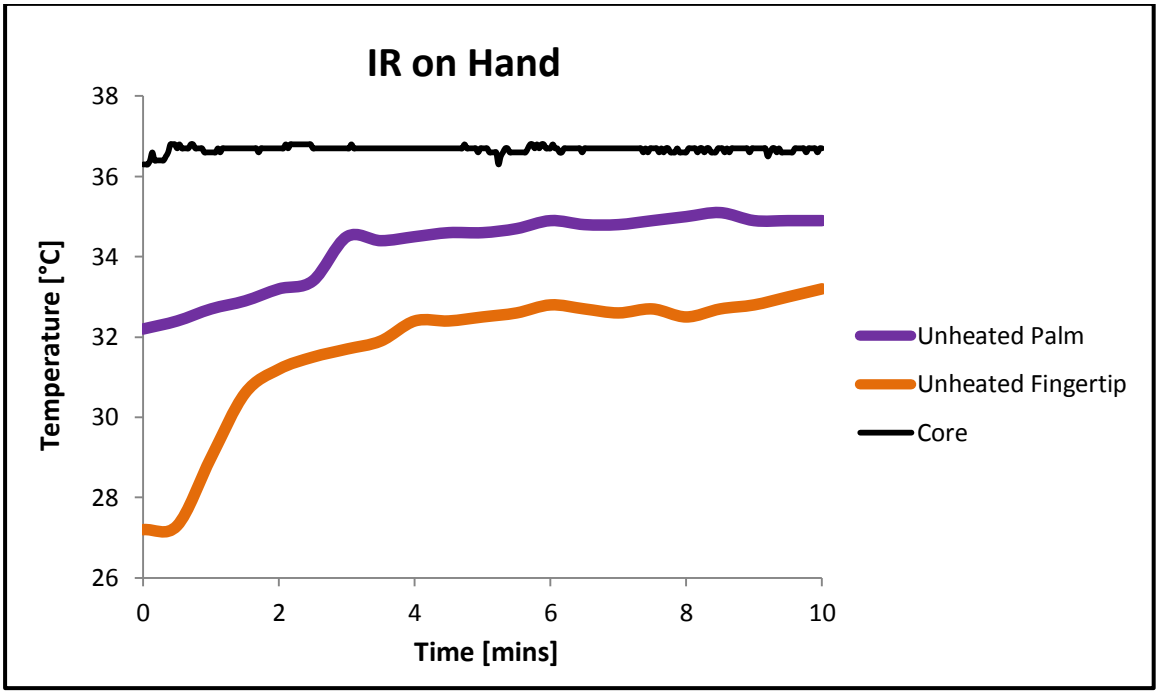

Figure 74 - Subject 1 Hand Test: Actual temperatures for IR on Hand test

Heat flux measurements have not been recorded for this test, but would be expected to behave in a similar manner as before; positive heat flux values throughout due to the air being cooler than the hand temperature, positive slope during increasing hand

temperatures, and negative or horizontal slope during periods of steady temperature or temperature decrease.

Comparison of Hand Heating under different conditions

It should be noted here that different start temperatures may cause discrepancies when comparing between the results over the three tests and comparisons should be made bearing this point in mind.

A comparative plot of the IR on Face and IR on Hand tests is shown in Figure 75. The palm temperature behaviour is very similar between the two tests in relation to both trend and temperature. The trends for the fingertips over the two tests are also comparable; steady state at the beginning followed by a sharp rise and then further steady state. The differences between the trends lie in the timing of the sharp rise which occurs between 0.5mins and 1.5mins for the IR on Hand test, and between 2.5mins and 4mins for the IR on Face test. The start temperatures for the fingertips are different for each of the tests, which makes it difficult to deduce which shows the better heating capability for the fingertip area, but an interesting point to note is that the fingertip temperatures converge over the two tests.

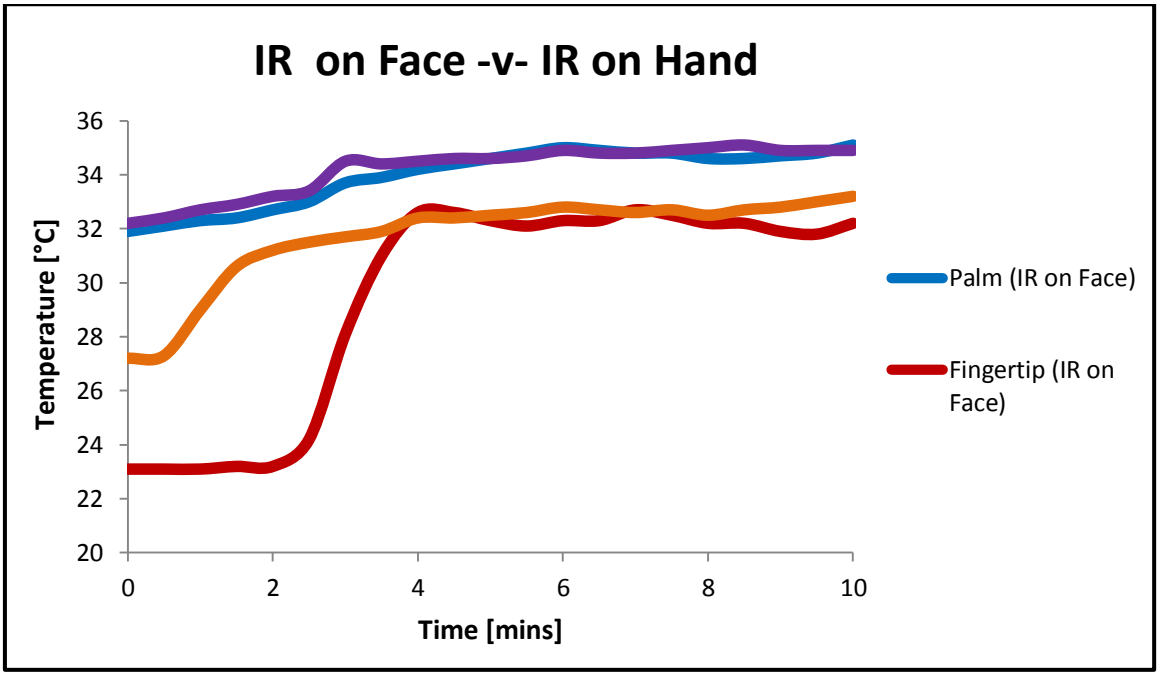

Figure 75 - Subject 1 Hand Test: IR on Face -v- IR on Hand

Comparisons between the Warm Room and both IR tests for the hand show surprisingly similar characteristics considering there is no heat directly applied to the hand in the IR tests.

The WR and IR on Face tests are compared in Figure 76. The overall temperature increase is only a small amount higher for the WR test, and the general shape of the curve produced for both the palm and fingertips is very similar in each case; the palm a gentle slope followed by a steady state, and the fingertips a steady temperature followed by a sharp increase followed by a steady state. The difference between the curves lies mainly in the time at which changes occur. The palm temperature reaches a steady state approximately 1.5mins later in the IR on Face test than in the WR test, and the fingertip temperature undergoes a sharp increase approximately 1.5mins later and reaches a steady state around 30seconds later in the IR on Face test than in the WR test. With relation to heat flux, the heat flux values for the IR on Face test are found to be higher than those for the WR test, suggesting a greater difference between the hand and the air temperatures in the IR on Face test than for the WR test.

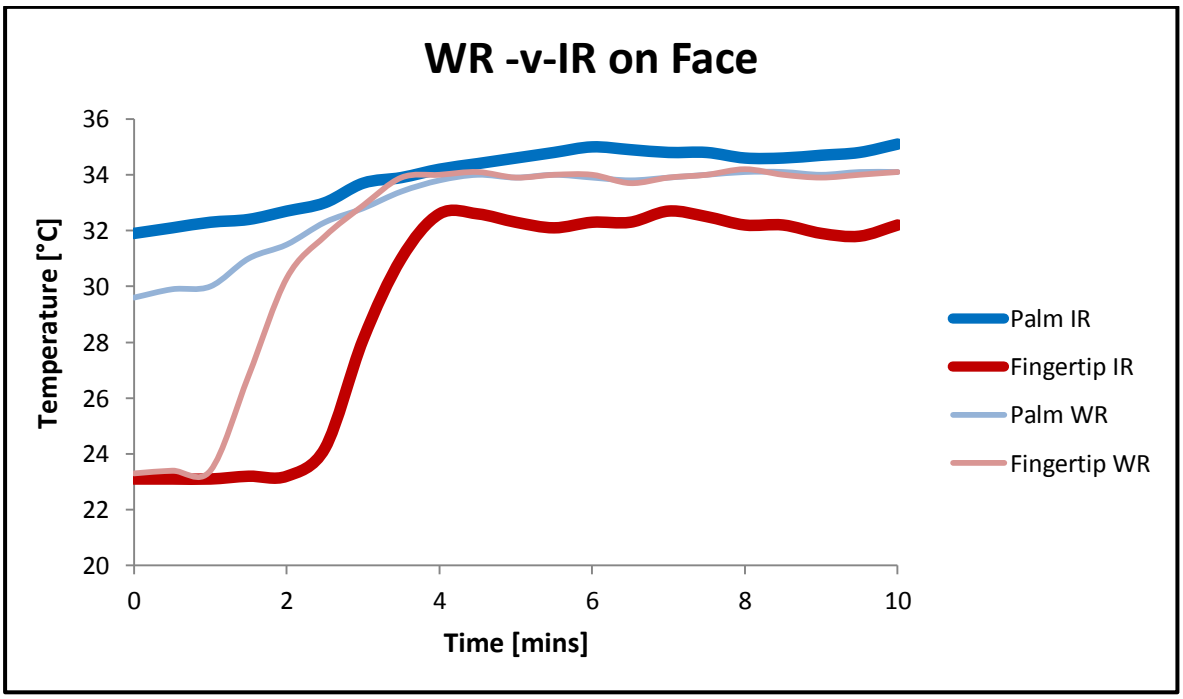

Figure 76 - Subject 1 Hand Test: WR -v- IR on Face

The Warm Room and IR on Hand tests are compared in Figure 77. The trends between the Warm Room and IR on Hand plots show several similarities. The initial palm temperatures differ between the test, but from their respective starting points show a fairly

similar trend, with a gradual rise over the first 4mins followed by a relatively steady state. The fingertip start temperatures also differ, but both show the trend of an initial steady state, followed by a rapid rise, followed by steady state. The difference in trend relates to timing, as the rapid increase occurs around 30seconds earlier and ends around 1.5mins earlier in the IR on Hand test than in the WR test. The fingertip temperature also reaches a fully steady state approximately 2.5mins later in the IR on Hand test than in the WR test.

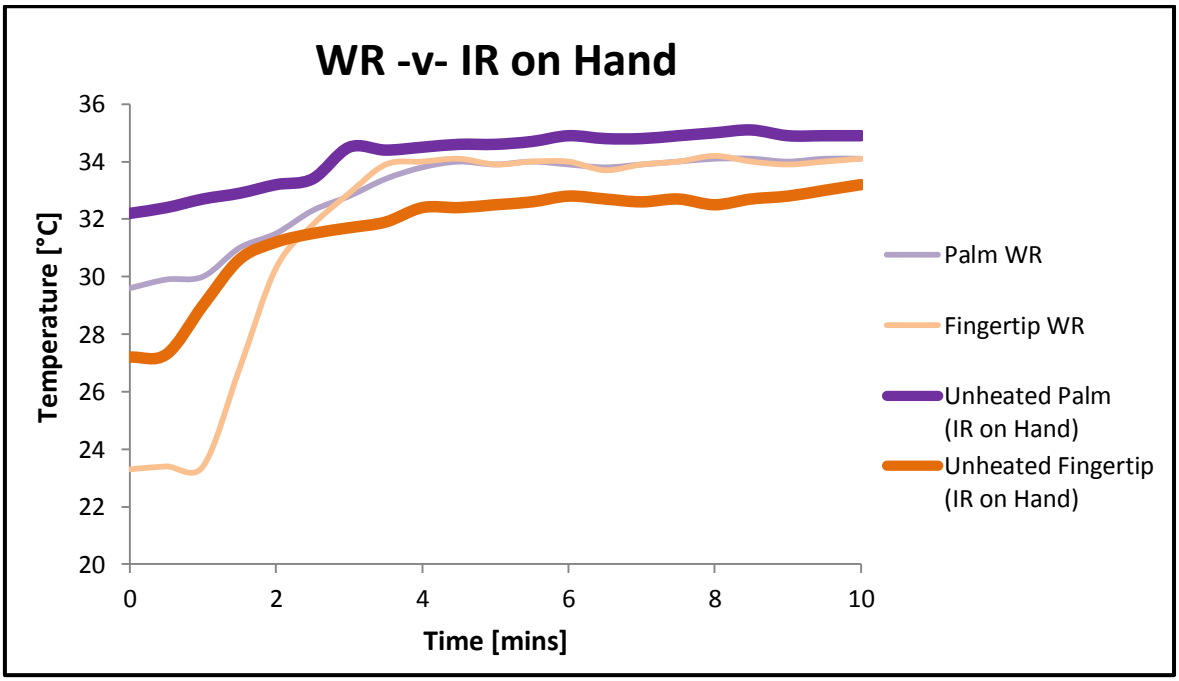

Figure 77 - Subject 1 Hand Test: WR -v- IR on Hand

4.3.1.2 Subject 2

Full Body Test - Warm Room

The subject is brought from a cold room (~18°C) into a warm room (~24.3°C). Figure 78 displays thermal images which show the resulting changes in skin temperature distribution about the body over the course of the 10min test. The most evident change observable from the images occurs in the hands, and the majority of this change appears to occur quite rapidly between the times of 2.5mins and 5mins. The nose area also becomes noticeably warmer during the test. This temperature change occurs more gradually than the change in the fingertips, and to a lesser extent. There are no other visible changes apparent from inspection of these images, and so to investigate more subtle changes, numerical data from the test will be analysed.

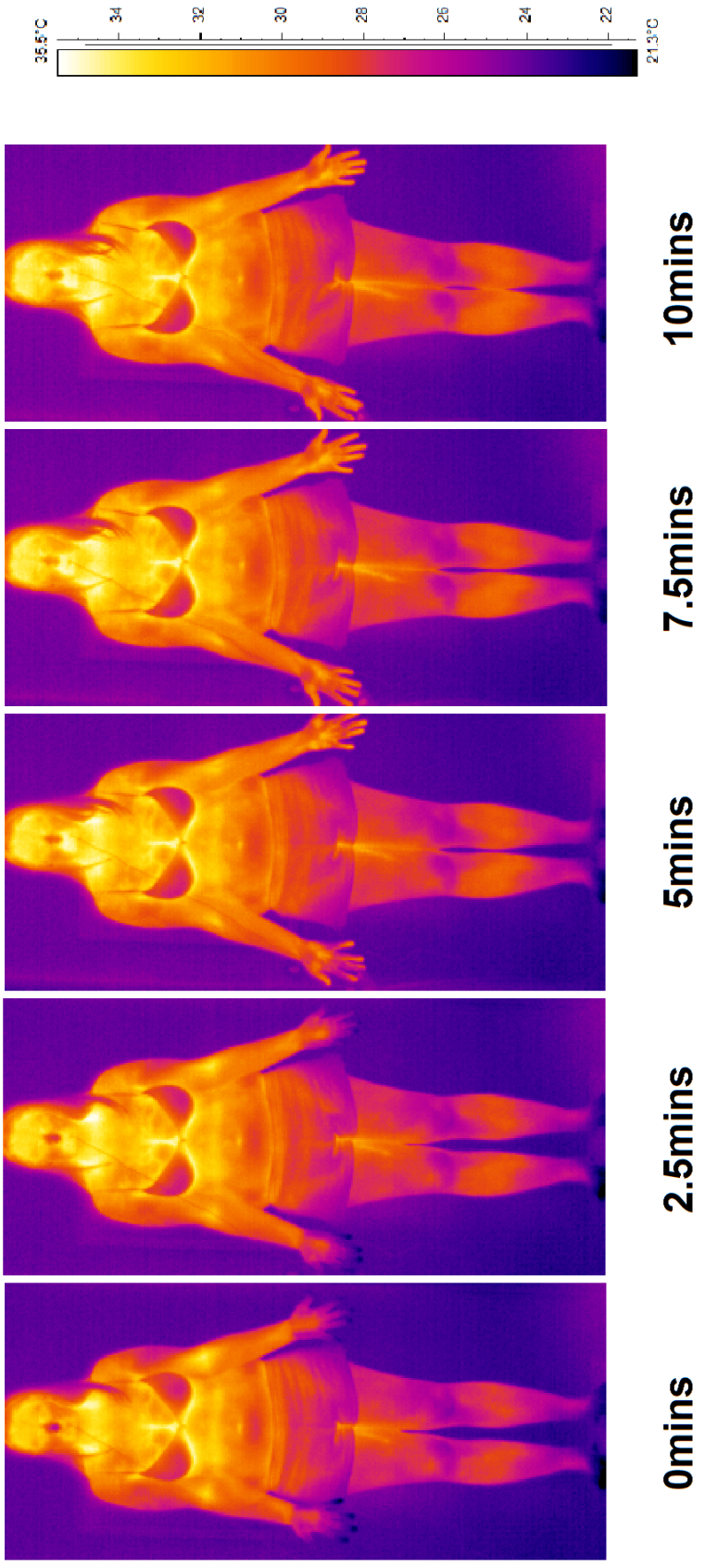

Figure 78 - Subject 2 Full Body Test: Thermal images of WR test

From Figure 79 the change in temperature of each area can be more clearly seen. The largest increases in temperature occur in the fingertip (8.4°C), nose (4.6°C) and palm (3°C) areas, as previously proposed. All other areas of the body increased in temperature by a small amount ranging between 0.3-1.3°C. The rapid rise in hand temperature that was observed between the 2.5min and 5min thermal images can also be further investigated here, and it can be seen that there is a fingertip temperature increase of 7.3°C between the times of 3.5min and 5.5min, almost 87% of the overall change.

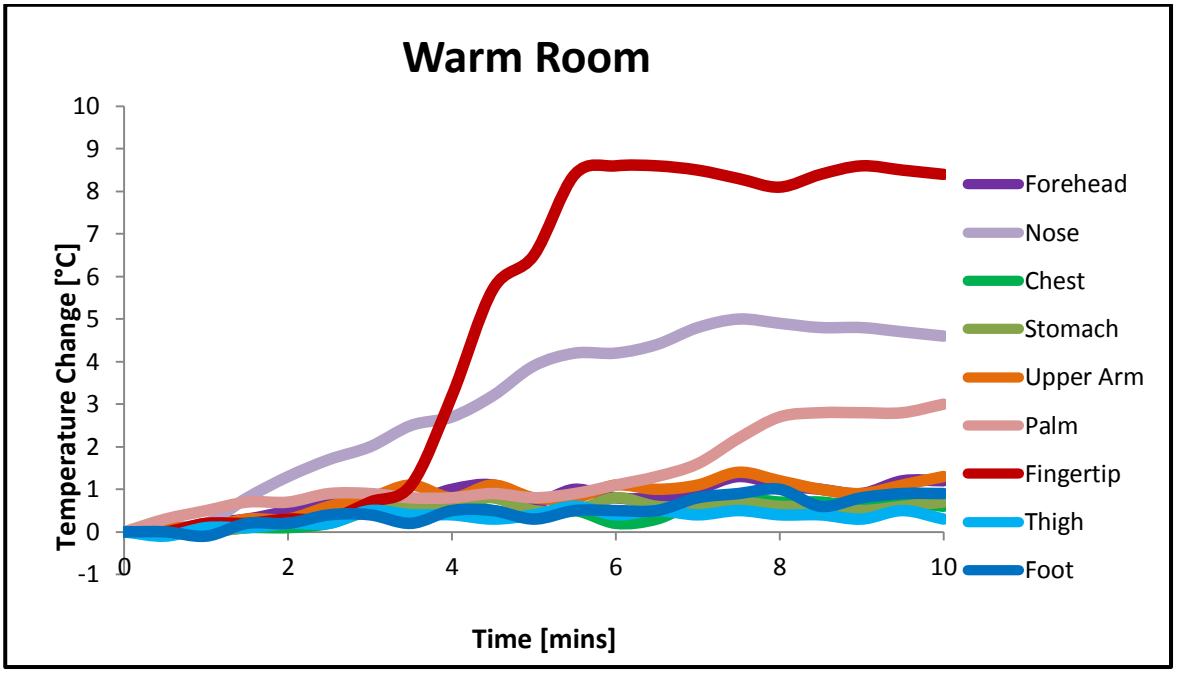

Figure 79 - Subject 2 Full Body Test: Temperature change data for WR test

Figure 80 shows the actual temperatures of several areas of the body during the test. The primary areas (forehead and chest), lie 2-3°C below the estimated core temperature throughout the test. The secondary areas of the thigh, palm, upper arm and stomach all begin at temperatures close to 8°C below the estimated core temperature and end the test between 6.5-7.7°C below (with the exception of the palm temperature which rises to just 4.7°C below the estimated core temperature). The nose and foot temperatures have similar initial temperatures around 10°C below the estimated core temperature but from this point on these extremities behave entirely differently; the nose temperature gradually rises, and by the end of the test lies only slightly below the palm temperature, which also shows good heating capabilities, whilst the foot temperature remains approximately 10°C below the estimated core temperature throughout. The fingertip shows an even better heating capability than the nose and palm. At 14°C below the estimated core temperature, the

fingertip has the lowest initial temperature out of all of the areas. By the end of the test however, the fingertip temperature lies slightly below the nose temperature, only 5.8°C below the estimated core temperature.

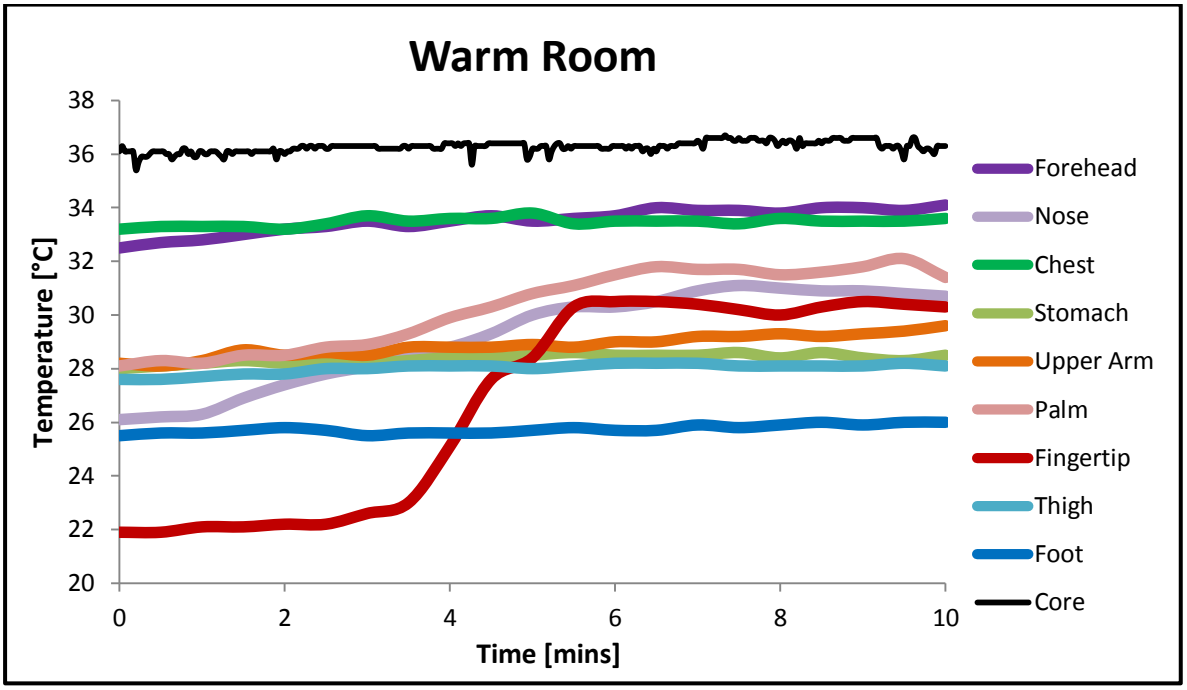

Figure 80 - Subject 2 Full Body Test: Actual temperature data for WR test

Full Body Test – IR on Face in Cold Room

The subject is positioned in a cold room (~17.6°C) and IR heat (26.5°C at the centre position) is applied to the face area. Figure 81 shows the resulting changes in temperature distribution around the body. The most obvious changes which can be seen from these images occur in the face, upper torso and hand regions. The face and upper torso can be seen to increase in temperature throughout the test as IR heat is applied, the most dramatic increase occurring within the first 2.5mins of the application of heat. The majority of the temperature increase in the hand area appears to occur between the 5min and 7.5min images. Changes in other areas of the body are not perceptible from these images.

Figure 82 shows the change in skin temperature experienced by different areas of the body regardless of initial temperature. From this figure it can be seen that the areas with the largest increase over the course of the test are indeed the areas that lie within the head, upper torso and hand regions; the forehead (4.8°C), the fingertip (3.9°C), the nose (3.1°C), the upper arm (2.6°C), the chest (2.5°C), and to a lesser extent the palm (1.4°C).

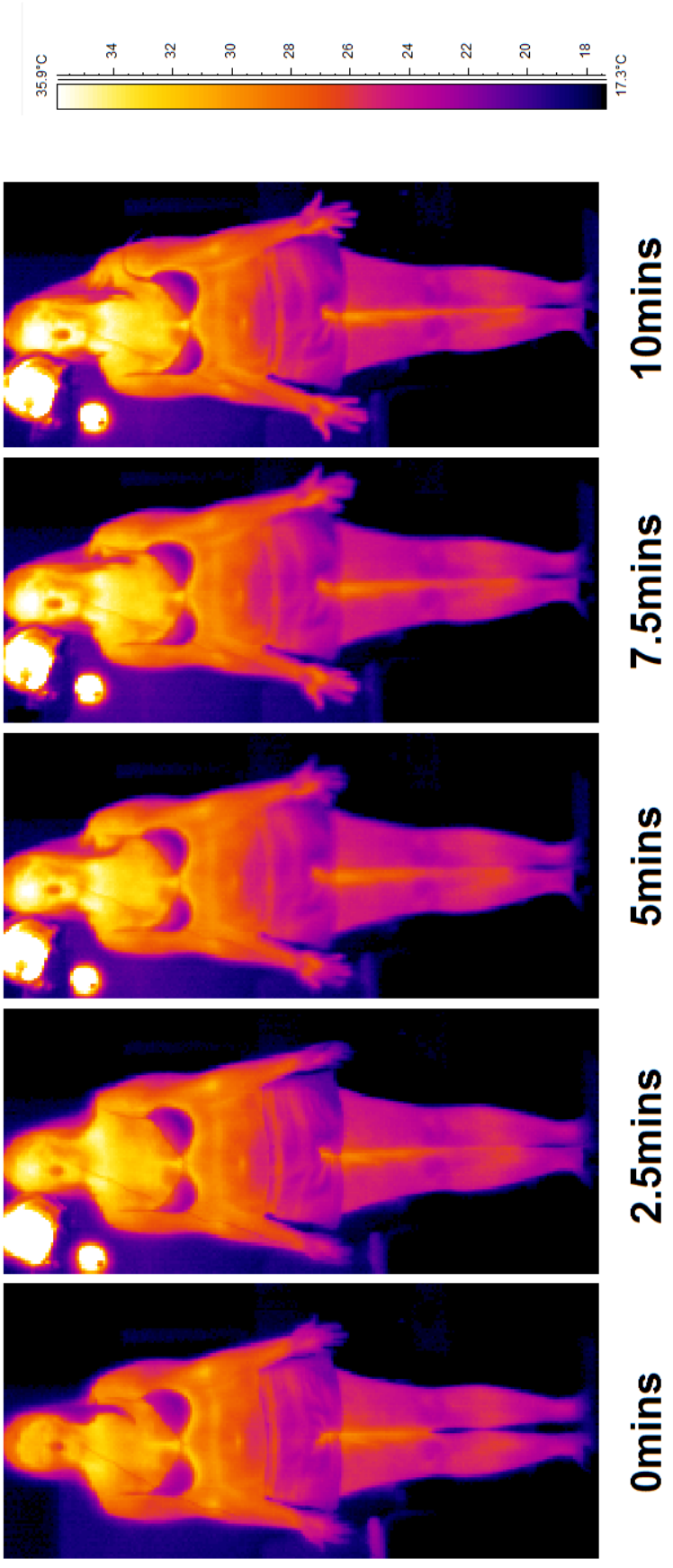

Figure 81 - Subject 2 Full Body Test: Thermal images of IR on Face test

The rise in temperature of the head and upper torso regions is expected as the main IR heat is focused on the face, with the peripheral emanating heat flux having a lesser heating effect on the upper torso and upper arm. Several areas of the body which are simply exposed to the cold air in the room (the foot, thigh, and stomach areas) show no temperature gain over the course of the test, with temperature change values fluctuating around the zero mark. The interesting observation to be made here is that both hand areas show a noticeable temperature increase, and are amongst the areas identified as having the largest rise in temperature over the course of the test. This is particularly true for the fingertip regions, which show the second largest temperature increase despite the fact that they are not in in the directional path of the IR heat. This would suggest that the hand area is being heated by thermoregulation.

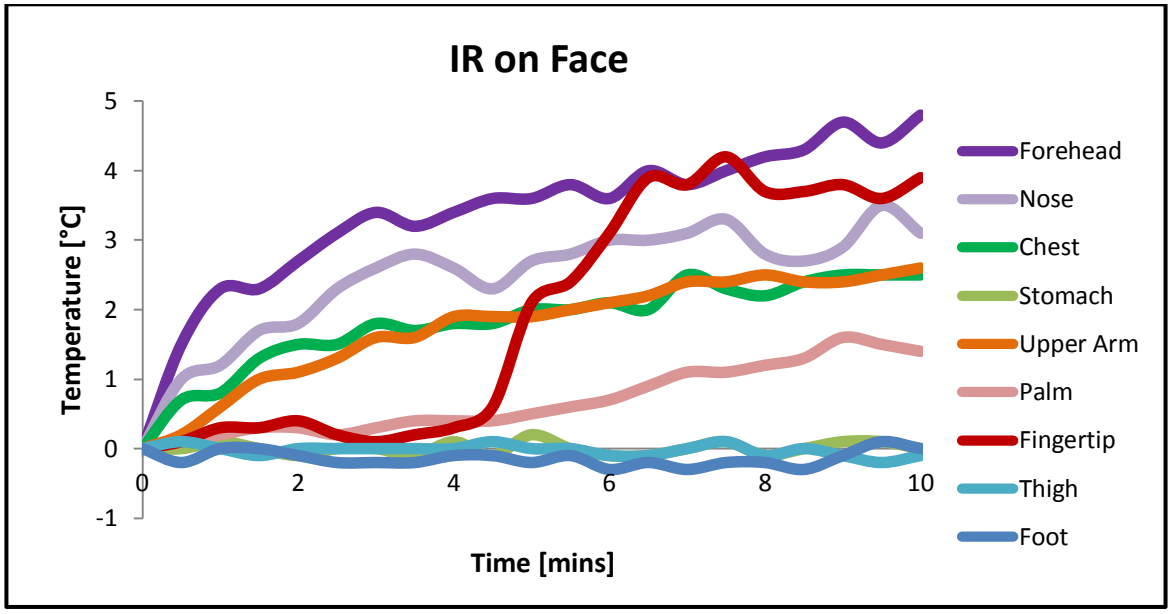

Figure 82 - Subject 2 Full Body Test: Temperature change data for IR on Face test

Figure 83 shows the actual temperatures of several areas of the body throughout the test. Grouping of the primary and secondary regions can again be seen here. High forehead and chest temperatures are apparent, with similar initial temperatures around 5.7°C below the estimated core temperature. However, these areas diverge in temperature as the test progresses, with a chest temperature 3.6°C below and a forehead temperature 0.5°C above the estimated core temperature. There is also a clear secondary grouping of lower stomach, upper arm, palm, nose, and thigh temperatures ranging 7.5-11.8 ° C below the estimated core temperature throughout the test. The foot temperature lies approximately 15°C below the estimated core temperature throughout the test. The fingertip temperature

initially lies16.5°C below the estimated core temperature, making it the coldest area of the body at the beginning of the test, but by the end of the test this area has warmed and lies only 12.7°C below the estimated core temperature, almost to within the secondary group range.

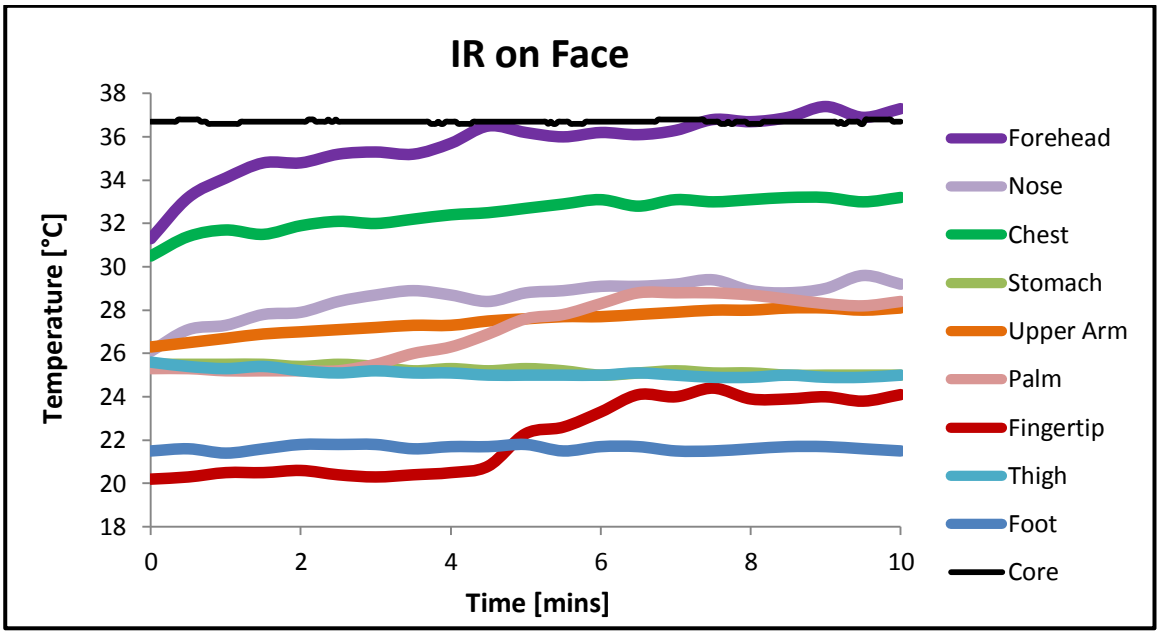

Figure 83 - Subject 2 Full Body Test: Actual temperature data for IR on Face test

Comparison of Full Body Heating under different conditions

Comparison of the WR and IR on Face tests show that the most noticeable differences between the tests relate to the forehead area of the face and the fingertip area of the hand, which are plotted together for comparison in Figure 84. The palm and nose temperatures have similar trends between tests, and show lesser overall temperature change than the forehead and fingertip regions. They both gain higher overall temperatures during the WR test. The nose areas differs in this way from the other areas of the body which are subjected to direct IR heat (forehead, chest and upper arm), as these all gained higher overall temperature increases during the IR on Face test. The forehead temperature is the best example of the difference in behaviour observed in the forehead, chest and upper arm areas between the tests, rising by 4.8°C during the IR test, above even the estimated core temperature, compared to a rise of only 1.2°C during the warm room test. Although the overall temperature increase in the fingertips is substantially higher in the WR test, a similar trend can be observed for both tests, consisting of an initial steady temperature followed by a sharp increase to a new steady temperature. This is an interesting result as it

shows that the fingertips are heated in a somewhat similar manner despite the fact that the WR case involves the direct application of warm air to the fingertips along with the movement of heat within the body, and the IR case involves only the latter of these.

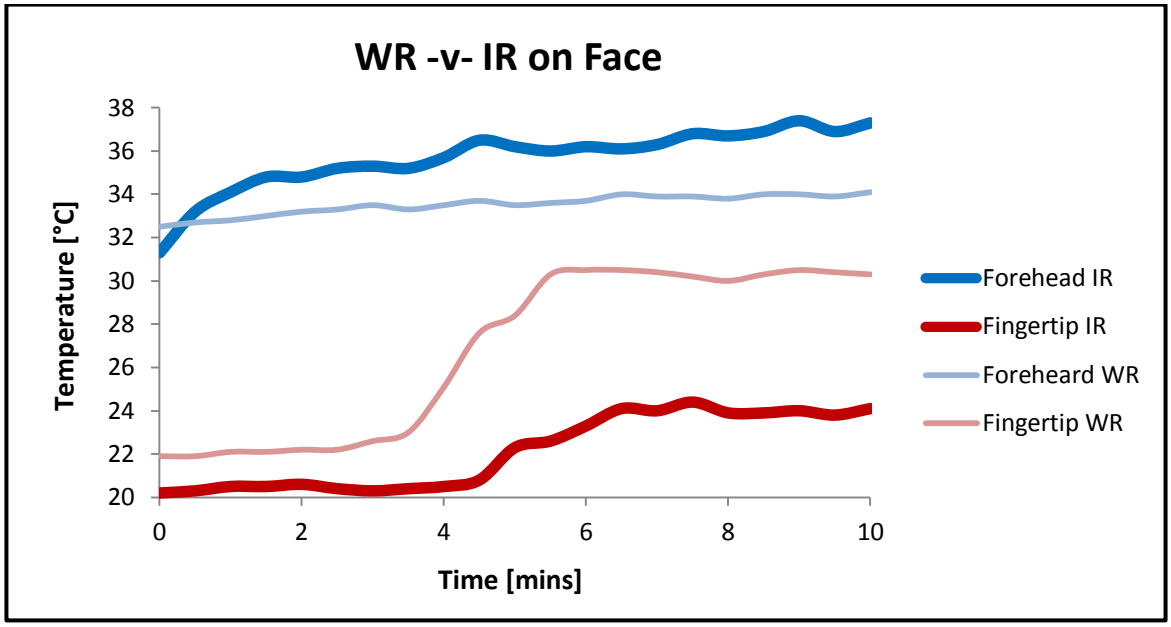

Figure 84 - Subject 2 Full Body Test: WR -v- IR on Face

As in the case of Subject 1, the hand and face areas have been identified as the most interesting areas for further investigation, and so for the same reasons, further testing will be carried out focusing on these areas.

Face Test - Warm Room

The subject is brought from a cold room (~18.2°C) into a warm room (~24.9°C), and the resulting changes in temperature distribution in the face over a 10min period are shown in Figure 85. Noticeable changes in temperature during the test can be seen to occur throughout the face, in areas including the nose tip, cheek, chin, and around the mouth. The warmest area of the face at the beginning of the test is around the mouth at 33°C, closely followed by the forehead at 32.5°C. The cheeks and chin are somewhat cooler than these areas, and the nose tip can be seen to be the coldest area at 25.7°C. The greatest temperature change occurs in the nose area, which gradually rises by a total of 7.1°C and approaches the forehead and chin temperatures at the end of the test. The end result is a more uniform overall face temperature.

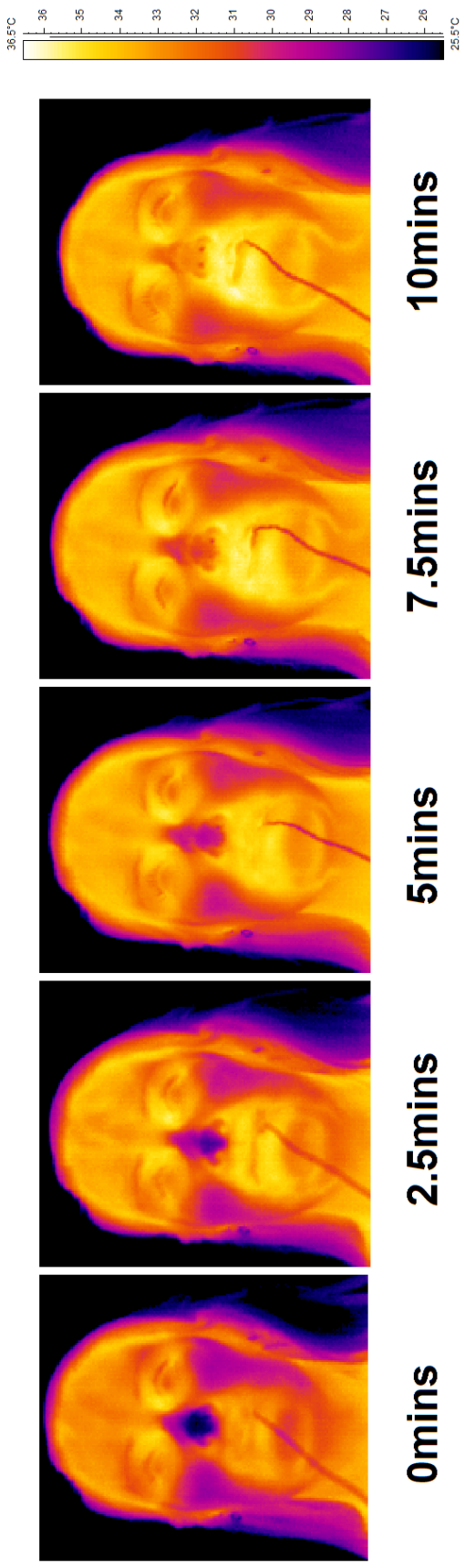

Figure 85 - Subject 2 Face Test: Thermal images of WR test

The numerical results derived from the thermal images are inspected further in Figure 86. The forehead is initially the second highest temperature area, but the chin area shows a larger temperature change during the test and by the end has converged with the forehead temperature, following an initial difference of 1.6°C. The mouth also heats to a greater extent than the forehead, resulting in an end temperature difference between the two of 1.8°C following an initial difference of just 0.5°C. The cheek temperature lies a little over 3°C below the forehead temperature throughout the test. All of these areas show an increase of between 1.5-3°C during the test. The nose temperature increase is very large in comparison at over 7°C, bringing it to a final temperature just below the forehead and chin regions. The change in uniformity of temperature can also be seen here, with an initial temperature range over the entire face of 7.3°C falling to 4.8°C by the conclusion of the test.

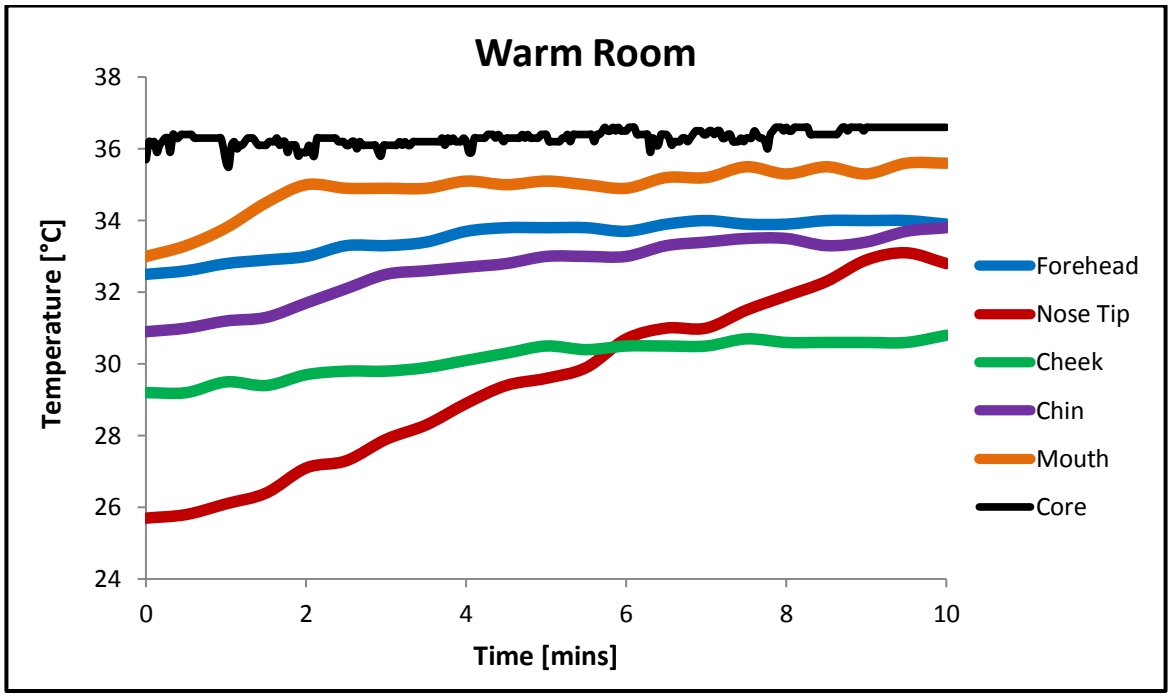

Figure 86 - Subject 2 Face Test: Actual temperature data for WR test

Face Test – IR on Face in Cold Room

The subject is positioned in a cold room (~17.1°C) and IR heat (26.5°C at the centre position) is applied to the face area. The resulting changes in temperature distribution are shown in Figure 87.

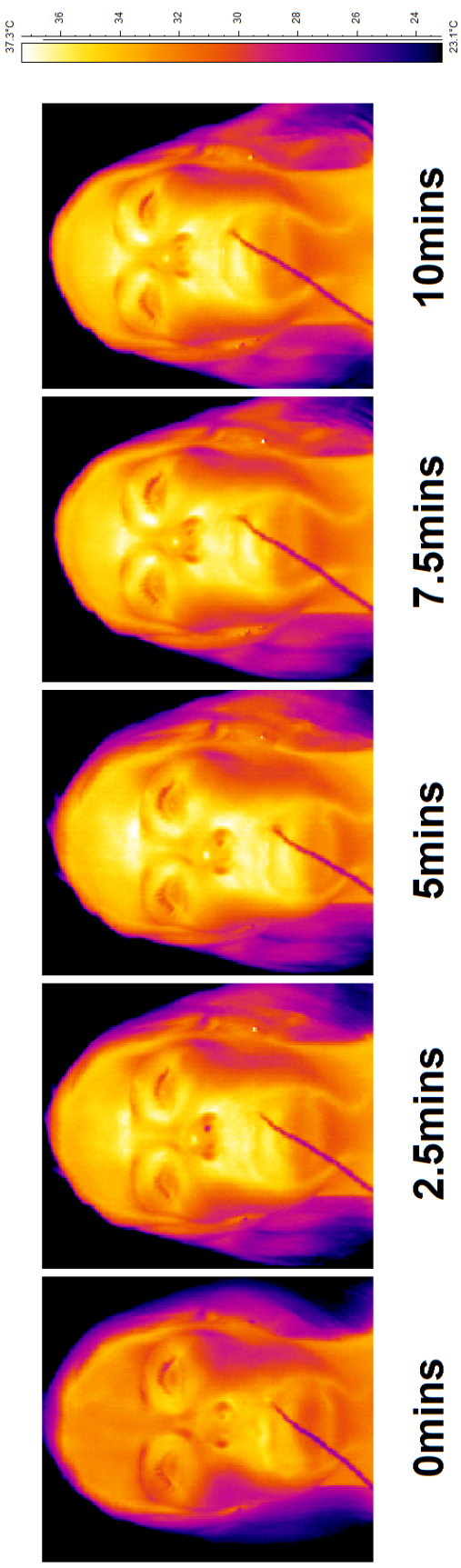

Figure 87 - Subject 2 Face Test: Thermal images of IR on Face test

At the beginning of the test the warmest area of the face is the mouth area at 33.9°C. The forehead and nose tip temperatures are similar at approximately 1.5°C below the mouth temperature. The chin area is somewhat cooler than this, and the cheek area has the lowest initial temperature at 28.9°C. At 2.5mins the temperatures of the entire face area can be seen to have risen, and hot spots have appeared in the forehead, nose tip and mouth regions. A reasonably steady state can be observed from 5mins showing a slightly more uniform temperature for the face area.

The numerical results for this test are shown in Figure 88. There is a distribution of temperatures across the face, with the nose tip and the area around the mouth being the most comparable in temperature. Both of these areas show a sharp temperature increase within the first 30seconds of the test followed by a relatively steady temperature which converges to around 36°C. The forehead, cheek and chin areas show a similar trend consisting of an initially larger slope which gradually decreases as the test progresses, the forehead area reaching a fairly steady state towards the end. The temperature distribution across the face becomes only slightly more uniform over the course of the test, from an initial range of 5°C to a final range of 3.6°C.

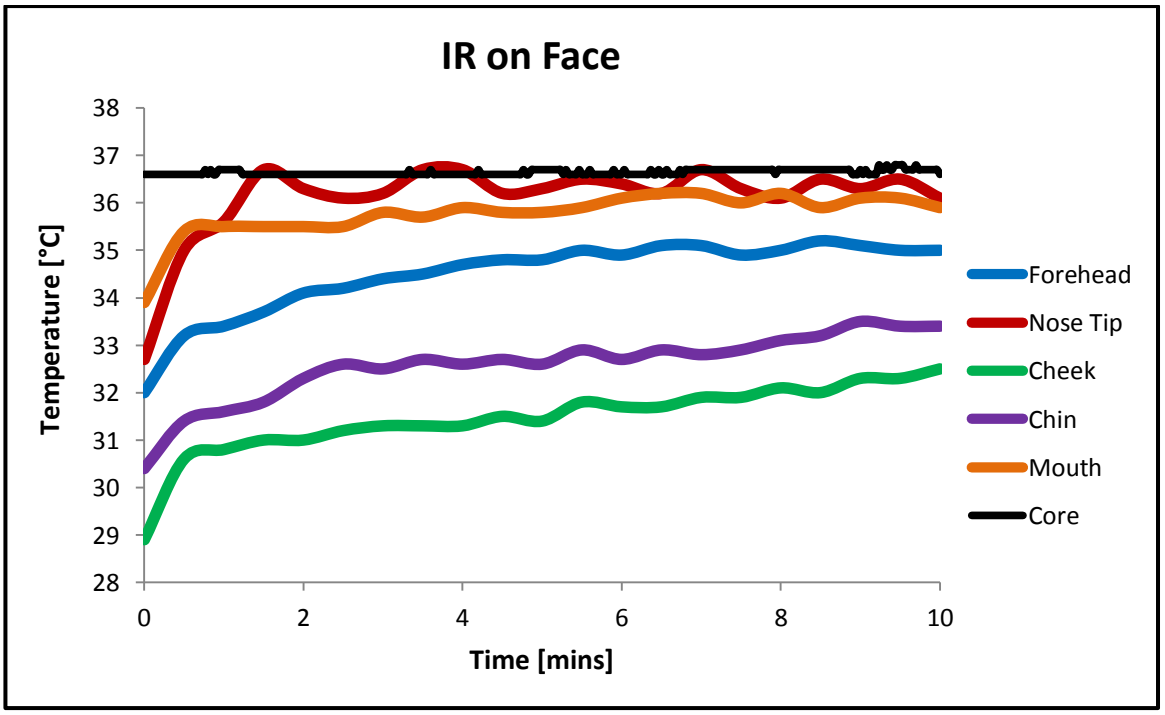

Figure 88 - Subject 2 Face Test: Actual temperature data for IR on Face test

Comparison of Face Heating under different conditions

When comparing the WR and IR on Face tests in Figure 89 it can be observed that although most areas have initial temperatures that are similar across the two tests, those for the mouth area are somewhat dissimilar, and those for the nose tip are very dissimilar. It is clear from the figure that the overall temperatures for the IR on Face test are higher for all face areas excluding the chin, which displays a similar temperature for both the WR and IR tests. With regards to temperature increases, the forehead and cheek show higher increases during the IR on Face test whilst the mouth and nose tip show higher increases during the WR test. However, with regards to these observations the nose and mouth area behaviour may have been influenced by somewhat different start temperatures. The common trend for the IR on Face test is that it occurs in two stages; a larger initial slope over the first 1.5mins, followed by a more gentle slope thereafter and in some cases a reasonably steady state, whilst the common trend for the WR test shows a more even slope throughout the test, with the exception of the mouth area which shows a sharper initial increase.

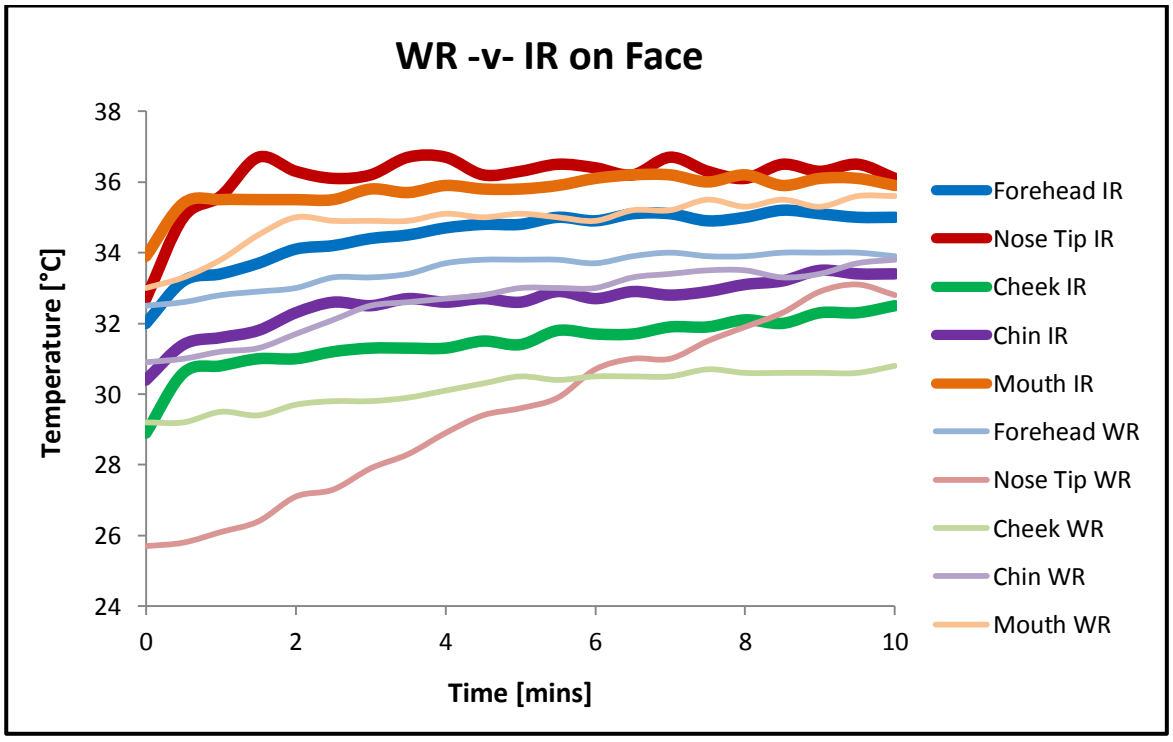

Figure 89 - Subject 2 Face Test: WR -v- IR on Face

The area with the greatest behaviour difference with respect to both temperature and trend is the nose tip temperature, but the dissimilar initial temperatures for the nose area mentioned previously make it difficult to make fair observations about these differences. However, it could be suggested here that the nose temperature in the IR test may have reached similar temperatures even had its initial temperature been lower by showing a more profound temperature rise at the beginning of the test. This is not an excessive suggestion to make as testing has already shown the capability of the nose temperature to increase dramatically under the direct application of IR heat. Assuming this suggestion, the nose area would hold to the discussed trends and would be an extreme example of the differences between the tests.

Hand Test - Warm Room

The subject is brought from a cold room (~17.6°C) into a warm room (~23.3°C). The resulting changes in temperature distribution about the hand over the test duration are shown in Figure 90. It is clear that the entire hand increases in temperature over the course of the test. Initially the warmest area of the hand is the centre of the palm at 31°C. The temperatures of the edges of the palm and the fingers are cooler and appear to be of fairly uniform, with the fingertip temperature measured at 26.8°C. From observation of Figure 90 the initially cooler areas of the hand can be seen to heat very rapidly within the first 2.5mins, with a fingertip temperature rise of 6.4°C making the entire hand more uniform in temperature at this point. For the remainder of the test the hand continues to heat, and a steady state could be approximated over the 7.5min and 10min images.

The numerical data from this test can be examined in Figure 91. The first point to note is the convergence of the palm and fingertip temperatures, from an initial difference of 4.2°C, approximately 2mins into the test. From this point the temperatures of these areas remain similar and rise only very slightly and gradually over the remainder of the test. A second point to note is that a large portion of the fingertip temperature occurs very rapidly, with a 4.5°C increase occurring between the times of 0.5min and 1.5mins; almost 60% of the overall fingertip temperature rise. In comparison to this the palm temperature can be seen to rise much more gradually over the course of the test, with a slightly steeper rise over the first 4mins than towards the end.

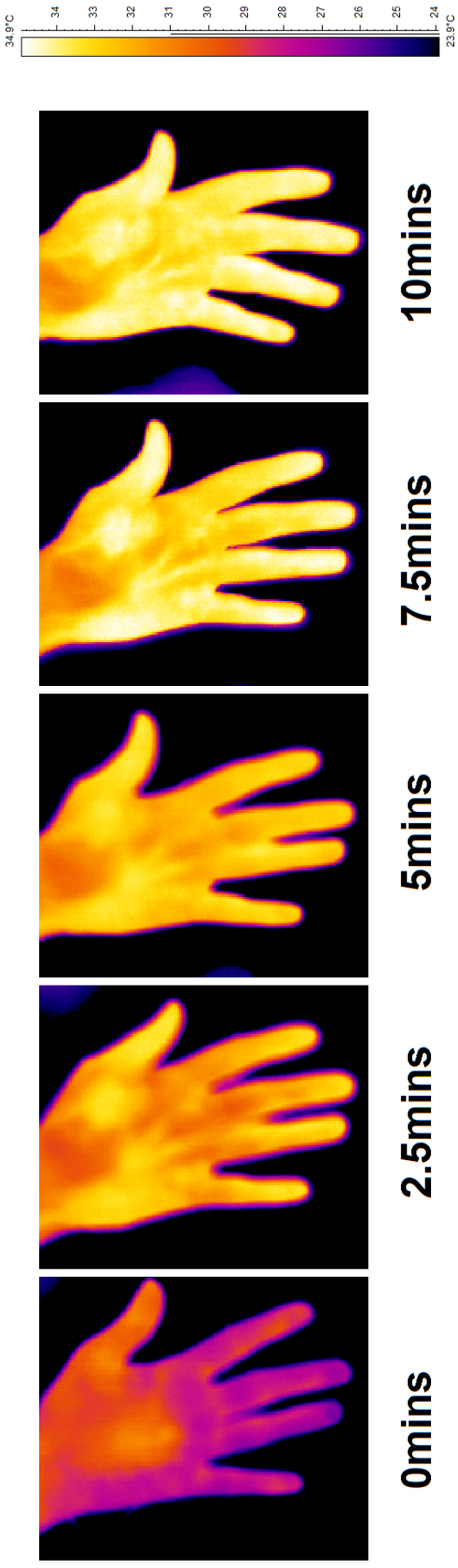

Figure 90 - Subject 2 Hand Test: Thermal images for WR test

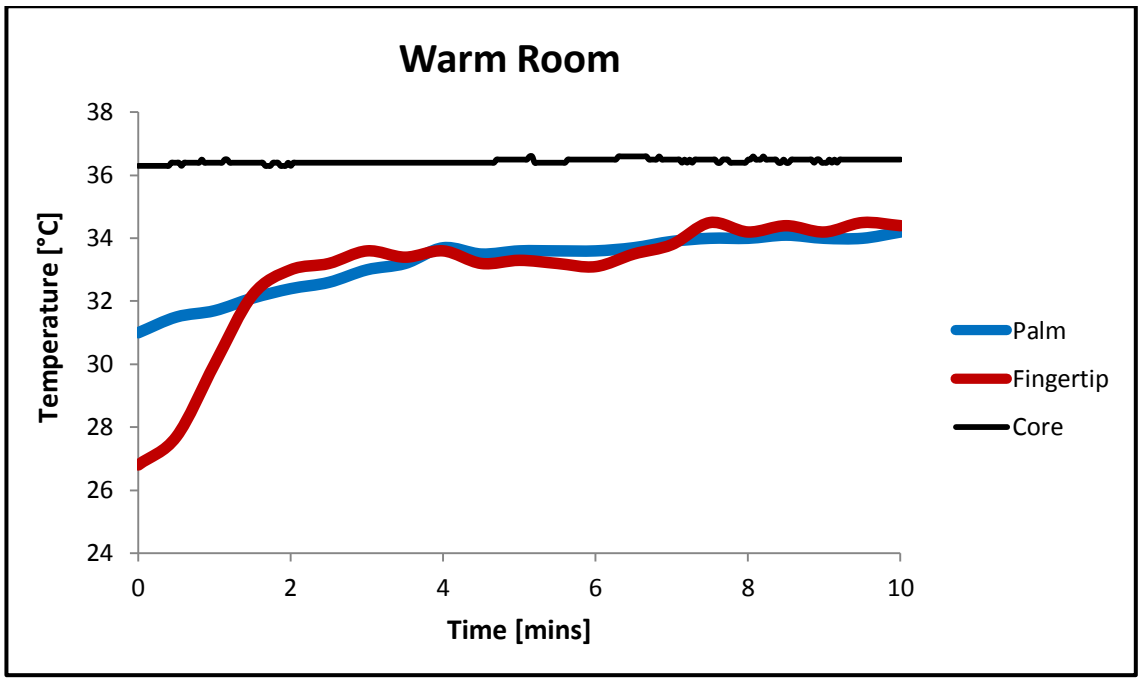

Figure 91 - Subject 2 Hand Test: Actual temperature data for WR test

The heat flux, shown in Figure 92, is positive for the entire test thus showing that the hand is at all times radiating heat to the surroundings. This corresponds to the fact that the temperatures throughout the hand are higher than the room temperature for the duration of the test.

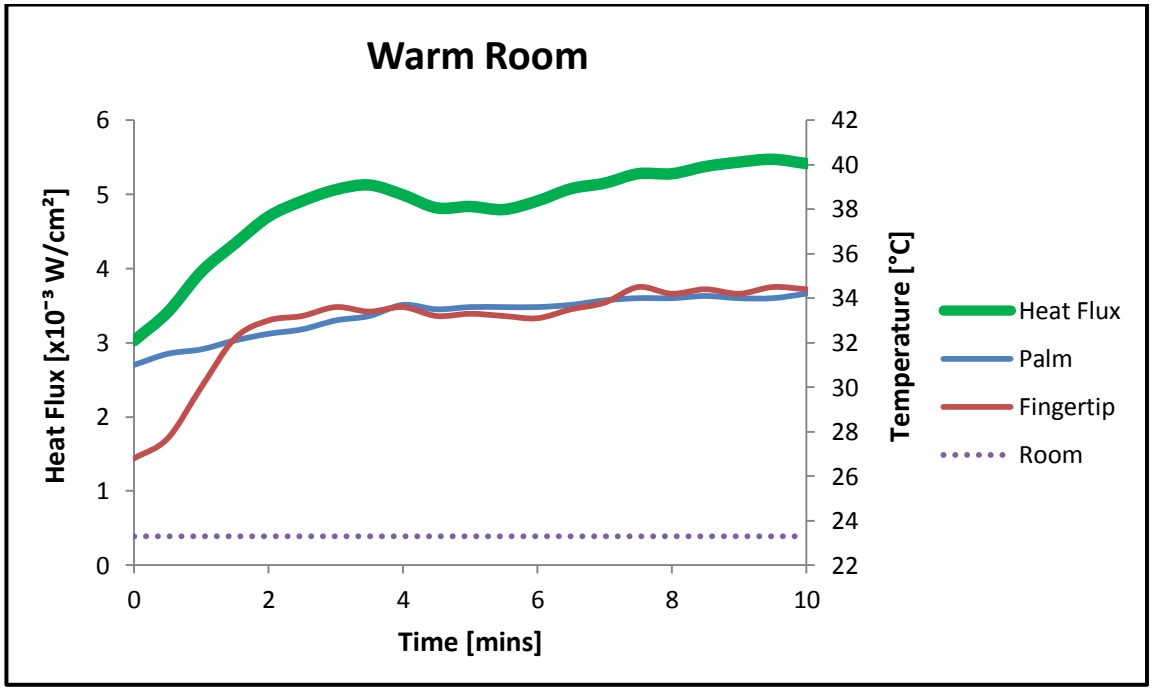

Figure 92 - Subject 2 Hand Test: Heat flux data for WR test

The slope of the heat flux is positive for almost the entire test, with the steepest portion corresponding to the most rapid palm temperature increase over the first 4mins. The heat flux value falls off from a value of $5.13 \times 10^{-3}\ W/cm^2$ at 3mins, corresponding to the point where the fingertip and palm temperatures reach a relatively steady state. Overall, the plot suggests that increasing temperature in the hand causes an increase in heat flux, and that when temperature stabilises so too does the heat flux.

Hand Test – IR on Face in Cold Room

The subject is positioned in a cold room (~17.9°C) and IR heat (26.5°C at the centre position) is applied to the face area. Figure 93 shows the resulting changes in temperature distribution about the hand over the course of the test; the most noticeable of which occur in the fingertip and palm centre areas. At the beginning of the test the hand can be seen to have two general areas of different temperature; the palm and the fingers. At this time the palm centre is 28.2°C whilst the fingertips have a substantially lower temperature of 20.6°C.

The most obvious temperature change occurs over the first 5mins of the test. At 2.5mins the temperature in several spots across the palm can be seen to rise along with the fingertips. There is also some less noticeable change in the rest of the fingers. At 5mins the heat in the palm lies mostly in the centre at 31.1°C, the fingers have heated to temperatures similar to the edges of the palm, and the fingertip temperatures have risen further to 28.9°C. For the remainder of the test the hand appears to maintain a relatively steady state, cooling very slightly towards the end.

Figure 94 displays the numerical results for this test. The rapid heating of the fingertip area can be further inspected here, and it can be seen that there is a 6.6°C rise between the times of 1.5mins 3mins; over 75% of the maximum temperature rise experienced in that area. The palm temperature displays a much more gentle slope throughout. As previously observed, both areas show a slightly declining temperature towards the end of the test. The uniformity of temperatures in the hand has greatly improved by the end of the test with a final range of less than half that of the initial range.

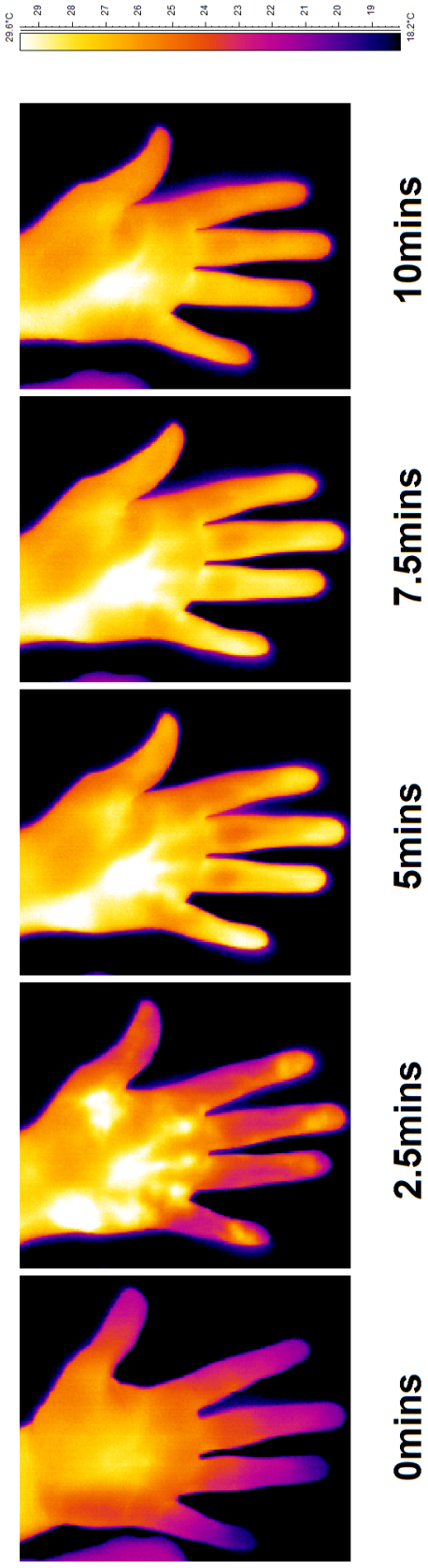

Figure 93 - Subject 2 Hand Test: Thermal images for IR on Face test

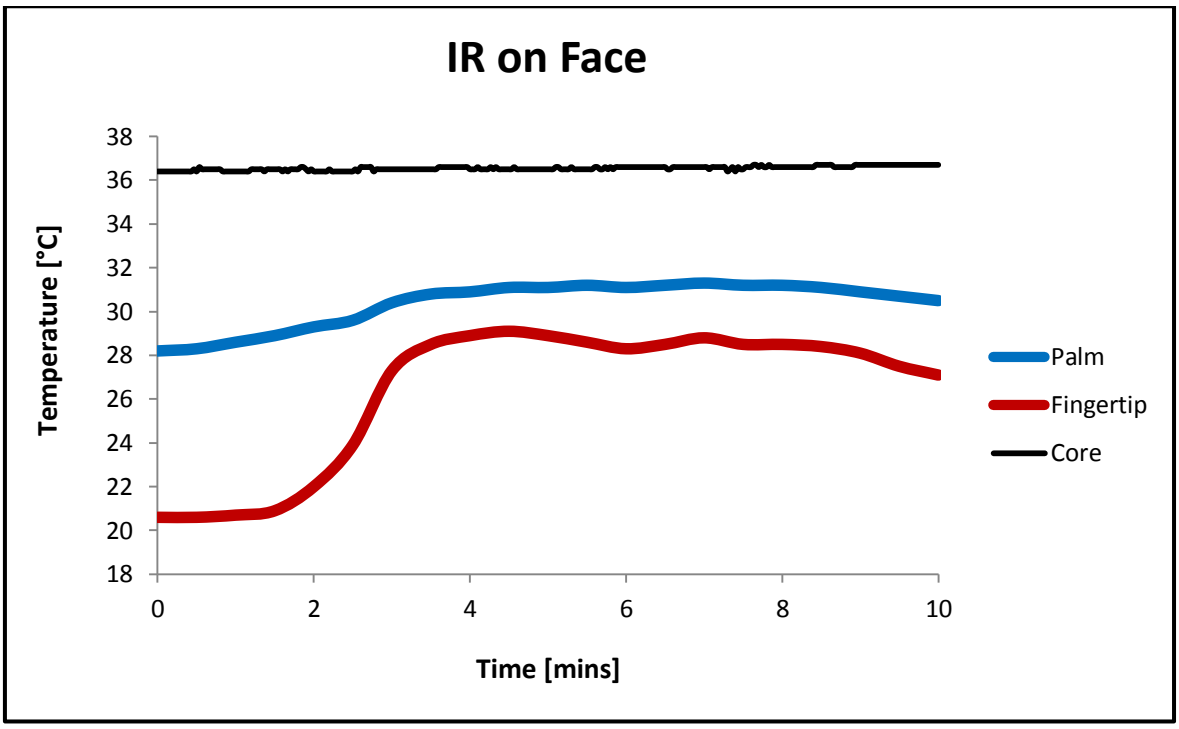

Figure 94 - Subject 2 Hand Test: Actual temperature data for IR on Face test

The heat flux recorded for the duration of this test is shown in Figure 95. The hand temperature was higher than the air temperature at all times during the test and the heat flux value is positive over the course of the test.

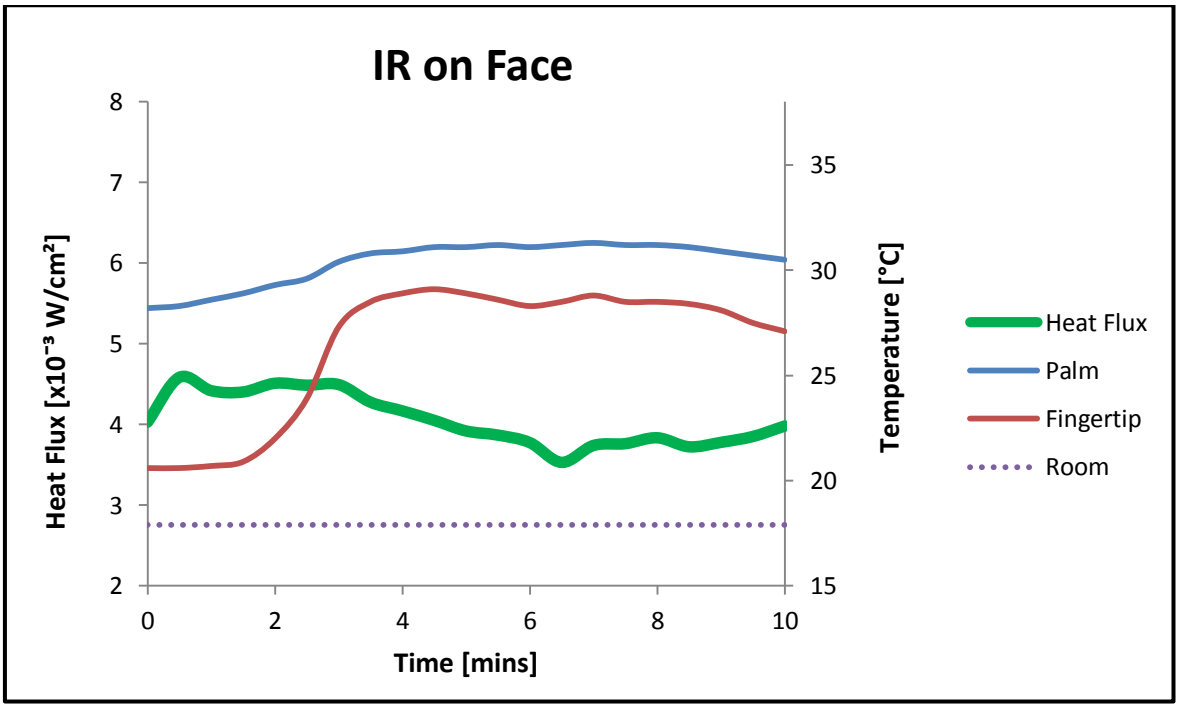

Figure 95 - Subject 2 Hand Test: Heat flux data for IR on Face test

There is little variation in heat flux shown during this test, with a maximum value of $4.58 \times 10^{-3}\ W/cm^2$ occurring within the first minute. The heat flux appears to remain fairly stable for the first 3mins of the test, within which time the palm and fingertip temperatures increase. From 3mins onwards the heat flux drops to a lower level and this corresponds to the time when the temperatures in the hand stabilise and then begin to fall.

Hand Test - IR on Hand in Cold Room

The subject is positioned in a cold room (~18.6°C) and IR heat (26.5°C at the centre position) is applied to the hand area. Figure 96 shows the resulting changes in temperature distribution about the unheated hand. The warmest area at the beginning of the test is the centre of the palm at 30.3°C. The majority of the hand appears to be at a lower temperature, just slightly warmer than the fingertips which are recorded at 26.3°C. Over the first 2.5mins the hand can be seen to heat throughout, with hot spots of up to 31.2°C appearing in several areas of the palm, as well as the palm centre. At 5mins these hot spot areas have also appeared on the fingertips, which show temperatures of 30.2°C. The 7.5min and 10min images show that the fingertips and edges of the palm drop in temperature towards the end of the test, with the palm centre remaining relatively steady.

The numerical results from this test are plotted in Figure 97. The palm shows a temperature increase of only 1°C over the course of the test. This occurs within the first 3.5mins after which a steady state is reached. The fingertip area shows a greater change, almost reaching the temperature of the palm centre after increasing by 4.1°C over the first 4.5mins of the test. For the second half of the test however, the fingertip temperature falls. A suggestion as to why this would occur could relate to the fact that the room temperature is quite cold in this case; the subject reported feeling very cold throughout the test. Perhaps the thermoregulatory system was responding to 'cold' impulses from the body, and was thus was reducing blood flow to the finger areas, or perhaps this is a case of 'overshoot' occurring with regards to vasodilation.

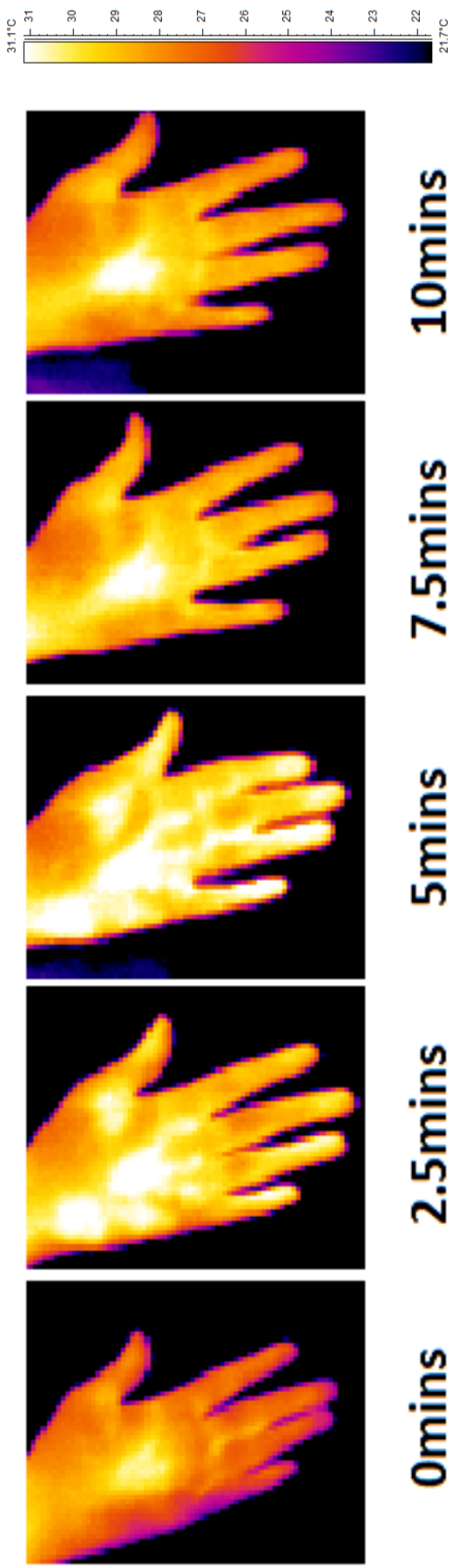

Figure 96 - Subject 2 Hand Test: Thermal images of IR on Hand test

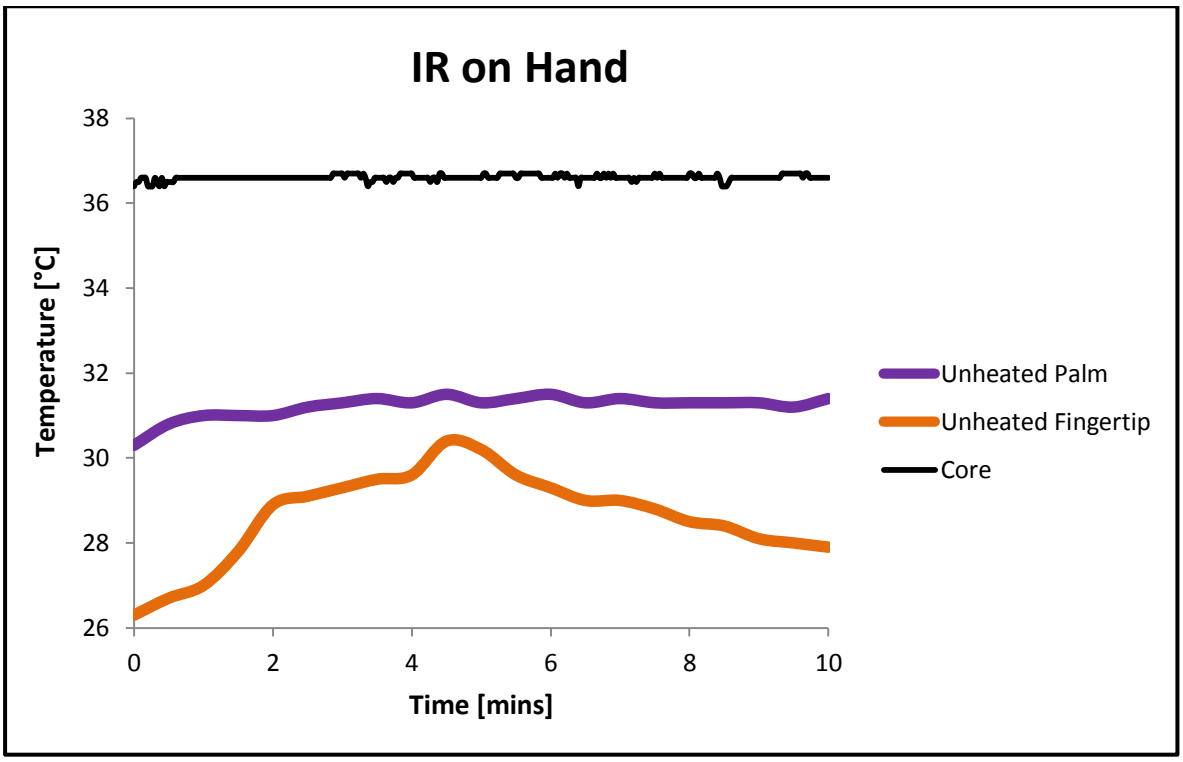

Figure 97 - Subject 2 Hand Test: Actual temperatures for IR on Hand test

Comparison of Hand Heating under different conditions

A comparative plot of the IR on Face and IR on Hand tests is shown in Figure 98. The start temperatures are higher for the IR on Hand test but by the end of the test duration the fingertip and palm temperatures respectively converge for the IR on Face and IR on Hand tests. The palm temperature is quite steady throughout the IR on Hand test. During the IR on Face test however the palm temperature rises over the first 4.5mins to converge with the IR on Hand palm temperature at this time. From this point onwards the palm temperatures remain together at around 31.4°C. The trends for the fingertip temperatures both show a portion of rapid temperature increase, and their temperatures converge at around 7mins. For the IR on face test the rapid rise occurs between 1.5mins and 3mins (over 75% of the overall rise) and for the IR on hand this occurs between 1min and 2mins (over 45% of the overall rise). The main differences to note between these tests for the fingertip area are that the IR on Hand test exhibits a peak fingertip temperature before decline around midway through the test (which can also be seen clearly in Figure 96), whilst towards the end of the IR on Face test steady state behaviour is seen before decline.

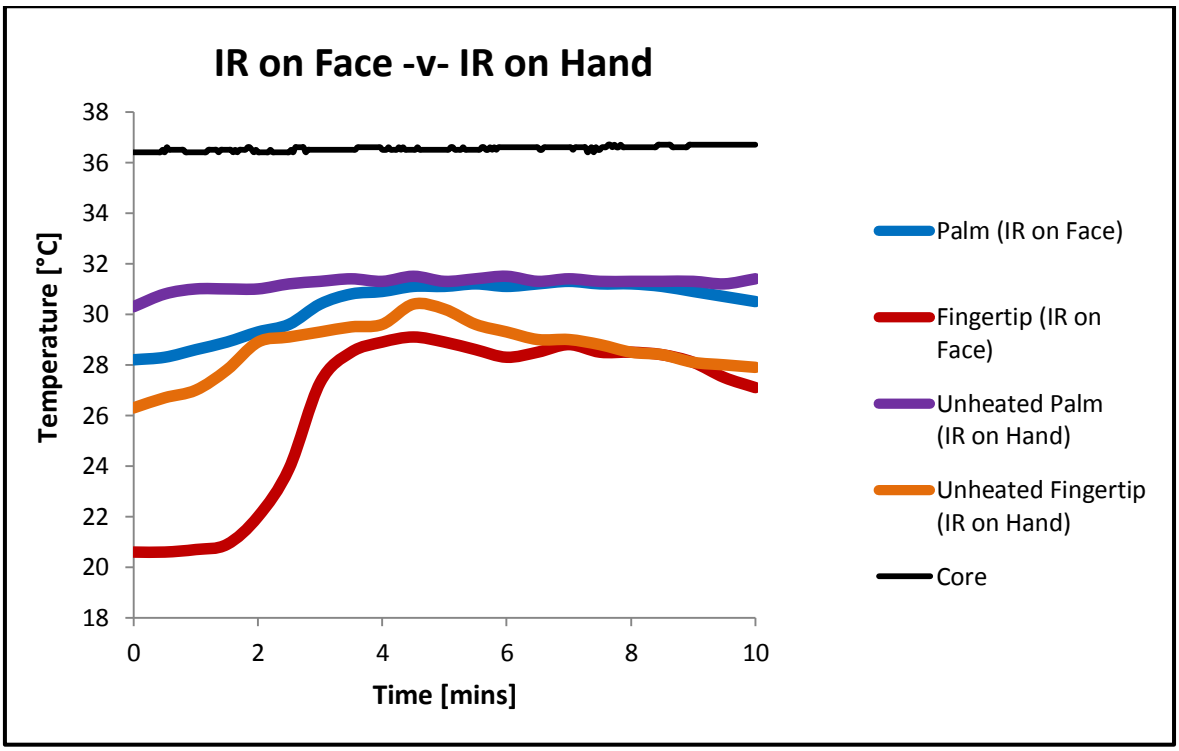

Figure 98 - Subject 2 Hand Test: IR on Face -v- IR on Hand

The results from the WR and IR on Face tests are shown together in Figure 99. With regards to overall temperature increase both hand areas show only a slightly higher increase during the WR test - even despite higher initial temperatures.

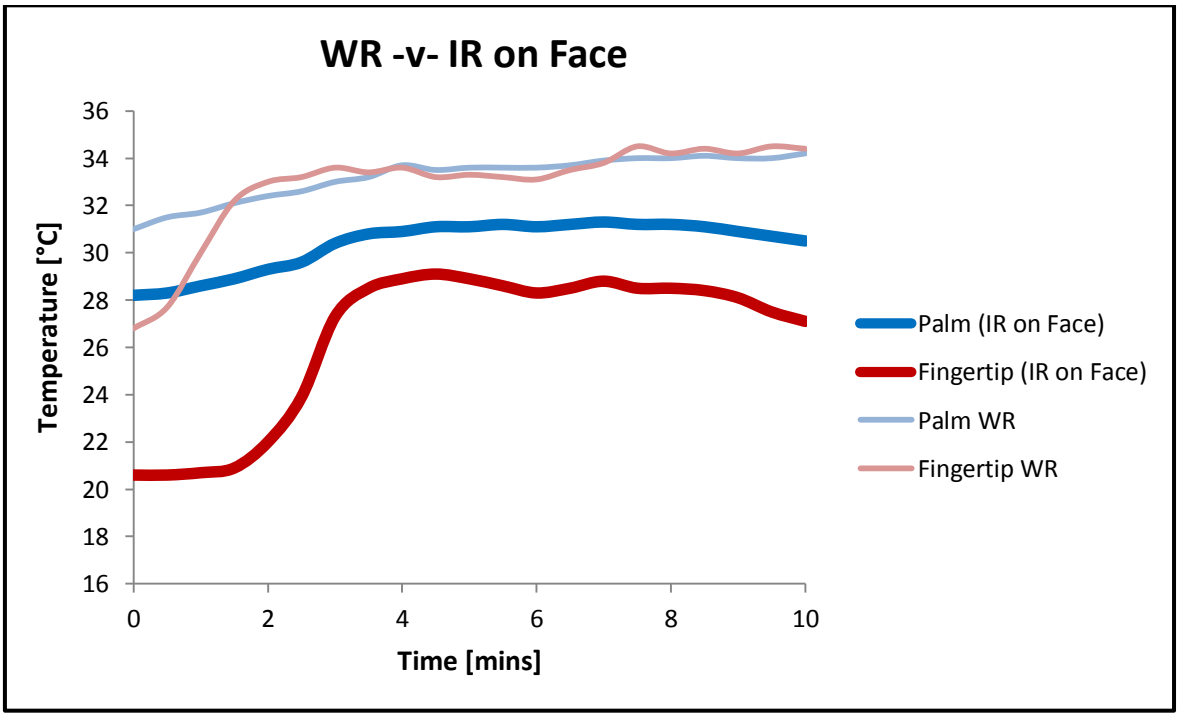

Figure 99 - Subject 2 Hand Test: WR -v- IR on Face

The shape of the curve for the palm temperature is almost identical between the tests, and the shape for the fingertip temperature is very similar. The differences between the fingertip curve shapes mainly relate to the time at which changes in slope occur. The fingertip temperature both undergoes a rapid increase and also reaches a steady state approximately 1.5mins later in the IR on Face test than in the WR test. Another difference pertains to the fact that the fingertip temperature rises by a small amount towards the end of the WR test and falls by a small amount towards the end of the IR on Face test. The heat flux is on average at slightly higher values during the IR on Face test suggesting a greater difference between the hand and the air temperatures in the IR on Face test than for the WR test.

The WR and IR on Hand tests are compared in Figure 100. Start temperatures are quite similar here allowing for a more accurate comparison of heating behaviour. It can be seen here that the WR conditions heat the hand areas more effectively than the IR on Hand conditions, even despite slightly higher start temperatures. The slope of the palm temperature for the WR test is greater for the majority of the time than that of the palm temperature for the IR on Hand test. In the case of the fingertip temperature, both trends show an early rapid rise, with the steeper slope for a longer period of time apparent in the WR test. Another fingertip area difference can be seen from observation of the trends during the second half of the test duration where the WR plot rises slightly in temperature whilst the IR on Hand plot falls.

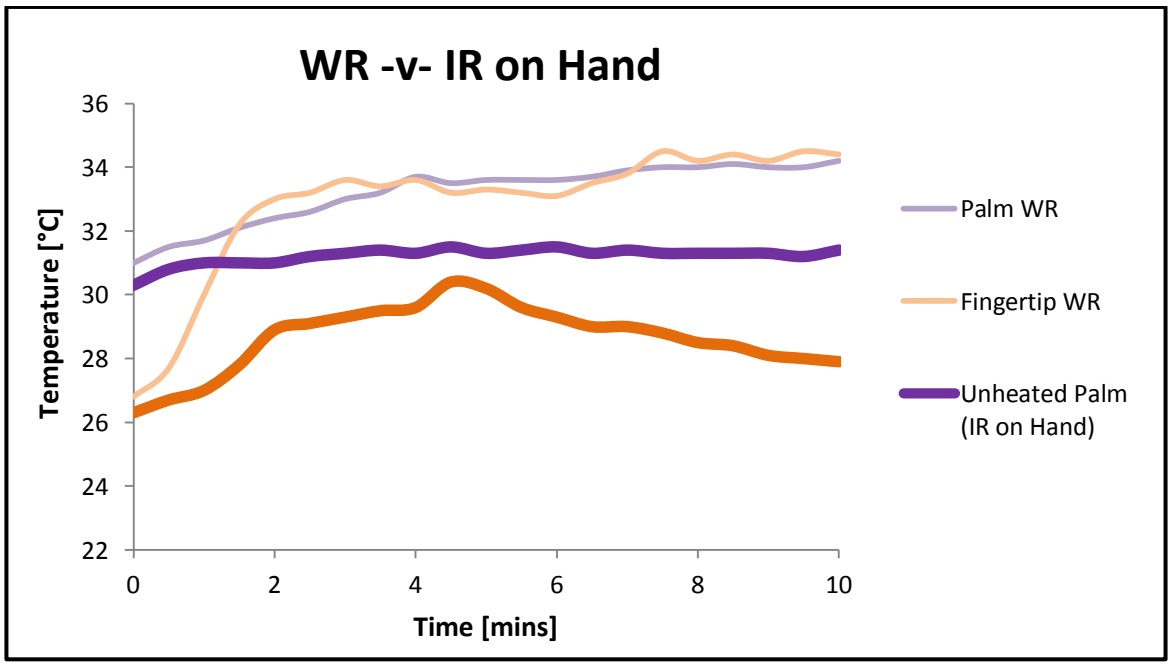

Figure 100 - Subject 2 Hand Test: WR -v- IR on Hand

4.3.1.3 Subject 3

Full Body Test - Warm Room

The subject is brought from a cold room (~19.9°C) into a warm room (~24.8°C). Figure 101 displays thermal images which show the resulting changes in skin temperature distribution about the body over the course of the test. The most obvious change that can be seen here occurs in the hands, particularly in the fingertips, and the majority of this change appears to occur quite rapidly between the times of 2.5mins and 7.5mins. The nose and mouth areas also become noticeably warmer during the test, mostly during the second part of the test and at a slower rate. There are no other changes immediately apparent from inspection of these images, and so numerical data will be analysed to investigate more subtle changes.

The change in temperature occurring in each area of the body can be more clearly seen from Figure 102. As previously observed, the largest increases in temperature occur in the fingertip (11.8°C), nose (5.5°C) and palm (4.1°C) areas., with the other areas of the body all showing small increases in temperature by amounts ranging from 0.1-0.8°C. The rapid rise in fingertip temperature can be clearly seen here. It shows a much higher increase than any other area, the majority of which occurs between 4mins and 6mins when the temperature rises by 9°C; over 75% of the overall temperature increase.

Figure 103 shows the actual temperatures of several areas of the body during the test. The primary areas (forehead and chest) lie between 2.1-3.8°C below the estimated core temperature for the test duration. The secondary areas of the thigh, palm, upper arm and stomach fall 4.6-8.1°C below the estimated core temperature throughout. The foot temperature also lies within this secondary group for the duration of the test, and the nose temperature begins just below. The upper arm begins the test as the warmest area within the secondary group, and the palm temperature the lowest, but by the end of the test the temperatures of these areas have converged, along with the nose temperature, at the high temperature end of the secondary group. As previously discussed, the fingertip shows by far the highest increase, beginning at by far the lowest initial temperature (14.7°C below the estimated core temperature) and reaching the chest temperature by the end.

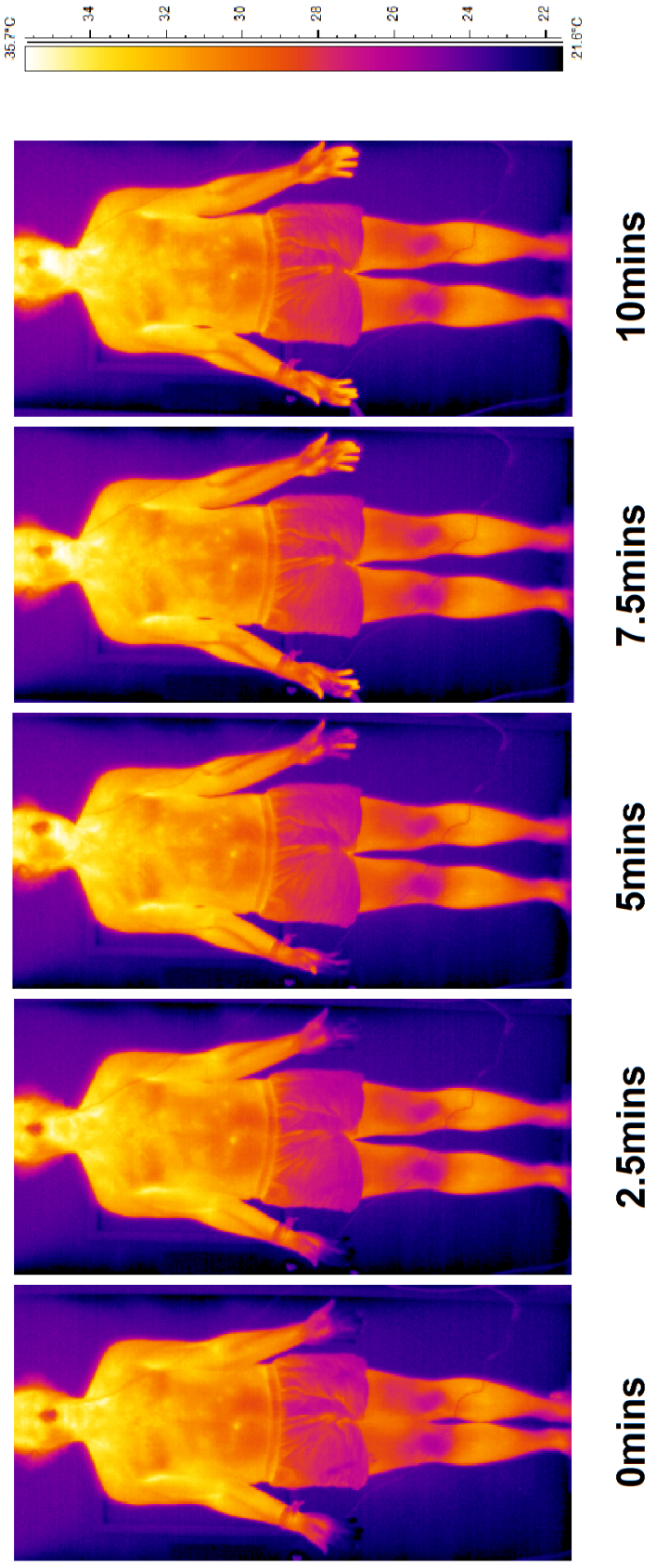

Figure 101 - Subject 3 Full Body Test: Thermal images of WR test

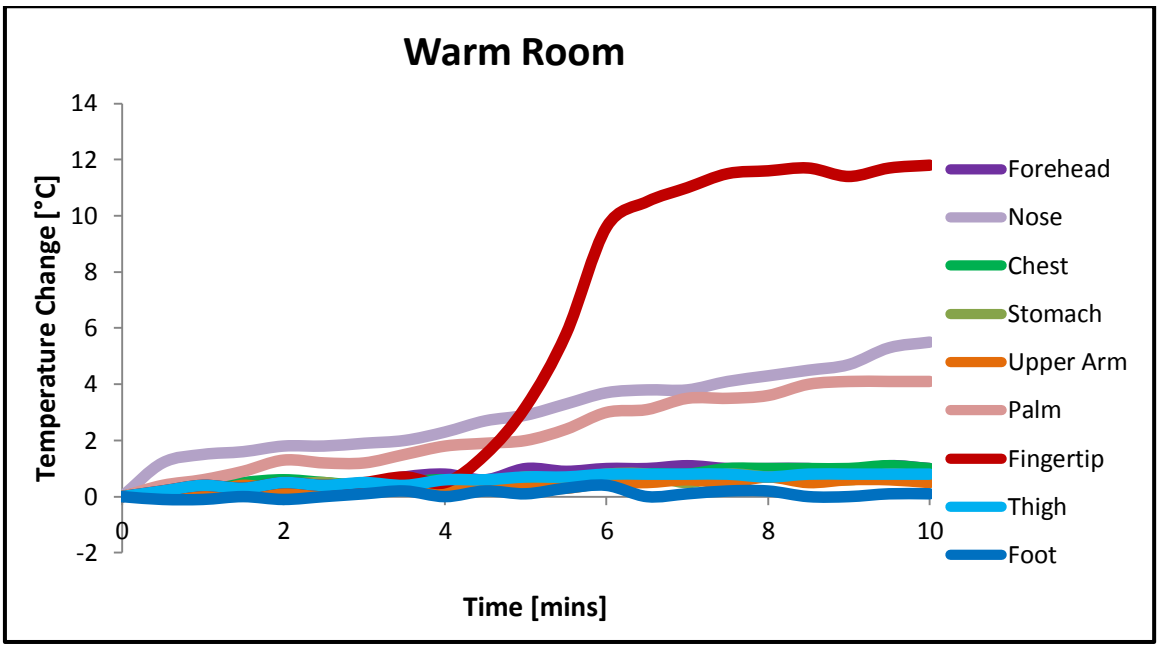

Figure 102 - Subject 3 Full Body Test: Temperature change data for WR test

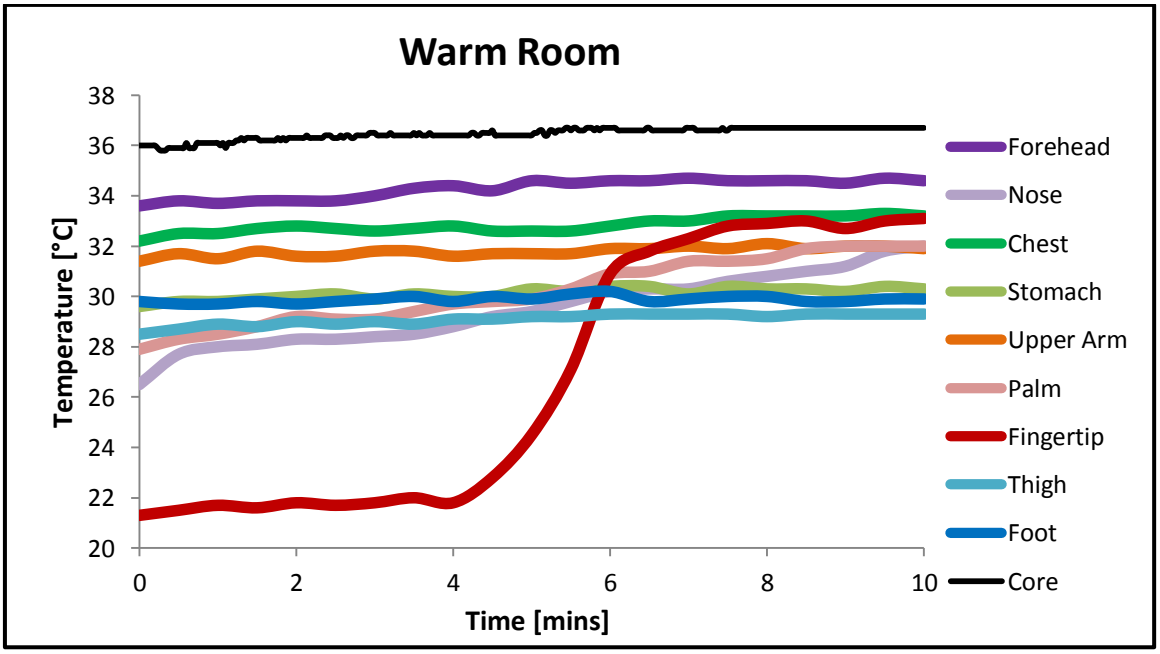

Figure 103 - Subject 3 Full Body Test: Actual temperature data for WR test

Full Body Test – IR on Face in Cold Room

For this test the subject is positioned in a cold room (~19.6°C) and IR heat (~26.5°C at the centre position) is applied to the face area. Figure 104 shows the resulting changes in temperature distribution around the body.

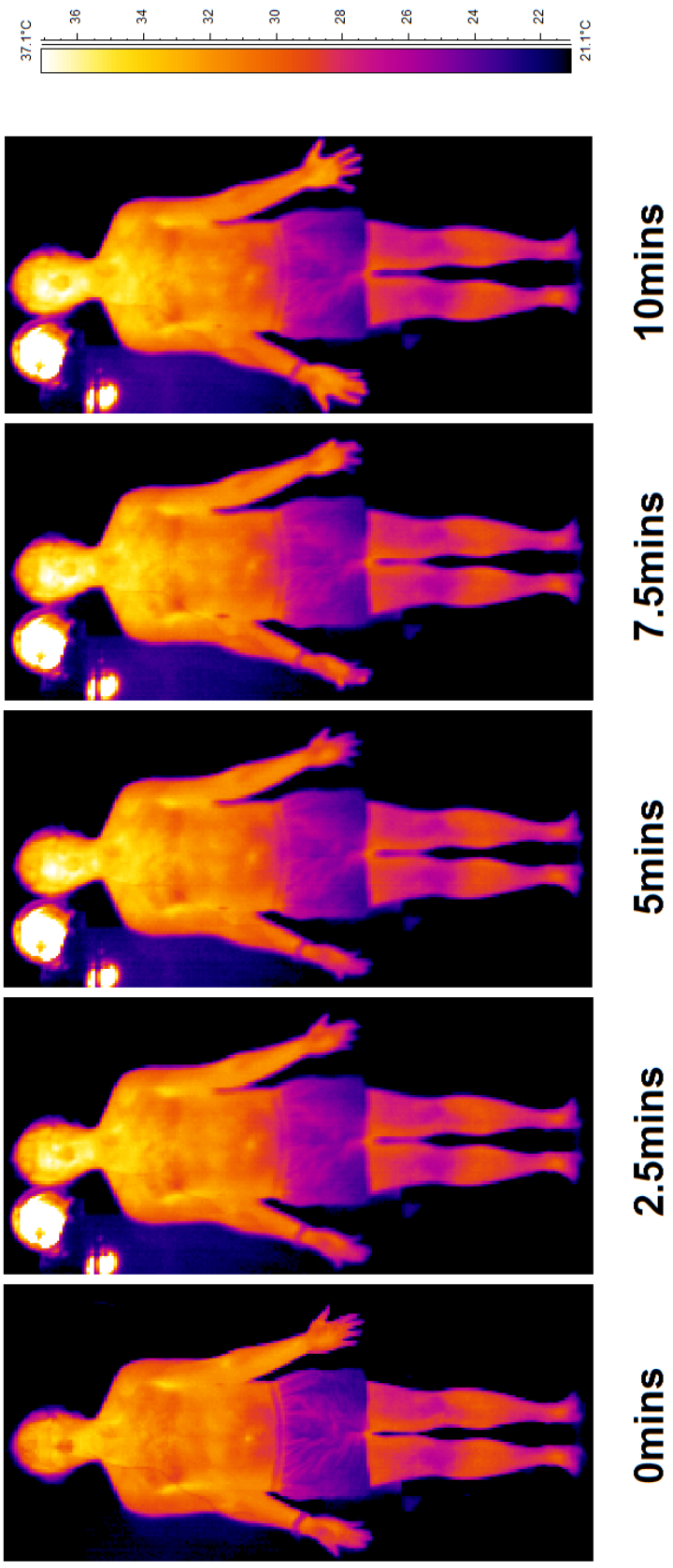

Figure 104 - Subject 3 Full Body Test: Thermal images of IR on Face test

The most obvious changes which can be seen from these images occur in the face, upper torso and hand regions. The temperature increase appears to occur quite rapidly in each case; mostly between 0mins and 5mins in the case of the face and upper torso, and mostly between 7.5mins and 10mins for the hand region. Other areas of the body cannot be visibly seen to change from these images.

Figure 105 shows the change in skin temperature experienced by different areas of the body regardless of initial temperature. It can be seen here that the areas with the largest temperature change are the areas that lie within the head, upper torso and hand regions. These are the nose (4.2°C), the forehead (3.9°C), the fingertip (3.7°C), the chest (3.3°C), and to a lesser extent the upper arm (1.9°C) and the palm (1.5°C). The head and upper torso regions would be expected to rise as the main IR heat is focused on the face, with the peripheral emanating heat flux also having an effect on the upper torso and upper arm. The face and chest areas show a sharp initial rise in temperature within the first 30seconds of the application of the IR heat, followed by a more gentle rise before a relatively steady state is reached at around 6mins. The fingertip and palm areas display different behaviour to this; the palm rises in temperature solely between the times of 6.5mins and 9mins, and the fingertip undergoes over 70% of its temperature rise between the times of 7.5mins and 10mins.

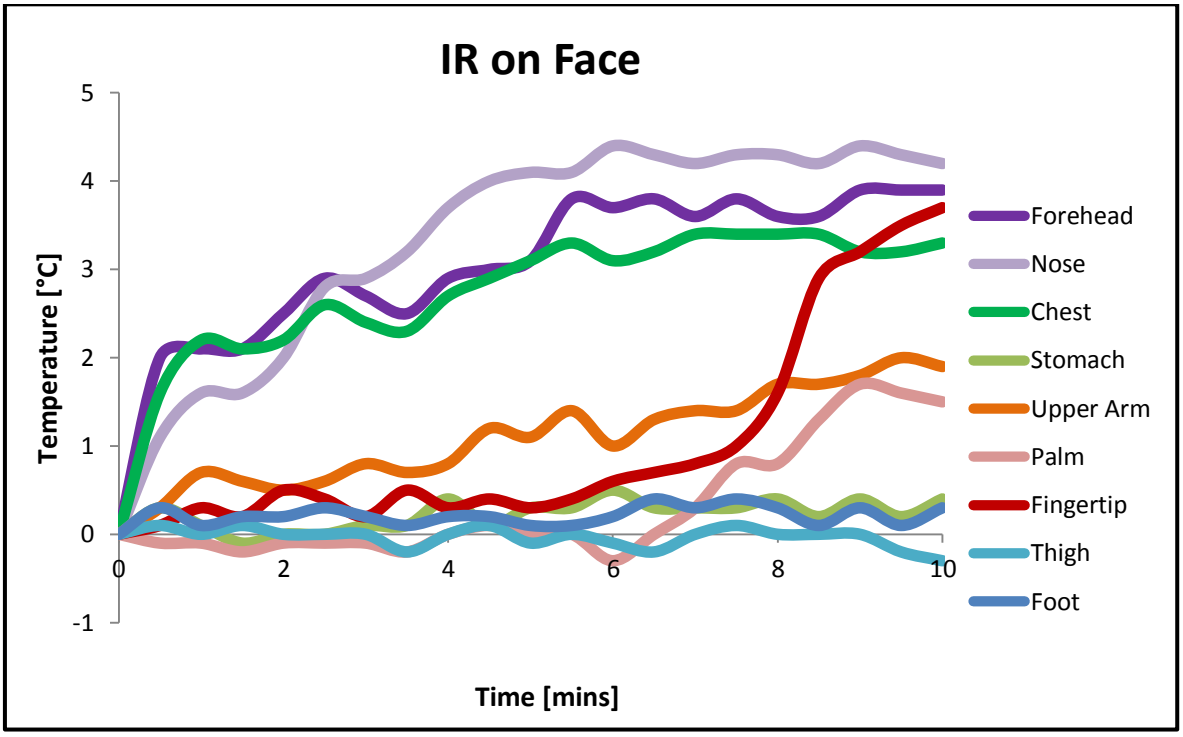

Figure 105 - Subject 3 Full Body Test: Temperature change data for IR on Face test

Several areas of the body which are not directly exposed to IR heat (the foot, thigh, and stomach areas) show temperature changes of less than ± 0.4°C. The fingertip and palm are also areas which do not receive any direct IR heat, however these areas still show a noticeable temperature increase thus suggesting that thermoregulation of the body is responsible for heating these areas.

Figure 106 shows the actual temperatures of several areas of the body throughout the test. Grouping of the primary and secondary regions shows an overlap at the beginning of the test, as the areas associated with these groups (and also the foot and nose areas) have initial temperatures within only a 3.7°C range, situated 4.2-7.9°C below the estimated core temperature. By the end of the test the primary forehead and chest areas have risen to within 0.8-3.1°C below the estimated core temperature, accompanied by the nose area. The secondary areas and the foot area are situated 4.4-8.1°C below the estimated core temperature at this time, and have been joined by the fingertip area which has risen from an initial temperature 11.1°C below the estimated core temperature

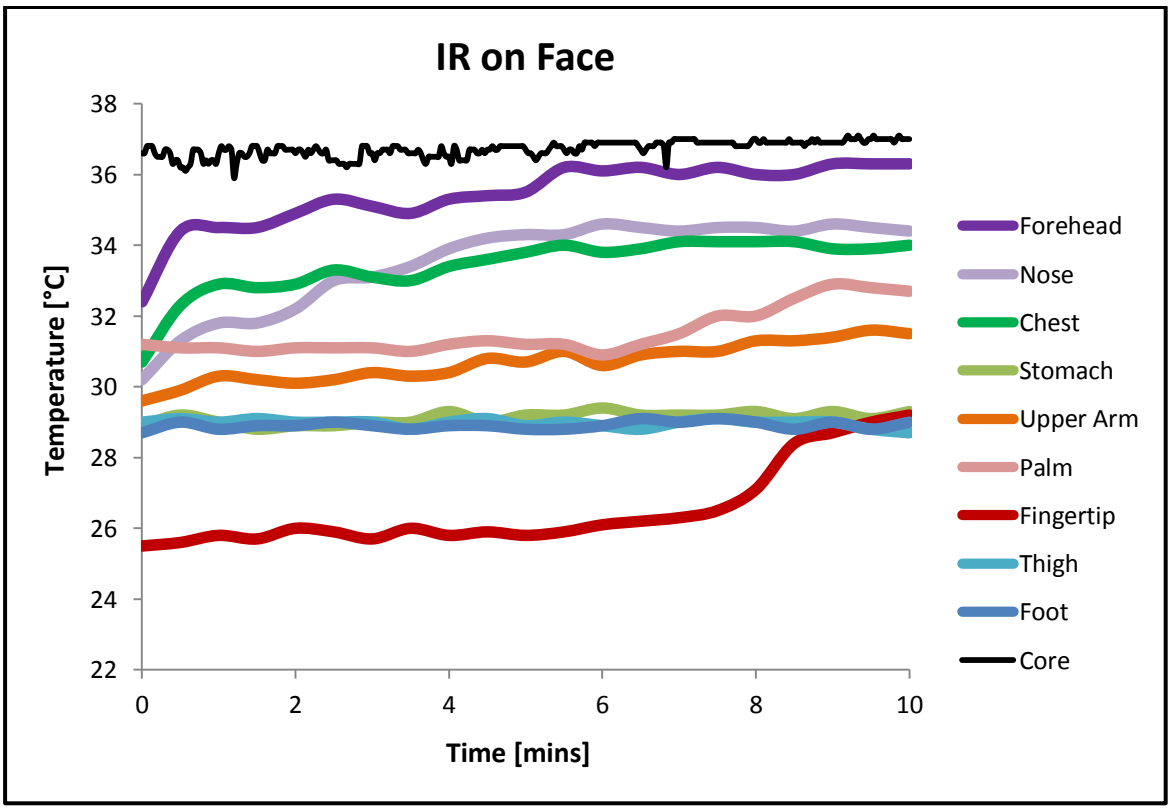

Figure 106 - Subject 3 Full Body Test: Actual temperature data for IR on Face test

Comparison of Full Body Heating under different conditions

In comparing the Warm Room and IR on Face tests, it can be seen that the most noticeable differences between the tests relate to the forehead area of the face and the fingertip area of the hand, which are plotted together for comparison in Figure 107.

The nose area shows a similar overall temperature change in both tests, but the trend differs in that most of the rise occurs towards the beginning of the IR on Face test, and occurs gradually throughout the WR test. The other areas which are directly subjected to IR heat (the forehead, chest and upper arm) all show higher temperature increases in the IR on Face test. The forehead shows the best example of this, rising 3.9°C during the first half of the IR on Face test (close to the estimated core temperature) but only 1°C during the WR test.

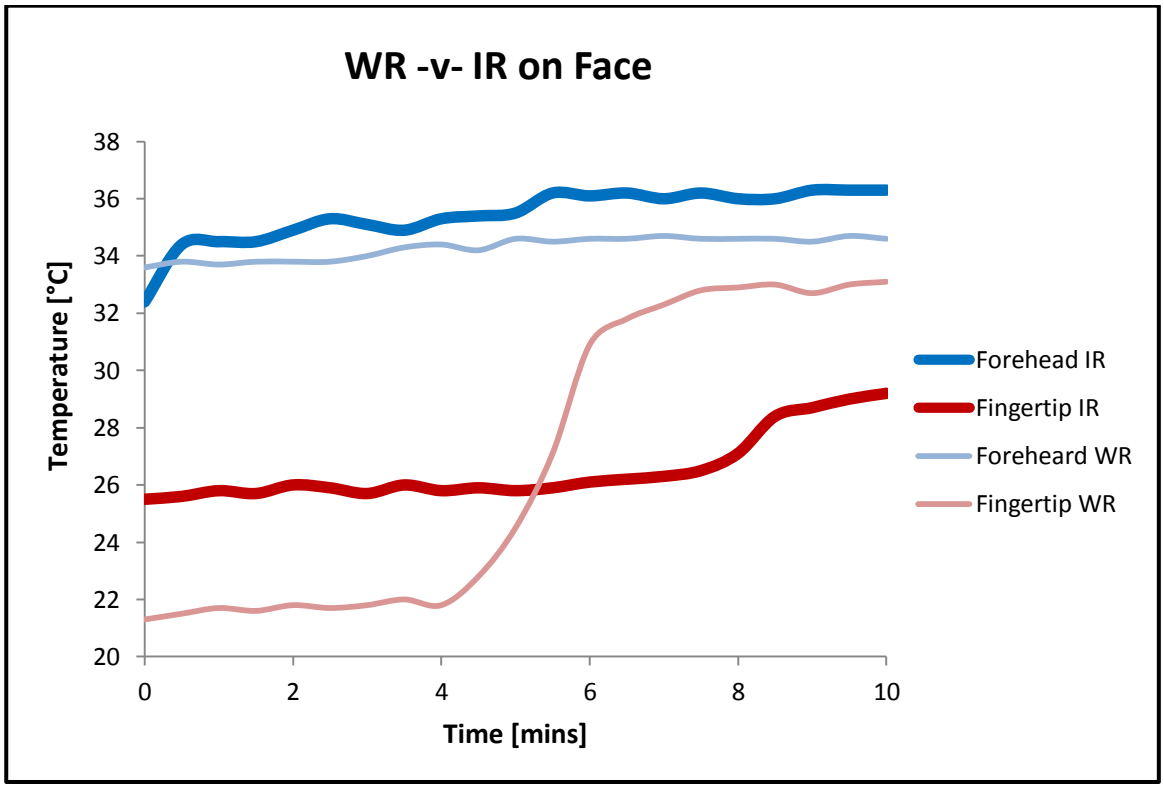

Figure 107 - Subject 3 Full Body Test: WR -v- IR on Face

The palm area achieves a higher temperature during the WR test, but also shows an increase during the IR on Face test. The trends between the tests also differ; a gradual rise is seen over the course of the WR test, and a sharp rise is seen towards the end of the IR on Face test following a period of no change. The fingertip area shows an even more

substantial increase during the WR test, but both IR on Face and WR tests show the trend of a rapid fingertip temperature increase at some stage during the test; in the WR case this occurs approximately midway through the test, and in the IR on Face case occurs towards the end of the test. This is an interesting point to note as it shows that the fingertips warm in a somewhat similar manner despite the different conditions between tests.

Again the hand and face areas have been identified as the most interesting areas for further investigation, and so for the same reasons, further testing will be carried out focusing on these areas.

Face Test – Warm Room

The subject is brought from a cold room (~19.9°C) into a warm room (~24.4°C), and the resulting changes in temperature distribution in the face over the testing period are shown in Figure 108. Change can be seen to occur throughout the face over the course of the test, appearing to result in a more uniform temperature distribution.

Initially the highest temperature exists around the mouth area at 35°C, closely followed by the nose tip and forehead areas at 34.4°C and 33.8°C respectively. The chin area is somewhat cooler at 32.1°C and the cheek is the coldest area, with an initial temperature of 29.9°C. The greatest temperature increases occurs in initially cooler areas, with a chin temperature rise of 3.1°C, and a cheek temperature rise of 1.6°C.

The results for this test are further inspected in Figure 109. It can be seen that the mouth and nose remain the highest temperature areas throughout the test. The forehead temperature remains slightly below those of these areas throughout. The trends of the chin and cheek plots appear to be comparable here, each showing noticeable increase, and the chin temperature rising to the nose tip temperature by the test conclusion. The overall effect appears to be a more uniform temperature distribution, an initial range of 5.1°C dropping to 3.4°C by the end of the test.

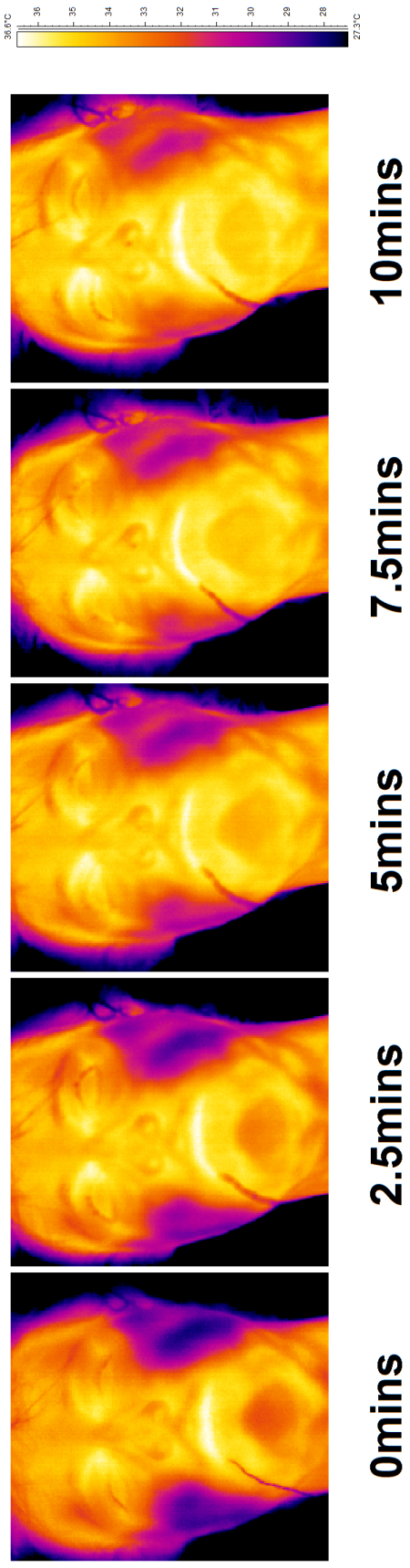

Figure 108 - Subject 3 Face Test: Thermal images of WR test

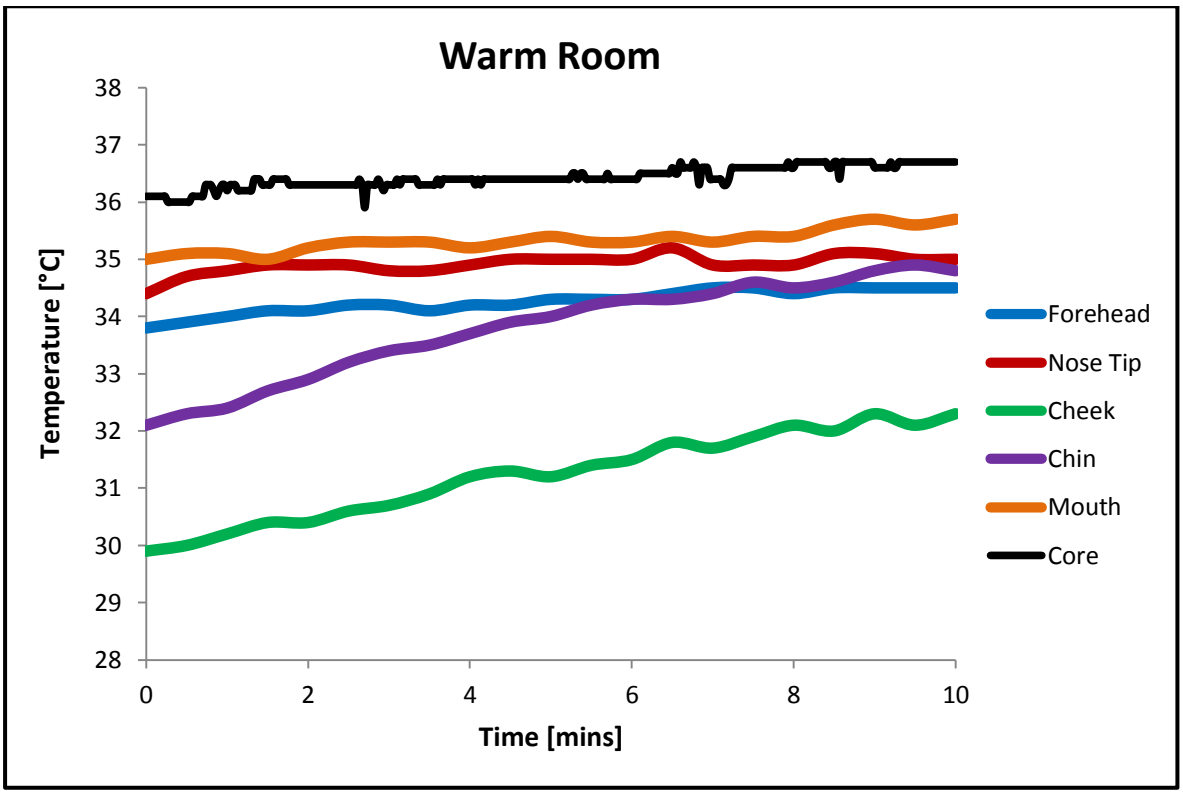

Figure 109 - Subject 3 Face Test: Actual temperature data for WR test

Face Test – IR on Face in Cold Room

The subject is positioned in a cold room (~19.9°C) and IR heat (26.5°C at the centre position) is applied to the face area. The resulting changes in temperature distribution are shown in Figure 110. The warmest area of the face at the beginning of the test can clearly be seen to be the mouth at 34.5°C. The nose tip is somewhat cooler at 33.5°C, and this is closely followed by the forehead and chin areas, both approximately 33°C. The coldest area initially is the cheek at 31.9°C. At 2.5mins the temperatures in the face appear much higher, with hot spots appearing on the forehead, nose tip, chin and mouth areas. From 7.5mins a steady state appears to have been reached, with a uniform temperature apparent over most of the face disregarding the hot spot areas and the sides of the face.

The numerical results for this test are shown in Figure 111. The distribution of temperatures about the face is fairly narrow both at the beginning and end of the test, at 2.9°C and 2.2°C respectively.

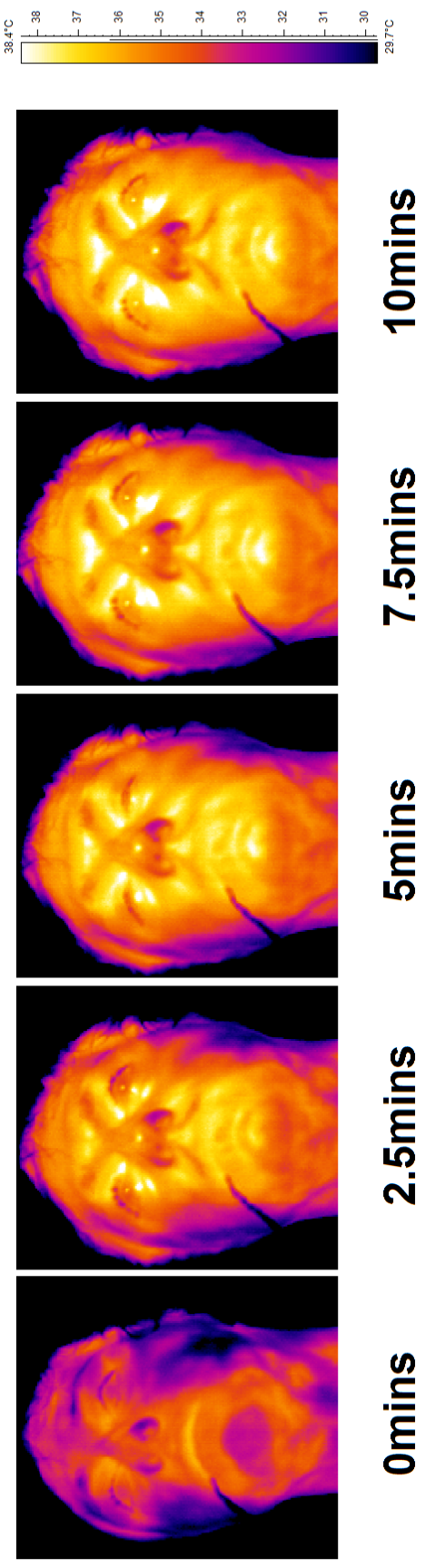

Figure 110 - Subject 3 Face Test: Thermal images of IR on Face test

The mouth, nose and chin areas show the most rapid initial increase due to the fact that the measurement positions for these areas correspond to hot spot areas, all of their temperatures exceeding the estimated core temperature by 2.5mins. The forehead and cheek areas show a less dramatic initial rise followed by a gentle decreasing slope. The nose tip and chin areas show the largest overall temperature increases at around 5°C each, whilst the other areas all warm by approximately 3-3.5°C. It can be seen that a reasonably steady state has been reached for all areas by 6mins.

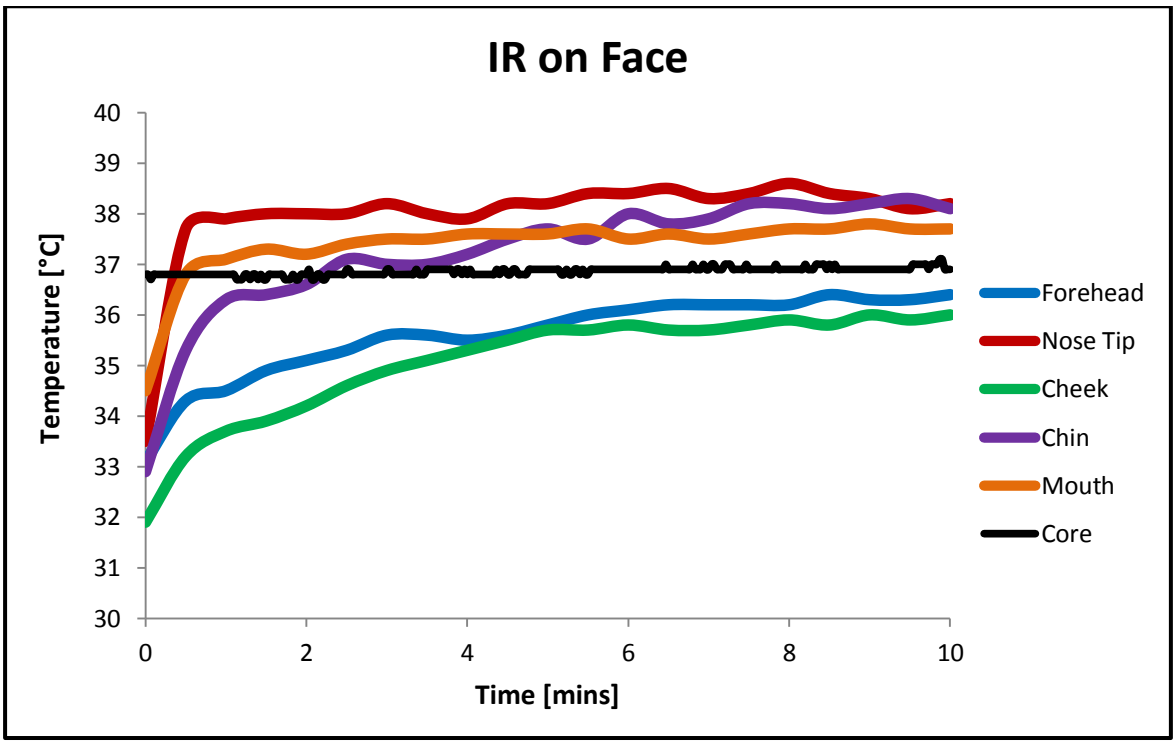

Figure 111 - Subject 3 Face Test: Actual temperature data for IR on Face test

Comparison of Face Heating under different conditions

When comparing the Warm Room and IR on Face tests for the face area it should be noted that the starting temperatures of some areas, particularly the cheek, are somewhat dissimilar for the two tests, but are considered significantly close for qualitative comparisons to be made. The temperatures and temperature increases for the IR on Face test are higher for all face areas, as shown in Figure 112. This suggests that the application of IR heat at a central temperature of 25.6°C heats the face more effectively than the warm air in a room maintained at an approximate temperature of 24.4°C. The WR test areas show a common trend of an even gradual slope throughout the test duration. This differs

from the trends displayed by the IR on Face test areas, which all show a sharp initial rise of varying magnitudes over the first 30seconds, followed by a more gentle decreasing slope and a relatively steady state at varying times. The nose tip area shows the greatest differences with respect to both overall temperature increase and trend. The overall temperature increase varies from just 0.6°C for the WR test to 4.7°C for the IR on Face test, and the even, gradual temperature increase during warm room test is in clear contrast with the swift initial increase followed by steady state observed during the IR on Face test.

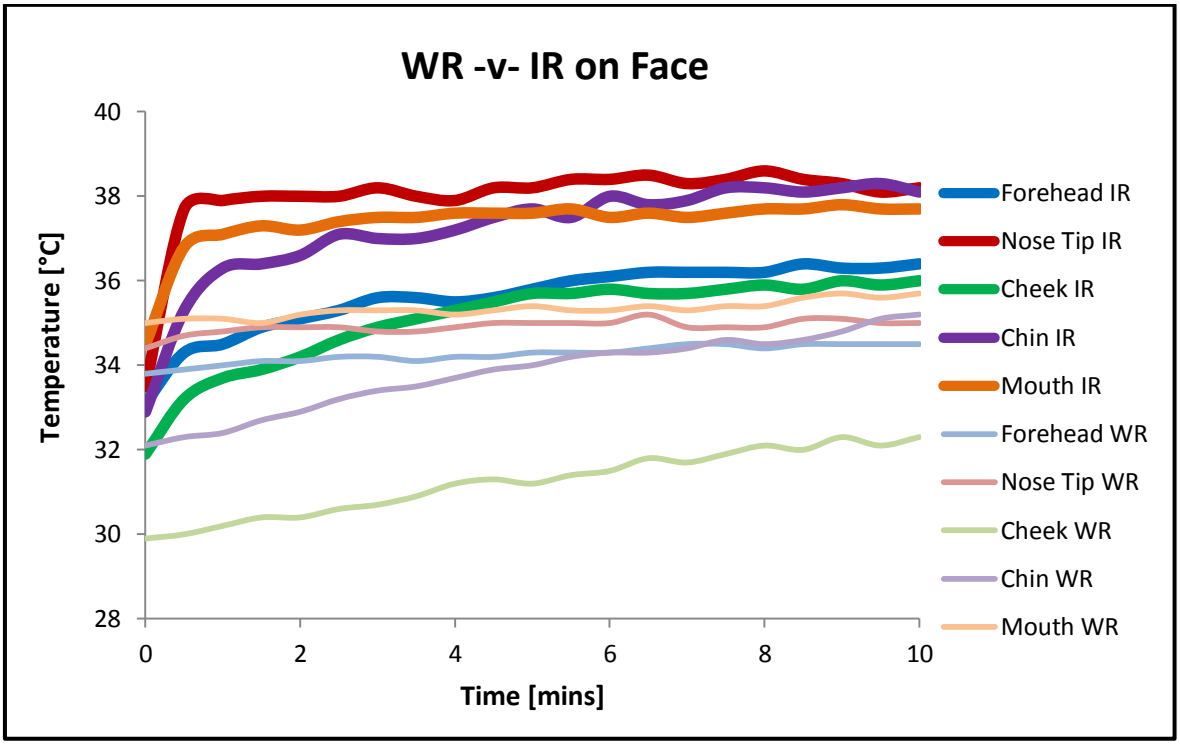

Figure 112 - Subject 3 Face Test: WR -v- IR on Face

Hand Test – Warm Room

The subject is brought from a cold room (~19.7°C) into a warm room (~25.3°C). The resulting changes in temperature distribution over the hand area for the test duration are shown in Figure 113. The hand shows noticeable increases in temperature in all areas during the test. The palm centre is initially the warmest area of the hand at 29.9°C, with cooler temperatures around the edges of the palm and the fingers. The fingertip areas are initially the coldest areas at around 22.1°C.

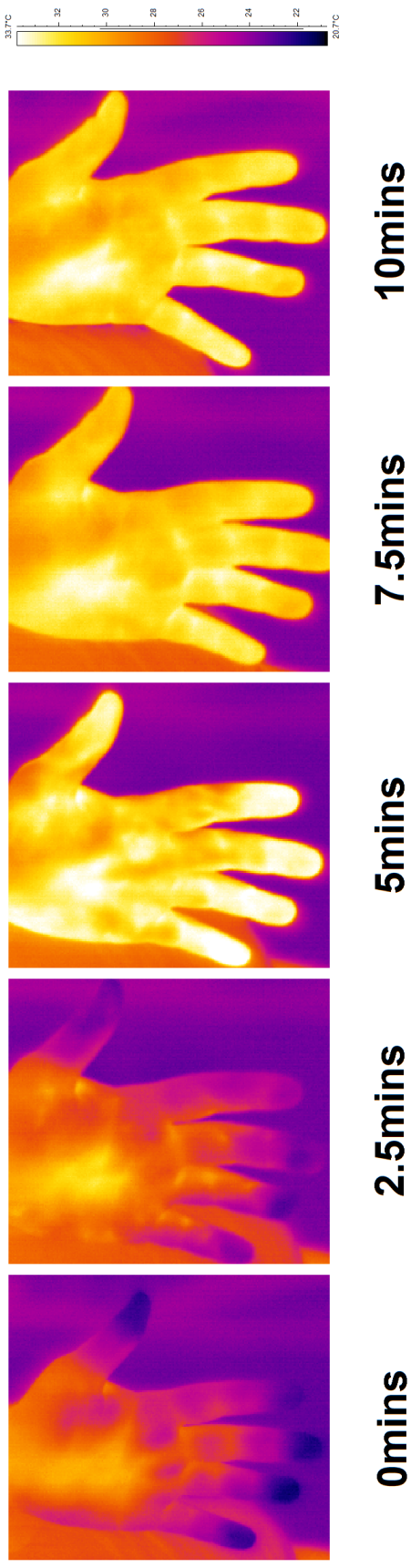

Figure 113 - Subject 3 Hand Test: Thermal images for WR test

Figure 113 shows that the initially cooler areas of the hand begin to heat within the first 2.5mins, and that very rapid change occurs between the times of 2.5mins and 5mins. The most prominent change over this time occurs in the fingertips which rise very rapidly in temperature to become, along with the palm centre, the hottest areas in the hand at around 33.5°C. Heat spots can also be seen to appear in the outer areas of the palm. Between 5mins and 7.5mins the hand can be seen to cool slightly in the fingers, and a steady state could be approximated over the 7.5min and 10min images, consisting of a uniform temperature for most of the hand with a slightly hotter palm centre temperature.

Figure 14 shows the numerical data from this test. The palm temperature can be seen to gradually climb over the first 4mins of the test before reaching a steady state, thus completing 100% of its temperature rise within 4mins. The fingertip temperature however exhibits an almost steady state for the first 2mins, a rapid rise between 2.5min and 4min, and then a slight drop to a reasonably steady state thereafter; thus completing nearly 90% of its maximum temperature rise in only 1.5mins. Another point to note is the convergence of the palm and fingertip temperatures at 4mins, after which time the fingertip temperature drops slightly but remains within about 2°C below the palm temperature. Thus the uniformity of temperatures in the hand has greatly improved from the initial difference of 7.8°C.

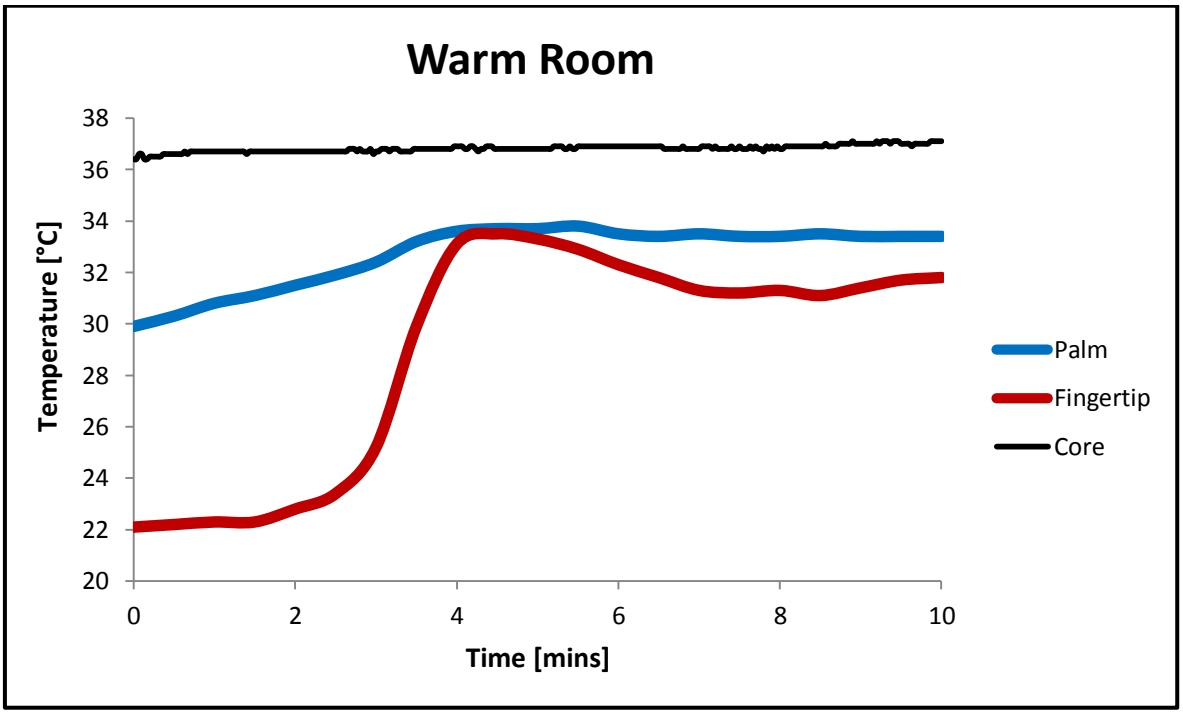

Figure 114 - Subject 3 Hand Test: Actual temperature data for WR test

The heat flux recorded during the test shown in Figure 115. Initially it is indicated by a negative heat flux value that the hand is receiving heat from its surroundings. However the slope of the heat flux is positive at this stage, indicating that the rate of heat intake is reducing, and the value very quickly becomes positive to indicate that the hand is radiating heat to its surroundings. This change from negative to positive value occurs when the palm and fingertip temperatures are 5.7°C above and 2.2°C below the room temperature respectively. A sharp rise in heat flux value over the first 4.5mins of the test corresponds to the time over which the temperatures of the hand are increasing. After 4.5mins the heat flux value drops somewhat and for the remainder of the test stays between values of $2.34 \times 10^{-3}\ W/cm^2$ and $2.58 \times 10^{-3}\ W/cm^2$, corresponding to the time during which the palm temperature remains steady and the fingertip temperature decreases. This behaviour would suggest that heat flux is directly affected by the hand temperatures.

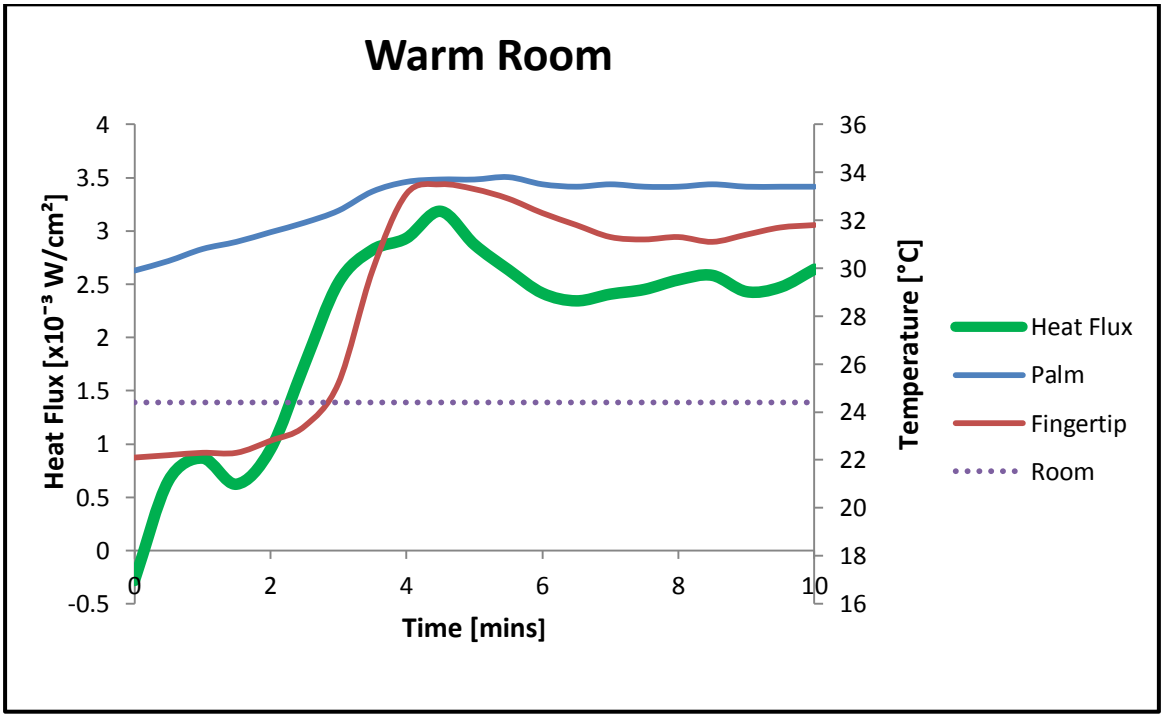

Figure 115 - Subject 3 Hand Test: Heat flux data for WR test

Hand Test –IR on Face in Cold Room

The subject is positioned in a cold room (~19.7°C) and IR heat (26.5°C at the centre position) is applied to the face area. Figure 116 shows the resulting changes in temperature distribution about the hand over the course of the test.

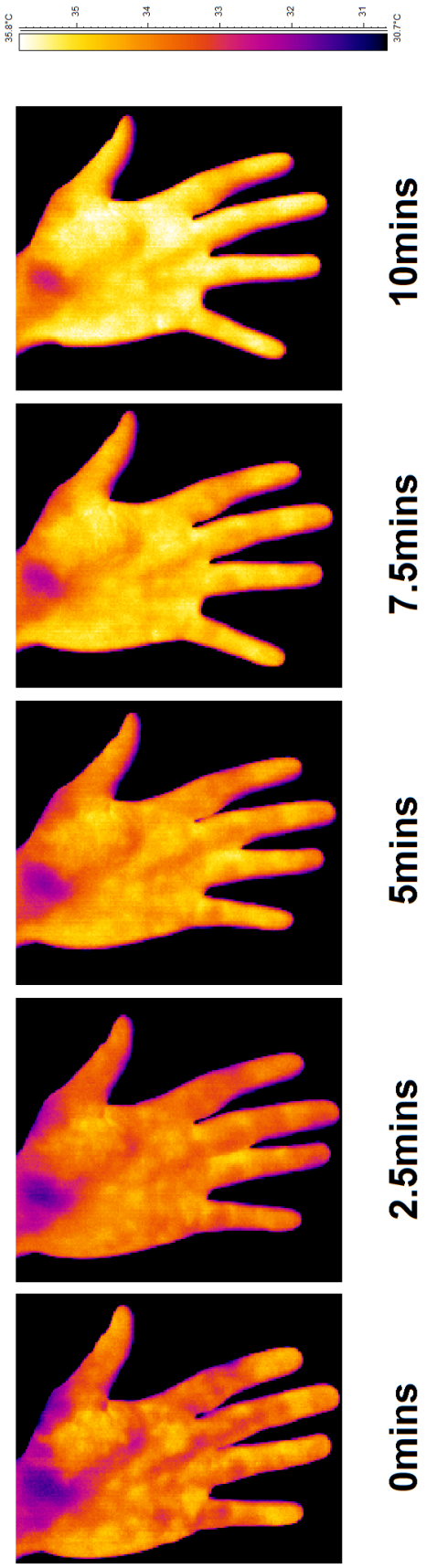

Figure 116 - Subject 3 Hand Test: Thermal images for IR on Face test

At the beginning of the test the temperature distribution is a blotchy pattern of temperatures between 33-34.5°C throughout most of the hand. Over the 2.5min and 5min images, the overall temperature of the hand can be seen to become more uniform, with temperatures ranging over the smaller amount of 33.8-34.6°C by 5mins. Temperatures over most of the hand continue to remain within a range of approximately 1°C from this point onwards, with final temperatures of 35.1 for the palm centre and 35.4 for the fingertip, with hotter regions up to temperatures of 35.9 existing as hot spots around the palm.

Figure 117 displays the numerical results for this test. It can be observed here that both the palm and fingertip temperatures rise gradually by less than 1.5°C over the course of the test, and that they both begin the test at unusually high temperatures. The temperatures of these areas also remain quite uniform throughout the test.

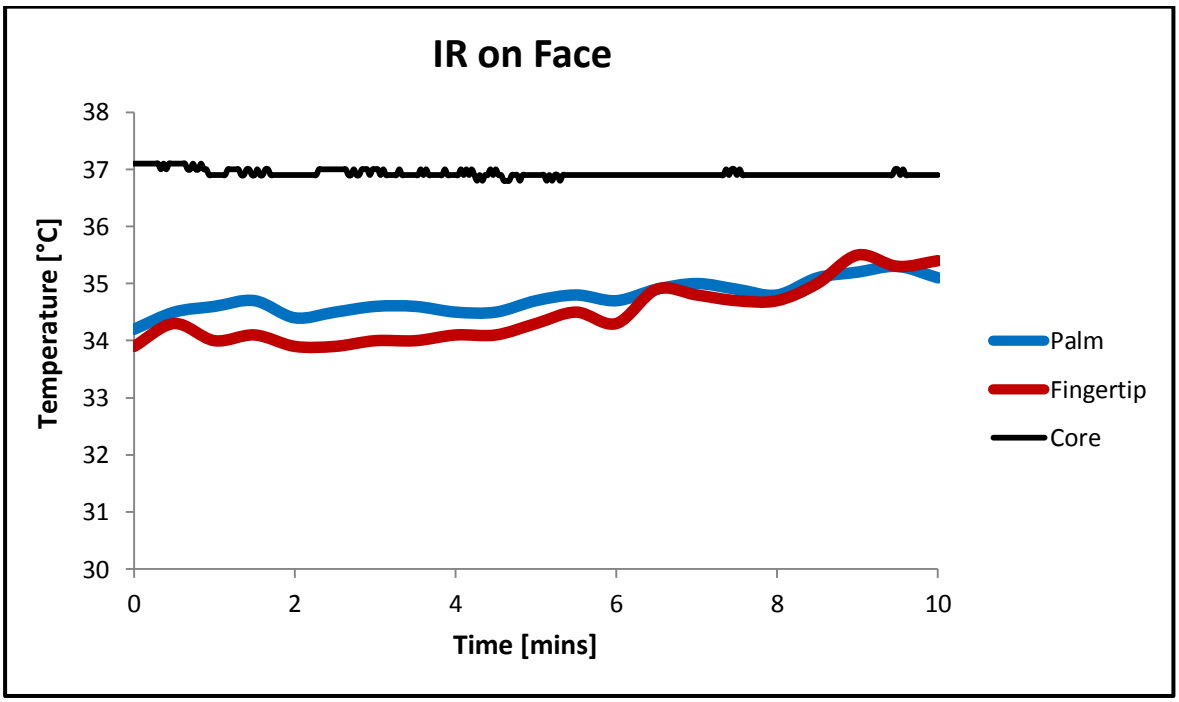

Figure 117 - Subject 3 Hand Test: Actual temperature data for IR on Face test

The heat flux recorded for the duration of this test is shown in Figure 118. The hand temperature was substantially higher than the air temperature (~19.7°C) for the duration of the test and so the heat flux value is positive over the course of the test. There is little variation in heat flux shown. The heat flux trend can be seen here to be very similar to those of the hand temperatures, with a maximum value of $9.16 \times 10^{-3}\ W/cm^2$ occurring

at the end of the test corresponding to maximum hand temperatures. Again, this suggests the direct influence of hand temperature on heat flux.

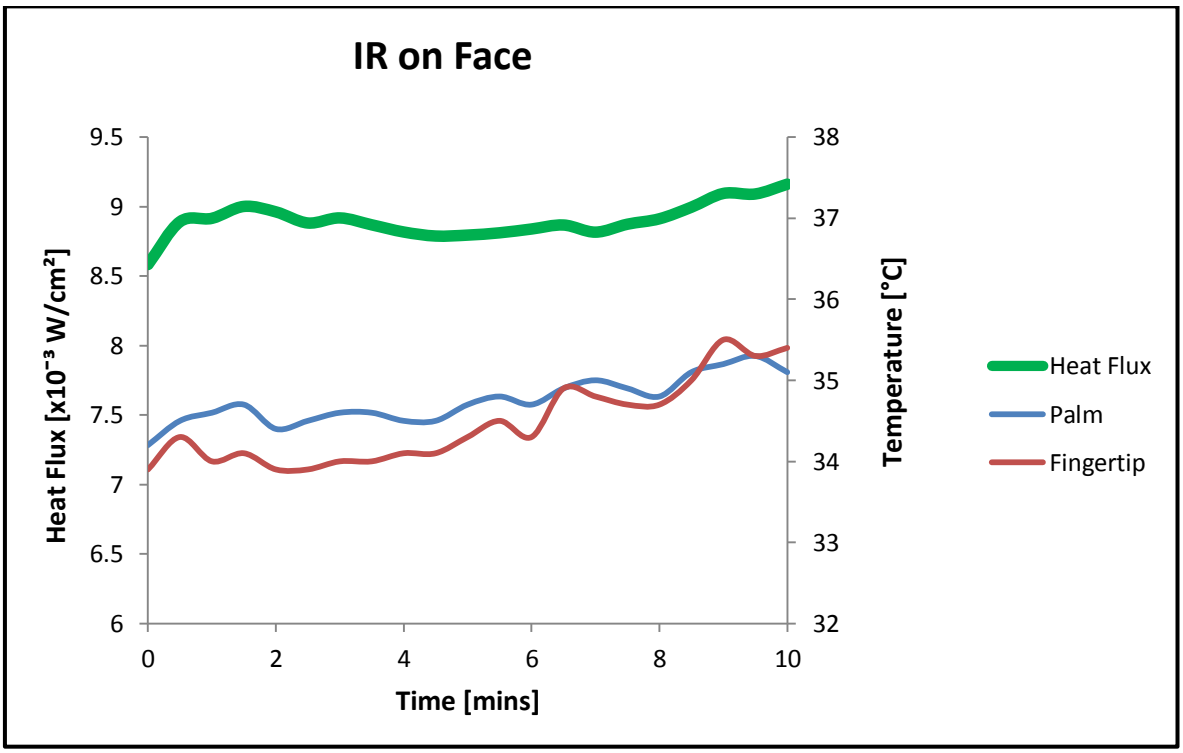

Figure 118 - Subject 3 Hand Test: Heat flux data for IR on Face test

Hand Test –IR on Hand in Cold Room

The subject is positioned in a cold room (~19.5°C) and IR heat (26.5°C at the centre position) is applied to the hand area. Figure 119 shows the resulting changes in temperature distribution about the unheated hand over the test duration. The hand appears to be fairly uniform in temperature throughout the test. At the beginning, the palm is the warmest area at 34.7°C in the centre with slightly warmer areas around the edges. The fingertips are a little cooler at 34.1°C. The temperatures throughout the hand can be seen to change the most noticeably over the first 2.5mins when palm and fingertip temperatures rise to 35.5°C and 34.8°C respectively. The hand can be seen to cool again between the times of 2.5mins and 5mins, and both palm centre and fingertip temperatures remain fairly constant for the second half of the test (35.2°C and 34.5°C respectively) with hotter areas of around 35.9°C appearing around areas of the palm towards the end of the test.

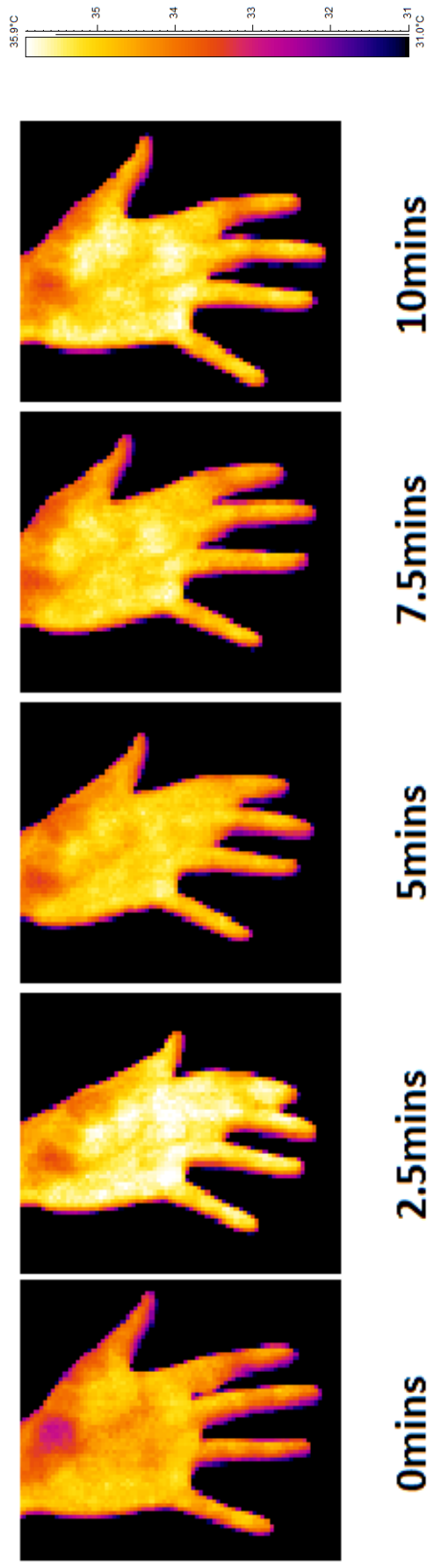

Figure 119 - Subject 3 Hand Test: Thermal images of IR on Hand test

Numerical results from this test are shown in Figure 120. Both palm and fingertip areas show similar trends here; an increase of less than 1°C which occurs within the first 2.5mins of the test. After this point temperatures for both areas fall slightly, then fluctuate around their final values for the remainder of the test.

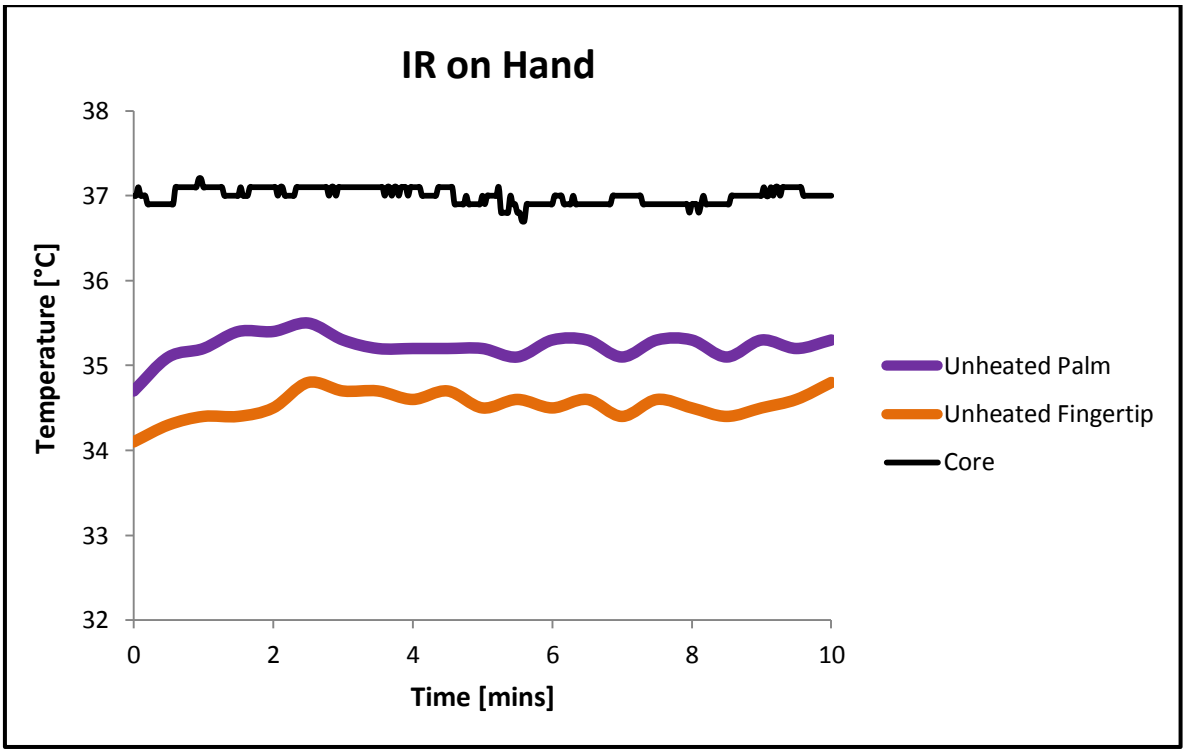

Figure 120 - Subject 3 Hand Test: Actual temperatures for IR on Hand test

Comparison of Hand Heating under different conditions

A comparative plot of the IR on Face and IR on Hand tests is shown in Figure 121. The IR on Face test shows a rise in temperature in both hand areas throughout the test. This differs from the behaviour shown by the hand areas during the IR on Hand test as both of palm and fingertip areas reach a relatively steady state at 4mins. The start temperatures for the fingertip area are very similar and so it can be seen that the IR on Face test produces a higher overall temperature increase whist the IR on Hand test produces a faster heating response. The start temperatures for the palm differ slightly, but their plots converge over the course of the test. It cannot be clearly seen whether the IR on Face test is producing a better heating response or whether this larger temperature increase occurred due to a lower start temperature, however from previous observations it is thought that the latter case is the more likely.

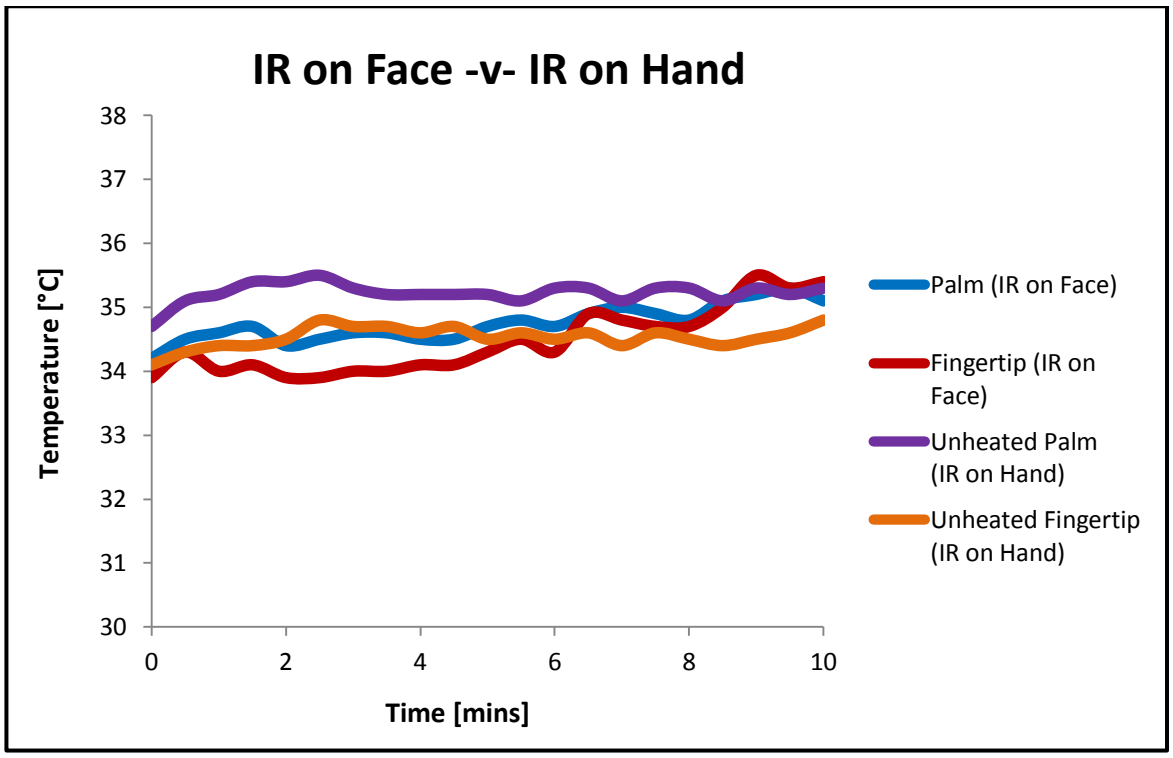

Figure 121 - Subject 3 Hand Test: IR on Face -v- IR on Hand

Comparisons between trends in the WR and IR on Face tests for the hand shown in Figure 122 may not be reasonable to make due to the very high initial temperatures of these areas in the IR on Face test.

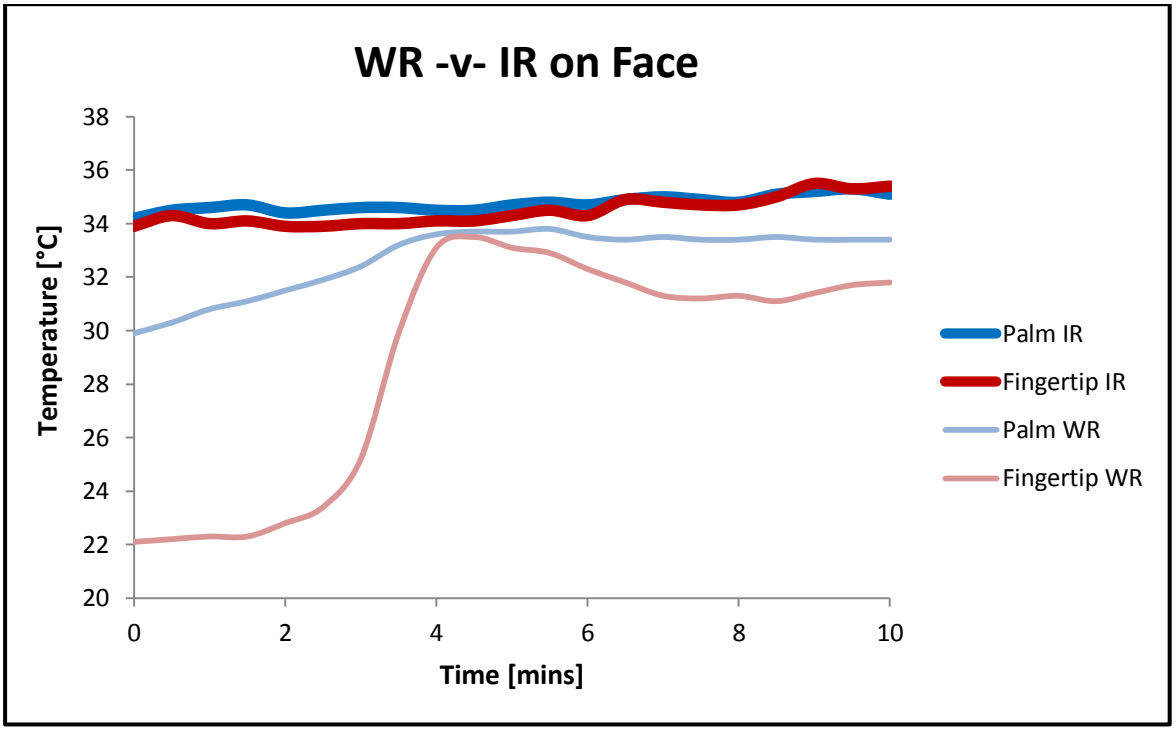

Figure 122 - Subject 3 Hand Test: WR -v- IR on Face

From investigation of the full body for this subject it had been previously found that the hand areas show a rise in temperature when the IR test is carried out with lower stating temperatures for these areas. In the IR on Face test the initial temperatures are so high that there is not much of a temperature increase possible in the hands. This would suggest that during the IR on Face test the blood flow to the hand area was already at a maximum, and this suggestion is supported by the high heat flux values shown in Figure 118. These observations can be similarly put to the comparison of the WR and IR on Hand tests shown in Figure 123. The similar nature of these two comparative plots would lend support to the theory that high initial temperature results cannot be accurately compared to low initial temperature results.

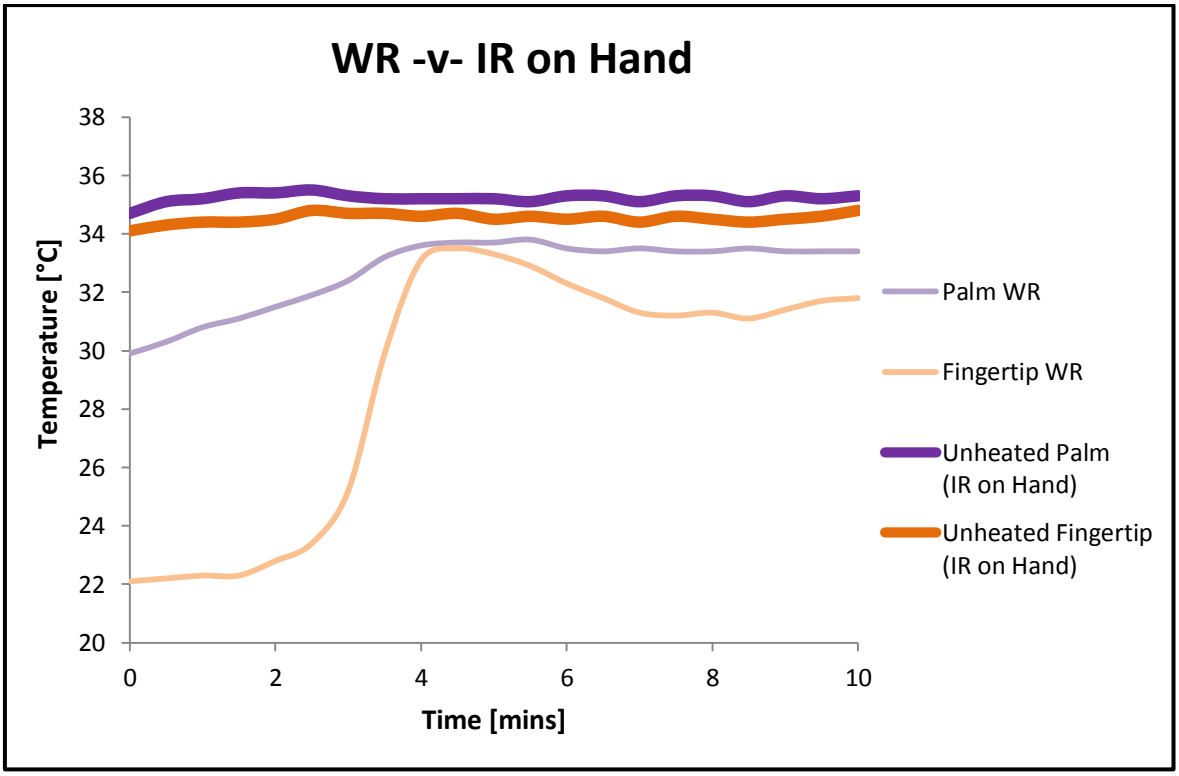

Figure 123 - Subject 3 Hand Test: WR -v- IR on Hand

4.3.1.4 Subject 4

Full Body Test - Warm Room

The subject is brought from a cold room (~17.4°C) into a warm room (~22°C). Figure 124 displays thermal images which show the resulting changes in skin temperature distribution about the body over the course of the test. The temperatures over the entire body appear to rise over the course of the test, particularly over the last 5mins. The greatest change can be seen in the face around the nose and mouth regions.

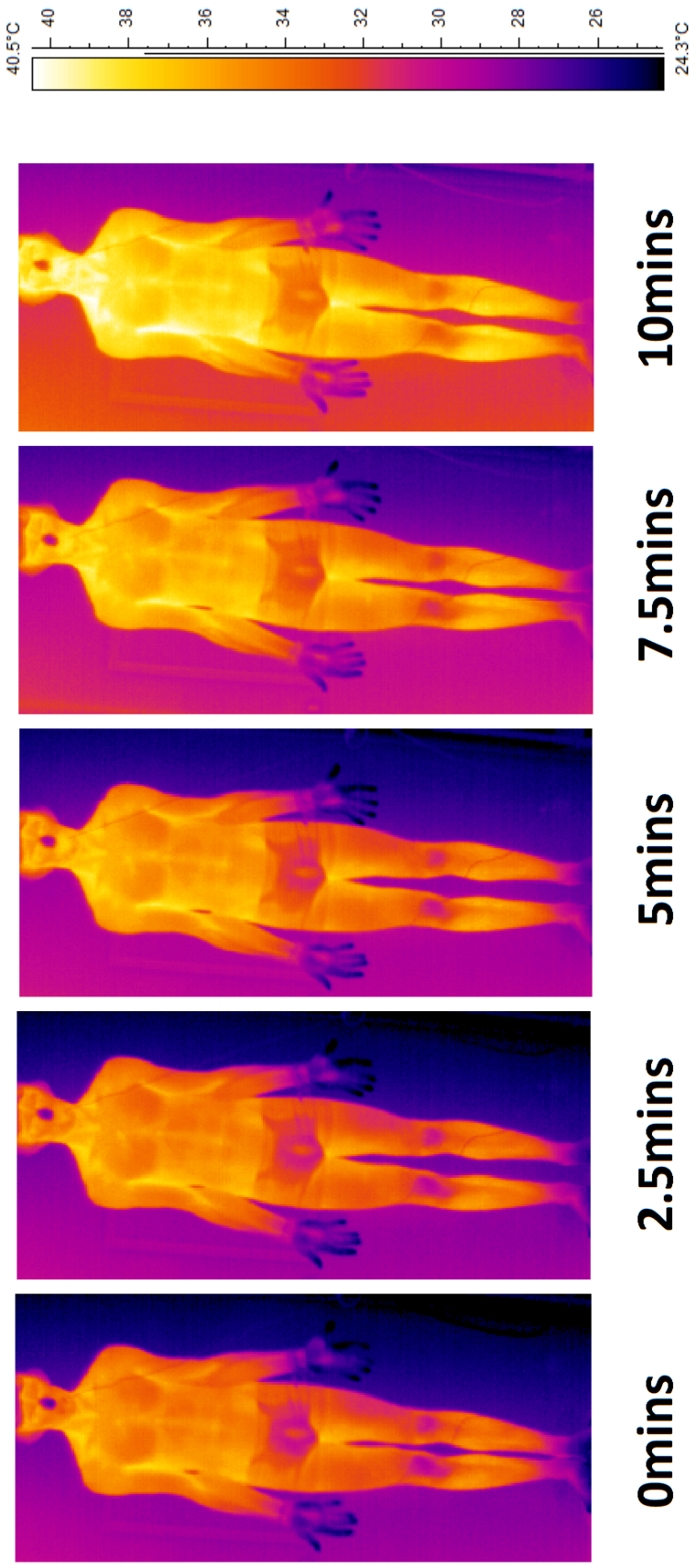

Figure 124 - Subject 4 Full Body Test: Thermal images of WR test

Analysis of the numerical data in Figure 125 shows that there are indeed temperature increases throughout the entire body, and that the temperatures increase most rapidly from 4mins into the test. The nose shows the greatest temperature increase (4°C), and 75% of this increase occurs between the times of 4mins and 10mins. The palm shows the least temperature increase (1.7°C), and all other areas of the body show an increase within the range of 2.3-3.2°C.

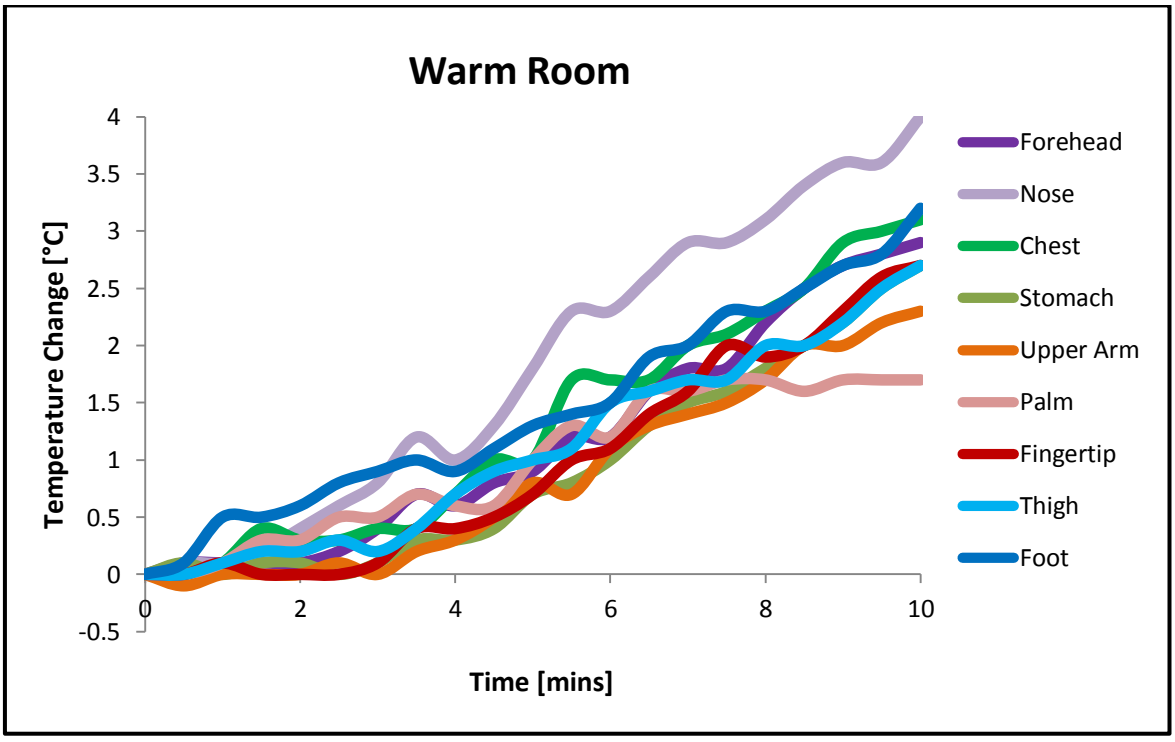

Figure 125 - Subject 4 Full Body Test: Temperature change data for WR test

The actual temperatures of several areas of the body during the test are shown in Figure 126. It can be seen here that the general groupings of primary and secondary temperature areas do not hold as strongly here. The primary forehead and chest areas are just slightly higher in temperature than the upper arm, stomach and thigh areas throughout, all of these areas lying within a range of 2.2°C below to 1.7°C above the estimated core temperature. The palm, as the final secondary area, is much closer to the nose and foot areas in temperature all of which fall between 4.9-8.1°C below the estimated core temperature throughout the test. The fingertip area has the lowest initial temperature at 10.4°C below the estimated core, and this area remains the coldest area by the end of the test, where it falls 9.1°C below the estimated core temperature.

Trends for all areas of the body are quite similar; relatively steady state or gently rising slope for the first 4mins followed thereafter by a steeper slope. It can also be seen here that the uniformity of the temperature distribution about the body remains fairly constant over the course of the test.

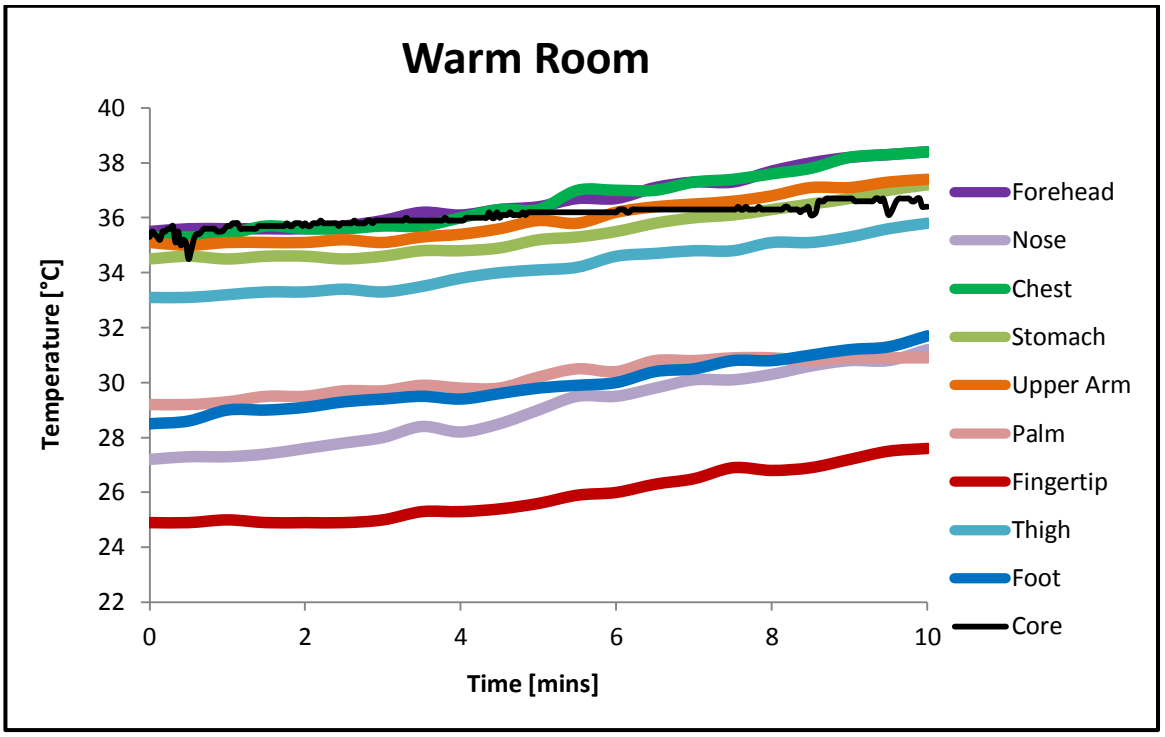

Figure 126 - Subject 4 Full Body Test: Actual temperature data for WR test

Full Body Test - IR on Face in Cold Room

The subject is positioned in a cold room (~17.5°C) and IR heat (26.5°C at the centre position) is applied to the face area. Figure 127 shows the resulting changes in temperature distribution around the body. The clearest temperature increases here appear mostly in the face and upper torso regions, and the majority of this change occurs over the first 2.5mins of the test. Other areas of the body cannot be seen to change from these images, but further analysis of the numerical data may allow more subtle changes to be observed.

Figure 128 shows the change in skin temperature experienced by different areas of the body regardless of initial temperature. It can be observed that the areas with the largest temperature change are indeed the areas that lie within the head and upper torso regions; the forehead (3.1°C), the nose (2°C), the chest (1.4°C), and also the upper arm (1.3°C).

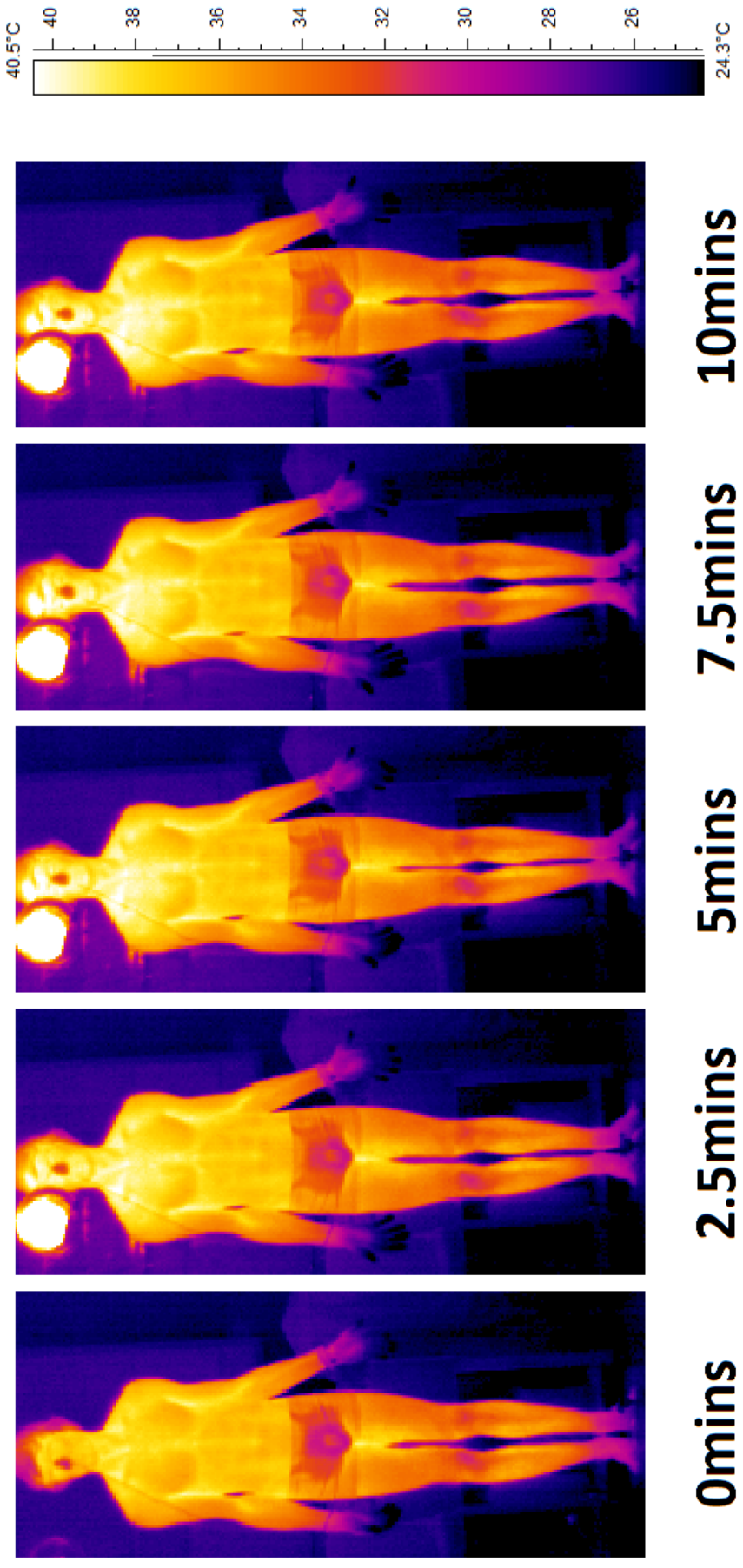

Figure 127 - Subject 4 Full Body Test: Thermal images of IR on Face test

It would be expected that the head and upper torso areas would rise in temperature as the main IR heat is focused on the face, with the peripheral emanating heat flux also having an effect on the upper torso and upper arm. Of these areas the forehead and nose in particular show an early sharp initial temperature rise which occurs over the first 3mins; this period includes around 80% of the overall temperature increases for each area. From 5mins all of these areas reach more stable temperatures and fluctuate around their final temperature values. The foot is the only other area that shows some amount of heating (a rise of 0.6°C occurring from 3mins into the test) with all other areas fluctuating around the zero temperature change mark.

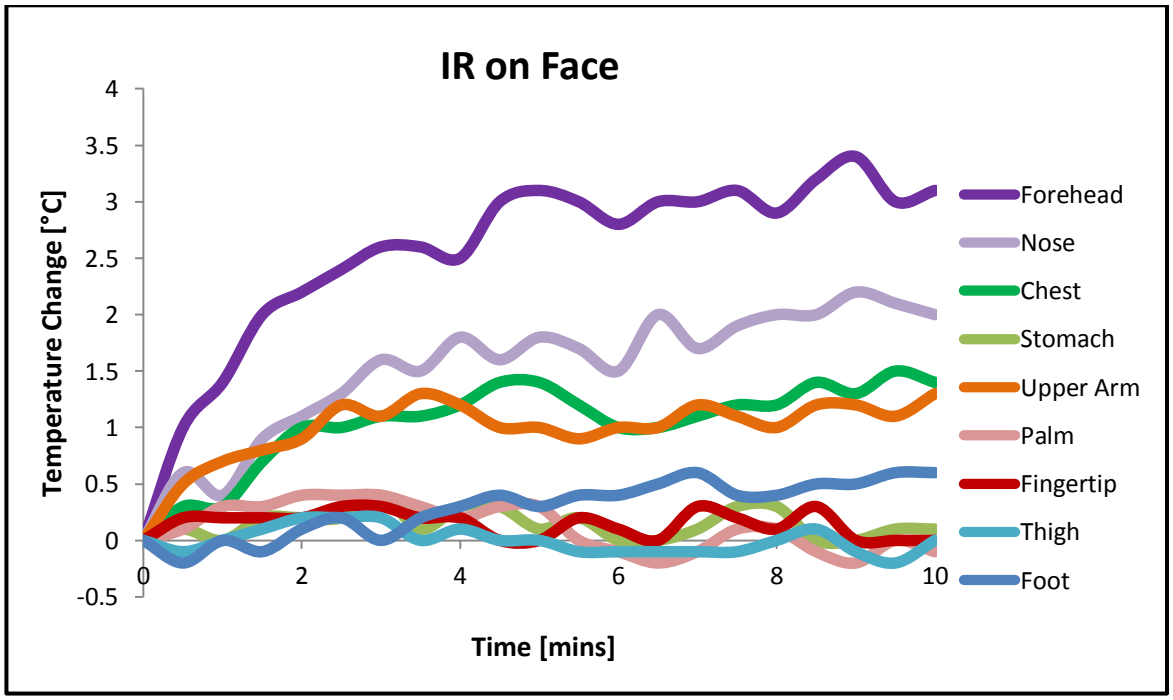

Figure 128 - Subject 4 Full Body Test: Temperature change data for IR on Face test

Figure 129 shows the actual temperatures of several areas of the body during the test. The primary forehead and chest areas begin the test at 3°C below the estimated core temperature and by the end of the test the forehead temperature matches its value, with the chest temperature lying only 1.9°C below. The secondary regions of the thigh, upper arm and stomach remain between 4.3-6.9°C below the estimated core temperature throughout the test. The palm temperature is substantially lower than this, and along with the nose and foot temperatures falls in a range of 9.4-13.2°C below the estimated core temperature for the test duration. The fingertip remains the lowest temperature area throughout the test at over 20°C below the estimated core temperature throughout the test.

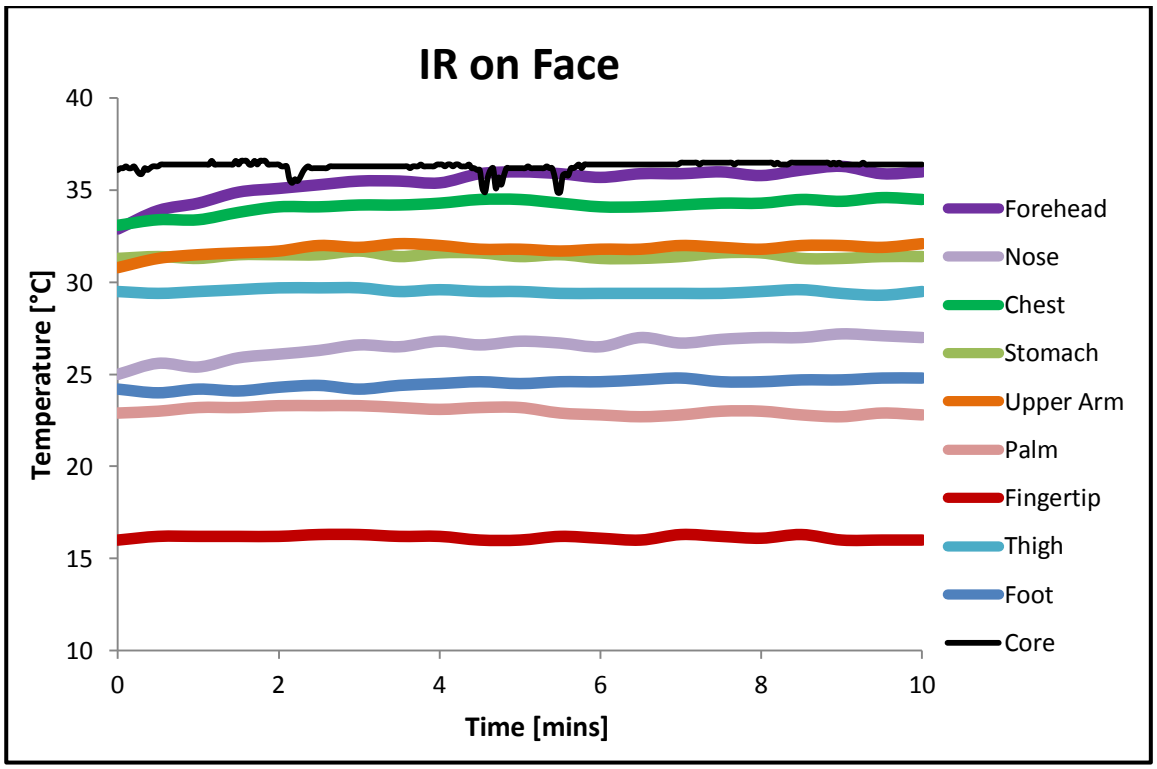

Figure 129 - Subject 4 Full Body Test: Actual temperature data for IR on Face test

Comparison of Full Body Heating under different conditions

In comparing the IR on Face test with the WR test the most noticeable differences can be best described by looking at the forehead and fingertip areas, which are shown for comparison in Figure 130. Each of these areas shows the same difference in trend between the two tests; an increasing slope for the WR test and a decreasing slope for the IR on Face test, and this can be seen most clearly from observation of the forehead area. During the WR test every area of the body showed a temperature increase similar to those shown here without exception.

Overall, the WR test gave the greatest temperature increases throughout all areas of the body, even for the areas exposed to direct IR heat during the IR on Face test (excepting the forehead area which showed a slightly higher temperature increase during the IR on Face test). The fingertip is the best example of this, showing an increase in temperature of 2.7°C during the warm room test as compared to no overall change during the IR on Face test.

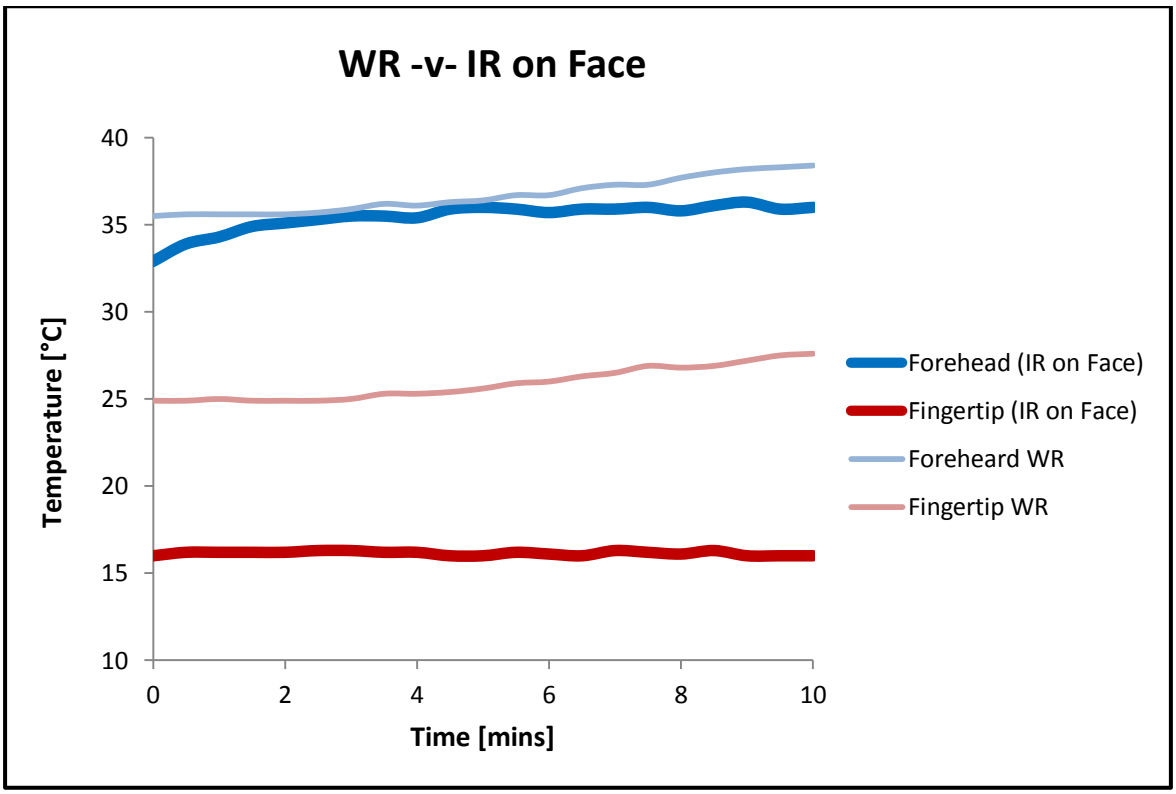

Figure 130 - Subject 4 Full Body Test: WR -v- IR on Face

Again the hand and face areas have been identified as the most interesting areas and so further testing will be carried out focusing on these areas.

Face Test – Warm Room

The subject is brought from a cold room (~17.8°C) into a warm room (~22°C), and thermal images showing the resulting changes in temperature distribution in the face over the test duration are displayed in Figure 131. Initially the highest temperature exists around the forehead area which is at 34.6°C. The chin and mouth areas are cooler than this at 32.8°C and 32.5°C respectively, closely followed by the cheek area at a slightly cooler 31.7°C. The nose tip temperature is by far the coldest area at the beginning of the test at only 23.8°C. From observation of the thermal images it can be seen that the greatest changes in temperature occur in the nose and mouth areas, which undergo a total temperature increase of 3.7°C and 3.4°C respectively. The chin, cheek and forehead areas can also be seen to grow warmer, all rising by temperatures of between 1.1-2.3°C over the course of the test.

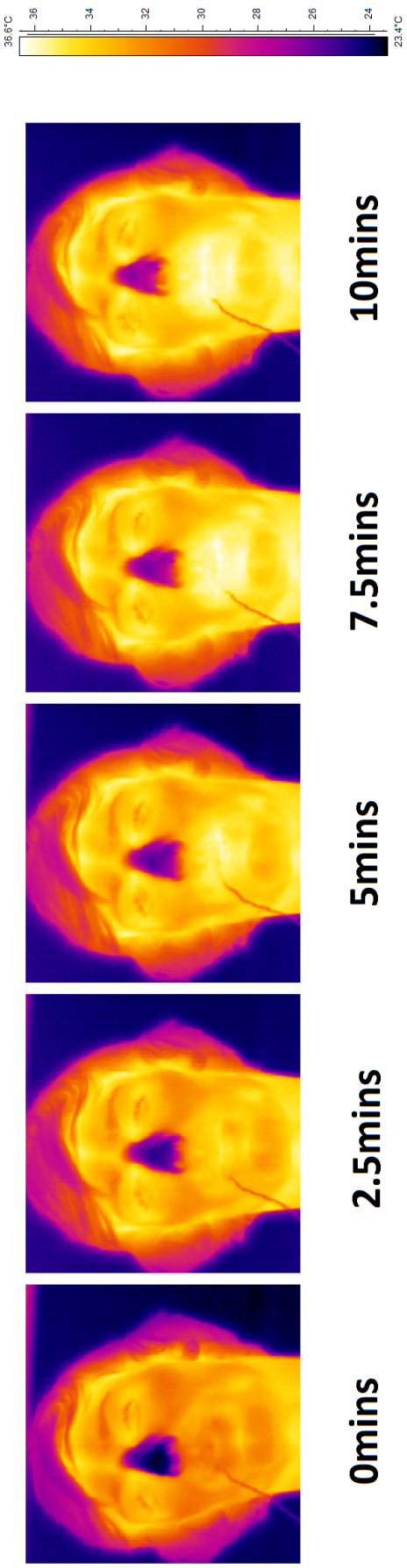

Figure 131 - Subject 4 Face Test: Thermal images of WR test

The results for this test are further inspected in Figure 132. Excluding the nose tip, the face areas remain within a fairly uniform 2.6°C range throughout the test. Initially at the lower end of this temperature range, the increase in mouth temperature causes this area to achieve the highest final temperature across the face. The nose tip however remains the coldest area of the face throughout due to its substantially lower initial temperature. The forehead, chin and cheek areas show a similar rate of increase, as can also be said for the nose tip and mouth areas. The overall effect is a somewhat more uniform temperature distribution over the entire face, an initial range of 10.8°C dropping to 8.4°C by the end of the test.

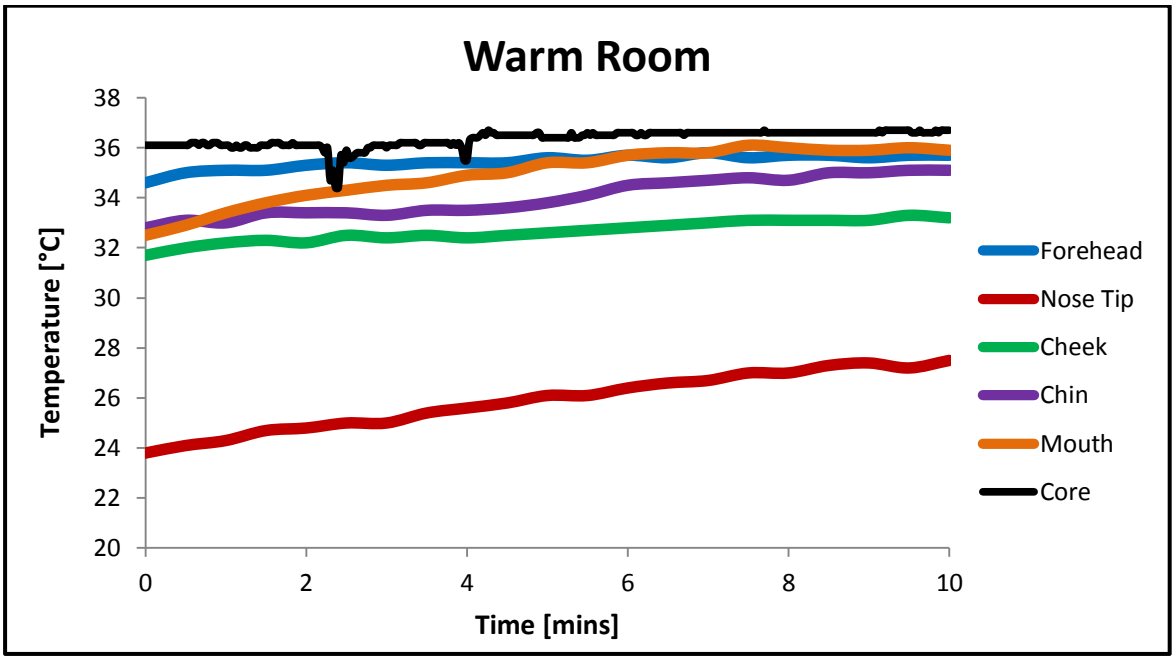

Figure 132 - Subject 4 Face Test: Actual temperature data for WR test

Face Test –IR on Face in Cold Room

The subject is positioned in a cold room (~18.4°C) and IR heat (26.5°C at the centre position) is applied to the face area. The resulting changes in temperature distribution over the following 10mins are shown in Figure 133. Initially the warmest area of the face can be seen to be around the mouth area at 34.7°C. The next warmest areas are the chin and forehead, both around 32°C, and the cheeks are a little cooler at 31.4°C. The coldest area at the beginning of the test is the nose with a temperature of 22.3°C. Within the first 2.5mins of the test the temperatures across the entire face can be seen to rise, and after this point the changes if any are much more gradual. The nose area remains by far the coldest area at the end of the test.

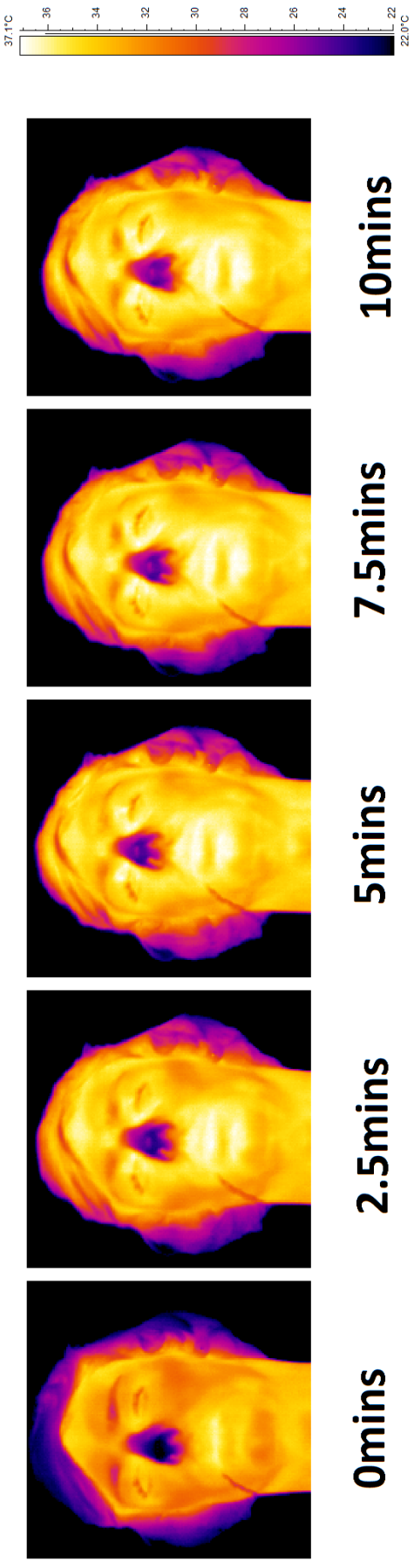

Figure 133 - Subject 4 Face Test: Thermal images of IR on Face test

Figure 134 allows for further inspection of the numerical results derived from the thermal images. The plots show that the majority of the temperature increase for each area occurs within the first 1min of the test; ranging from 52% of the total temperature increase for the nose tip area to 75% for the moth area. It can also be seen that the forehead and chin temperatures are very similar at the beginning of the test, but later diverge as the chin area shows an overall higher temperature increase. Overall the temperatures over the entire face become more uniform, from an initial range of 12.4°C to a final range of 10°C.

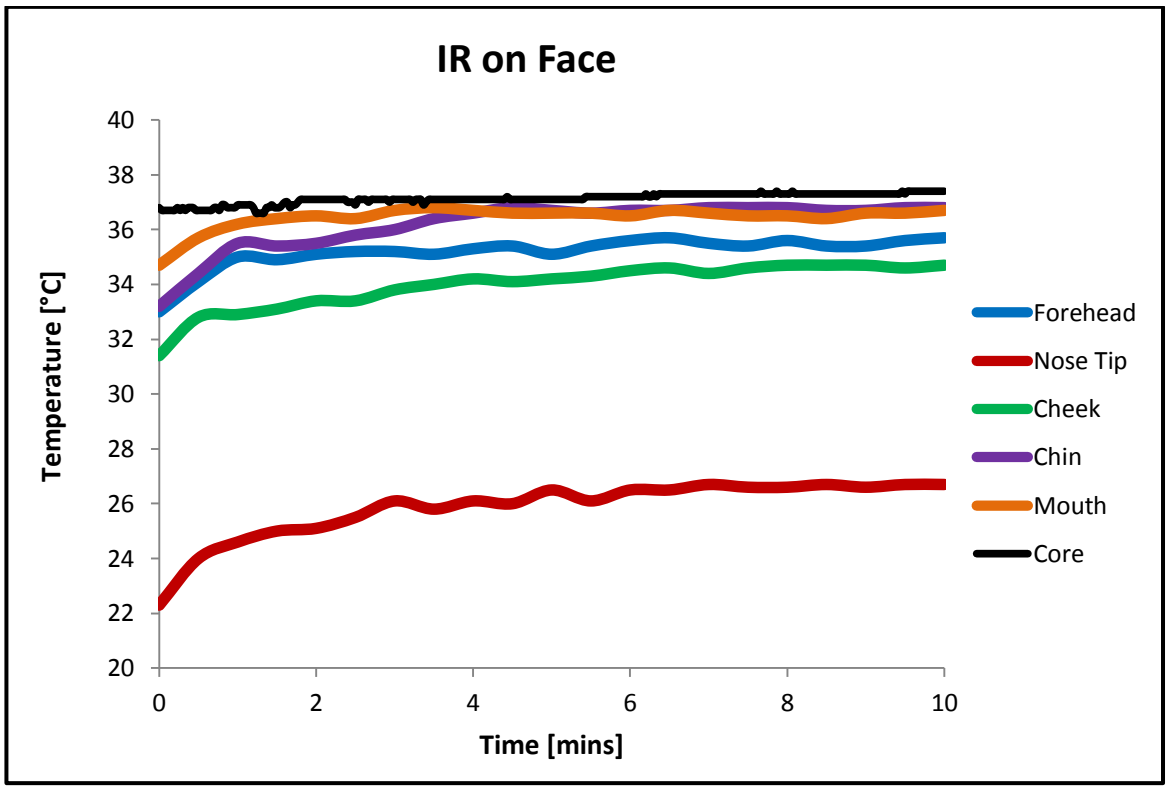

Figure 134 - Subject 4 Face Test: Actual temperature data for IR on Face test

Comparison of Face Heating under different conditions

A comparative plot of the WR and IR on Face tests is shown in Figure 135. The overall temperatures achieved are higher for the IR on Face test than for the WR test for all areas excluding the nose tip, however this statement is only truly meaningful for areas with similar start temperatures, i.e. the cheek and chin areas. The temperature increases during the IR on Face test are greater than those which occur during the WR test (excepting the mouth area which shows a higher overall temperature increase during the WR test, but this possibly due to its noticeably lower initial temperature). The forehead area also shows relatively different start temperatures between the tests and so the results for this area may

likewise be less reliable. The common trend for the IR on Face test is a two stage process consisting of a sharp initial rise followed by a more gentle slope, whilst the common trend for the WR test is a gentle slope throughout the test.

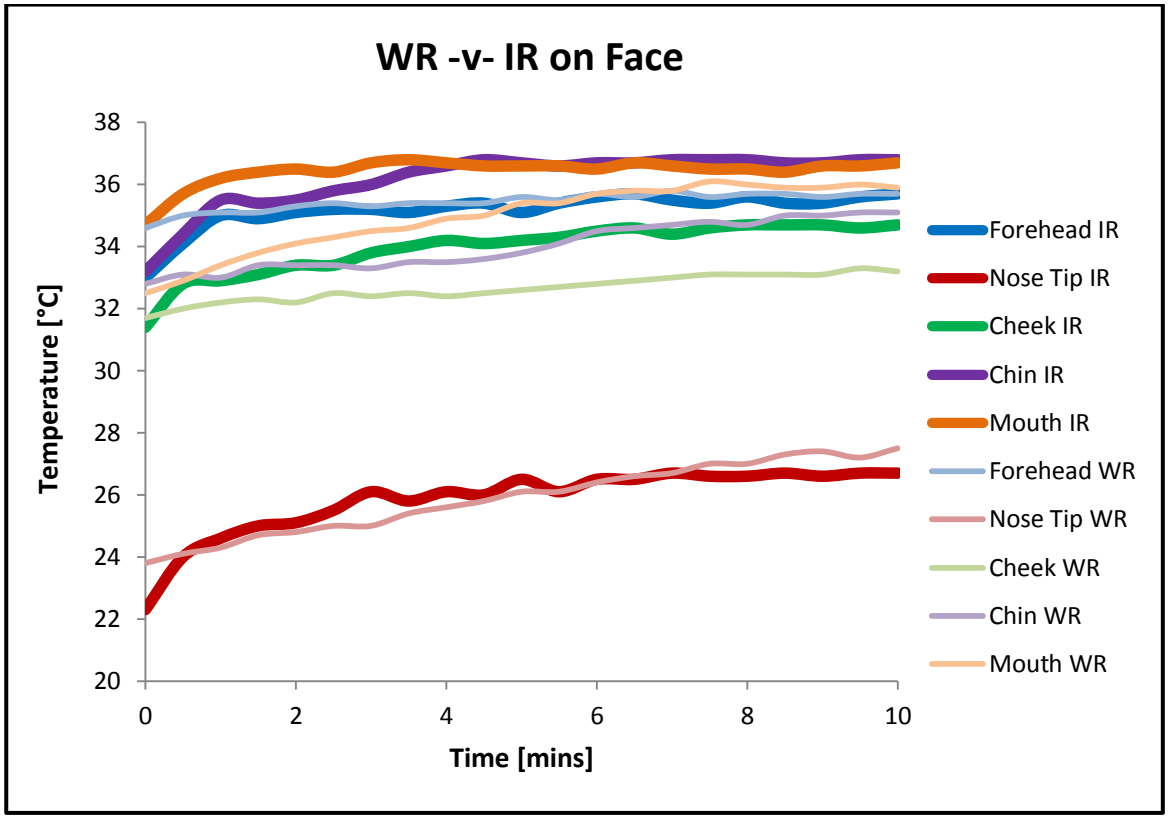

Figure 135 - Subject 4 Face Test: WR -v- IR on Face

Hand Test – Warm Room

The subject is brought from a cold room (~17.8°C) into a warm room (~22.2°C). Thermal images of the resulting changes in temperature distribution in the hand area are shown in Figure 136. At the beginning of the test the palm centre is the warmest area of the hand at 24.5°C. Temperatures drop towards the edges of the palm and the fingers, and the coldest are of the hand is the fingertip area at 18.4°C.

From these thermal images it can be seen that the greatest temperature change occurs in the fingertips, which show a 2.4°C rise over the course of the test, the majority of which appears to occur over the final 2.5mins. The palm cam also be seen to increase in temperature (25.8°C after 10mins), with the hot centre spot moving across more of the palm towards the end of the test.

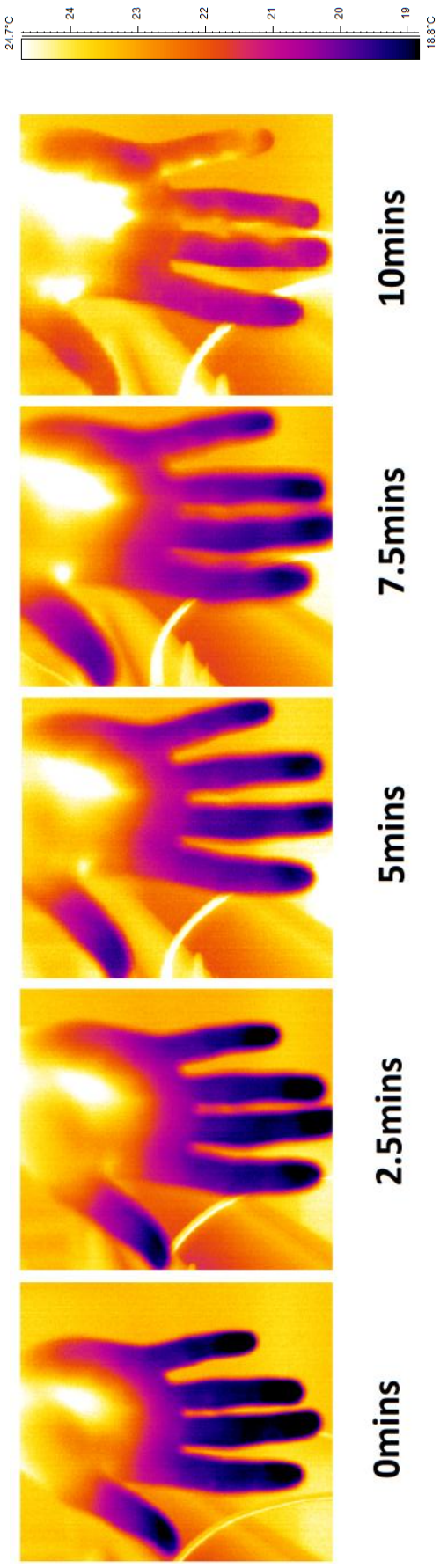

Figure 136 - Subject 4 Hand Test: Thermal images for WR test

The numerical data from this test can be examined in Figure 137. *[Note: the estimated core temperature has not been displayed here, or in the hand plots to follow, as its significantly higher temperature interfered with the clarity of the hand temperature plots. It remained reasonably constant throughout each test duration].* Both the palm and fingertip areas can be seen to increase in temperature by a small amount during the test; 1.3°C and 2.4°C respectively. For both areas this increase occurs mostly between 4mins and 10mins, when the palm experiences over 75% of its total temperature increase, and the fingertip over 90% of its total temperature increase. The hand becomes slightly more uniform over the course of the test; an initial range of 6.1°C dropping to a final range of 5°C.

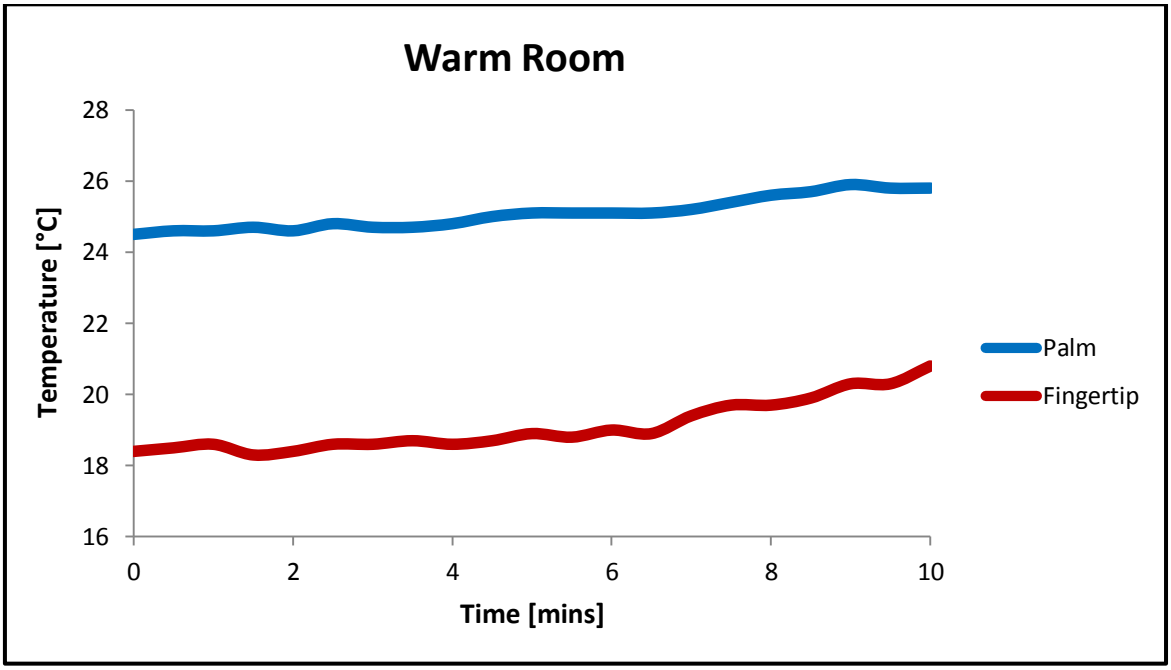

Figure 137 - Subject 4 Hand Test: Actual temperature data for WR test

The heat flux recorded for this test is shown in Figure 138. The heat flux value is negative for the duration of the test indicating that the hand is receiving heat from the surroundings at all times. It can be seen that the fingertip temperature remains below the room temperature throughout the test and that the palm temperature is less than 4°C above it at its highest temperature point. This suggests that the overall temperature of the hand is likely quite cold in comparison to the room temperature. As the test progresses the heat flux plot displays a gradually decreasing slope to a minimum value of $-1.42 \times 10^{-3}\ W/cm^2$, suggesting that the rate of heat intake to the hand is being increased. This corresponds to a rise in temperature over the hand.

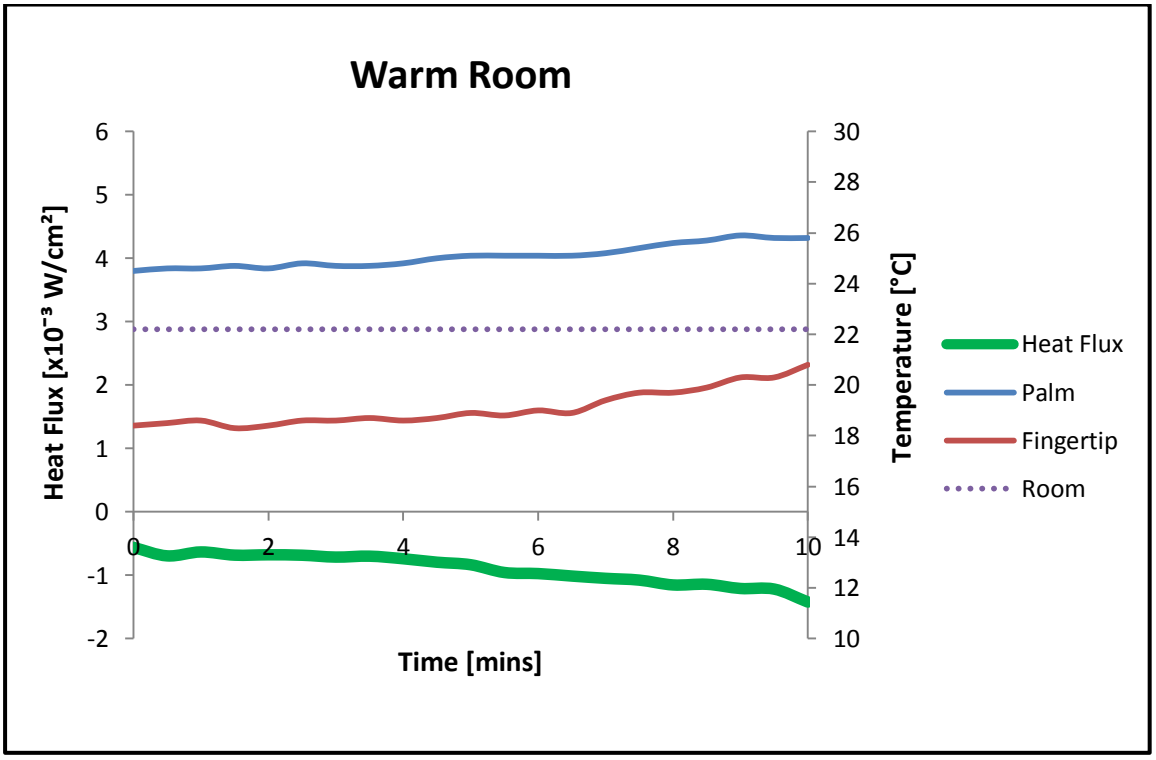

Figure 138 - Subject 4 Hand Test: Heat flux data for WR test

Hand Test –IR on Face in Cold Room

The subject is positioned in a cold room (~17.3°C) and IR heat (26.5°C at the centre position) is applied to the face area. Figure 139 shows the thermal images of the hand recorded for the test. From observation of these images there is no clear change apparent.

The results are further inspected in Figure 140 and it can be seen that the temperatures for the palm and fingertip areas remain reasonably constant for the entire test. An initial palm temperature of 24.4°C changes by only 04°C over the test duration, ending at a slightly lower temperature of 24°C. Similarly the fingertip area barely changes from its initial temperature of 16.7°C.

Figure 141 displays the heat flux data recorded for the test. The heat flux value is positive throughout the test, indicating that the hand is radiating heat to the surrounding cold air. There is little variation in heat flux over the test duration and it maintains a value of a little over $2 \times 10^{-3}\ W/cm^2$ throughout. This corresponds to an unchanging hand temperature, the temperature of which is higher than the room temperature except for in the fingertip areas which lay slightly below the room temperature.

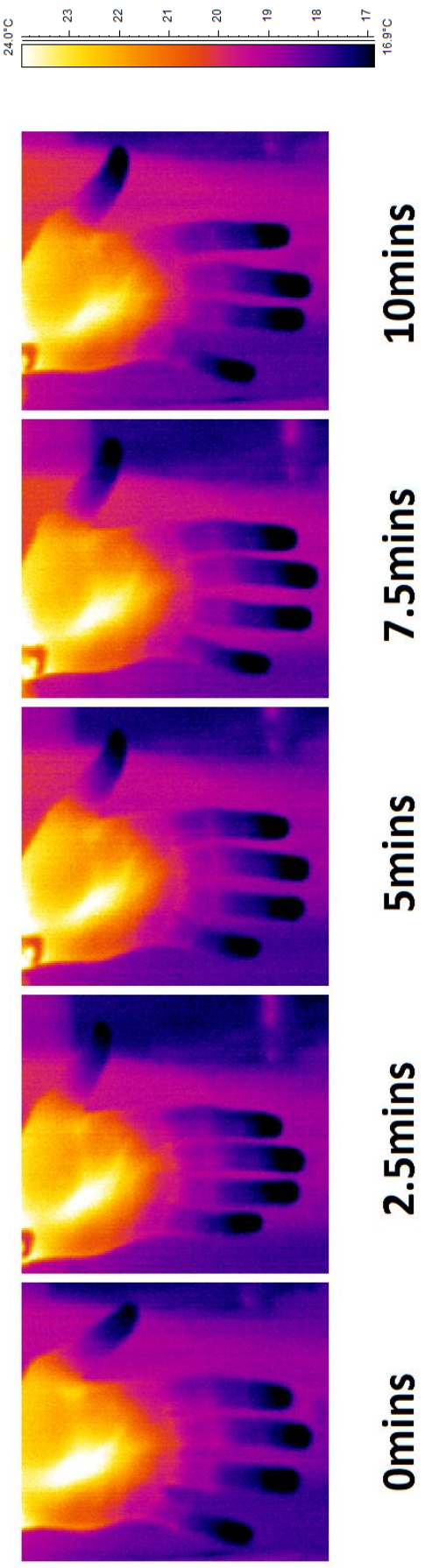

Figure 139 - Subject 4 Hand Test: Thermal images for IR on Face test

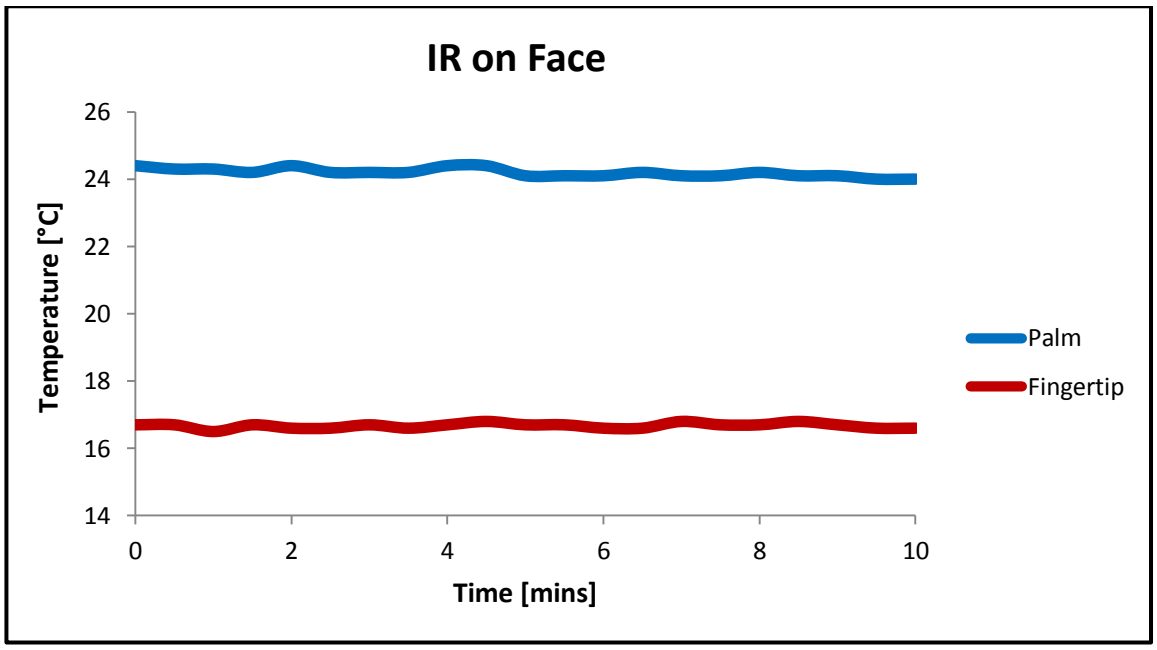

Figure 140 - Subject 4 Hand Test: Actual temperature data for IR on Face test

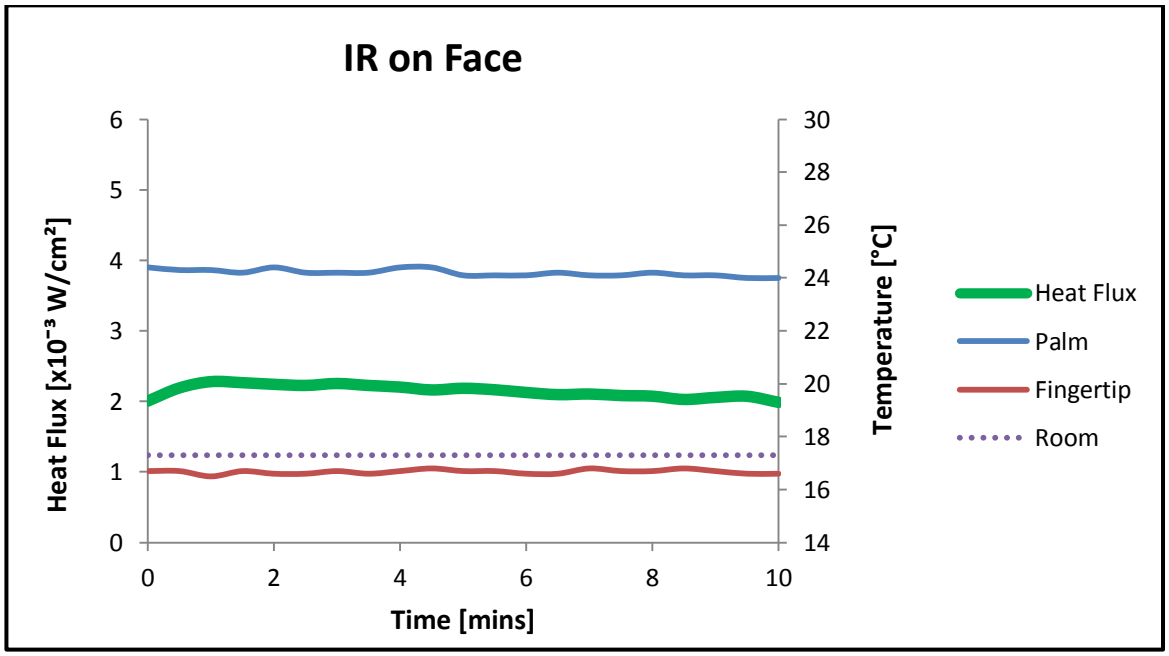

Figure 141 - Subject 4 Hand Test: Heat flux data for IR on Face test

Hand Test –IR on Hand in Cold Room

The subject is positioned in a cold room (~18.2°C) and IR heat (26.5°C at the centre position) is applied to the hand area. Figure 142 shows the thermal images of the unheated hand recorded for the test. From observation of these images there is no change apparent.

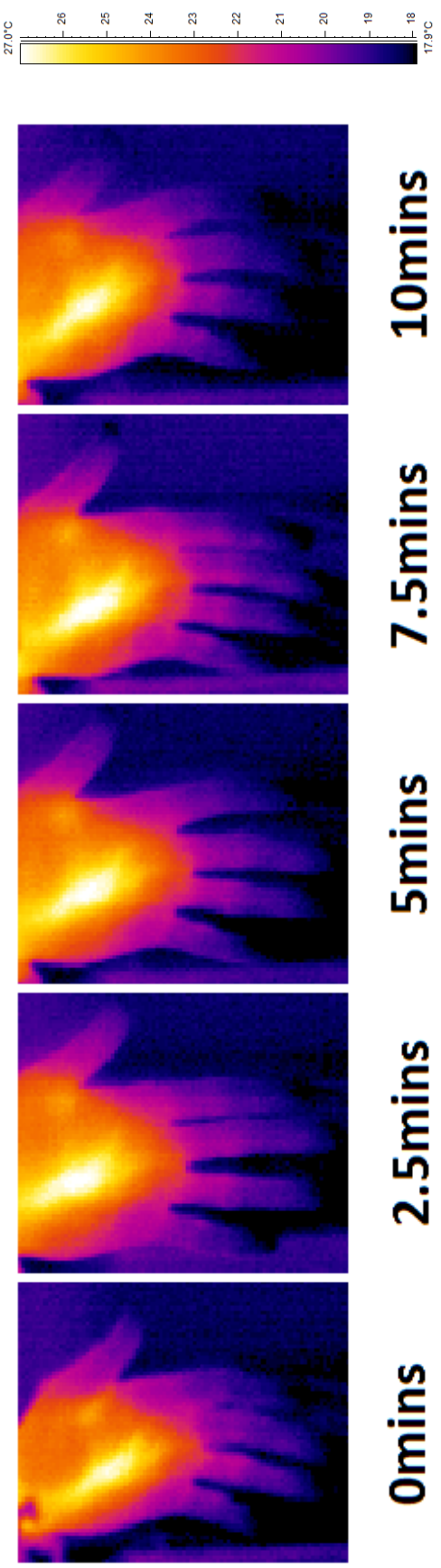

Figure 142 - Subject 4 Hand Test: Thermal images of IR on Hand test

These results are inspected further in Figure 143. As deduced from observation of the thermal images, it can be seen that the palm and fingertip areas remain fairly constant in temperature for the entire test. The palm temperature rises from an initial temperature of 26.8°C by a maximum of 0.4°C over the course of the test. The fingertip temperature shows even less change than that of the palm; fluctuating around a temperature of 18.3°C for the entire test.

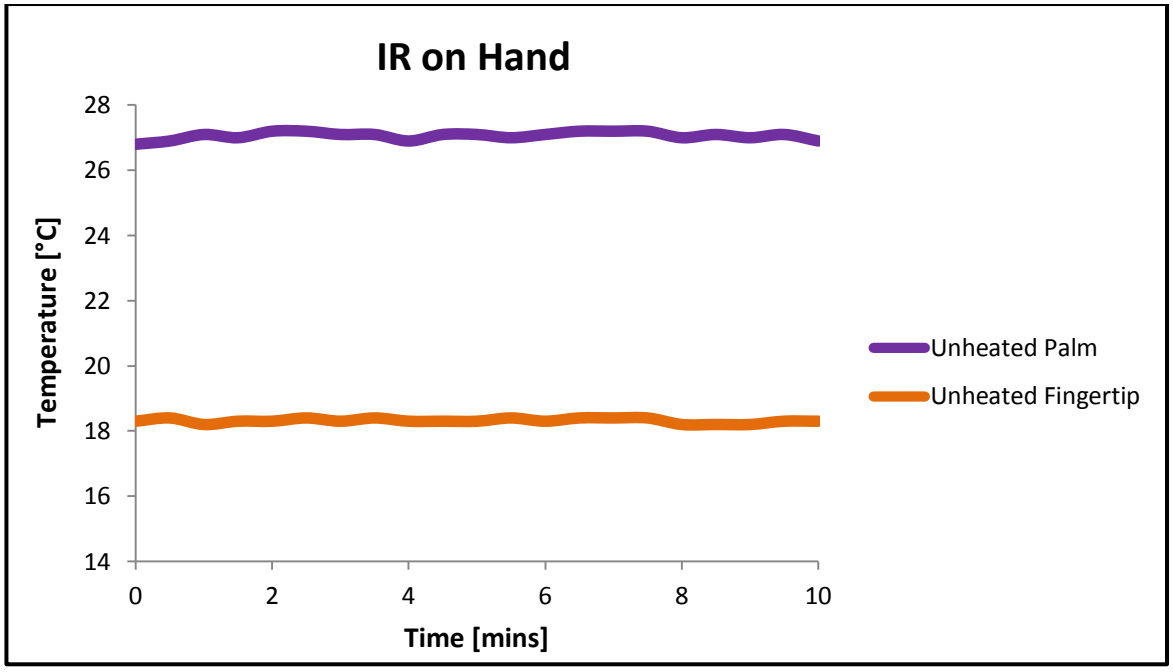

Figure 143 - Subject 4 Hand Test: Actual temperatures for IR on Hand test

Comparison of Hand Heating under different conditions

The IR on Face and IR on Hand tests are compared in Figure 144. It can be seen here that the palm and fingertip behaviour is the highly similar for each of the tests, and that this behaviour is not affected by initial temperature.

The IR on Face and WR tests are compared in Figure 145, and the IR on Hand and WR tests are compared in Figure 146. As the behaviour of both hand areas over the two IR tests has proven to be highly similar, it is convenient to compare the palm temperature between the IR on Face and WR tests, and the fingertip temperature between the IR on Hand and WR tests. This allows comparison to be made with relation to similar starting temperatures.

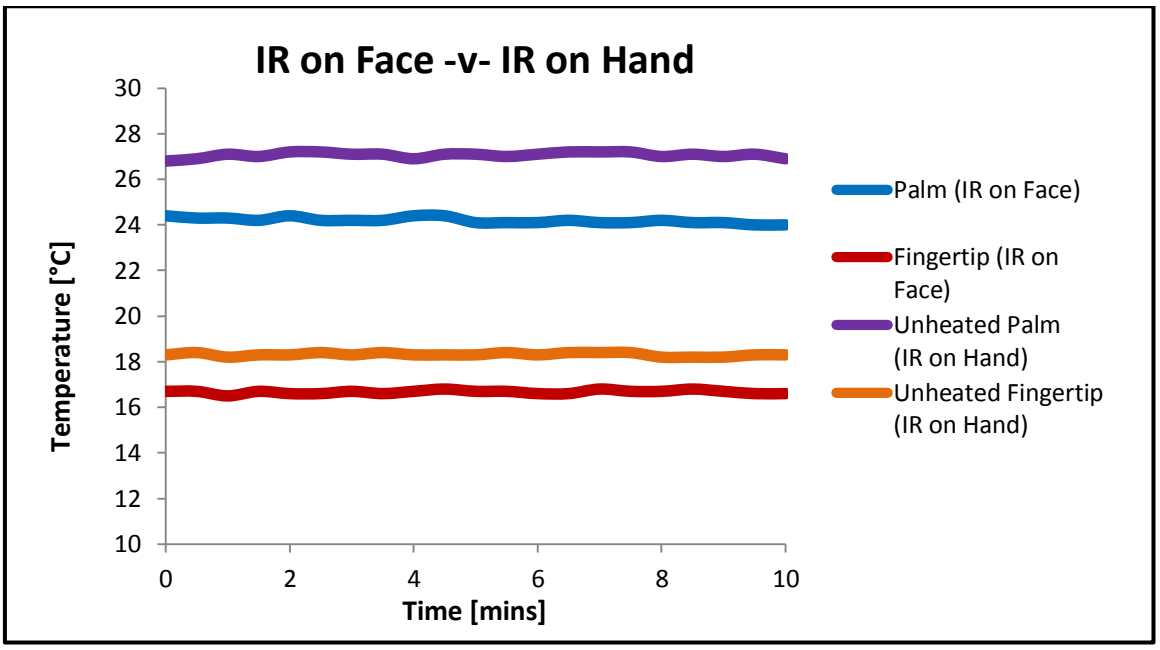

Figure 144 - Subject 4 Hand Test: IR on Face -v- IR on Hand

From Figure 145 the palm temperature can be seen to increase gradually over the course of the WR test by 1.3°C, whilst the palm temperature over the IR on Face test remains relatively constant. From Figure 146 the fingertip temperature over the WR test can be seen to increase slowly between the times of 2.5mins and 6.5mins, then more rapidly for the remainder of the test. It achieves a total temperature increase of 2.4°C, whilst the fingertip temperature over the IR on Hand test remains relatively constant.

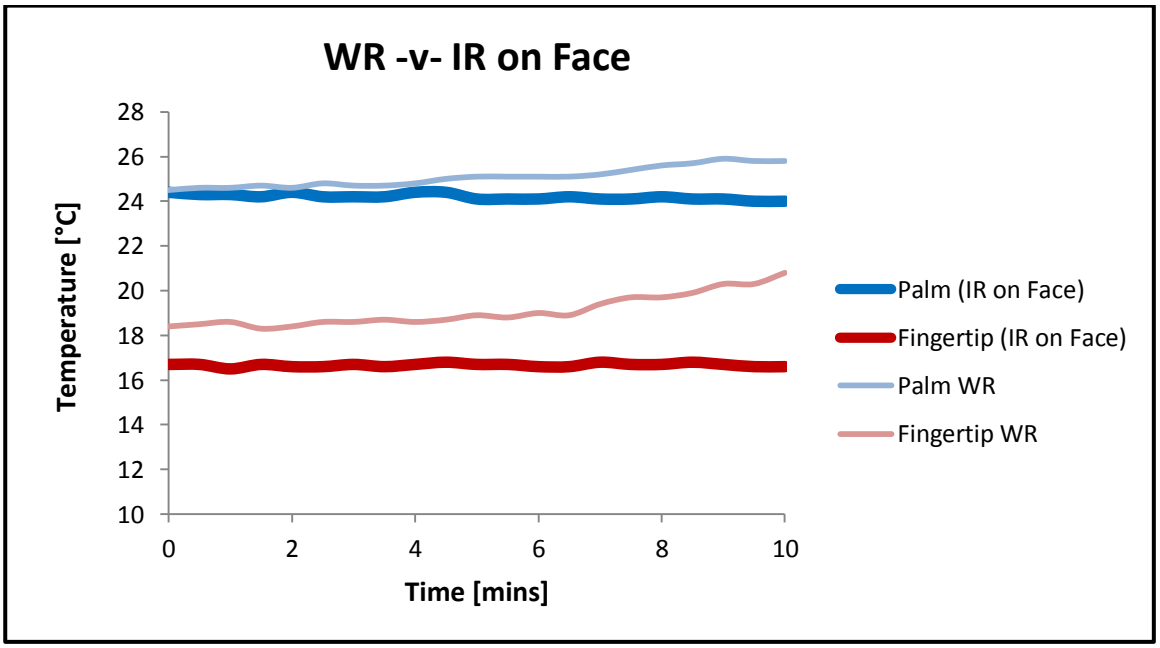

Figure 145 - Subject 4 Hand Test: WR -v- IR on Face

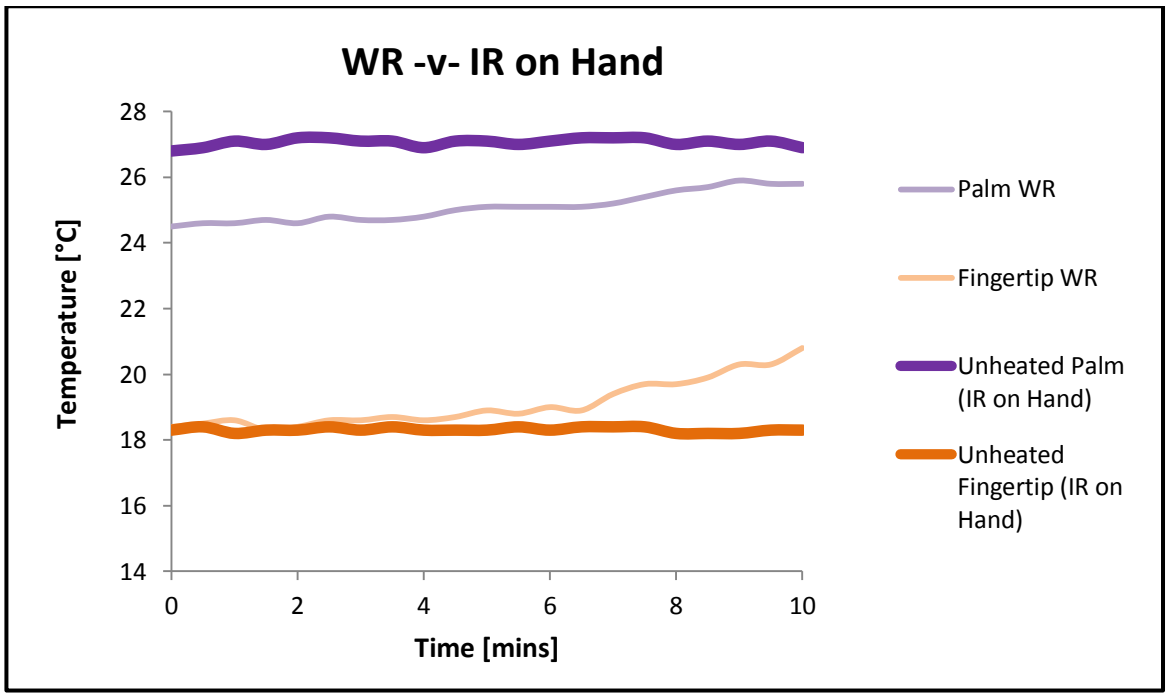

Figure 146 - Subject 4 Hand Test: WR -v- IR on Hand

4.3.2 Overall Findings

It has been made clear from the analysis of the individual results for the test subjects that the heating behaviour of the body under a set of imposed conditions will differ widely between individuals. The similarities and differences between subjects will be identified in this section and discussed with respect to the thermoregulatory system and its response to different heating conditions.

At the beginning of many of the tests the coldest areas can easily be identified as extremities of the body, i.e.: the hand, nose tip, and foot areas. The initial images from many tests suggest that the test subjects are cold from being exposed to a cold environment, and that at this time the thermoregulatory system has activated its vasoconstriction response in an attempt to conserve heat in the core of the body by reducing blood flow to these areas and closing the ateriovenous shunts.

During the WR tests the warm air is received by convection both directly to the extremities and also to other areas of the body. As the whole body warms up vasodilation allows excess heat to be moved from the core to other areas of the body in order to regulate the core temperature. Hence the extremities are being heated both directly by the warm air and also by thermoregulation. In contrast to this, the IR tests involved the application of

localised heat to the body. The IR heat is received by radiation directly to the areas of the body in the directional path of its waves, in the case of these tests to either the face or the hand area. The other areas of the body are in contact with only the cold air in the room, and so any heating of areas outside the directional path of the IR heat must be caused by thermoregulation alone.

The different ways in which the body is heated by warm air and direct IR heat conditions has been shown clearly during analysis of the tests which focused on the face area. In the case of the WR test the face slowly heats over the duration of the test, whilst almost the entire temperature increase over the face during the IR on Face test is achieved within the first minute. This is a major difference between IR and warm air heating conditions; the latter requires a longer exposure time to achieve the same effects. Analysis of the IR on face tests also showed that in general the application of IR heat caused the face areas to heat more significantly over the 10min period than during the WR tests (sometimes even above the estimated core temperature, which never occurred during WR testing). These key differences hold for all of the test subjects.

Temperature distributions in the face area at the beginning and end of a WR test are shown for all subjects in Figure 147. It can be seen that the nose temperature is initially very low in comparison to the rest of the face temperature for Subjects 1, 2 and 4.

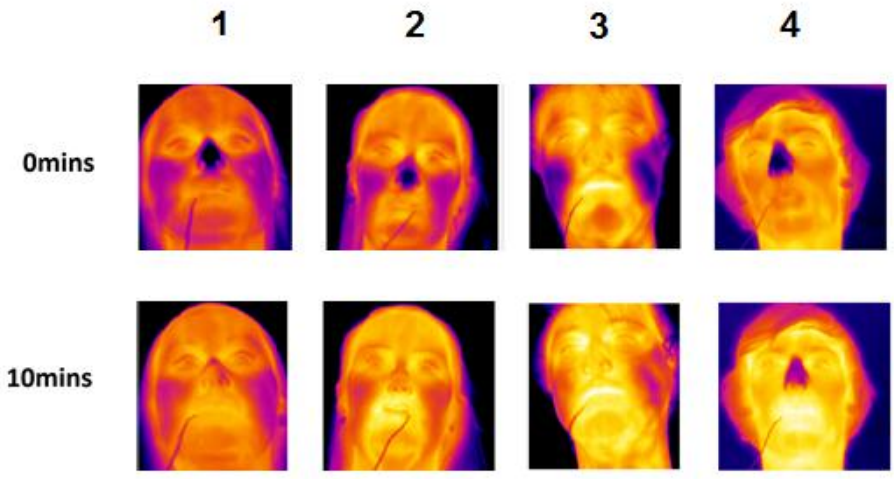

Figure 147 - Face temperature distributions at start and end of WR testing

For Subjects 1 and 2 it can be seen that the nose area rises significantly in temperature over the course of the test thus making the overall temperature of the face more uniform. For Subject 4 this change is not as extreme, thus suggesting that there is not as much warm

blood flowing in the nose area for this subject. This is the first of many examples of the poor circulation to the extremities displayed by Subject 4. Subject 3 has a high nose temperature at the beginning of the test which remains fairly constant throughout showing that the area is at no point during the test cut off from the blood flow to conserve heat, i.e. the subject is relatively warm before the test begins. *[Note: the temperature scales are not the same for the images that are shown together for comparison in this section - they are the same as those outlined for each test in section 4.3.1].*

Temperature distributions at the beginning and end of the IR on Face test are shown in Figure 148. For Subjects 1 and 4 the coldest area is initially the nose temperature as in the corresponding WR test. Again the heating behaviour of Subjects 1 and 4 differs in that Subject 1's nose area rises significantly in temperature thus making the overall temperature in the face more uniform, whilst for Subject 4 there is a less substantial increase in the nose temperature which remains well below the temperatures of other areas of the face. Again this would suggest poor circulation to the nose area for Subject 4. There is no blood restriction to the nose of Subjects 2 and 3 at the beginning of the test thus suggesting that the subjects are relatively warm at the beginning of the test.

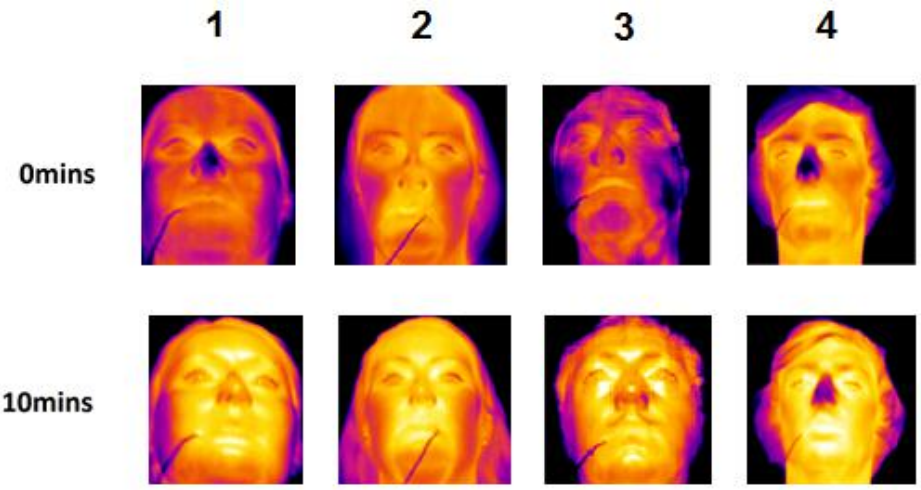

Figure 148 - Face temperature distributions at start and end of IR on Face testing

In the case of Subjects 1, 2 and 3, it is clear that the hand area is used by the body as a favoured region to which heat should be moved for dissipation to the surroundings in both the WR and IR tests. The hands are particularly suited to the dissipation of heat as they have a large surface area and little insulating fat, and in the case of these tests also frequently have low initial temperatures.

When focusing on the hand area during the WR test it can be seen that the temperature distribution about the hand is similar for all subjects at the start of the test; a warm palm centre with temperatures falling towards the edges of the palm and the fingers. At the end of the tests the temperatures in the hands of Subjects 1, 2 and 3 become quite uniform, but Subject 4 differs in that the palm temperature remains much warmer than the fingers, as shown in Figure 149. During the WR test the hand areas of Subjects 1, 2 and 3 can be seen to heat substantially over the course of the testing period, with the greatest temperature increase seen in the fingertip area, also shown in Figure 149. Again Subject 4 displays different behaviour than the other test subjects; throughout testing in warm conditions the overall temperature increases experienced by the hand areas of Subject 4 are much lower than those experienced by the other test subjects (showing only 27% for the fingertip and 42% for the palm of the average temperature rise shown by the same areas of the other test subjects). This suggests that heating is not occurring to the same extent in the hand area of Subject 4 as occurs for the other three subjects, likely due to the poor circulation that has been observed for this subject.

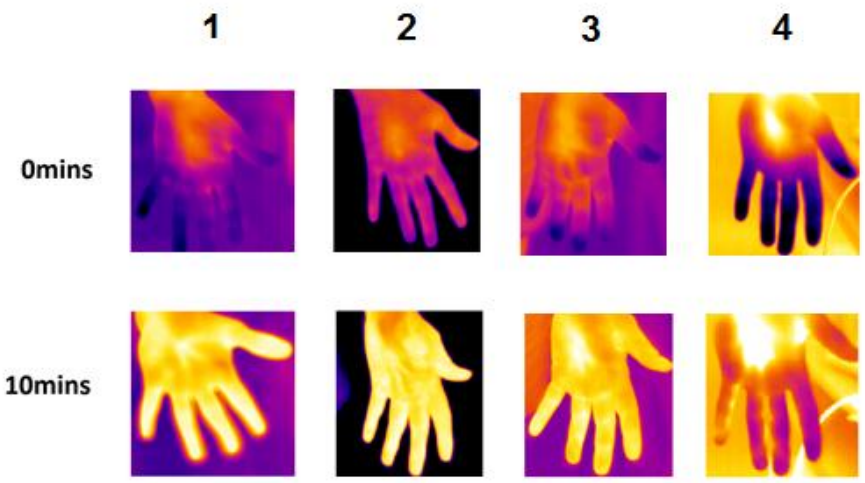

Figure 149 - Hand temperature distributions at start and end of WR testing

It can be seen from Figure 150 and Figure 151 that at the beginning of the IR on Face and IR on Hand tests the temperature distributions in the hands of Subjects 1, 2 and 4 are similar, consisting of a warm palm area with cooler fingers. Subject 3 has a more even temperature distribution in both cases and it is known from previous analysis that the hand is already close to being fully warmed at this time; therefore Subject 3 will be neglected from discussion here. During the both IR tests the whole hand area for Subjects 1 and 2

can be seen to rise in temperature and become more uniform despite the absence of a direct heat source to the area.

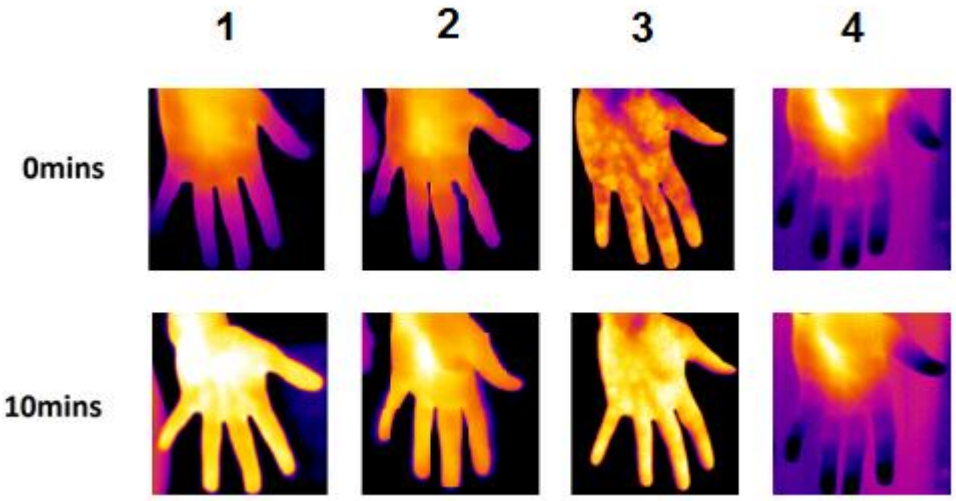

Figure 150 - Hand temperature distributions at start and end of IR on Face testing

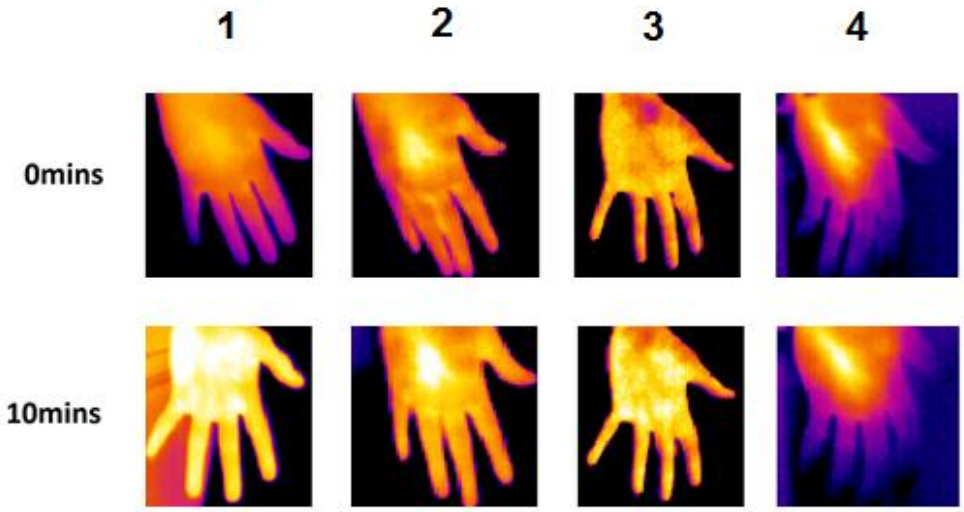

Figure 151 - Hand temperature distributions at start and end of IR on Hand testing

Because the hand area is not directly exposed to a heat source during the IR on Face and IR on Hand tests this temperature increase must come from within the body, i.e. through the process of thermoregulation. A temperature increase in the core body areas due to the direct application of IR heat has caused vasodilation to occur in the monitored hand in response to heat stress experienced by the body. This cooling mechanism has caused increased blood flow to the skin where the heat can be readily released to the environment. The heating effect on the hand when IR heat is focused on the opposite hand is less

substantial in magnitude than when heat is focused on the face, likely due to the fact that excess heat is being applied away from the core areas thus causing a lesser thermoregulatory response. These are very interesting results as they show the ability of the body to transfer IR heat from warm areas to cooler areas of the body through blood flow.

It has been generally shown from analysis in section 4.3.2 that the overall temperature increases in the hand area are lower for the IR tests than those that occur in the hands during the WR test. Hence it can be seen that during the WR tests both thermoregulation under heat stress conditions and direct contact with the warm air contribute to the overall heating effect. In both IR cases there is no observable change in the temperature distribution in the hand of Subject 4 which shows that the increase in hand temperature for Subject 4 during the WR test was likely due solely to direct contact between the hand and the warm air. Again this suggests very poor circulation in the hand areas of Subject 4.

The fact that less heat is not allowed to move to the hand area of Subject 4 leads to another notable difference between this subject and the other three subjects during the WR test. From analysis of the whole body during the WR test, Subjects 1, 2 and 3 all show a high temperature increase in the fingertip area, lesser increases in the palm and nose areas, and only very small temperature increases (less than 1.3°C) for all other areas of the body. Subject 4 shows very different behaviour; the highest temperature increase occurs in the nose area, the lowest in the palm area, and mid-range increases occur in all other areas (changes of 2.3-3.2°C).

Figure 152 shows the differences between the heating behaviour of Subject 4 and the other three subjects during the Full Body WR test very clearly; it can be seen from comparison of the 0min and 10min images recorded that Subjects 1, 2 and 3 show high increases in hand temperature and low increases (if any) in other areas of the body resulting in a more uniform body temperature overall by the end of the test, whilst the images of Subject 4 show a lesser increase in hand temperatures than the other subjects and a temperature increase throughout the rest of the body that is more pronounced, resulting in hand temperatures that remain substantially colder than other areas of the body. This temperature increase throughout the whole body of Subject 4 is likely due to the fact that vasodilation does not occur extensively enough in the hand. The heat must still be dissipated however, and so skin temperatures throughout the body rise in order to lose the excess heat. A further point to note here is that Subjects 1, 2 and 3 felt comfortably warm

during the WR tests, but Subject 4 felt uncomfortably warm and experienced perspiration. This is a sign that vasodilation was not sufficient to regulate the core temperature, and so the thermoregulatory system employed the perspiration response in order to more effectively reduce core temperature.

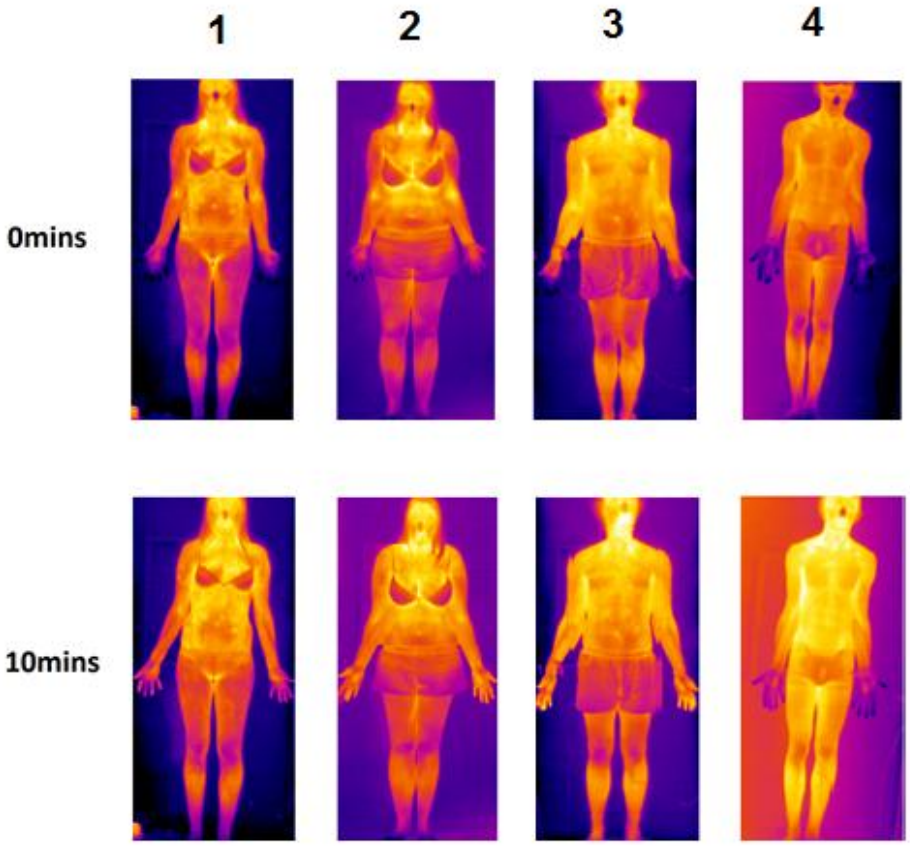

Figure 152 - Full body temperature distributions at start and end of WR testing

The overall results for heat flux measurements taken during the test suggest that heat flux is directly related to temperature, as it has been seen that in general for each subject increasing temperature in the hand causes an increase in heat flux, and that when temperature stabilises so too will heat flux. Heat flux values are positive throughout the IR on Face tests for each subject when the hand area is in direct contact with the cold air. During the WR tests the change from negative to positive heat flux value seems to occur when the palm temperature is approximately 6°C above the room temperature (as seen in the cases of Subjects 1 and 3 during the WR test), possibly relating to the point when the back of the hand (where the heat flux sensor is situated) rises above room temperature.

There are some cases where the heat flux shows slightly varying behaviour from these norms, and some possible reasons for this could include that the back of the hand is

undergoing further temperature increase at this time, that the thermoregulatory system has increased blood flow but the temperature in the hand is already at a maximum temperature for that area, that there is error in the results due to draft or movement of the hand, or potentially that other unknown factors are also contributing.

5 Future Work

The directional output of the IR heaters could be better assessed in a controlled environment and using a hemispherical test area rather than a 2D plane. Hence the output of the heater could be assessed at different radial distances from the heater, rather than at a flat plane at a given distance normal to the heater. This would be a preferable as it would mean that the entire output of the heater in all directions is being accounted for (assuming an efficient level of insulation at the rear of the heater).

The testing of the human thermoregulatory system in response to IR heating conditions could be improved and added to in many ways;

- Use of a controlled thermal environment.
- Ensuring that the initial skin temperatures of the subject are the same or at least very similar in all body areas between baseline WR and IR heating tests.
- Inclusion of skin moisture level analysis.
- Testing of the application of direct IR heat to further areas of the body, both singly and in combination.
- Generation of baseline tests at various room temperatures.
- Testing of IR heat application at various distances from the body.
- Positioning of the test subject in a sitting or lying down posture.
- Use of a wall of heaters to apply heat IR to the entire body.
- Analysis of the impact of the combinational effects of conventional and IR heating when used together in a space.
- Use of a higher resolution thermal imaging camera to obtain improved image quality of the full body.

6 Conclusion

The following conclusions are made with regards to the temperature distribution for each heater, and their suitability for use in comfort heating applications;

- As would be expected, the temperature distribution for both heaters varies most dramatically at the closest point to the heat source, and decreases with increased distance from the source. The variations in temperature are most noticeable within the 0.5m closest to the source, whilst after that point the temperature variation settles down to within 2-3°C for both heaters.
- A human will feel warm in the 30°C rays of the sun [49]. An estimate of an appropriate ESER placement for comfort applications could be given as at least 0.3m from the subject, giving a maximum central temperature of just under 30°C. Resultss for the Double FTE would suggest that it should be placed at least 0.5m from the subject for comfort applications, giving a maximum central temperature of just over 30°C. These distances give appropriately warm temperatures and quite uniform temperature distributions across the horizontal section.
- It could be suggested that the distance from the heat source at which the optimum combination of heat output and temperature distribution occurs is at around 0.3m. At this point the maximum temperatures from both of the heaters lies in the 30 – 40°C range, and the temperature difference across the test area is close to its lowest.

The following conclusions are made with regards to the heat flux distribution for each heater;

- As would be expected, the heat flux distribution for both heaters varies most dramatically at the closest point to the heat source, and decreases with increased distance from the source. The changes are most noticeable within the 0.4m closest to the source, after which the variation in heat flux settles down to within $8.6 - 11 \times 10^{-3}\ W/cm^2$ for both heaters.
- It could be suggested that the distance from the heat source at which the optimum combination of heat flux magnitude and heat flux distribution occurs is at around 0.4m with magnitudes of $30.8 \times 10^{-3}\ W/cm^2$ and $45 \times 10^{-3}\ W/cm^2$ for the

ESER and Double FTE respectively at the centre position. At this point the maximum and minimum heat flux values are within a range of between 20-30 $\times 10^{-3} W/cm^2$ across the horizontal section for both heaters.

- The heat flux and temperature distributions are compared at a distance of 0.4m from the source and are shown to be similar in trend.

The following conclusions are made with regards to the response of the thermoregulatory system to IR heating;

- Human thermoregulatory behaviour differs with each individual tested, and thus must be dependent on many individual factors.
- Temperatures across the body become more uniform when the subject is moved from a cold to a warm environment.
- Exposure of the face to warm air causes a steady rise in temperature over a 10min period. Exposure of the face to IR heat causes a sharp initial temperature rise within the first minutes of the testing period which is followed by a period of very gentle rise or steady state.
- IR heat from the ESER heater directly applied at 0.4m from the face area gives a higher magnitude heating response of the areas in its directional path over a 10min period than the effect of contact with warm air at a similar or slightly lower temperature. Direct IR heating at times causes skin temperatures to rise even above the estimated core temperature, which does not occur during WR testing.
- The nose and fingertip areas of the body are cut off from blood flow when the body is in a cold environment. For individuals with adequate circulation, these extremities tend to heat by a large magnitude when exposed to a direct heat source or to increased warm blood flow.
- The thermoregulatory system has the ability to redistribute IR heat effectively around the body. This is shown by the IR on Face and IR on Hand testing of the hand area, where sizeable temperature increases are recorded within the 10min period despite the fact that the monitored hand is not exposed directly to a heat source.
- The thermoregulatory response is greater when IR heat is applied to the face area than when it is applied to the hand area.

- The thermoregulatory system makes use of the large surface area and lack of insulating fat in the hand area by using it as a primary means of dissipating heat to the surroundings.
- In the case of poor circulation to the hand for an individual, the thermoregulatory system has trouble regulating the core temperature by vasodilation. The excess heat is distributed through the entire body in an effort to dissipate heat, and the thermoregulatory system employs the further cooling response of perspiration.
- The heat flux between the hand and the environment is dependent on the relationship between the temperature of the hand and the temperature of the surroundings, with energy moving from the warmer to the cooler of the two.

The overall objective of this project was to investigate the suitability of IR heating for use in human thermal comfort applications by obtaining qualitative information about the response of the human thermoregulatory system to IR heating. This objective has been realised.

With respect to this overall objective it can be concluded that there is much potential for the use of IR heating for thermal comfort applications.

- It has the potential to rapidly warm individuals placed in its directional path, and thus could be considered very useful for intermittently used areas.
- Human thermal comfort applications require relatively low temperatures to avoid excessive heating. An appropriate range of temperatures can be provided by IR heating for any given requirement by careful choice of heater and installation position.
- Although skin temperatures have been shown to rise substantially in areas where direct heat is applied, the subjective sensation is pleasant.
- The human thermoregulatory system has shown the ability to effectively redistribute directly applied IR heat around the body. This means that areas of the body that lie outside the directional path of IR waves can still be heated by thermoregulation.

REFERENCES

[1] Incropera, F.P., and DeWitt, D.P., 1996. *Introduction to Heat Transfer*, 3rd ed. USA: John Wiley and Sons.

[2] Murray, D., 2011. *Heat Transfer*, 4B4 Heat Transfer, [online via internal VLE] Trinity Collage Dublin. Available at <webct.tcd.ie> [Accesses Date 01 December 2011]

[3] Lahti, C., 2011. *The heat is on – an explanation of how far infrared heat works*. SaunaTime® blog [blog] 05 October, Available at <http://www.finnleo.com/blog/2011/5/10/the-heat-is-on---an-explanation-of-how-far-infrared-heat-works---by-craig- lahti.aspx> [Accessed date 04 December 2011]

[4] Murray, D., 2011. *Radiation*, 4B4 Heat Transfer, [online via internal VLE] Trinity Collage Dublin. Available at <webct.tcd.ie> [Accesses Date 01 December 2011]

[5] Omron Healthcare, 2010. *Body Temperature and Fever* [online] Available at <http://www.omron-healthcare.com/en/health_information/Fever/> [Accessed Date 13 February 2012]

[6] Emery, A. F., 2011. *Human Comfort and Health Requirements* [pdf] ME425, HVAC Engineering. University of Washington. Available at <http://courses.washington.edu/ me333afe> [Accessed Date 04 December 2011]

[7] Walsh, S., 2010. *Infrared imaging analysis for thermal comfort assessment* [pdf] Dublin: TrinityHaus. Available at < http://www.trinityhaus.tcd.ie/publications/2010-seminar-simeonwalsh.pdf> [Accessed Date 04 December 2011]

[8] Melikov, A.K., 2010. *Human Physiology Body's Heat Balance*, [pdf], Prague: International Centre for Indoor Environment and Energy Department of Civil Engineering, Technical University of Denmark. Available at <http://www.ib.cvut.cz/sites/default/files/temporary/Human%20Physiology-Body%20heat%20balance-AMelikov-CTU%20in%20Prague-Oct2010O.pdf> [Accessed Date 04 November 2011]

[9] Griffith, J.M. et al, 2004. *Human Skin Temperature Response to Absorbed Thermal Power* [pdf] Availale at <http://www.syneurgy.com/images/Downloads/Reference-9.pdf> [Accessed Date 04 December 2011]

[10] Snell Infrared, 2007. *Think Thermally – Practical news for practicing thermographers* [pdf] Vermont: Snell Infrared. Available at < http://www.thesnellgroup.com/storage/fck/File/thinkthermally/ThinkThermally_2007_Winter.pdf> [Accessed Date 04 December 2011]

[11] Sessler, D.I., 2007. *What's Hot in Thermoregulation*, ASA Refresher Courses, 36, pp.153-164.

[12] King, J., 2004. *Thermoregulation: Physiological Responses and Adaptions to Exercise in Hot and Cold Environments*, J.Hyperplasia Research, 4(3).

[13] Diaz, M., and Becker, D.E., 2010. *Thermoregulation: Physiological and Clinical Considerations during Sedation and General Anesthesia* [online] Available at <http://www.ncbi.nlm.nih.gov/pmc/articles/PMC2844235/> [Accessed Date 05 February 2012]

[14] White, I.H., 2006. *Homeostasis* [pdf] Available at <http://www.biologymad.com/resources/A2%20Homeostasis.pdf> [Accessed 06 November 2011]

[15] Stevenson, P., 2002. *Thermoregulation*, Australian Naturopathic Network [online] Available at <http://www.ann.com.au/MedSci/rmoregul.htm> [Accessed Date 05 February 2012]

[16] Kenney, W.L., 1998. *Physiological Responses to the Thermal Environment*, Encyclopaedia of occupational health and safety, Volume II, Ch42. Geneva: International Labour Organisation

[17] Tuomaala, P. et al, 2009. *New energy-efficient building concepts affecting human thermal comfort and sensation*, Eleventh International IBPSA Conference, Glasgow. 27-30 July 2009. Available at <http://www.ibpsa.org/proceedings/BS2009/BS09_1468_1475.pdf> [Accessed Date 06 November 2011]

[18] The Engineering Toolbox. *Met – Metabolic Rate* [online] Available at <http://www.engineeringtoolbox.com/met-metabolic-rate-d_733.html> [Accessed Date 02 February 2012]

[19] Bougdah, H., and Sharples, S., 2010. *Environment, Technology and Sustainability*. Abingdon: Taylor & Francis.

[20] ASHRAE Standards, 2004. *ASHRAE Thermal Environmental Conditions for Human Occupancy* [pdf] Available at <http://c0131231.cdn.cloudfiles.rackspacecloud.com/ASHRAE_Thermal_Comfort_Standard.pdf> [Accessed Date 24 November 2011]

[21] Djongyang, N., Tchinda, R., Njomo, D., 2010. *Thermal comfort: A review paper.* Renewable and Sustainable Energy Reviews, 14, pp.2626-2640.

[22] Prek, M., 2006. *Thermodynamical analysis of human thermal comfort,* Energy, 31(5), pp.732-743.

[23] Fanger, P.O., 1973. *Assessment of man's thermal comfort in practice*. British Journal of Industrial Medicine, 30, pp.313-24.

[24] International Standards Office, 2005. *ISO 7730. Ergonomics of the thermal environment - Analytical determination and interpretation of thermal comfort using calculation of the PMV and PPD indices and local thermal comfort criteria*. Geneva: ISO.

[25] Peeters, L. et al, 2009. *Thermal comfort in residential buildings: comfort values and scales for building energy simulation*. Applied Energy, 86(5), pp.772-780.

[26] Melikov, A., 2010. *Thermal Comfort Local Thermal Discomfort* [pdf] Available at <http://www.ib.cvut.cz/sites/default/files/temporary/Local%20thermal%20discomfort-AMelikov-CTU%20in%20Prague-Oct2010.pdf> [Accessed Date 29 November 2011]

[27] Olesen, B. W. Ph.D., 1994. *Introduction to the new revised draft of EN ISO 7730,* Ashrae Standard, 55(1992), pp.31-44

[28] Fanger, P.O. et al, 1985. *Comfort limits for asymmetric thermal radiation*, Energy and Buildings, 8(3), pp.225-236.

[29] Nicol, J.F., and Humphreys, M.A., 2002. *Adaptive thermal comfort and sustainable thermal standards for buildings*, Energy and Buildings, 34(2002/6) pp.563-573.

[30] Lifestyle Home Solutions Ltd. *Electric Heaters* [online] Available at <http://www.lifestylewindowsandconservatories.com/Products/Accociated/Electric_HeaterH.asp> [Accessed Date 07 December 2011]

[31] Total Health Marketing Inc. *Far Infrared Heater* [online] Available at <http://www.thmi.com/FIR/heater.html> [Accessed Date 07 December 2011]

[32] Celmec International Ltd. *Electric Infrared Heaters* [online] Available at <http://www.celmec.com.au/products/heatray/electric-infrared-heaters-general-information.html> [Accessed Date 07 December 2011]

[33] Glen Dimplex Ireland. *Benefits of Electric Heating* [online] Available at <http://www.glendimplexireland.com/corporate_information/benefits-of-electric-heating.htm> [Accessed Date 27 November 2011]

[34] Delta T. *Introduction to Radiant/Infrared heating* [online] Available at <http://www.deltat.com/radiant_infrared_heating_intro.html> [Accessed Date 04 December 2011]

[35] Protherm. *Infrared Basics* [online] Available at <http://www.pro-therm.com/infrared_basics.php> [Accessed Date 04 December 2011]

[36] Sunlight Saunas. *What is far Infrared?* [pdf] Available at <http://jjukurispa.com/pub/What+is+Far+infrared[20].pdf> [Accessed Date 04 December 2011]

[37] Ceramicx Ireland Ltd. *Ceramic Elements* [online] Available at <http://www.ceramicx.com/en/ceramic-elements> [Accessed Date 29 November 2011]

[38] Glen Dimplex Ireland. *Radiant Heaters* [online] Available at <http://gdhi.live.4.i-ntarsia.com/catalogue/commercial_heating/radiant_heaters/index.htm> [Accessed Date 27 November 2011]

[39] SSTS Infrared Ireland. *Ceramic Infrared Heater: Overview* [online] Available at <http://www.infraredireland.com/products.html> [Accessed Date 02 December 2011]

[40] Dimplex. *Electric Heating Products* [pdf] Available at <http://dimplexheating.com/cms-staging/publications/Commercial_Catalogue_2011.pdf> [Accessed date 04 December 2011]

[41] Knauf Insulation. *Glossary of Insulation Terms* [online] Available at <http://www.knaufinsulation.co.uk/design/glossary.aspx> [Accessed Date 27 November 2011]

[42] Vatell Corporation. *Thermogage Circular Foil Heat Flux Gauges* [online] Available at <http://www.vatell.com/thermogage.htm> [Accessed Date 13 January 2012]

[43] Vatell Corporation. *Use of the Thermogage Circular Foil Heat Flux Gage* [pdf] Available at <www.vatell.com/use%20of%20thermogage.pdf> [Accessed Date 11 January 2012]

[44] Vatell Corporation. *Thermogage Specification Sheet* [pdf] Available at <http://www.vatell.com/thermogage.pdf> [Accessed Date 11 January 2012]

[45] Art is fun. *Henna hand designs art lesson* [online] Available at <http://www.art-is-fun.com/henna-hand-designs.html> [Accessed Date 03 March 2012]

[46] Clker. *Hand 2 clip art* [online] Available at <http://www.clker.com/clipart-13908.html> [Accessed Date 03 March 2012]

[47] Portal Parejajoven. *Outline Human Body Blank* [online] Available at <http://parejajoven.com/ei-outline-human-body/> [Accessed Date 03 March 2012]

[48] istockphoto. *Human head surface anatomy outline* [online] Available at <http://www.istockphoto.com/> [Accessed Date 03 March 2012]

[49] Sunjoy, 2006. *Medicinal Effects of Far-Infrared Rays* [online] Available at <http://www.sunjoy.co.kr/eng/product/far-infrared-heating.html> [Accessed Date 15 January 2012]

APPENDIX A: Ceramicx Heater Information

Technical Details

Ceramic Full Trough Element (FTE)		
Wattage	300	$[W]$
Voltage	230	$[V]$
Mean surface temperature	400	$[°C]$
Max permissible working temperature	750	$[°C]$
Max power density	18	$[kW/m^2]$
Useful wavelength range	2-10	$[\mu m]$
Dimensions	245 x 60 x 31	$[mm]$
Average weight	180	$[g]$
Ceramic Edison Screw Bulb (ESER)		
Wattage	250	$[W]$
Voltage	240	$[V]$
Mean surface temperature	516	$[°C]$
Max permissible working temperature	750	$[°C]$
Useful wavelength range	2-10	$[\mu m]$
Dimensions	95 x 140	$[mm]$
Average weight	165	$[g]$

Table 3 - Technical details for FTE and ESER [37]

Schematic Diagrams

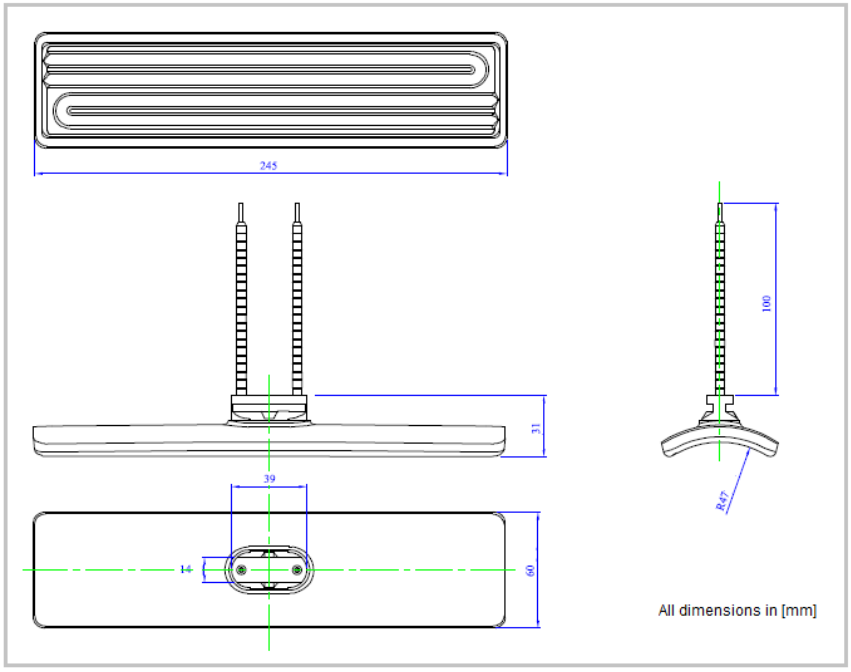

Figure 153 - FTE Schematic [37]

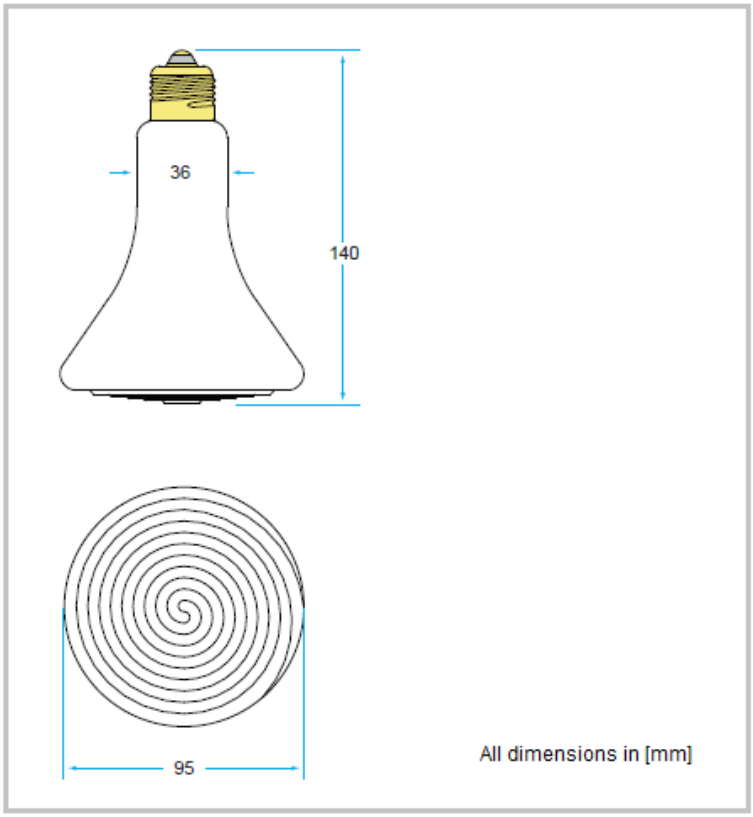

Figure 154 - ESER Schematic [37]

Heating Up Curves

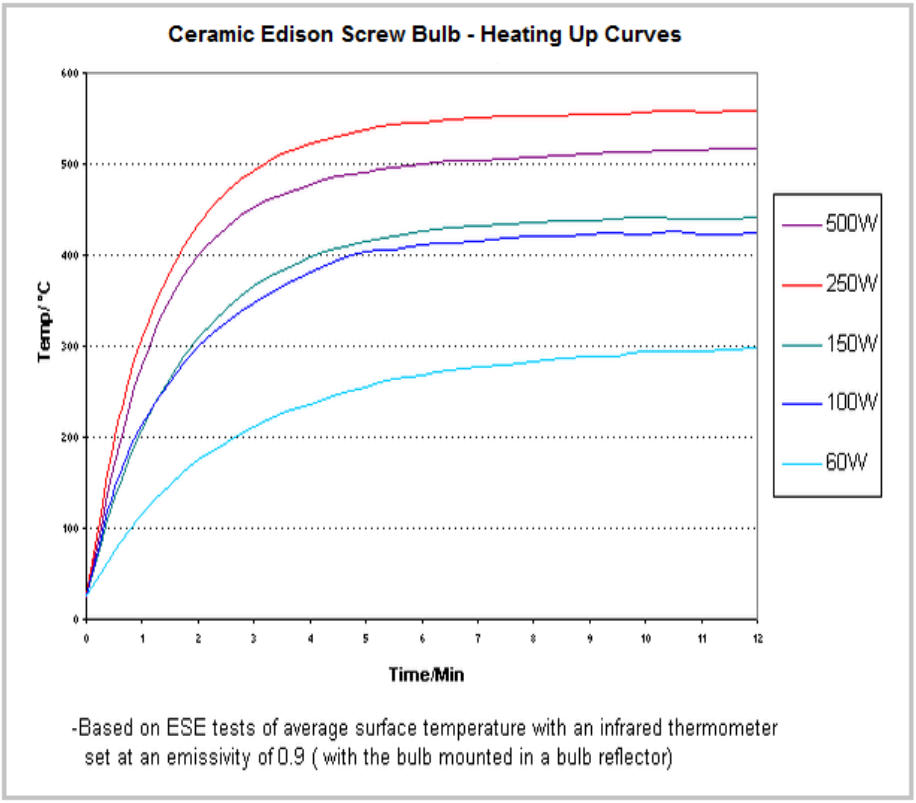

Figure 155 - Heating Up Curves for ESER [37]

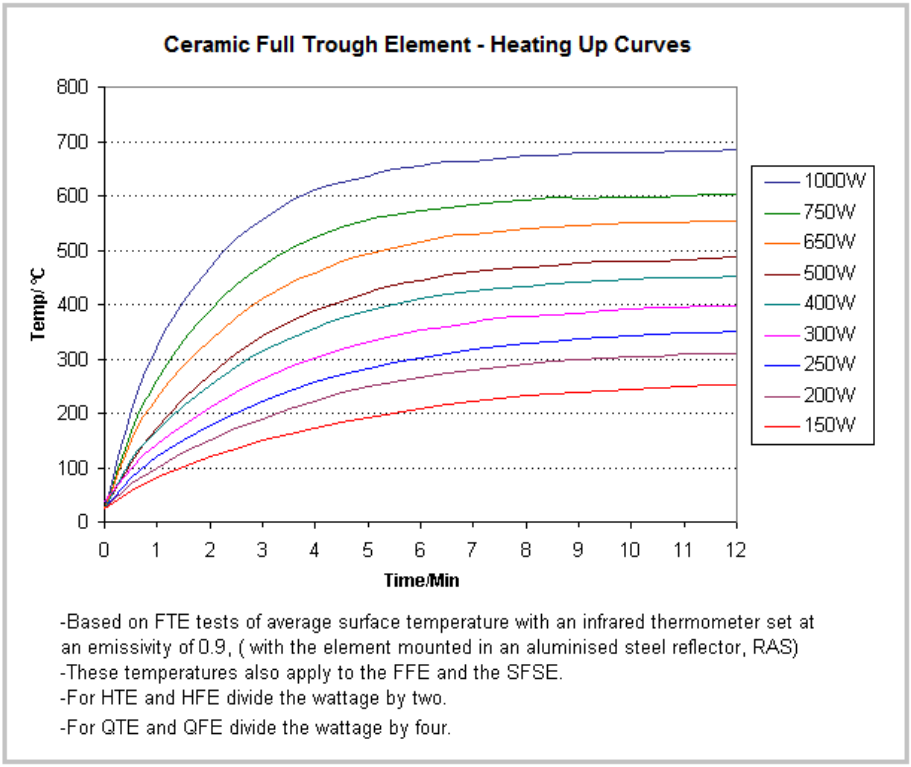

Figure 156 - Heating Up Curves for FTE [37]

Cooling Down Curves

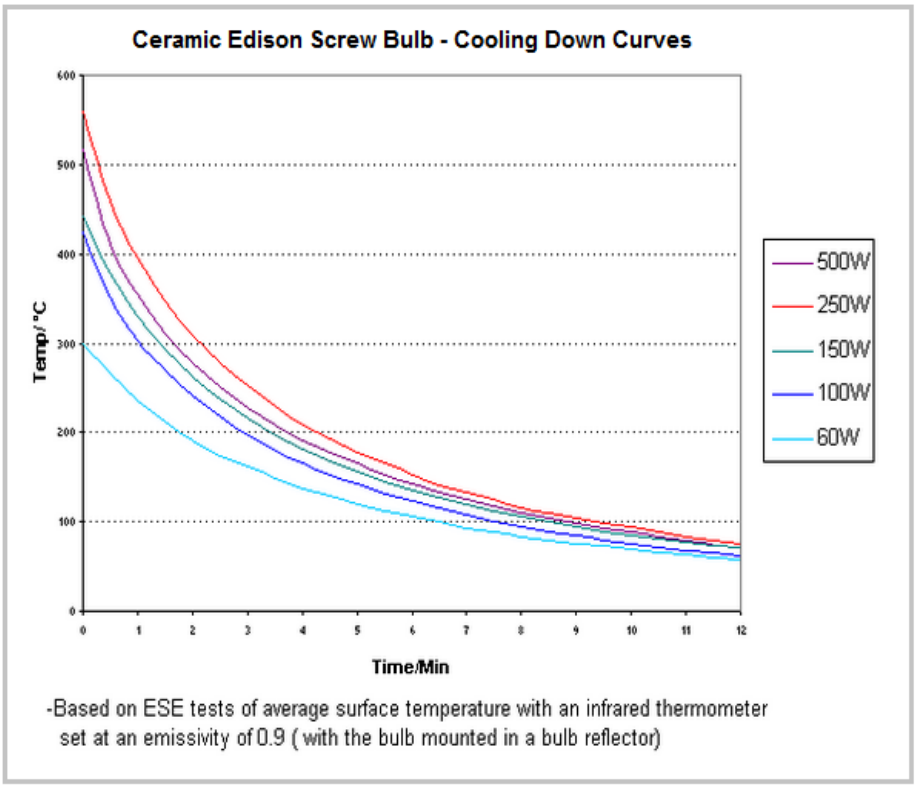

Figure 157 - Cooling Down Curves for ESER [37]

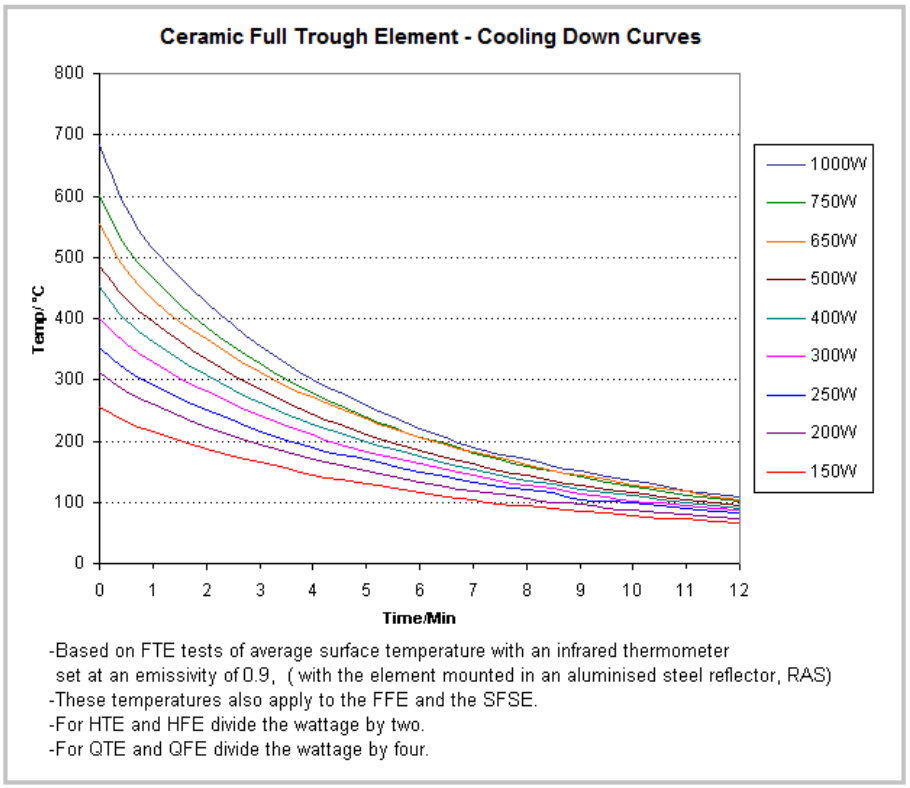

Figure 158 - Cooling Down Curves for FTE [37]

APPENDIX B – MATLAB Code

Temperature Distribution Code

```
close all; clear all;  clc; warning off;

% Set folder path
folder1 ='file location\';
% Load IR image file
load([folder1 'file name']);

% Change temperature value from Kelvin to Degrees Celcius
Z_C = filename - 273.15;
% Scale image to change X, Y axis values from pixels to mm
Z_C = imresize(Z_C, 2.569);


% Create figure
figure('NumberTitle', 'off', 'name', 'Rectangle Heater 10cm contourf')
% Filled contour plot with 15 colour segments
[C, h] = contourf(Z_C, 12);
% Set labels for X and Y axis
xlabel('X [mm]'), ylabel('Y [mm]'), zlabel('Temperature [^oC]');
% Set title for colourbar
title(colorbar,'[^oC]')
% Formatting options
colormap ('jet');  shading flat;
```

Heat flux distribution code

```
close all; clear all;  clc; warning off;

% Read in data from Excel file
Data =  xlsread (‘filename');
```

```
% Create figure
figure ('NumberTitle', 'off', 'name', 'Contour');
% Filled contour plot with 15 colour segments
[C,h] = contourf  (Data, 15);
% Set labels for X and Y axis
set(gca,'XTickLabel',{'0';'100';'200';'300';'400';'500';'600';'700';'800'});
set(gca,'YTickLabel',{'0';'100';'200';'300';'400';'500';'600';'700';'800'});
xlabel ('X [mm]'),  ylabel ('Y [mm]')
% Set title for colourbar
title (colorbar,'[x10^-^3 W/cm^2]')
% Formatting options
colormap ('jet');  shading flat;
```

APPENDIX C - Control Box Design and Bill of Materials

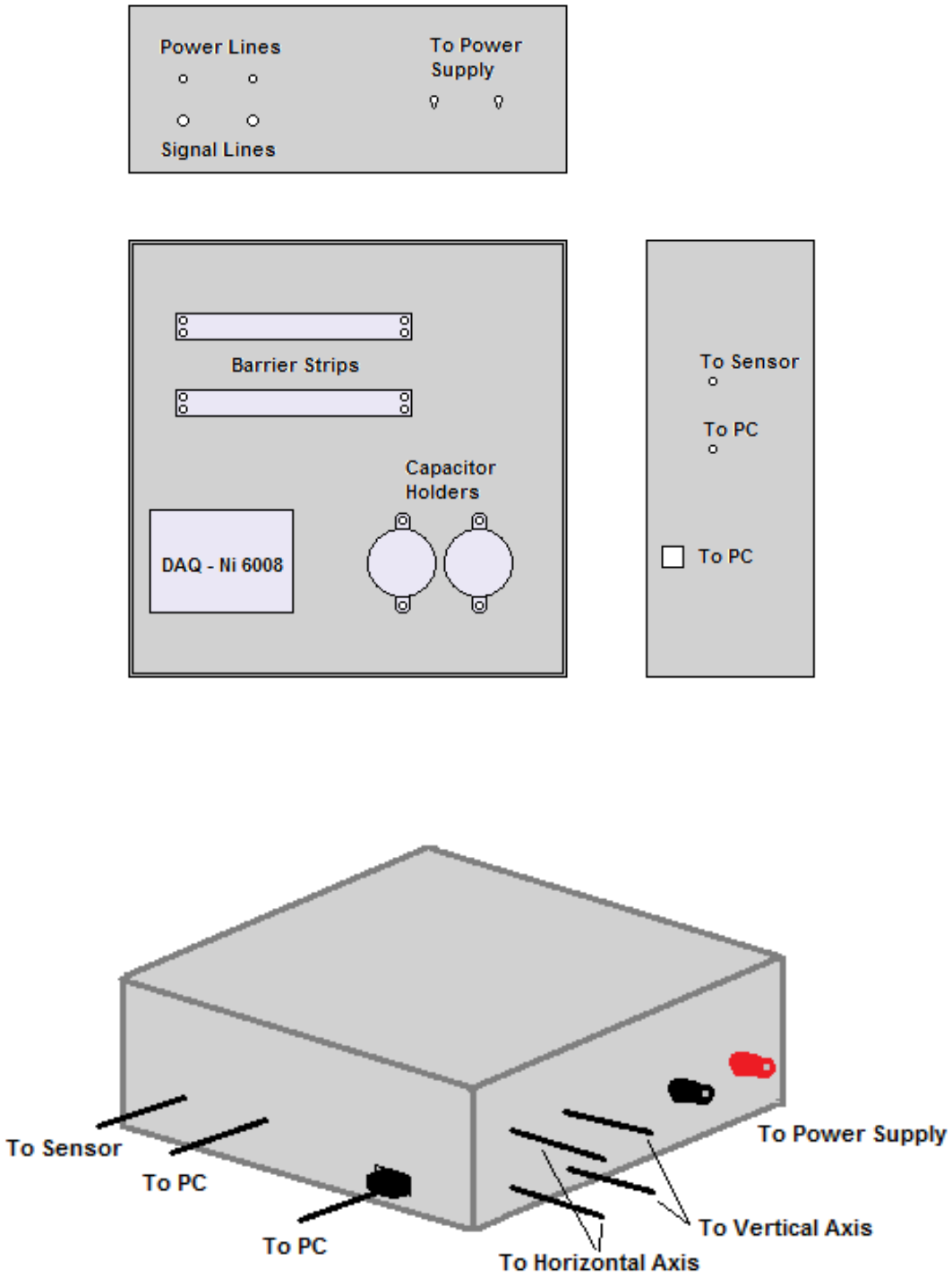

Figure 159 - Control Box Design

APPENDIX D: Sensor Calibration Sheets

TG9000 Radiant Heat Flux Sensor

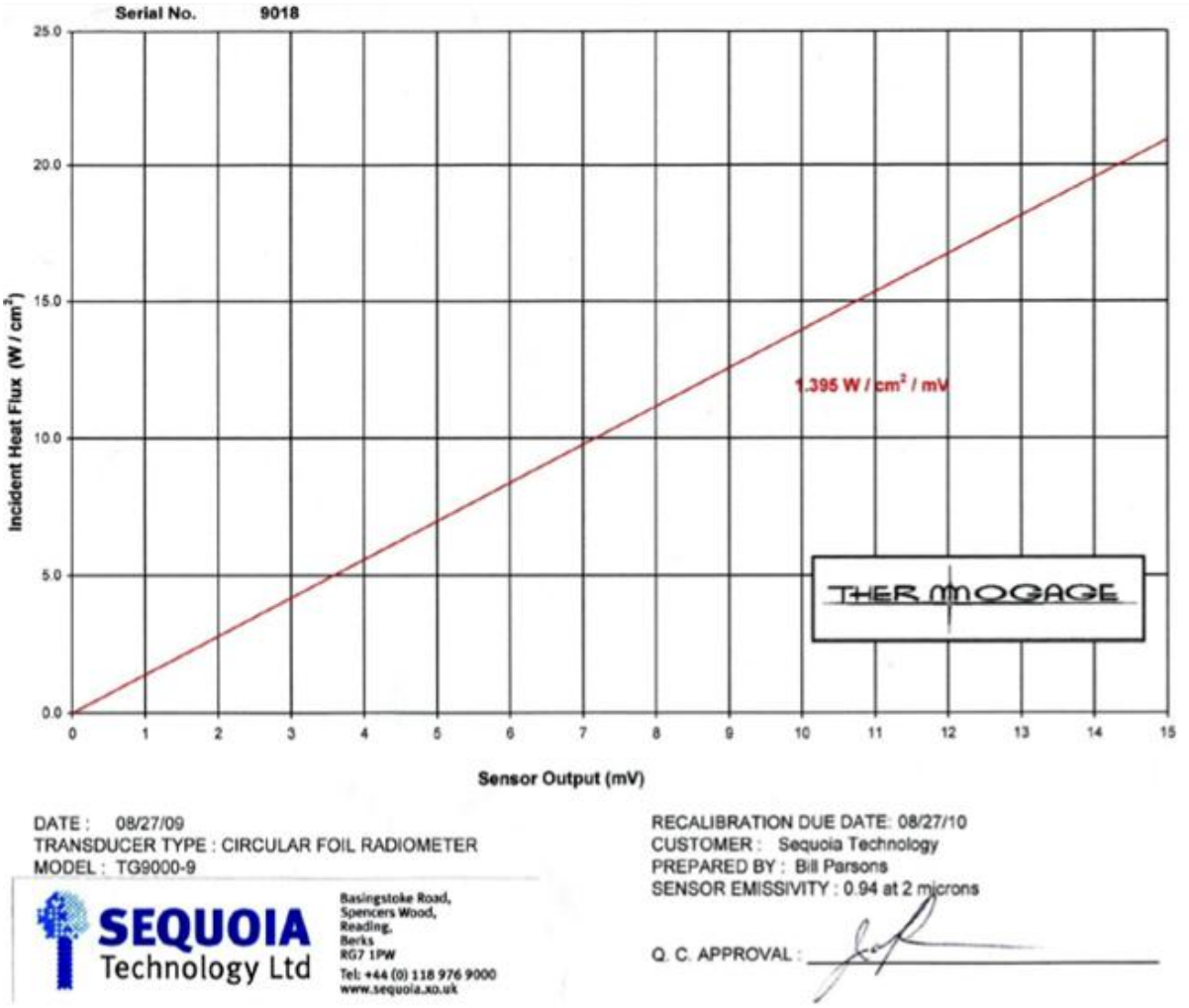

Figure 160 - TG9000 Radiant heat Flux Sensor Calibration Sheet

Thin Foil Radiant Heat Flux Sensor

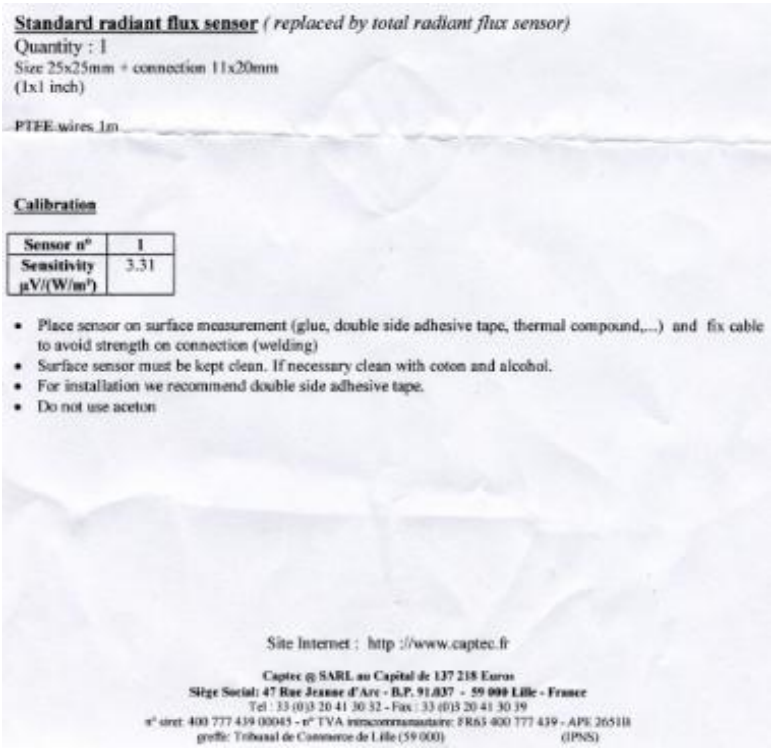

Standard radiant flux sensor *(replaced by total radiant flux sensor)*
Quantity : 1
Size 25x25mm + connection 11x20mm
(1x1 inch)

PTFE wires 1m

Calibration

Sensor n°	1
Sensitivity µV/(W/m²)	3.31

- Place sensor on surface measurement (glue, double side adhesive tape, thermal compound,...) and fix cable to avoid strength on connection (welding)
- Surface sensor must be kept clean. If necessary clean with coton and alcohol.
- For installation we recommend double side adhesive tape.
- Do not use aceton

Site Internet : http ://www.captec.fr

Captec @ SARL au Capital de 137 218 Euros
Siège Social: 47 Rue Jeanne d'Arc - B.P. 91.037 - 59 000 Lille - France
Tel : 33 (0)3 20 41 30 32 - Fax : 33 (0)3 20 41 30 39
n° siret: 400 777 439 00045 - n° TVA intracommunautaire: FR65 400 777 439 - APE 2651B
greffe: Tribunal de Commerce de Lille (59 000) (IPNS)

Table 4 - Thin Foil Radiant Heat Flux Sensor Calibration Sheet

APPENDIX E – Use of AcIA Easy and LabVIEW Programs

AcIA Easy Program

The AcIA Easy control screen is shown in Figure 161. The procedure for the use of this program is outlined as follows;

1) Connect drive unit to software.
2) Enable outputs. This turns off the brake and allows movement of the units.
3) Write motion sequence. The data sets can be specified in terms of increments or in terms of mm, where a 1mm target movement corresponds to a movement of 2000 increments. This allows for very high precision with accurate movements as small as 0.0005mm possible. The motion sequence shown makes each movement with respect to the previous data set. This requires manual location of the [0,0] position. Alternatively, the home position reference can be used which moves the unit directly to the [0,0] position by means of a limit switch.
4) Download the data set motion sequence to the drive unit.
5) Set test mode to allow step by step progression through the data set positions.
6) Testing can now begin. The step button is used to progress through the data set positions.

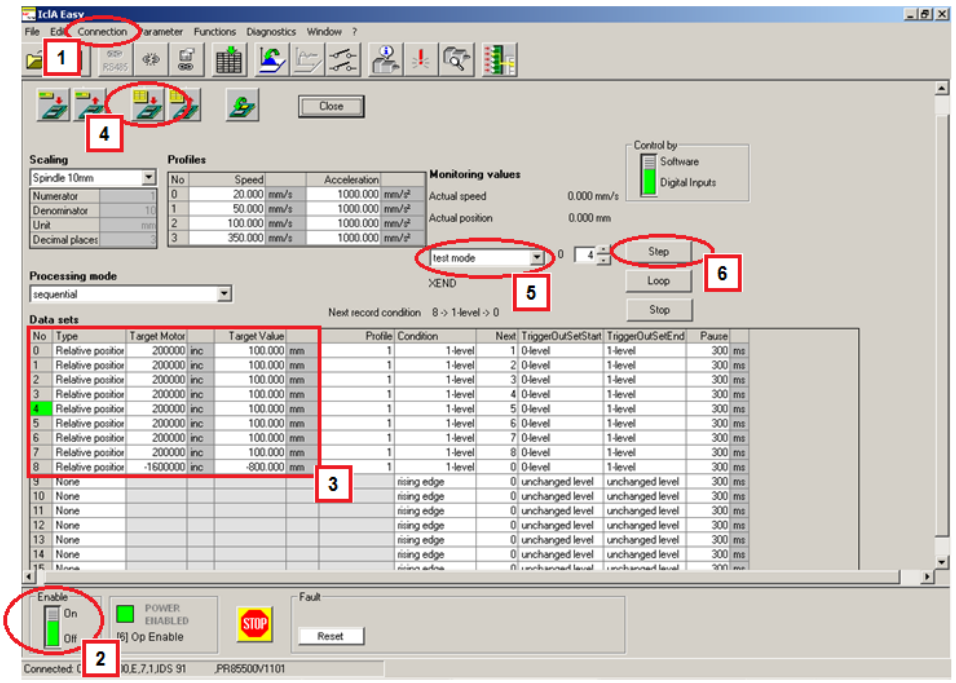

Figure 161 - AcIA Easy Motion Sequence Screen

LabVIEW Program

The LabVIEW front panel and block diagrams are shown in Figure 162 and Figure 163 respectively. The operation steps for this program are as follows;

1) Run the program.
2) Testing can now begin. Heat flux data is read in through the Ni 6008. There is a large amount of variation in the raw data and so the data is averaged to allow its mean value to be seen on the front panel waveform chart along with the raw data.
3) An initial data set should be recorded at this point without the heater present. This will be used to 'zero' the data at the data reduction stage.
4) A record of horizontal and vertical axes position is manually incremented on the front panel screen to show the sensor position for the current data set.
5) Data is saved for 5 seconds when the 'Save data for' button is activated. The number of seconds can be altered on the front panel screen. The raw data is stored in a .lvm file along with the current horizontal and vertical positions and its time stamp. The file number is set to automatically increment each time the program is run. The indicator labelled 'Saving data' indicates when data is being saved. The sensor must not be moved to the next position until this indicator turns off.
6) When testing is complete, stop the program to close the current .lvm file.

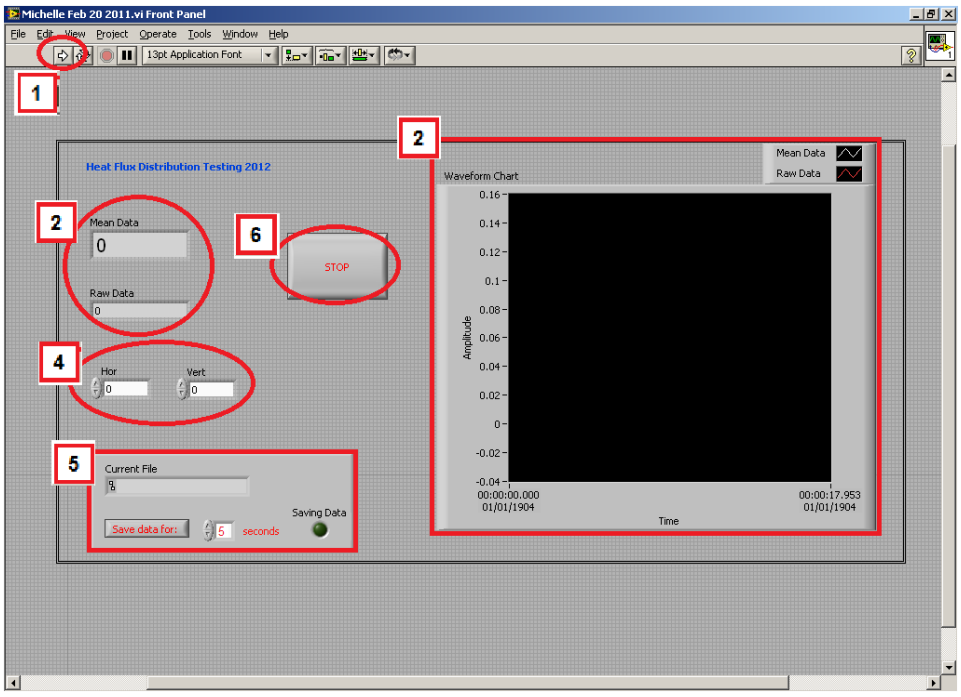

Figure 162 - LabVIEW Front Panel

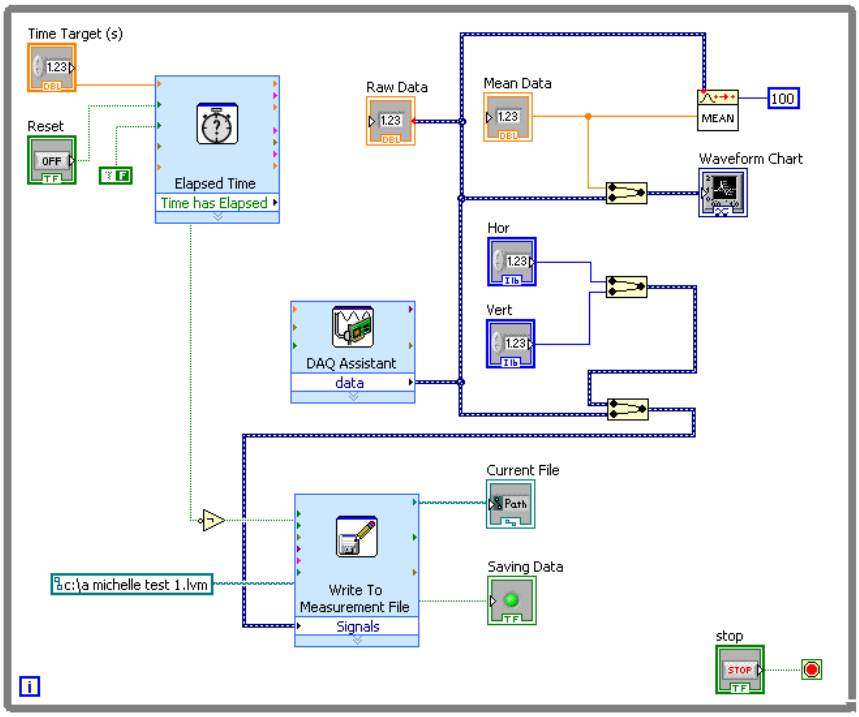

Figure 163 - LabVIEW Block Diagram

APPENDIX F: Bill of Materials

Control Box

Item	RS Part Number	Quantity	Cost [€]
High Temperature Enclosure	517-3428	1	29.60
Barrier Strip	423-330	2	4.96
Nylon Capacitor Mounting Clamp ϕ 40mm	203-5705	2	2.50 – pack of 5
Standard PVC Grommet, cable hole ϕ 9.5mm	543-210	2	5.34 - pack of 100
Standard PVC Grommet, cable hole ϕ 6.4mm	543-204	2	4.10 - pack of 100
Standard PVC Grommet, cable hole ϕ 4mm	543-197	2	2.65 - pack of 100

Table 5 - Bill of Materials for Control Box components

Radiant Heat Flux Sensing

Item	Supplier	Size	Quantity	Cost [€]
Thin Foil Radiant Heat Flux Sensor	Captec Enterprise	$25 \times 25mm$	1	157.00

Table 6 - Bill of Materials for Radiant Heat Flux Sensing